Fall 2010

# The synthesis and development of novel multi-component polyacridine gene delivery systems

Nicholas Jay Baumhover
*University of Iowa*

# THE SYNTHESIS AND DEVELOPMENT OF NOVEL MULTI-COMPONENT POLYACRIDINE GENE DELIVERY SYSTEMS

by

Nicholas Jay Baumhover

An Abstract

Of a thesis submitted in partial fulfillment
of the requirements for the Doctor of
Philosophy degree in Pharmacy (Medicinal and Natural Products Chemistry)
in the Graduate College of
The University of Iowa

December 2010

Thesis Supervisor: Professor Kevin G. Rice

# ABSTRACT

Non-viral gene therapy offers the potential to deliver nucleic acids producing therapeutic proteins to treat genetic diseases without the limitations observed with viral vectors. Before the therapeutic potential of non-viral gene delivery can be realized, several barriers to efficient gene delivery must be overcome. One delivery barrier of interest is the enhancement of endosomal escape to prevent vehicle and DNA degradation within the lysosome. However, to properly investigate the generation of analogues designed to enhance endosomal escape, one must also develop a gene delivery vector capable of addressing the deficiencies of traditional cationic polymer vectors.

The overall scope of this thesis project is to address the deficiencies and concerns encountered with traditional non-viral vectors. This has led to the hypothesis involving the development of novel systems based on polyintercalation afforded by incorporation of multiple acridine moieties within a modular polyacridine peptide. Initial studies focused on proof of principle experiments in vitro to assess the polyacridine peptides viability as a gene delivery vector by tethering the fusogenic peptide melittin to polyacridine. Polyacridine-melittin allowed us to conduct SAR (Structure Activity Relationship) studies relating to the sequence and structure of the polyacridine peptides using biophysical measurements and luciferase expression levels in cell culture to dictate peptide design. This data led to the discovery of $(Acr\text{-}Arg)_4$-Cys as the optimal in vitro polyacridine-peptide scaffold.

$(Acr\text{-}Arg)_4$-Cys was chosen as the lead polyacridine peptide for further development for in vivo mouse studies following PEGylation of the C-terminal cysteine. Polyplexes formulated with the $(Acr\text{-}Arg)_4$-PEG peptide demonstrated the ability to produce efficient in vivo gene transfer after delayed hydrodynamic (HD) stimulation. Further in vivo polyacridine peptide SAR studies resulted in identification of $(Acr\text{-}Lys)_6$-Cys as a PEGylated analogue that offered superior delivery capability by moderating

stimulated gene expression comparable to HD pGl3 after a 1 hr delay between formulation dose and hydrodynamic stimulation.

The properties of $(Acr\text{-}Lys)_6$-Cys allowed the in vivo study of multi-component complexes composed of polyacridine PEG, N-glycan targeting ligand, and fusogenic peptide to overcome the delivery barriers, most notably endosomal escape and nuclear localization. Multi-component complexes were formulated with 25 μg of pGL3 and liver gene expression was evaluated by bioluminescence imaging (BLI). Multi-component complexes containing polyacridine-PEG, N-glycan targeting ligand, and/or the charge neutral fusogen PC-4 produced detectable luciferase expression. Alternatively, multi-component complexes formed with the cationic fusogen melittin or anionic fusogen JTS-1 were unable to produce a BLI response, suggesting that multi-component complexes are intolerant of excessive charge. Upon further optimization, polyacridine peptides hold great therapeutic potential due to their modular design and unique nucleic acid binding properties to produce delivery vehicles capable of enabling efficient gene transfer in vivo.

Abstract Approved: _____
Thesis Supervisor

_____
Title and Department

_____
Date

# THE SYNTHESIS AND DEVELOPMENT OF NOVEL MULTI-COMPONENT POLYACRIDINE GENE DELIVERY SYSTEMS

by

Nicholas Jay Baumhover

A thesis submitted in partial fulfillment
of the requirements for the Doctor of
Philosophy degree in Pharmacy (Medicinal and Natural Products Chemistry)
in the Graduate College of
The University of Iowa

December 2010

Thesis Supervisor: Professor Kevin G. Rice

Graduate College
The University of Iowa
Iowa City, Iowa

CERTIFICATE OF APPROVAL

_____

PH.D. THESIS

_____

This is to certify that the Ph.D. thesis of

Nicholas Jay Baumhover

has been approved by the Examining Committee
for the thesis requirement for the Doctor of Philosophy
degree in Pharmacy (Medicinal and Natural Products Chemistry) at the
December 2010 graduation.

Thesis Committee: _____
Kevin G. Rice, Thesis Supervisor

_____
Jonathan A. Doorn

_____
Michael W. Duffel

_____
David L. Roman

_____
Paul B. McCray

To: My wife, parents, and the rest of my family that supported me through my many years of education.

ACKNOWLEDGMENTS

To begin, I want to thank my advisor, Dr. Kevin Rice, for his guidance during last 5 years to prepare me for a career as a scientist and introducing me to peptide chemistry and all the skills that go with it. On a personal note, I would also like to thank him for letting Nadiya take research credits during her P3 year, without it, chances are that we would have never met. I would also like to thank the members of my thesis committee, Dr. Duffel, Dr. Doorn, Dr. Roman, and Dr. McCray, for serving on the committee and for the advice and helpful comments during the entire process. To my lab-mates, past and present, for all the assistance and opportunities to collaborate and for keeping me sharp with endless questions and requests for advice, thank you. Thank you to my wonderful wife, Nadiya, for tolerating my long nights while writing this thesis and for making all the hard work worthwhile, Я люблю тебе без кінця, моя дружина. Finally, I want to thank my friends, my parent, the rest of my family, and my "other family" (those that I served with in Iraq) for your guidance, support, and giving me the initiative and persistence to get through anything life has to throw at me, especially graduate school.

## ABSTRACT

Non-viral gene therapy offers the potential to deliver nucleic acids producing therapeutic proteins to treat genetic diseases without the limitations observed with viral vectors. Before the therapeutic potential of non-viral gene delivery can be realized, several barriers to efficient gene delivery must be overcome. One delivery barrier of interest is the enhancement of endosomal escape to prevent vehicle and DNA degradation within the lysosome. However, to properly investigate the generation of analogues designed to enhance endosomal escape, one must also develop a gene delivery vector capable of addressing the deficiencies of traditional cationic polymer vectors.

The overall scope of this thesis project is to address the deficiencies and concerns encountered with traditional non-viral vectors. This has led to the hypothesis involving the development of novel systems based on polyintercalation afforded by incorporation of multiple acridine moieties within a modular polyacridine peptide. Initial studies focused on proof of principle experiments in vitro to assess the polyacridine peptides viability as a gene delivery vector by tethering the fusogenic peptide melittin to polyacridine. Polyacridine-melittin allowed us to conduct SAR (structure-activity relationship) studies relating to the sequence and structure of the polyacridine peptides using biophysical measurements and luciferase expression levels in cell culture to dictate peptide design. This data led to the discovery of $(Acr\text{-}Arg)_4$-Cys as the optimal in vitro polyacridine-peptide scaffold.

$(Acr\text{-}Arg)_4$-Cys was chosen as the lead polyacridine peptide for further development for in vivo mouse studies following PEGylation of the C-terminal cysteine. Polyplexes formulated with the $(Acr\text{-}Arg)_4$-PEG peptide demonstrated the ability to produce efficient in vivo gene transfer after delayed hydrodynamic (HD) stimulation. Further in vivo polyacridine peptide SAR studies resulted in identification of $(Acr\text{-}Lys)_6$-Cys as a PEGylated analogue that offered superior delivery capability by moderating

stimulated gene expression comparable to HD pGl3 after a 1 hr delay between formulation dose and hydrodynamic stimulation.

The properties of $(Acr\text{-}Lys)_6$-Cys allowed the in vivo study of multi-component complexes composed of polyacridine PEG, N-glycan targeting ligand, and fusogenic peptide to overcome the delivery barriers, most notably endosomal escape and nuclear localization. Multi-component complexes were formulated with 25 μg of pGL3 and liver gene expression was evaluated by bioluminescence imaging (BLI). Multi-component complexes containing polyacridine-PEG, N-glycan targeting ligand, and/or the charge neutral fusogen PC-4 produced detectable luciferase expression. Alternatively, multi-component complexes formed with the cationic fusogen melittin or anionic fusogen JTS-1 were unable to produce a BLI response, suggesting that multi-component complexes are intolerant of excessive charge. Upon further optimization, polyacridine peptides hold great therapeutic potential due to their modular design and unique nucleic acid binding properties to produce delivery vehicles capable of enabling efficient gene transfer in vivo.

TABLE OF CONTENTS

LIST OF TABLES

Table

LIST OF FIGURES

Figure

LIST OF SCHEMES

Scheme

# LIST OF ABBREVIATIONS

*ACM*.. ..... acetamidomethyl

*ACN*.. ..... acetonitrile

*AFM*.. ..... atomic force microscopy

*ASGP-R* ..... asialoglycoprotein receptor

*ATP*... ..... adenosine 5'-triphosphate

*BLI*..... bioluminescence imaging

*Boc*... ..... t-butyloxycarbonyl

*CHO*... ..... chinese hamster ovary cells

*DCM*..... dichloromethane

*DIC*..... diisopropylcarbodiimide

*DIPEA*.. ..... diisopropylethylamine

*DMEM*..... Dulbecco's modified eagle medium

*DMF*.. ..... *N,N*-dimethylformamide

*DMSO*.. ..... dimethylsulfoxide

*DNA*..... deoxyribonucleic acid

*DTDP*.. ..... 2-2'dithiodipyridine

*DTT*.. ..... DL-dithiothreitol

*EDTA*..... ethyenediaminetetraacetic acid

*EDT*.. ..... 1,2-ethanedithiol

*ESI*... ..... electrospray ionization

*FBS*..... fetal bovine serum

*Fmoc*.. ..... 9-fluorenylmethoxycarbonyl

*HATU*..O-(7-Azabenzo-triazol-1-yl)-N,N,N',N'-tetramethylurionium hexafluorophosphate

*HBTU*.. ..... O-(Benzotriazole)-N,N,N',N'-tetramethyluronium hexafluorophosphate

*HepG2*.. ..... human hepatocellular carcinoma cells

*HBM*.. .....Hepes buffered mannitol

*HD* ..... hydrodynamic dose

*HOBt*.. ..... 1-hydroxybenzotriazole

*HPLC*.. .....high performance liquid chromatography

*i.p.*… ..... intraperitoneal

*i.v.*… .....intravenous

*LC*.... ..... liquid chromatography

*MALDI-TOF*.. ..... matrix assited laser desorption ionization-time of flight

*MEM*.. ..... minimum essential media

*MS*… .....mass spectrometry

*MTT*..... 3-(4,5-dimethyl-2-thiazolyl)-2,5-diphenyl-2H-tetrazolium bromide

*mV*… .....millivolt

*MWCO* .....molecular weight cut-off

*NLS*.....nuclear localization signal

*NMP*.. .....*N*-methylpyrrolidone

*NMR*.. ..... nuclear magnetic resonance

*N:P*.. ..... nitrogen to phosphorous ratio

*NPC*..... nuclear pore complex

*OBut*.. .....t-Butyl ester

*Pbf*.... ..... 2,2,4,6,7-pentamethyldihydrobenzofuran-5-sulfonyl

*PBS*.. ..... phosphate buffered saline

*PEG*..... poly(ethylene)glycol

*PEI*... .....polyethyleneimine

*PLL*..... poly(L-lysine)

*QELS*... .....quasi-elastic light scattering

*SAR*..... structure-activity relationship

*SPPS*..... solid-phase peptide synthesis

*RP*……reverse phase

*RT*……room temperature

*TCEP*……tris(2-carboxyethyl)phosphine

*TFA*……trifluoroacetic acid

*TIS*……triisopropylsilane

*TP*……thiolpyridine

*TRI*……Triantennary N-Glycan

*3T3*……Mouse Fibroblast Cells

*Trt*……trityl

# CHAPTER 1

# LITERATURE REVIEW


## Abstract

Chapter 1 reviews the current literature of peptides used in non-viral gene delivery systems. Areas of discussion will include the major barriers to efficient non-viral gene transfer and focus largely on the mechanisms employed to enhance endosomal escape. The discussion will also include a brief history of acridine and its role in non-viral gene delivery as an alternative to using cationic peptides or polymers to interact with and deliver DNA or siRNA.


## Introduction

Viral vectors currently remain the most effective and efficient method of delivering genetic material in vitro and in vivo. Even though viral vectors have seen much success, their therapeutic use is limited by immunogenicity, insertional mutagenesis, and cytotoxicity (*1-6*). Conversely, synthetic vectors are much less efficient, but yet hold the promise of eliminating many of the issues observed with viral vectors. Some well known examples of non-viral vectors include polyethylenimine, dendrimers, poly-L-lysine, cationic lipids, chitosan, peptides with various biological functions, and to a lesser extent intercalator based systems (*7-11*). However it should be noted that some of these intercalator based systems still rely upon cationic polymers to condense DNA.

Several barriers to efficient non-viral gene therapy currently exist (Figure 1-1). First, the polymer or peptide systems must interact and in most cases condense DNA. Furthermore, a proper system should incorporate targeting ligands to enhance uptake by specific cell types and protect the DNA from premature degradation while exposed to the systemic circulation. Once the targeted polyplex has reached the cell of interest, it must be taken in by receptor mediated endocytosis and avoid lysosomal degradation by incorporating an endosomal disruption mechanism to transfer the nucleic acid to the

cytosol (*12*). One of the final barriers to overcome is the trafficking of the DNA from the cytosol to the nucleus (*13, 14*). An intuitive and yet often overlooked barrier to non-viral gene transfer involves the timely release of DNA near or inside the nucleus after polyplex dissociation, otherwise transgene expression cannot occur (*15*). To accomplish the goals of overcoming the barriers to efficient non-viral gene delivery, researchers have either employed peptide based delivery systems or peptides conjugated to polymeric or lipid based systems (*12*). This chapter will discuss the progress and deficiencies regarding cationic peptide mediated non-viral gene delivery with a focus on a diverse and bioactive class of peptides known as the fusogens. Additionally, attention will be given to the well characterized intercalator acridine and its utility in non-viral gene delivery.

## Peptide Enhancement of Non-Viral Gene Delivery

The use of peptides in conjunction with non-viral gene delivery systems has seen several advances over the past few decades, evolving from the use of highly heterogeneous poly-L-lysine (PLL) oligomers to characterizable multi-functional gene delivery vehicles designed to incorporate strategies overcoming various barriers to efficient gene delivery. These multifunctional peptide vehicles are capable of high affinity interaction with DNA and condensing DNA into compact particles, providing limited DNA protection from premature degradation, targeting specific cellular receptors, encouraging endosomal escape, addressing nuclear translocation of plasmid DNA, and preventing proteasomal degradation of peptide vectors (*16-18*).

### DNA Interaction and Condensation with Cationic Peptides

Gene delivery vehicles consisting of cationic peptides bind through an ionic interaction with the negatively charged DNA phosphate backbone. It is this binding that leads to compaction of DNA into what is commonly refered to as a nanoparticle or polyplex. Wu et al were among the first to report the use of polylysine as a non-viral gene delivery reagent to condense and deliver DNA (*19-21*). One potential benefit that exists

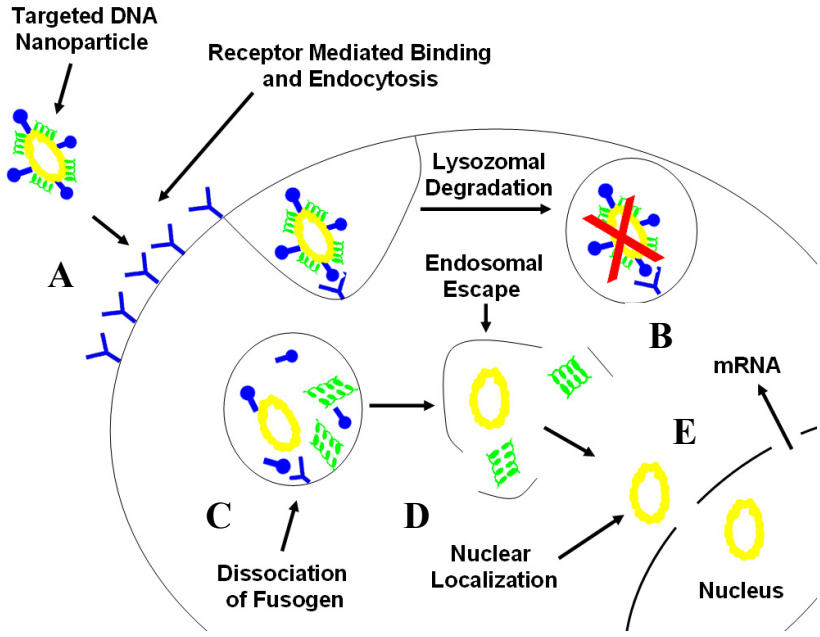


Figure 1-1. *The Intracellular Barriers to Efficient Fusogen Mediated Non-Viral Gene Delivery.* Once a targeted DNA nanoparticle has survived the trip through the systemic circulation, the nanoparticle must target a specific receptor on the cell to undergo receptor mediated endocytosis (**A**). To prevent lysosomal degradation (**B**), nanoparticle disassembly must occur (**C**) to release the fusogen to enhance endosomal escape (**D**). The cytosolically located plasmid must then be transported to the nucleus for gene expression to occur (**E**).

for use of PLL in vivo is its biodegradability by proteases; conversely, polymers such as PEI are not readily degraded and can lead to toxicity. Even though PLL is degradable, it can be cytotoxic, especially where the degree of polymerization (dp) (dp is defined as the number of lysine residues in the average polymer) is high, which generally ranges from 90-450 dp (*22*). Not only is the use of PLL limited by its toxicity, it is also limited by modest transfection efficiencies that it mediates, and if used in vivo, must be further modified with poly(ethylene)glycol to prevent plasma protein binding in an effort to stealth (stealthing is defined as the apparent neutralization of overall polycationic charge of a polyplex through incorporation of PEG on the delivery vector in an effort to reduce

non-specific interactions encountered within the systemic circulation) the net cationic charge of the polyplex (*23-25*).

As PLL is sold as a heterogeneous mixture of oligomers, several efforts were undertaken to generate homogenous cationic peptides of a desired length, capable of undergoing a high degree of characterization in hopes of generating reproducible biological results. Additionally, synthetic polycationic peptides offered the opportunity to modify the peptides in a specific fashion, allowing discrete modifications anywhere in the sequence to incorporate functionalities such as targeting ligands or fusogenic peptides by utilizing modern orthogonal peptide chemistry techniques (*22, 26-28*). Earlier work done in the group led to the observation that peptides minimally containing 13 lysine's were sufficient to tightly condense plasmid DNA (*29*). Further optimization by Adami et al generated a polylysine peptide that afforded protection from salt sonication and serum endonucleases (*30*). This resulted in the peptide sequence containing an alkylated cysteine, a tryptophan for detection purposes, followed by 18 sequential lysine residues ($AlkCWK_{18}$) (*22, 29*). It is useful to note that other research groups evolved similar cationic condensing peptides as well, such as Gottschalk's $YKAK_8WK$ peptide (*31*).

With $AlkCWK_{18}$ serving as the basic prototype for DNA complexing peptides, efforts were undertaken to strengthen the interaction of the peptide for plasmid DNA to offer greater protection and stability. One approach involved the crosslinking of amine groups between peptides on DNA with glutaraldehyde, which resulted in very stable polyplexes but prevented the timely release of DNA from the polyplex, ultimately resulting in a 10 day low-level steady-state luciferase expression in vitro (*32*). Another method involved reversible crosslinking that was mediated by interpeptide disulfide bond formation, which strengthened the interaction of the carrier for DNA and integrated a bioresponsive trigger to release the plasmid once inside the reducing environment of the cell (*33, 34*).

To adapt the $CWK_{18}$ system for use in vivo, it was necessary to functionalize the peptides with targeting ligands and "stealthing" reagents (*35*). Generation of the targeting ligands included the modification of $CWK_{18}$'s cysteine with an iodoacetamide triantennary N-glycan (I-TRI) (*36*) or high mannose N-glycan (I-Man9) (*37*) to form a thiol ether linkage. Functionalizing $CWK_{18}$ with I-TRI or I-Man9 allowed the selective targeting of the asialoglycoprotein receptor (ASGP-R) found on hepatocytes (*36, 38*) or mannose receptor located on Kupffer cells (*37, 39*). The stealthing peptide was afforded through selective PEGylation of $CWK_{18}$'s cysteine.

The evolution of $CWK_{18}$ as an in vivo gene transfer peptide led to more synthetically elegant systems that formed targeted gene transfer vectors through cysteine mediated polymerization. Park and Kwok pioneered early work involving sulfhydryl crosslinked polymeric PEGylated glycopeptides targeting either Kupffer cells or hepatocytes, respectively (*40, 41*). The PEGylated glycopeptides were synthesized utilizing two cysteine residues orthogonally protected with acetamidomethyl (Acm) groups, allowing selective modification of the N-terminal cysteine with PEG or glycopeptide. Following the removal of Acm groups with silver tetrafluoroborate in TFA, this allowed template driven polymerization to occur in the presence of DNA.

Chen and coworkers pushed this technology forward by inclusion of a cysteine modified melittin peptide capable of enhancing endosomal escape in vitro (*26, 42*). The core polylysine DNA binding peptide also included a centrally located TFA labile protected cysteine, resulting in the following sequence; $C(Acm)W(K)_8C(K)_9C(Acm)$, allowing the selective modification of cysteine with PEG or N-glycan targeting ligand. After Acm deprotection from PEG and TRI peptides, they were allowed to polymerize with each other and with a terminal cysteine flanked melittin analogue to form polymers containing stealthing reagent, targeting ligand and endosomal escape agent (*26*). Upon polyplex dosing by a standard tail vein injection into mice, the polymers were unable to mediate expression unless stimulated through a 5 min delayed blank hydrodynamic dose.

Furthermore, the stimulated expression levels were independent of fusogenic effect and the polyplexes lost their ability to be stimulated after 30 minutes, indicating rapid plasmid degradation (*26*).

While the polymeric PEGylated glycopeptide system represents an elegant approach integrating a variety of gene delivery components, there are several deficiencies that were discovered through the study (*26*). One deficiency that was discovered during the development of the PEGylated glycoprotein system relates to the synthetic difficulty to form the polymers between PEG, glycopeptide and melittin (*26*). To encourage polymerization, the peptide concentration must be very high to promote disulfide bond formation, which does not represent an issue for hydrophilic PEG or glycopeptide species (*26, 42*). In regards to melittin, this presents a challenge to prevent peptide aggregation and precipitation with hydrophobic peptides when present in high concentration (*26*). In a related item of interest, it was originally discovered that to encourage polymerization and strengthen DNA binding, melittin needed to be modified with additional lysine residues at the N and C-terminus of the peptide, which resulted in a neutralization of melittin's hemolytic activity at pH 4.5, which is the proposed pH of the late endosome (*26, 42*). It is this lack of low pH activity that may have contributed to the melittin independent effect as observed by BLI. Lastly, in an effort to keep the polyplex charge near neutral and avoid aggregation and flocculation, one must limit the amount of carrier that can be used to condense DNA, which may limit the carriers' ability to protect DNA from degradation in vivo (*26*). However, the formation of cationic polyplexes may be unavoidable as the system relies upon polycationic interactions to condense DNA, which inevitably leads to undesirable interactions with blood proteins (*35, 43*).

To overcome formation of cationic polyplexes and avoid subsequent undesirable blood protein interactions, there is a need to investigate alternative methods of DNA binding that does not rely entirely upon cationic polymers to deliver DNA in vivo (*44*). Even with the limitations of cationic polymers and peptides, there has been considerable

effort in the field to address and overcome the variety of barriers presented to a non-viral gene delivery vector. One area of such effort focuses on the investigation and incorporation of efficient endosomal escape mechanisms to prevent formulation degradation within the lysosome.

## Escaping the Endosome

Researchers have attempted to increase the efficiency of non-viral vectors by incorporating reagents capable of enhancing endosomal escape through ionic interactions, chemical ligation, or building the endosomal escape reagent into the vehicle backbone (*31, 42, 45-53*). There are several mechanistic theories to achieve endosomal release of nanoparticles to the cytosol, such as endosomal buffering or proton sponge effect and inclusion of membrane lytic entities such as fusogenic peptides. The small molecule chloroquine and polymers such as PEI are reported to enhance endosomal escape through an endosomal buffering mechanism (*17*). Briefly, as the endosome undergoes acidification by ATP dependent proton pumps, the protons are sequestered by the secondary amines of PEI, resulting in a net movement of anionic counter ions and influx of water, eventually bursting the endosome and releasing the PEI condensed polyplex into the cytosol (*54-56*). Efforts were undertaken to apply this proton sponge effect into peptide systems containing histidine (*57-63*). The imidazole side chain of histidine has a pKa of approximately 6.0, which allows for protonation to occur within the endosome while the side chain remains relatively neutral at physiological pH (*63*).

Several researchers have synthesized polyhistidine containing peptides to investigate the probable proton sponge effect. Midoux and Monsigny were among the first to successfully test the polyhistidine hypothesis in vitro and eventually developed a histidine rich peptide based upon the N-terminal sequence of the HA-2 subunit of influenza hemagglutinin (*59, 60*). The resulting peptide, H5WYG, demonstrated pH dependent cell membrane destabilization through a chimeric mechanism involving the

proton sponge effect and membrane destabilization (*59, 60*). Recently there have been reports involving the synthesis of hyperbranched polyhistidine peptides for use as antifungal agents and demonstrating promise as both in vitro plasmid and siRNA delivery agents (*64-67*).

In efforts to recreate the mechanism that viruses, such as influenza mediate endosomal escape, researchers have incorporated relatively short membrane lytic peptide segments or fusogens, either derived from virus proteins or from venoms of various species (*45, 53, 68-70*). The general characteristics of fusogenic peptides are that they adopt an alpha helical conformation, contain a variety of charged residues (anionic or cationic), exhibit pH specific activity, and are amphipathic (have a hydrophilic and hydrophobic face). These characteristics relate to their mechanism of action regarding membrane lysis. Generally the peptides form an alpha helical structure when encountering membranes, which allows for the hydrophobic and hydrophilic faces of the peptides to interact with membranes, followed by peptide aggregation and membrane disruption or pore formation (*68, 71*). Pore formation then allows for a disruption of the internal ion concentration or osmolarity, leading to an influx of counter ions and water which eventually results in the membrane bursting (*68, 71*).

Several attempts have been undertaken to incorporate fusogenic peptides into non-viral vectors to increase endosomal escape and gene transfer efficiency. Plank and Wagner attempted to exploit the endosomal escape mechanism employed by the influenza virus through truncation of the N terminal region of hemagglutinin HA-2 protein, resulting in the peptide known as INF, an anionic fusogen. To overcome the natural repulsion of INF for DNA, the peptide was chemically conjugated to PLL, resulting in a 10-10,000-fold increase in gene transfer efficiency in vitro over controls lacking INF (*72-74*).

On the other hand, the Szoka group conducted pioneering efforts regarding the development of artificial synthetic fusogens meant to mimic those found in viruses (*50-*

*52, 75*). These efforts led to the development of fusogenic peptides GALA and KALA, which their design was based on the N-terminal region of influenza hemagglutinin HA-2 protein template with pH dependent membrane lytic activity (*50, 52, 75*). The mechanism of lysis of both GALA and KALA have been studied extensively and both have been utilized as endosomal escape agents in non-viral gene delivery formulations (*51, 52*).

Gottschalk and co-workers designed an anionic fusogen designated JTS-1 first in silico using software capable of determining the secondary structure of the peptide (*31*). Upon synthesis and purification of JTS-1, the peptide exhibited low pH fusogenic activity in a liposome leakage and hemolysis assay where the peptide was devoid of activity at neutral pH. When ion paired to DNA complexes formed with a polylysine peptide, JTS-1 generated a 1000-fold increase in gene transfection activity as compared to polylysine only polyplexes. Vlasov and coworkers have also reported the successful use of JTS-1 in vitro when ion-pairing the anionic peptide with lysine dendrimers to polyplex DNA (*76, 77*). Unfortunately, JTS-1's utility exists only in vitro without chemical ligation to the cationic carrier as physiological salt concentrations can disrupt the ion-pairing between JTS-1 and poly-lysine peptide, resulting in premature liberation of fusogen from the polyplex if introduced systemically. To overcome the natural repulsive natures between JTS-1 and DNA, the five negatively charged glutamic acid residues were replaced with the cationic residues lysine or arginine, resulting in two unique peptides, ppTG1 and ppTG20, respectively. Both peptides were found to retain their secondary structures and membrane lytic potential, with the added ability to condense DNA and mediate gene transfer in vitro and in vivo following i.v. injection of a 50 μg plasmid dose delivered with a liposomal/peptide polyplex (*78*).

While several viruses employ anionic fusogens to mediate endosomal escape, investigators have looked at cationic fusogenic peptides to overcome repulsions associated with the anionic peptide and phosphate backbone of DNA. Several reports have incorporated the cationic fusogen melittin into gene transfer formulations (*46-48,*

*79, 80*). Melittin is a 26 amino acid cationic, amphipathic peptide which comprises 50% of the dry weight of honey bee (*Apis mellifera*) venom and is renowned for a potent lytic activity against various cell types and especially erythrocytes (*81-85*). Melittin is composed of two alpha-helical segments separated by an interrupting proline and has been observed to organize as a tetramer in solution while producing transient membrane pores of approximately 3-5 nm in diameter (*86-88*).

Researchers have attempted to harness melittin's robust lytic activity to increase polyplex endosomal escape in several reported studies. Legendre et al were among the first to utilize melittin through the reversible conjugation to dioleoylphosphatidyl-ethanolamine to generate dioleoymelittin, rivaling commercially available lipid formulations available at that time (*80*). Additionally, melittin has demonstrated increased in vitro gene transfer activity when bound to PEI versus transfectants generated with PEI alone (*46*). Several structure activity studies conducted by the Wagner group demonstrated that melittin's pH activity profile and toxicity can be shifted when linked to a carrier through its' C or N terminus (*47*). The C-terminally linked melittin is optimally membrane lytic at neutral pH which translates to increases in cytotoxicity while the N-terminal linkage produces a conjugate that is optimally active at endosomal pH, translating to higher gene transfer efficiency (*47*). Additionally, it was found that substitution of the neutral C-terminal QQ repeat with glutamic acid residues shifted the optimal pH profile to endosomal pH as well, increasing melittin-PEI conjugates toxicity and gene transfer profile (*48*). Further attempts to reduce melittin's cytotoxicity involved the transient masking of lysine residues with maleic anhydride derivatives that inhibited hemolytic activity at neutral pH, but were hydrolyzed off at low pH and demonstrated a recovery of lytic activity along with increased in vitro gene transfer efficiency (*79*). The transient masking of melittin has also found utility in siRNA delivery in vitro and in vivo while being reversibly bound to a cationic carrier system (*89-91*).

Studies from our lab eliminated the reliance of a cationic carrier system such as PEI or polylysine by transforming melittin into a gene transfer peptide capable of sulfhydrl mediated polymerization while condensing DNA (*42*). The concept of polymelittin was adapted to an in vivo gene transfer system composed of PEG peptide, glycopeptide targeting ligand, and melittin polymerized together at discrete ratios produced hydrodynamically stimulated gene expression although it was independent of melittin presence and composition as was discussed in the previous section describing polylysine based derivatives (*26*).

While there are several more cationic fusogens that have been utilized in non-viral gene transfer systems, many of them operate by the same mechanism of action and share some homology with the well characterized melittin. Most systems utilizing fusogenic peptides usually suffer from the same deficiencies when it comes to optimizing the systems for in vivo use. Many of the systems are highly cationic, even when formulated with PEG to stealth the overall charge, which leads to non-specific binding to serum proteins and less than desirable biodistribution to target organs. These non-specific binding issues are not only due to the cationic fusogen, but also to the cationic carrier that they are conjugated to, leaving the need to develop a unique gene delivery system that does not solely rely upon cationic charges to bind and associate with DNA or siRNA.

Recently there have been reports regarding the discovery of a neutrally charged fusogen that could have future utility in the design of non-viral vectors. Hirosue and Weber reported the discovery of a relatively short and hydrophobic peptide designated PC-4 (SSAWWSYWPPVA) identified from a phage display that possessed pH dependent fusogenic activity against a variety of liposomes (*92*). Interestingly, PC-4's activity is not dependent on the traditional alpha-helical secondary structure characteristic of many fusogenic peptides as circular dichroism measurements revealed a random coil secondary structure. Sun et al independently demonstrated early endosome activity in CHO cells with fluorescently labeled N-alkyl-3β-cholesterylamine PC-4 bioconjugates,

demonstrating the peptides' potential to disrupt endosomes in a cell model (*93*). If PC-4's endosomal lysis activity translates when incorporated into a non-viral vector, this could allow for the generation of charge controlled multi-component vectors capable of minimizing undesirable blood/polyplex interactions in vivo.

## Nuclear Localization

Once the DNA polyplex has achieved endosomal escape into the cytosol, the polyplex must be translocated into the nucleus before gene expression can occur. As the nuclear pore complex (NPC) is only estimated to be about 9 nm in diameter, it is very unlikely that free diffusion of polyplexes through the complex will generate robust gene transfer (*94*). In an attempt to coax the active transport of DNA polyplexes through the nuclear pore complex, several attempts have been made by researchers to develop and optimize short peptide sequences known as nuclear localization signals (NLS), that are generally recognized by a cluster of cationic residues that bind to intracellular proteins called importans that transport or chaperone macromolecules through the NPC (*46, 95-100*). One of the most utilized and well known NLS sequences is derived from the simian virus 40 (SV-40) large tumor antigen, resulting in the minimal NLS sequence needed for activity comprised of PKKKRKV (*101*). The minimal SV-40 NLS sequence has been reported to increase the localization of plasmid DNA 100-fold faster than a reversed NLS sequence (*102-105*). Furthermore, mutation of the sequence of the second N-terminal lysine to a threonine or asparagine negates any NLS activity (*106-108*). Behr's group has also reported that only one NLS peptide per plasmid is sufficient to gain nuclear entry where additional NLS copies per plasmid inhibit nuclear transport (*13*).

Several attempts have been made to incorporate NLS sequences into polyplex formulations through ionic interactions, mono and polyintercalation, chemical ligation, or to sequence specific sites on the plasmid DNA with PNA clamps, all producing contradictory and controversial results regarding their effectiveness in vitro (*10, 11, 13*).

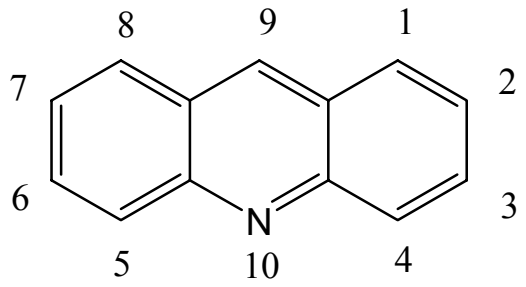


Figure 1-2 *Acridine Structure and the Numbering System Developed by Graebe (109).*

The source of these controversial reports may be addressed by simply analyzing the physical dimensions of common polyplex diameters and size of the nuclear pore complex. As most artificially formed polyplexes are generally around 100 nm in diameter (*110*), it is very difficult to conceive that a polyplex of this size can readily pass through a pore size of 9 nm to produce a significant increase in gene transfer.

In an alternative strategy to promote nuclear localization, Rebuffat and coworkers conjugated the steroid dexamethasone to their DNA binding vehicle, designated DR9NP. The overall rationale was to promote specific binding to the glucocorticoid receptor by DR9NP-DNA polyplexes to promote transport through the nuclear pore complex and demonstrated a 5-fold increase in transfection efficiency over control lacking the steroid ligand (*111*).

## Non-Viral Gene Delivery with Polyintercalators

Acridine has a long studied history of 140 years in scientific and medical research and has been used in applications as an antiviral, antimicrobial, and antiprion agent (*112-115*). Physical properties of acridine include a robust and vivid chromophore and fluorophore which can be attributed to the tricyclic heteroaromatic ring system (Figure 1-2). It is widely accepted that much of acridine's biological activity rests in its ability to intercalate nucleic acids, while some attribute biological activity to direct protein

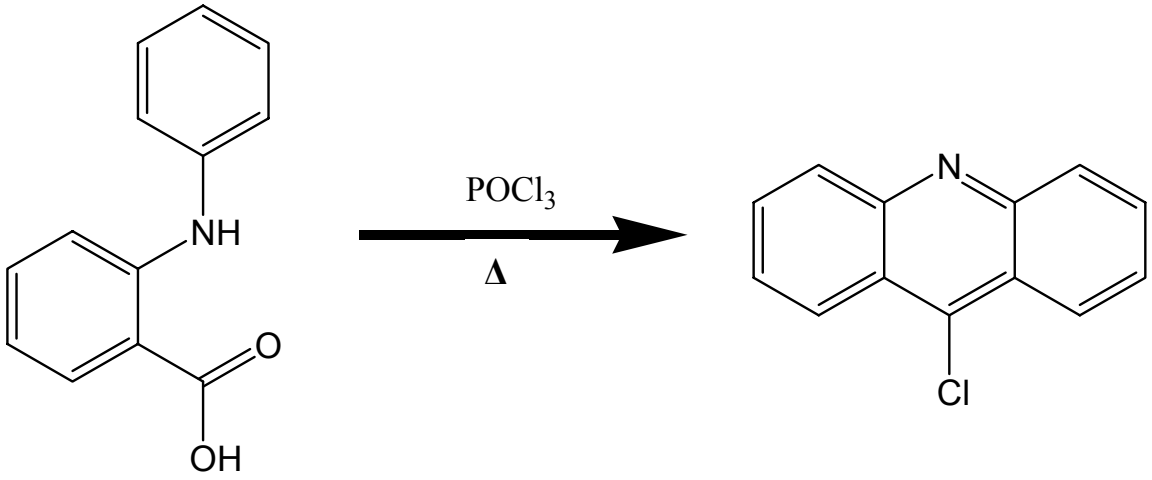


Scheme 1-1. *Synthesis of 9-Chloroacridine.* N-phenylanthranilic acid is heated at 140ºC for 2 hrs in the presence of phosphorous oxychloride to yield the reactive 9-chloroacridine product (*117*).

interaction. Acridine was originally discovered by Graebe and Caro after they isolated the compound from the anthracene fraction of coal tar (*109, 116*).

Since Caro and Graebe's initial discovery, several organic syntheses have been reported to obtain acridine analogues and their reactive intermediates. One acridine reactive intermediate of interest is 9-chloroacridine (*117*), which allows for further nucleophilic activation of acridine at the C-9 position with a labile leaving group such as phenol (*118*). Substitution of chlorine with phenol allows for functionalization of nucleophilic species such as primary amines at lower temperatures, which is of importance considering that the desired product may contain heat sensitive functional groups such as peptide bonds or protecting groups.

9-chloroacridine is easily obtained on large scale by reaction with N-phenylanthranilic acid in the presence of excess phosphorus oxychloride ($POCl_3$) at 140ºC for two hours and the reaction terminated by distillation to remove excess $POCl_3$ (Scheme 1-1). The 9-chloroacridine product is then extracted into the organic layer of a

mixture of chloroform/ammonia, dried with calcium chloride, and the solvent removed by distillation followed by a final heating to obtain the dry product (*117*).

9-phenoxyacridine is obtained by solvation of 9-chloroacridine in an excess of phenol and sodium hydroxide heated to 110ºC for 2-3 hours (Scheme 1-2). The product is precipitated from the sodium hydroxide phenol solution with aqueous 2 N NaOH, filtered via a Buchner funnel, washed several times with $H_2O$, and allowed to dry in vacuo overnight to afford 9-phenoxyacridine, generally in nearly quantitative yield (*119*).

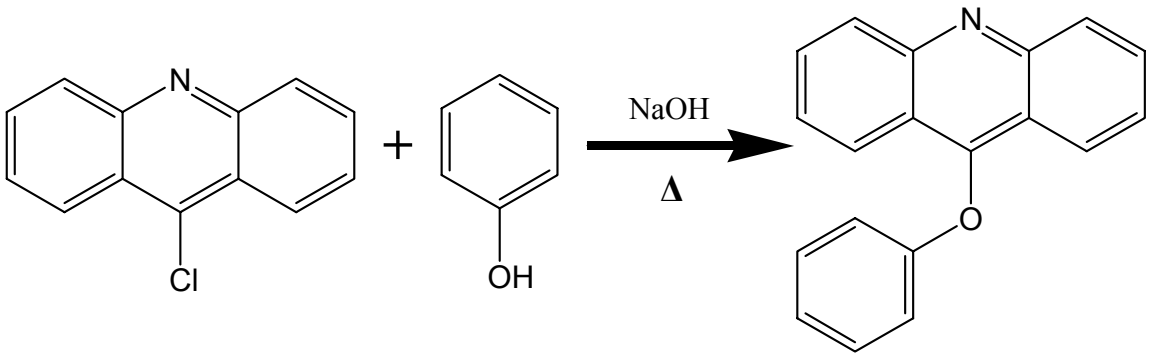


Scheme 1-2. *Synthesis of 9-Phenoxyacridine.* 9-Chloroacridine is dissolved in molten phenol and sodium hydroxide at 110ºC for 3 hours to yield 9-phenoxyacridine (*119*).

9-phenoxyacridine can then be used to modify primary amines that are present on solid phase peptide reagents containing free amines, such as lysine (Fmoc or Boc-Lys-OH) or N-amino 6-hexanoic acid which, allow for the synthesis of single or multiple valent acridine containing bioconjugates for use as non-viral gene delivery agents (*118, 120-122*).

The Szoka group initially pioneered the efforts to synthesize multi-valent intercalating bioconjugates as gene delivery agents by generating a trigalactosyl dilysyl bisacridine compound (Figure 1-3) capable of intercalating DNA and binding to the

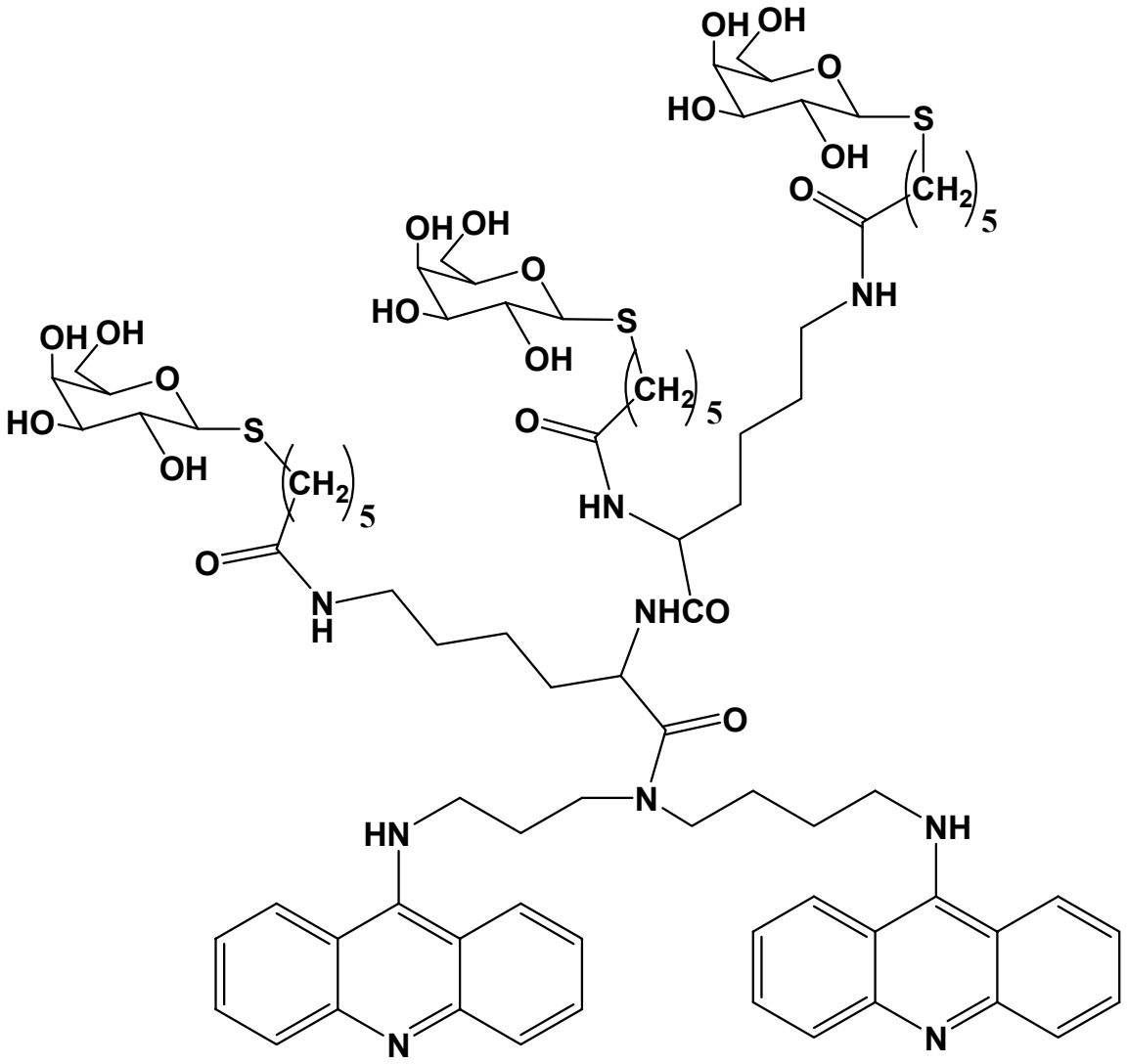


Figure 1-3. *Szoka's Trigalactosyl-bisacridine (123).*

soluble galactose receptor *Ricinus communis* lectin and asialoglycoprotein receptor of isolated primary rat hepatocytes (*123*). Unfortunately, the binding of polyplexes formed with the trigalactylated bisacridine compounds did not translate to increases in luciferase gene expression (*123*).

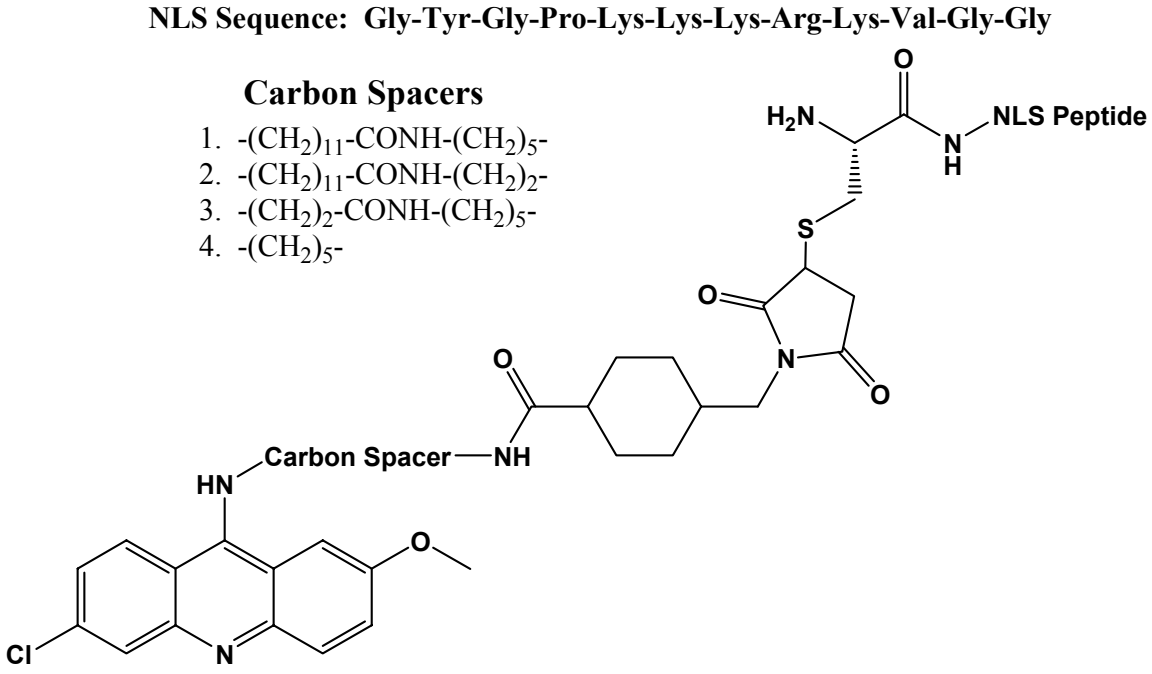


Figure 1-4. *Vierling's Mono-Acridine-NLS Peptides (11)*.

The Vierling and Nielsen groups independently reported mono-acridine (Figure 1-4) modified nuclear localizing peptide (*11*) and di and tri acridine substituted NLS peptides (Figure 1-5) (*10*), respectively. The transfection results reported for these compounds are controversial; as the Vierling group reported that gene transfection efficiency was not improved upon addition of an acridine-NLS to the formulation where Nielsen's group reported transfections were improved optimally with a triacridine-NLS construct included within a PEI-DNA polyplex. Explanations for the inconsistent reports may lie in insufficient binding affinity of a mono-acridine-NLS peptide for DNA given that nuclear transport of macromolecules relies upon active transport with the NLS sequence serving as the integrin attachment point, essentially pulling the acridine-NLS peptide away from the plasmid. In addition, the report by Nielsen relies upon PEI to condense DNA. At low N:P ratios (Nitrogen (cationic) to Phosphate (anionic) ratio), inclusion of triacridine-NLS results in a significant increase in gene transfer versus

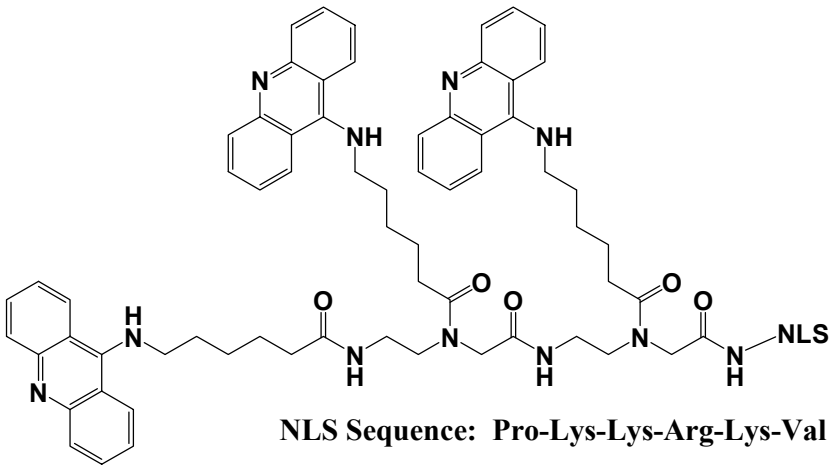


Figure 1-5. *Nielsen's Triacridine-NLS Peptide (10).*

control omitting NLS, however as the N:P ratio increases, the differences between PEI polyplexes with NLS decrease versus control polyplexes, leaving the question of whether an NLS effect is truly at work here and the increase in gene transfection is not merely a function of NLS's cationic character. This doubt could be removed if a control NLS sequence had been utilized, as formulating with triacridine-control NLS and PEI should produce similar expression levels to PEI only polyplexes, however, this was not reported in the manuscript.

Recently, the Vinogradov group has reported an advancement of acridine-NLS work initially begun by the Nielsen and Vierling groups with the synthesis of NLS-PEG-triacridine dendrimer (Figure 1-6) used in combination with Lipofectamine and Exgen 500 (sterile PEI solution in water). Their first report describes the synthesis of NLS-PEG-triacridine dendrimers and using in vitro gene transfer to conduct SAR to optimize the ideal PEG length to efficiently present NLS and encourage polyplex nuclear localization (*8*). Unlike Nielsen, Vinogradov's second report included a control-NLS-

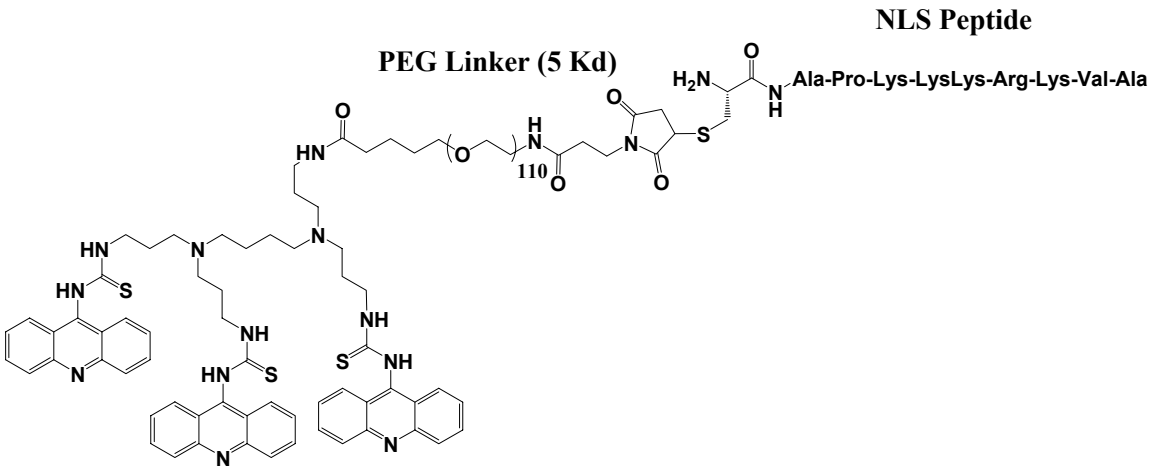


Figure 1-6. *Vinogradov's Tri-Acridine-PEG-NLS Conjugate (7-9).*

PEG-triacridine dendrimer, which resulted in a significant decrease in transfection efficiency when formulated with Lipofectamine 2000 or PEI polyplexes when compared to formulations containing NLS-PEG-triacridine dendrimer (*7*). The most recent report sought to investigate the replacement of commercial transfection reagents with bio-degradable and reducible polycations in formulations with NLS-PEG-triacridine dendrimer to reduce cytotoxicity associated with PEI (*9*). Secondly, the study sought to investigate the system for use in transfection of brain capillary endothelial cells. The overall results suggest that the new bio-reducible cationic polymers are less toxic than PEI. More importantly, the results observed in regards to transfection efficiencies of formulations containing NLS-PEG-triacridine dendrimer produces a modest increase over control even upon substitution of cationic polymer and may have utility in brain capillary endothelial cell transfections (*9*).

With exception to the pioneering work done by Szoka, many of the investigations involving acridine still rely upon the traditional cationic lipids or polymers to condense and deliver plasmid DNA and have overlooked the opportunity presented by poly-intercalation. Furthermore, the chemical synthesis of these acridine bioconjugates is

somewhat rate limiting and complicated, requiring several purification steps that prohibit the generation of polyacridine conjugates containing greater than three acridines. With the synthetic difficulty and meager increases in gene expression, it is understandable to see why development of polyacridine gene delivery systems were not optimized and advanced after the initial reports. Finally, all reported data pertains to in vitro gene transfer systems where the results do not necessarily dictate that an improvement will be observed if modified for in vivo delivery of nucleic acids. However, as many in the field of non-viral gene delivery are aware, in vitro results rarely translate to successful in vivo gene expression simply due to the complexity that exists in whole animal models. This does not preclude the usefulness of in vitro models, as one can investigate proof of principle ideas such as the design and appropriateness of a synthetic vector when used in conjunction with an entity to boost non-viral gene transfer to generate lead compounds to investigate in mouse models.

## Research Objectives

Cationic polymers and peptide systems have demonstrated their limitations to delivery nucleic acids in vivo. Partially due to the inability to completely shield an overall positive charge from serum proteins, premature polyplex dissociation due to ionic interference from physiological salt concentrations, and prevent plasmid degradation from serum DNAse activity (*43, 44, 124*). With the deficiencies of polycationic systems in mind, there is an incredible need to develop a novel delivery vehicle capable of high affinity interaction with DNA to withstand premature dissociation in high salt environments and capable of protecting DNA from premature degradation when delivered systemically. Furthermore, it would be beneficial to conduct SAR studies relating to vector design in vitro, where one can essentially conduct high throughput screenings to investigate various parameters. As mentioned before, the gene therapy literature is rich with gene expression data demonstrating a radical disconnect between in

vitro and in vivo success. However, if one were to couple an entity known to increase gene transfer efficiency in vitro to an experimental carrier system, data trends could be examined to provide rationale regarding the design of a carrier system to develop lead compounds capable of the most rudimentary functions required for an in vivo gene delivery system.

The overall scope of this thesis project is to address these concerns that have led to the hypothesis of developing a novel delivery system based on polyintercalation or a mixed intercalative/ionic interaction afforded by incorporation of multiple acridine moieties to provide sufficient affinity for nucleic acids (plasmid DNA and siRNA). The overall hypothesis regarding the development of polyacridine gene delivery systems is that the combined binding properties of intercalation and ionic interaction will provide a carrier system that is capable of withstanding premature dissociation and transgene degradation in vivo and allow the incorporation of multiple components to overcome the barriers to successful non-viral gene delivery. To successfully investigate this hypothesis, the polyacridine gene delivery systems must prevent the premature dissociation of the carrier, increase serum stability, enable targeting to specific organs and cells in vivo, and attempt to address the multitude of barriers that exist before successful non-viral gene delivery can be realized. Our ultimate aim is to deliver nucleic acids using a multi-component approach to instill PEG, targeting ligand, and endosomal escape reagent capable of overcoming the deficiencies related to the use of cationic polymer and peptides as gene delivery vehicles (Figure 1-7).

In the initial SAR studies regarding the discovery of desirable properties for a polyacridine peptide, the highly characterized fusogen melittin will be tethered to polyacridine in a reducible or non-reducible fashion to provide a positive readout consisting of luciferase transgene expression. The in vitro gene transfer properties of polyacridine-melittin will be studied to determine if gene transfer is dependent upon polyacridine chain length and what is the effect of a spacing amino acid between acridine

moieties. Furthermore, we wish to identity linker properties between polyacridine and melittin (or other bioactive molecules) that will lead to desirable gene transfer properties and distinguish which polyacridine polyplex physical properties lead to increased gene expression in vitro. Additionally, the synthetic strategy to incorporate acridine and obtain polyacridine peptides on large scale with good yields will be examined in depth. These results will be used to identify lead polyacridine anchor peptides on which to base the development of complex in vivo gene transfer systems designed to overcome the physical delivery barriers preventing reliable and robust gene expression in vivo.

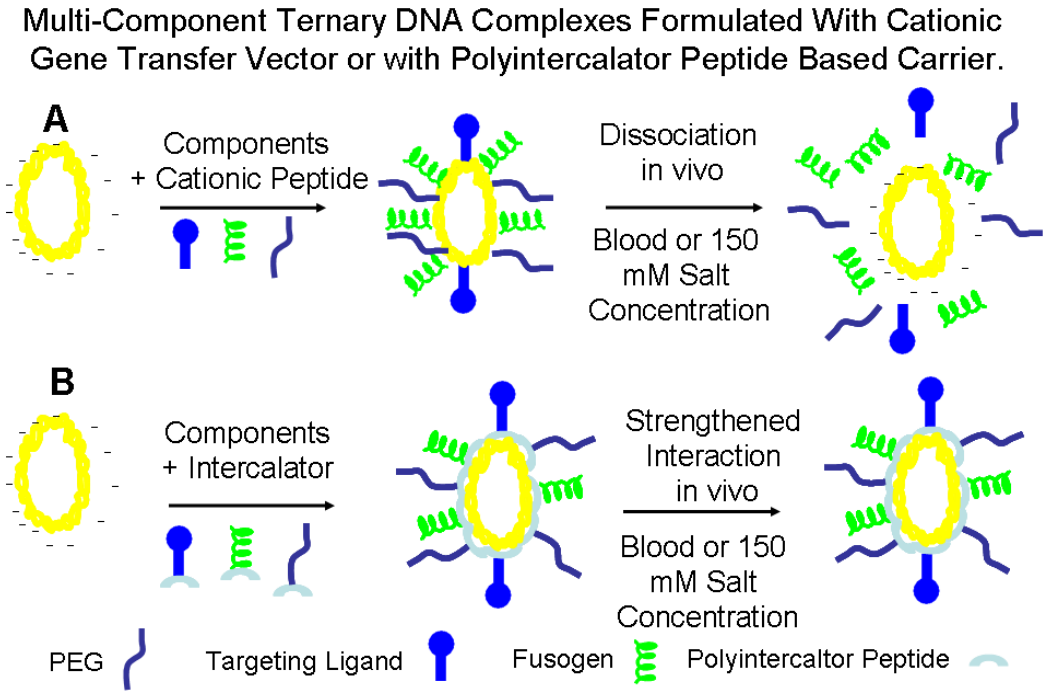


Figure 1-7. *A Comparison of Multi-Component Ternary DNA Complexes Formulated With Cationic Gene Transfer Vector or with Polyintercalator Peptide Based Carrier.* Polyplexes are formed with polycationic peptides or polymers modified with PEG, targeting ligand, and fusogenic peptide to form ternary complexes that dissociate upon exposure to physiological salt concentration or systemic circulation (**A**). Conversely, multi-component ternary complexes are formed with polyintercalator peptides modified with PEG, targeting ligand, and fusogenic peptide in which we hypothesize the combination of intercalative and ionic interactions with nucleic acids will generate a gene transfer vector resistant to dissociation and degradation in vivo (**B**).

# CHAPTER 2
# INITIAL SYNTHESIS AND IN VITRO EVALUATION OF POLYACRIDINE-MELITTIN GENE DELIVERY PEPTIDES


## Abstract

Chapter 2 describes the synthesis of polyacridine peptides following the post solid phase peptide synthesis (SPPS) modification of short DNA binding precursor peptides C(Acm)W$(KR)_2$K-$NH_2$ (peptide **1**) and W$(KR)_2$KC(Acm)-$NH_2$ (peptide **2**) primary amines with the acridine analogue 6-(9-acridinylamino) hexanoic acid to form Acr-CW(K(Acr)R$)_2$K(Acr)-$NH_2$ (peptide **5**) or Acr-W(K(Acr)R$)_2$K(Acr)Cys-$NH_2$ (peptide **6**), respectively. Following Acm deprotection from Cys, the peptides were conjugated to the membrane lytic peptide melittin by a reducible or non-reducible tether to generate polyacridine-melittin. These bioconjugates were employed to conduct proof of principle experiments to investigate the feasibility of a polyacridine peptide as a DNA delivery vector incorporating melittin as an endosomal escape agent. The results demonstrate that a reducibly linked polyacridine-melittin produces gene transfection comparable to PEI in CHO cells and demonstrate the effectiveness of polyacridine peptides as a DNA binding peptide and delivery vector in vitro. The results also warrant further SAR and optimization relating to the structure and sequence of the polyacridine anchor peptide.


## Introduction

An important element of many polyplex non-viral gene delivery systems is a releasable fusogenic peptide that can effect endosomal lysis (*12*). The endosomal escape of DNA is especially essential for receptor-targeted gene delivery systems to avoid polyplex degradation by the lysosome (Figure 1-1) (*46, 73, 125*).

To improve the endosomal escape of DNA, several prior studies have incorporated fusogenic peptides, including GALA, KALA, HA2, JTS-1 and melittin, into a non-viral gene delivery system (*31, 42, 47, 48, 50-52*). Most applications in gene

delivery have utilized melittin because of its relative ease of chemical synthesis and because its mechanism of membrane lysis has been extensively studied (*81-83*). Melittin has been covalently attached to polylysine, PEI, cationic lipids and even self-polymerized by terminal disulfide bonds and demonstrated to increase in vitro gene transfer efficiency (*46-48, 79, 80*).

While DNA anchoring polymers such as PEI, polylysine, dendrimers and chitosan are known to bind ionically to the phosphate backbone of plasmid DNA, this strategy leads to the formation of cationic polyplexes that favor in vitro gene transfer but to a much lesser degree in vivo gene transfer (*124*). This is partly because positively charged polyplexes bind non-specifically to proteins and cells (*44*). Attempts at masking the charge with PEG still results in a residual positive charge as measured by zeta potential (*35, 43*). The non-specific binding of PEGylated cationic polyplexes in vivo complicates strategies that attempt to combine a receptor ligand and releasable fusogenic peptide into a non-viral delivery system (*26, 41*). Consequently, it would be beneficial to reversibly bind fusogenic peptides, receptor ligand and PEG to DNA while simultaneously controlling the charge of polyplexes. Likewise, it would be advantageous if the DNA binding anchor were sufficiently small in size to allow for its chemical manipulation and specific functionalization with PEG, targeting ligand and fusogenic peptide (*26*).

Previous research performed within the group regarding the well characterized fusogen melittin resulted in the transformation of melittin into a polymerizable gene transfer reagent, capable of promoting endosomal escape and increasing gene transfer efficiency in vitro (*42*). Upon adaptation of polymelittin for in vivo gene delivery by co-polymerization with the terminal cysteines of a DNA binding peptide whose central cysteine was functionalized with PEG or N-glycan targeting ligand resulted in undetectable gene transfer without the presence of a stimulatory hydrodynamic dose (HD) (*26*). The failure of the polymerizable melittin system is believed to lie within the transformation of melittin to a gene transfer reagent. Upon addition of several lysine

residues at the N and C terminus of the peptide, the membrane lytic potential dropped dramatically at low pH, which is essential as the environment within the late endosome is proposed to have a pH of 4.5 (*26*). A second hypothesis behind the failure to provide meaningful gene expression in vivo lies within the cationic reliance of polymelittin to interact and condense plasmid DNA and the subsequent dissociation of this ionic interaction when exposed to physiological salt concentrations (*26, 36*). My research attempts to overcome this reliance upon cationic interactions between fusogenic peptide and ultimately the delivery vehicle with plasmid DNA.

My initial efforts involved the synthesis of photolabeling fusogenic peptides melittin (GIGAVLKVLTTGLPALISWIKRKRQQ) and JTS-1 (GLFEALLELLESLWE-LLLEA) by incorporation of an N-terminal photolabel capable of alkylating and covalently labeling the fusogen to DNA base pairs upon exposure to 330 nm light accomplished by photo flash. This methodology of incorporating a fusogen into a gene transfer formulation proved to be ineffective as photolabeling often damaged the transgene region of the plasmid (Unpublished observations by N. Baumhover), resulting in diminished expression and often limited the amount of fusogen that could be incorporated.

To overcome the limitations of ionic interaction and covalent modification of DNA, polyacridine peptides have been shown to reversibly bind with high affinity by intercalating into double stranded DNA (*120*). An early study by Szoka demonstrated the synthesis of a divalent acridine neoglycopeptide for delivery of DNA to cells expressing the asialoglycoprotein receptor (*123*). More recently, polyacridine-nuclear localization sequences (NLS) possessing up to three acridines were shown to improve in vitro gene transfer (*7-11*). However to date, a polyacridine DNA binding peptide has not been substituted with a fusogenic peptide, therefore we initially investigated the modification of melittin or JTS-1 with the classic intercalator dye acridine in an effort to incorporate a fusogen in a reversible fashion, yet provide enough affinity to avoid premature

dissociation of the acridine labeled fusogen from the plasmid. The initial synthesis of a mono-acridine melittin or JTS-1 provided evidence that modification of the N-terminus of the fusogenic peptide resulted in retention of fusogenic activity, but a single acridine was not sufficient to supply enough affinity for DNA (Unpublished observations by N. Baumhover). This work led to the development of a hypothesis in that incorporation of fusogenic peptide reducibly linked to a multi-valent polyacridine DNA anchor would generate a vector capable of producing robust in vitro gene transfer due to the strong, but reversible binding affinity of polyacridine for DNA. Furthermore, these preliminary experiments would provide proof of principle data indicating that polyacridine is a viable alternative to the use of polycationic polymers as gene delivery vehicles. These efforts yielded the generation of multi-valent acridine DNA binding peptides that were conjugated to melittin in a reducible or non-reducible fashion, enabling co-delivery of a fusogenic peptide and plasmid to facilitate efficient endosomal escape and a subsequent increase in gene expression.

## A Note Regarding Peptide Nomenclature in Chapter 2

Due to the chemical complexity of the polyacridine peptides presented in Chapter 2, I have employed a numbering system to identify compounds as an intuitive description designating sequence and structural features is not available. The numbering system is defined in Table 2-1, Scheme 2-1, Scheme 2-2, Scheme 2-3, and defined throughout the text, which is represented by a bold number (i.e. **1**) and may be preceded by the word peptide (i.e. peptide **3**). The numbered nomenclature system is used only in Chapter 2 as the polyacridine peptides presented in Chapters 3, 4, and 5 are adequately named through a system that utilizes an abbreviated and intuitive system to designate sequence and structural features.

## Materials and Methods

Unsubstituted Rink Amide and Wang resin for peptide synthesis, 9-hydroxybenzotriazole, Fmoc-protected amino acids, 1,3-Diisopropylcarbodiimide (DIC), and N-Methyl-2-pyrrolidinone (NMP) were obtained from Advanced ChemTech (Lexington, KY). N,N-Dimethylformamide (DMF), trifluoroacetic acid (TFA), and acetonitrile were purchased from Fisher Scientific (Pittsburgh, PA). Diisopropylethylamine (DIPEA), piperdine, acetic anhydride, Tris (2-carboxyethyl)-phosphine hydrochloride (TCEP), 9-chloroacridine, 6-aminocaproic acid, phenol, maleic anhydride, 2-2'dithiodipyridine (DTDP), and thiazole orange were obtained from Sigma Chemical Co. (St. Louis, MO). Triisopropylsilane (TIS) and polyethylene amine (PEI 25 KDa) were purchased from Aldrich (Milwaukee, WI). D-Luciferin and luciferase from *Photinus pyralis* were obtained from Roche Applied Science (Indianapolis, IN). CHO cells were acquired from the American Type Culture Collection (Manassas, VA). Inactivated qualified fetal bovine serum (FBS) was from Life Technologies, Inc. (Carlsbad, CA). BCA reagent was purchased from Pierce (Rockford, IL). pGL3 control vector, a 5.3 kb luciferase plasmid containing a SV40 promoter and enhancer, was obtained from Promega (Madison, WI). pGL3 was amplified in a DH5α strain of *Escherichia coli* and purified according to manufacturer's instructions.

### Synthesis of 9-phenoxyacridine (In collaboration with Kevin Anderson)

9-phenoxyacridine was synthesized with modification from the methods of Karup et al (*118*). Briefly, 12 g of phenol (127.5 mmol) and 0.72 g of sodium hydroxide (18 mmol) were heated to 100ºC. To the liquified phenol, 2.8 g of 9-chloroacridine (13.105 mmol) was added and stirred vigorously for 1.5 hrs. The reaction was quenched by the addition of 100 ml of 2 M sodium hydroxide then allowed to sit at RT overnight. A yellow precipitate was filtered, washed with water and dried in vacuo (3.4822g, 12.835

mmol, 97.9%, M.P. 123 – 124 º C, TLC, 15 : 5 : 1 : 0.5, ethyl acetate / methanol / hexane / acetic acid, $R_f = 0.18$). $^1H$ NMR (DMSO-$d_6$) δ 8.23 (d, 2H), 8.04 (d, 2H), 7.88 (t, 2H), 7.59 (t, 2H), 7.32 (t, 2H), 7.08 (t, 1H), 6.88 (d 2H).

Synthesis of 6-(9-acridinylamino)hexanoic acid (In collaboration with Kevin Anderson)

6-(9-acridinylamino) hexanoic acid was prepared according to a prior published procedure (*10, 118*). Briefly, 9-Phenoxyacridine (1.5 g, 5.5 mmol) was added to 3 g phenol under an argon atmosphere and stirred while heating to 50ºC. After the solid was in solution, 6-aminocaproic acid (725 mg, 5.5 mmol) was added and the temperature increased to 100ºC for 6 hr. The reaction was cooled to 50ºC, 25 ml of ethyl ether was added with vigorous stirring and the precipitant was collected on filter paper, washed with ethyl ether, ethanol, and water, and dried overnight in vacuo. The reaction produced 1.59 g (5.5 mmol) at 94% yield of 6-(9-Acridinylamino) hexanoic acid, which had a M.P. of 192ºC. (300 MHz $^1H$ NMR, $CF_3CO_2D$): δ=8.39 (d, 2H), 7.99 (dd, 2H), 7.63 (dd, 2H), 7.26 (br, 2H), 4.28 (t, 2H), 2.60 (tri, 2H), 2.13 (qui, 2H), 1.89 (m, 4H).

Synthesis of Maleimide Glycine (Mal-Gly-OH)

Glycine (5 g, 66.6 mmol) and maleic anhydride (6.6 g, 66.6 mmol) were suspended in 80 ml of acetic acid and allowed to react for 3 hrs at RT (*126*). The resulting white precipitate was collected by filtration, washed with cold water, and dried in vacuo (10.95 g, 63.3 mmol, 95 %, M.P. 187-189ºC**,** TLC: 2:1:1:1 isopropyl alcohol / acetic acid / ethyl acetate / water, $R_f = 0.5$). The glycine maleic acid intermediate was characterized by proton NMR (300 MHz, DMSO-d6): δ = 9.2 (s, 1H) 6.397 (d, 1H, j = 8.57 Hz), 6.310 (d, 2H, j = 12.86 Hz), 2.0 (d, 2H j = 6.86 Hz).

Glycine maleamic acid (5.2 g, 30.04 mmol) and 2.1 equivalents of triethylamine (6.37 g, 63 mmol) were refluxed for 3 hrs in 500 ml toluene with removal of water with a Dean-Stark apparatus. Upon reaction completion, the toluene solution was decanted and

dried. The resulting solid was acidified with 2 M HCl, extracted with ethyl acetate, dried with $MgSO_4$ and evaporated to yield Mal-Gly-OH (1.7 g, 11 mmol, 36.5%, M.P. 99-110ºC**,** TLC: 2:1:1:1 isopropyl alcohol / acetic acid / ethyl acetate / water, $R_f = 0.72$). The product was characterized by proton NMR (300 MHz, DMSO-d6): $\delta = 7.108$ (s, 2H), 4.105 (s, 2H) (*126*).

## Synthesis and Characterization of DNA Binding Precursor Peptides Cys(Acm)-Trp-(Lys-Arg)$_2$-Lys-$NH_2$, W(Lys-Arg)$_2$-Lys-Cys(Acm)-$NH_2$ and Melittin Analogue*s*

Melittin analogues were prepared by solid phase peptide synthesis using standard Fmoc procedures with 9-hydroxybenzotriazole and DIC double couplings on a 30 µmol scale on an Advanced ChemTech APEX 396 synthesizer using an Fmoc-Gln(Trt)-Wang resin. Cys(Acm) protected DNA binding precursor peptides were prepared on either a Fmoc-Cys(Acm)-Rink amide for W(KR)$_2$-Lys-Cys(Acm)-$NH_2$ or Fmoc-Lys(Boc)-Rink amide resin for Cys(Acm)-W(KR)$_2$-Lys-$NH_2$ using 9-hydroxybenzotriazole and DIC double couplings on a 30 µmol scale. Mal-melittin was prepared by coupling Mal-Gly-OH to the N-terminus of side-chain protected full-length melittin on resin utilizing a 6-fold excess of Mal-Gly-OH, DIC and HOBt, and reacted for 4 hrs while stirring. The resin was filtered, washed with DMF, DCM and methanol, and then dried. Peptides were removed from resin and side chain deprotected using a cleavage cocktail of TFA/triisoproylsilane/water (95:2.5:2.5 v/v/v) for 3 hrs followed by precipitation in cold ethyl ether. Precipitates were centrifuged for 10 min at 4000 rpm at 4ºC and the supernatant decanted. Peptides were then reconstituted with 0.1 v/v % TFA and purified to homogeneity on RP-HPLC by injecting 0.5-2 µmol onto a Vydac C18 semipreparative column (2 x 25 cm, 218TP1022) eluted at 10 ml/min with 0.1 v/v % TFA with an acetonitrile gradient of 20-45 v/v % for melittin or 15-25 v/v % for DNA binding peptide precursors over 30 min while monitoring tryptophan (Abs 280 nm). The major peak was

collected and pooled from multiple runs, concentrated by rotary evaporation, lyophilized, and stored at -20ºC. Purified peptides were reconstituted in 0.1 v/v % TFA and quantified by absorbance (tryptophan $\varepsilon_{280\ nm} = 5600\ M^{-1}\ cm^{-1}$, thiolpyridine and tryptophan $\varepsilon_{280\ nm} = 10915\ M^{-1}\ cm^{-1}$, or acridine $\varepsilon_{409\ nm} = 9266\ M^{-1}\ cm^{-1}$) to determine isolated yield. Purified peptides were characterized on an Agilent 1100 Series LC-ESI-MS by injecting 2 nmol onto a Vydac C18 analytical column (0.47 x 25 cm, 218TP54) eluted at 0.7 ml/min with 0.1 v/v % TFA and an acetonitrile gradient of 10-55 v/v % over 30 min while acquiring ESI-MS in the positive ion mode.

## Post-Synthetic Modification of DNA Binding Precursor's Primary Amines with 6-(9-acridinylamino) hexanoic acid

20 µmol of C(Acm)W$(KR)_2$K-$NH_2$ (peptide **1**) or W$(KR)_2$KC(Acm)-$NH_2$ (peptide **2**) were freeze dried prior to functionalization with 6-(9-acridinylamino) hexanoic acid and reconstituted in 2 ml DMF. Six equivalents (148.02 mg, 480 µmol) of 6-(9-acridinylamino) hexanoic acid per amine were activated with 30 equivalents of DIC (302.88 mg, 2.4 mmol) and 30 equivalents HOBt (367.56 mg, 2.4 mmol) in 6 ml NMP were added to the DMF solvated peptide, resulting in a solution of 80/20 v/v % NMP/DMF. DIPEA (100 µl) was added at a 1 v/v % as a proton scavenger. The reaction was allowed to proceed for 8 hrs while stirring vigorously at RT to yield Acr-C(Acm)W$(K(Acr)R)_2$K(Acr)-$NH_2$ (peptide **3**) or Acr-W$(K(Acr)R)_2$K(Acr)Cys(Acm)-$NH_2$ (peptide **4**) (Scheme 2-1). Upon reaction completion, the reaction mixture was precipitated in 40 ml aliquots of cold ethyl ether to remove the organic solvent and 6-(9-acridinylamino) hexanoic acid and reconstituted in 10 ml methanol. After reconstitution in methanol, the acridine functionalized peptide was loaded onto a G-10 gel filtration column (2.5 x 50 cm) to remove excess 6-(9-acridinylamino) hexanoic acid and coupling reagents and eluted with 0.1 v/v % TFA while monitoring at 280 nm with an ISCO UA-5 absorbance detector and collected on an ISCO Retriever II fraction collector. The

acridine functionalized peptide eluted in the void volume and the fractions corresponding to the peptide peak were collected, pooled, concentrated and lyophilized. Gel-filtration purified acridine peptides were characterized by LC-MS by injecting 2 nmol onto a Vydac C18 analytical column (0.47 x 25 cm) eluted at 0.7 ml/min with 0.1 v/v % TFA and an acetonitrile gradient of 10-55 v/v % over 30 min while acquiring ESI-MS in the positive ion mode.

Removal of the Acm protecting group on cysteine was accomplished as previously described (*26, 40*). Briefly, 20 μmol of peptide (peptide **3** or **4**) were reconstituted in 10 ml methanol and 15 ml cold TFA and removal of Acm to generate the free thiol was afforded by addition of 400 μmol or 20 equivalents each per thiol of silver tetrafluoroborate ($AgBF_4$) and anisole in 1 ml TFA, followed by reaction at 4ºC for 1.5 hrs. The Acm deprotected acridine peptides Acr-CW(K(Acr)R)$_2$K(Acr)-$NH_2$ (peptide **5**) or Acr-W(K(Acr)R)$_2$K(Acr)Cys-$NH_2$ (peptide **6**) were precipitated as the silver salt in 60 v/v % cold diethyl ether and centrifuged at 4000 rpm for 10 min at 4ºC and the supernatant decanted. The precipitate was redissolved in 5 ml of 0.2 M acetic acid containing 40 equivalents of DTT per Acm group and reacted by mixing for 4 hrs (Scheme 2-1). Following removal of insoluble material by centrifugation, the peptide was desalted by loading onto a G-10 gel filtration column as previously described, and analyzed by LC-ESI-MS to ensure complete removal of the Acm protecting group from cysteine. Polyacridine peptides were then purified by RP-HPLC as described previously.

Cys-melittin was reacted with 10-eq of DTDP in 2-propanol/2 N acetic Acid (10:3) for 8 hrs at RT to generate the thiolpyridine protected peptide (*127*). The reaction mixture was concentrated by rotary evaporation and applied to a Sephadex G-10 column eluted (2.5 x 50 cm) with 0.1 v/v % TFA while monitoring absorbance at 280 nm to remove excess DTDP. The peptide peak fractions were pooled, concentrated, lyophilized, and purified to homogeneity by RP-HPLC as described previously.

Reducible polyacridine-melittin (peptide **7**) and non-reducible polyacridine-melittin (peptide **8**) were synthesized on a 1 μmol scale based on melittin, using 1.25 equivalents (1.25 μmol) of the reduced polyacridine peptide **5** or **6**. Mal-melittin (1 μmol) was prepared in 4 ml of 10 mM ammonium acetate pH 5 and added to peptide **5** and 1 ml of methanol to facilitate solubility (Scheme 2-2). The reaction occurred over 24 hrs at RT as determined by analyzing aliquots by LC-MS. At reaction completion, the mixture was concentrated by rotary evaporation and lyophilized prior to purification of peptide **8** by RP-HPLC eluted with 0.1 v/v % TFA and acetonitrile gradient (35-45% over 30 min) while detecting at 409 nm. Following quantification by absorbance (acridine $\varepsilon_{409\ nm}$ = 9266 $M^{-1}$ $cm^{-1}$) to determine isolated yield, peptide **8** was characterized by LC-MS by injecting 2 nmol and eluting with 0.1 v/v % TFA and an acetonitrile gradient of 20-45 v/v % over 30 min while acquiring ESI-MS in the positive ion mode.

Alternatively, thiolpyridine-Cys-melittin (1 μmol) was prepared in 6 ml of 5 mM Hepes buffer pH 7.5 and added to 1.6 μmol of peptide **6** in 4 ml of methanol (Scheme 2-3). After 48 hrs, peptide **7** was purified and characterized by LC-MS as described above.

## Polyacridine-Melittin Hemolysis Assay

Whole blood was obtained from male ICR mice by heart puncture with heparinized 22G needles and collected in conical tubes containing 10 ml of 0.15 M PBS (pH 7.4) prewarmed to 37ºC. Erythrocytes were immediately separated from plasma by centrifugation at 2000 rpm for 2 min, washed three times with 10 ml of PBS, and then diluted to 1.5 x $10^8$ cells/ml. Peptides were prepared at 15 μM and serially diluted to 10-0.01 μM, after which 100 μl was pipetted in triplicate into a Millipore MultiScreenHTS BV 96 well plate. Erythrocytes (50 μl, 7.5 x $10^6$ cells) were added to the peptides and incubated at 37ºC for 1 h followed by filtration on a Multiscreen vacuum manifold (Millipore Corporation, Billerica, MA). The filtrate was measured for $Abs_{410nm}$ on a BioTEK plate reader (BioTEK Instruments Incorporated., Winooski, VT) and compared

to the 100% (100% lysis control, $Abs_{410\ nm}$: 1.7 absorbance units (au)) hemolysis caused by replacing PBS (background, $Abs_{410\ nm}$: 0.34 au) with water.

## Formulation and Characterization of Polyacridine-Melittin Polyplexes

The relative binding affinity of peptides for DNA was determined by a fluorophore exclusion assay (*22*). pGL3 (200 µl of 4 µg/ml in 5 mM Hepes pH 7.5 containing 0.1 µM thiazole orange) was combined with 0, 0.05, 0.1, 0.25, 0.35, 0.5, 1, and 2 nmol of peptide in 300 µl of Hepes and allowed to bind at RT for 30 min. Thiazole orange fluorescence was measured using an LS50B fluorometer (Perkin-Elmer, U.K.) by exciting at 498 nm while monitoring emission at 546 nm with the slit widths set at 10 nm. A fluorescence blank of thiazole orange in the absence of DNA was subtracted from all values before data analysis. The data is presented as nmol of peptide per µg of DNA versus the percent fluorescence intensity ± the standard deviation determined by three independent measurements.

## In Vitro Gene Transfer of Polyacridine-melittin DNA Polyplexes

CHO cells ($5 \times 10^5$) were plated on 6 x 35 mm wells and grown to approximately 50% confluency. Transfections were performed in MEM supplemented with 2% FBS, sodium pyruvate (1 mM), and penicillin and streptomycin (100 U and 100 µg/ml). Polyplexes were prepared at a DNA concentration of 30 µg/ml and a stoichiometry of 0.5 nmol peptide per µg of DNA in Hepes buffered mannitol (HBM). Polyplexes (10 µg of DNA in 0.3 ml of HBM) were added drop wise to wells in triplicate and incubated 24 hrs. After 24 hrs, the cells were washed twice with 2 ml of ice-cold phosphate-buffered saline ($Ca^{2+}$ - and $Mg^{2+}$ - free) and then treated with 0.5 ml of lysis buffer (25 mM Tris Chloride, pH 7.8, 1 mM EDTA, 8 mM magnesium chloride, and 1% Triton X-100) for 10 min at 4ºC. Cell lysates were scraped, transferred to 1.5 ml microcentrifuge tubes, and

centrifuged for 10 min at 13,000 g at 4ºC to pellet cell debris. Lysis buffer (300 µl), sodium-ATP (4.3 µl of a 165 mM solution at pH 7, 4ºC) were combined in a test tube, mixed briefly, and immediately placed in the luminometer. Luciferase relative light units were measured by a Lumat LB 9501 (Berthold Systems, Germany) with 10 s integration after automatic injection of 100 µl of 0.5 mM D-luciferin. The relative light units were converted to fmol using a standard curve generated by adding a known amount of luciferase to 35 mm wells containing 50% confluent CHO cells. The resulting standard curve had an average slope of $2.6 \times 10^4$ relative light units/fmol enzyme. Protein concentrations were measured by a BCA assay using bovine serum albumin as a standard (*128*). The amount of luciferase recovered in each sample was normalized to mg of protein and reported as the mean and standard deviation obtained from triplicate transfections. PEI pGL3 polyplexes were prepared by mixing 35 µg of DNA in 525 µl of HBM with 43.8 µg PEI in 525 µl of HBM while vortexing to create DNA complexes possessing a charge ratio ($NH_4^+/PO_4^-$) of 9:1. Cells were transfected with 10 µg PEI-DNA polyplexes as previously described.

## Results

### Synthetic Strategy for Polyacridine-Melittin Peptides.

Naturally occurring melittin isolated from bee venom is a 26 amino acid peptide amide composed of two α-helices conjoined through an interrupting proline (*81-83*). Numerous studies have been conducted to investigate the mechanism and sequence specificity of melittin's membrane lytic activity.

Natural melittin contains a single aromatic Trp at residue 8 and does not contain a Cys residue. To improve the synthesis of polyacridine-melittin, we replaced Trp 8 with Leu, and reinstalled a single Trp near the N-terminus in Cys-Trp-Lys-Lys. The reactivity of the Cys residue was increased by flanking Lys residues. This also allowed selective chromatographic detection of full length melittin at 280 nm. These modifications resulted

Table 2-1. *Sequences of Peptide and Peptide Conjugates*

| **Polyacridine Peptides (Acr)= N-terminal acridine or Lys-ε-amine acridine** | | Mass[a](calc/obs) |
|---|---|---|
| **Peptide** | | |
| **1** | C(Acm)WKRKRK-$NH_2$ | 1074.4 / 1074.3 |
| **2** | WKRKRKC(Acm)-$NH_2$ | 1074.4 / 1074.4 |
| **3** | Acr-C(Acm)W(K(Acr)R)$_2$K(Acr)-$NH_2$ | 2235.8 / 2235.8 |
| **4** | Acr-W(K(Acr)R)$_2$K(Acr)C(Acm)-$NH_2$ | 2235.8 / 2236.2 |
| **5** | Acr-CW(K(Acr)R)$_2$K(Acr)-$NH_2$ | 2164.7 / 2164.6 |
| **6** | Acr-W(K(Acr)R)$_2$K(Acr)C-$NH_2$ | 2164.7 / 2165.0 |
| **Melittin Analogues (thiolpyr= thiol pyridine, Mal =maleimide)** | | |
| Melittin | GIGAVLKVLTTGLPALISWIKRKRQQ | 2847.5 / 2847.4 |
| Cys-melittin | CWKKGIGAVLKVLTTGLPALISLIKRKRQQ | 3320.1 / 3320.4 |
| Thiolpyr-melittin | C(tp)WKKGIGAVLKVLTTGLPALISLIKRKRQQ | 3429.2 / 3428.4 |
| Mal-melittin | (m)GWKKGIGAVLKVLTTGLPALISLIKRKRQQ | 3354.0 / 3454.0 |
| **Polyacridine-Melittin (SS = reducible, Mal=non-reducible)** | | |
| **7** | Acr-W(K(Acr)-R)$_2$K(Acr)C-CWKKGIGAVLKVLTTGLPALISLIKRKRQQ | 5482.8 / 5482.4 |
| **8** | Acr-CW(K(Acr)R)$_2$K(Acr)(m)GWKKGIGAVLKVLTTGLPALISLIKRKRQQ | 5518.8 / 5518.8 |

[a] Calculated and observed mass as determined by ESI LC-MS

in a Cys-melittin analogue: CWKKGIGAVLKVLTTGLPALISLIKRKRQQ, that SOPMA analysis (*129*) predicted to maintain α-helical character. A similar Mal-melittin analogue (Mal-GWKKGIGAVLKVLTTGLPALISLIKRKRQQ), possessing an N-terminal maleimide-glycine (Mal-G) in place of Cys, was also prepared (Table 2-1).

Polyacridine DNA binding peptides were synthesized following the post-synthetic modification of short DNA binding peptide precursors possessing either an N or C-terminal protected cysteine to prevent unwanted cysteine acylation products, resulting in the following sequences; C(Acm)WKRKRK-$NH_2$ (peptide **1**) or WKRKRKC(Acm)-$NH_2$ (peptide **2**), respectively. The peptides were also synthesized on peptide amide forming resin to eliminate peptide polymerization or cyclization by-products via amide formation between the N and C-terminus of the peptides during acridine functionalization. To increase water solubility and binding affinity for DNA, peptides were designed with an arginine residue separating the acridine functionalized lysine residues. Inclusion of

arginine allowed the incorporation of a cationic residue without the need to incorporate an additional orthogonal protecting scheme due to the guanidine's un-reactivity during peptide bond formation between primary amines and 6-(9-acridinylamino) hexanoic acid.

The peptide precursors **1** and **2** were prepared and purified at 45 and 59% yields after preparatory RP-HPLC, respectively. Both Acr-C(Acm)W(K(Acr)R)$_2$K(Acr)-NH$_2$ (peptide **3**) or Acr-W(K(Acr)R)$_2$K(Acr)C(Acm)-NH$_2$ (peptide **4**) were synthesized following the post-synthetic modifications of the N-terminus and ε-amines of lysine by using six equivalents per amine of 6-(9-acridinylamino) hexanoic acid activated with an excess of DIC/HOBt (30 equivalents per amine) with 1 v/v % DIPEA to serve as a proton scavenger (Scheme2-1). It is interesting to note that usage of 6-(9-acridinylamino) hexanoic acid, HOBt, and DIC at a six fold equivalency failed to functionalize all primary amines, perhaps due to sluggish activation of 6-(9-acridinylamino) hexanoic acid with DIC/HOBt. Optimization of the reaction protocol included the modification of the coupling conditions to include 30 equivalents of DIC/HOBt while coupling 6 equivalents of acridine per amine, resulting in complete amine functionalization with a reaction time of 8 hrs (Figure 2-1A), with ESI-MS demonstrating a doubly charged positive ion consistent with the calculated mass of peptide 4 (Figure 2-1A, inset).

Following reaction completion, the crude reaction mixture was precipitated in cold diethyl ether and reconstituted. The remaining 6-(9-acridinylamino) hexanoic acid and coupling reagents were separated from the cysteine protected polyacridine peptide by G-10 gel filtration (Figure 2-1B), resulting in an 89 to 96.1% recovery of peptide **3** and **4**, respectively. LC-MS analysis revealed complete removal of acridine and coupling reagents (Figure 2-1C), with ESI-MS producing a doubly charged positive ion corresponding to the calculated mass of the desired peptide product (Figure 2-1C, inset). Final deprotection of Acm protected cysteine was afforded by treatment with $AgBF_4$ and anisole for 1.5 hrs (Scheme 2-1). Following a precipitation step in diethyl ether and

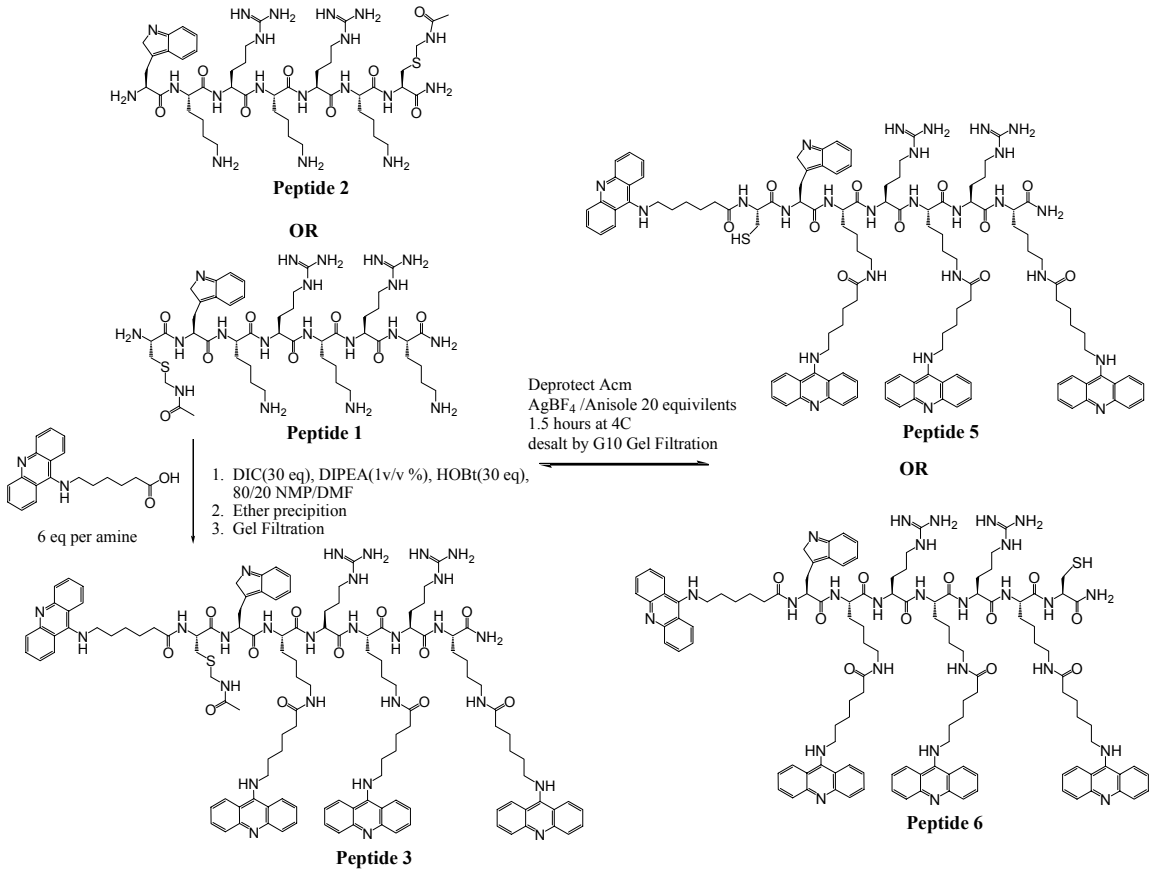


Scheme 2-1. S*ynthetic Scheme of Polyacridine Peptide Preparation.* 20 µmol of polyacridine precursor peptides C(Acm)W$(KR)_2$K-$HN_2$ (**1**) or W$(KR)_2$KC(Acm)-$NH_2$ (**2**) are reacted with 6 equivalents per amine of 6-(9-acridinylamino) hexanoic acid with 30 equivalents each of DIC/HOBt (relative to available amine) and 1 v/v % DIPEA for 8 hrs to yield **3** and **4** (Not shown). After determining reaction completion, the reaction mixture is precipitated in diethyl-ether to partially remove excess reactants and organic solvent. The peptide is reconstituted in methanol and subjected to Sephadex G-10 gel filtration chromatography to remove remaining 6-(9-acridinylamino) hexanoic acid and coupling reagents. The Acm group is removed by reaction with 20 equivalents of $AgBF_4$/anisole for 1.5 hrs, ether precipitated and centrifuged to obtain the peptide-silver salt. To reveal **5** or **6** as the free thiol peptide, 40 equivalents of DTT are added and mixed for 4 hrs, followed by desalting on a G-10 gel filtration column. Peptides are then purified to homogeneity by preparatory RP-HPLC.

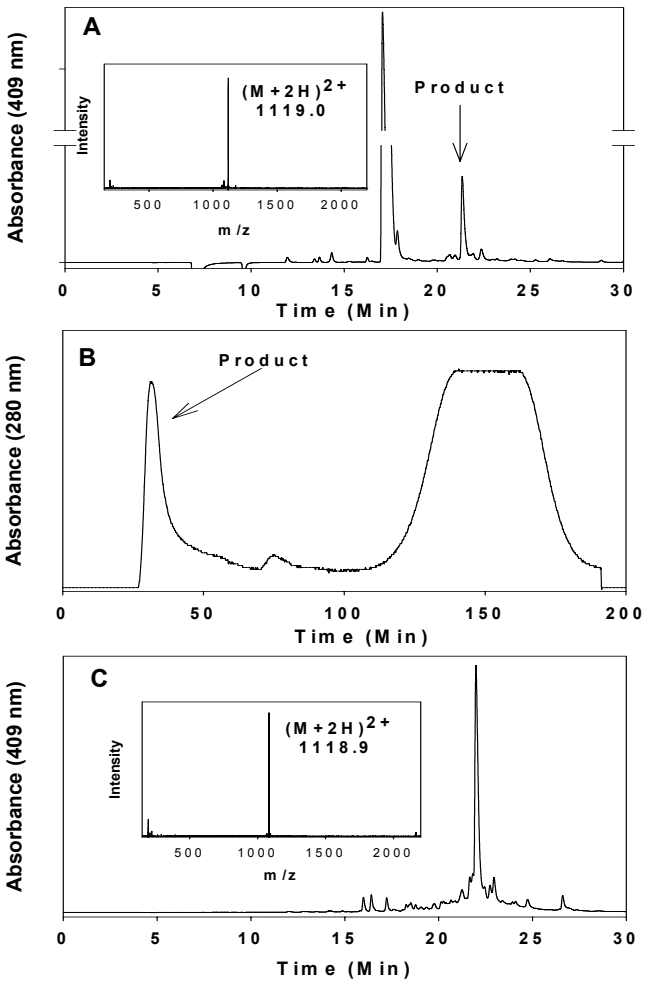


Figure 2-1. *Reaction Monitoring and Purification of the Acm Protected DNA Binding Peptide **4***. The reaction monitoring of $W(KR)_2KC(Acm)$ with 6-(9-acridinylamino) hexanoic acid to synthesize peptide **4** is determined to be complete at 6 hrs after injection of 2 nmol of crude peptide eluting with a 0.1 v/v % TFA with an acetonitrile gradient of 10-55 v/v % over 30 min while monitoring absorbance at 409 nm (Panel A). LC-MS analysis confirms functionalization of primary amines by producing a doubly charged ion of 1118.9 (Panel A, inset), corresponding to a mass of 2235.8 amu. Removal of excess 6-(9-acridinylamino) hexanoic acid and coupling reagents is accomplished with purification by G-10 gel filtration chromatography where peptide **4** elutes in the void volume and elution of excess 6-(9-acridinylamino) hexanoic acid follows much later as a broad peak (Panel B). Rechromatograph of the G-10 purified peptide reveals complete removal of excess acridine (Panel C) and ESI-MS analysis produces a doubly charged positive ion as previously described (Panel C, inset).

treatment with 40 equivalents of DTT in 0.2 M acetic acid to dissociate the peptide silver salt, the polyacridine peptides were desalted and purified by G-10 gel filtration chromatography (Figure 2-2A) and recovered at 34.3 to 54.7% for either Acr-CW(K(Acr)R)$_2$K(Acr)-NH$_2$ (peptide **5**) and Acr-W(K(Acr)R)$_2$K(Acr)C-NH$_2$ (peptide **6**), respectively. LC-MS analysis of G-10 purified peptides after Acm removal from peptide **6** produced an ion consistent with the Acm deprotected peptide (Figure 2-2A, inset). Complete removal of Acm was confirmed by LC-MS analysis for both polyacridine peptides. Both peptides were purified to homogeneity by preparatory RP-HPLC (Figure2-2C), recovered in 14.5% (peptide **5**) and 8% (peptide **6**). Final LC-MS analysis of peptide **6** revealed a single peak upon rechromatograph, producing a doubly charged positive ion of 1083.3 *m/z*, corresponding to an observed mass of 2164.6 amu, demonstrating a 71.2 amu decrease in mass due to loss of the Acm protecting group (Figure 2-2C, inset).

The synthesis of non-reducible polyacridine-melittin (peptide **8**) was designed to incorporate a non-reducible maleimide linkage preventing separation of the polyacridine DNA binding peptide from melittin (Table 2-1 and Scheme 2-2). The synthetic strategy of producing a non-reducible polyacridine-melittin utilized a maleimide modified glycine that was coupled to the N-terminus of a fully protected melittin peptide on resin. Upon workup and purification, Mal-melittin (1 μmol) was reacted with 1.25 μmol of peptide 5 for 24 hrs (Scheme 2-2 and Table 2-1) and purified by preparatory RP-HPLC. Peptide **8** was obtained in 48% yield and analytical RP-HPLC of the purified product resulted in a major peak (Figure 2-3A) and ESI-MS established structure by producing quadruply (1380.7 m/z) and triply (1840.7 m/z) charged positive ions corresponding with the calculated mass (Figure 2-3A, inset).

Reducible polyacridine-melittin (peptide **7**) incorporated a reducible disulfide linkage (Table 2-1 and Scheme 2-3) to allow dissociation of polyacridine peptide from melittin moiety upon exposure to reducing environments. To direct the formation of disulfide bonding between Cys-melittin and peptide **6**, the cysteine of melittin was

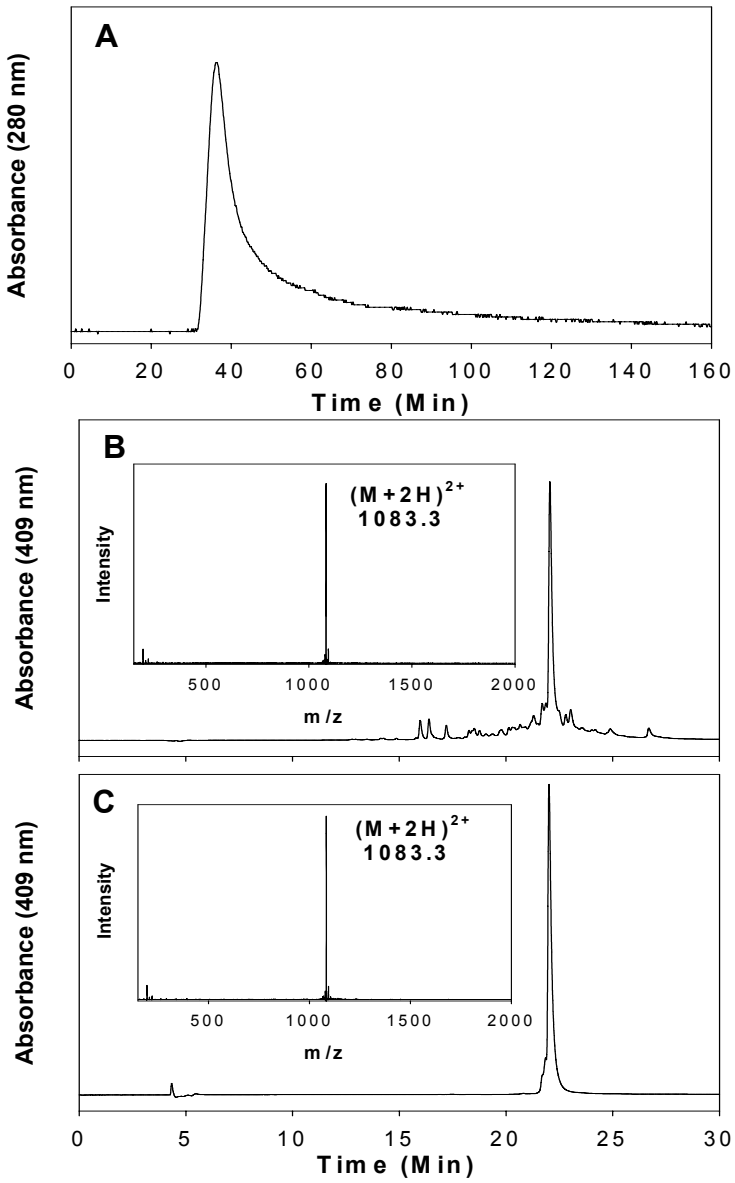


Figure 2-2. *Acm Removal and Purification of Peptide **6***. Desalting and purification is conducted by G-10 gel filtration chromatograph of peptide **6** after Acm deprotection (Panel A). 5 nmol of G-10 purified peptide is injected on RP-HPLC eluted with a 0.1 v/v % TFA over an acetonitrile gradient of 10-55 v/v % over 30 min while monitoring absorbance at 409 nm (Panel B). LC-MS analysis confirms complete Acm deprotection of the cysteine residue by producing a doubly charged ion of 1083.3 *m/z* (Panel B, inset), corresponding to a mass of 2164.6 amu, resulting in a loss of 71.2 amu, accounting for the loss of Acm from cysteine. Final purification of peptide **6** reveals a single peak upon rechromatograph following preparative RP-HPLC (Panel C) and ESI-MS analysis produces the doubly charged positive ion as previously described (Panel C, inset).

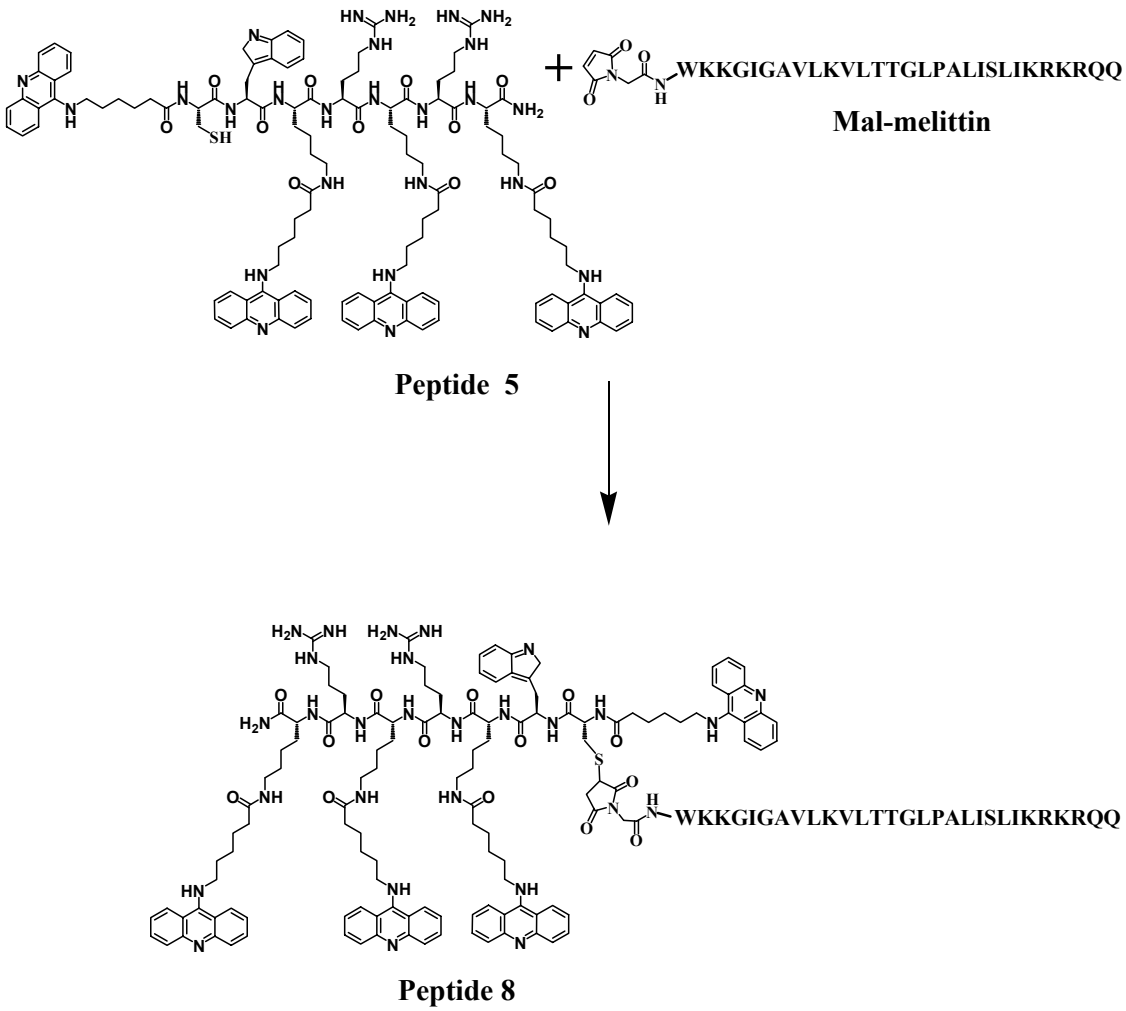


Scheme 2-2. *Synthesis of Non-Reducible Polyacridine-Melittin (Peptide **8**)*. Maleimide-melittin (1 μmol) is reacted for 24 hrs with 1.25 μmol of polyacridine peptide (**5)** at pH 6 to yield the non-reducible polyacridine-melittin (**8**) gene transfer peptide.

reacted with DTDP to generate the thiolpyridine protected Cys-melittin peptide (Table 2-1). Following preparative RP-HPLC of TP-Cys-melittin, synthesis of peptide **7** was afforded by reacting 1.7 μmol of peptide **6** with 1 μmol TP-Cys-melittin for 48 hrs due to the apparent slow reaction kinetics. Peptide **7** was obtained in 37% yield following preparatory RP-HPLC purification, analytical RP-HPLC analysis revealed a major peak (Figure 2-3B), producing an ESI-MS spectrum with quadruply (1371.6 *m/z*) and triply

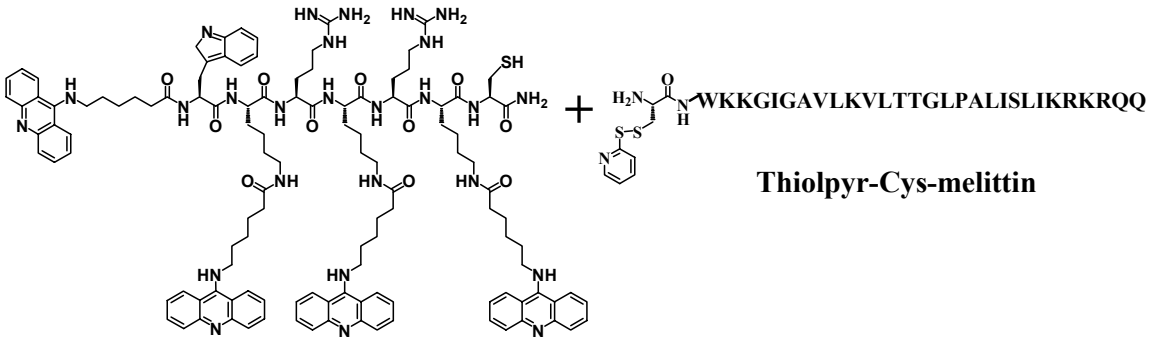


**Peptide 6**

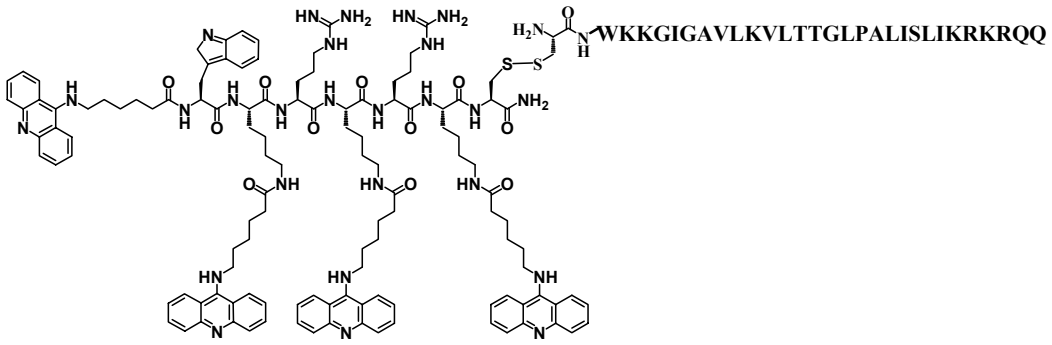


**Peptide 7**

Scheme 2-3. *Synthesis of Reducible Polyacridine-Melittin (Peptide 7).* Thiolpyridine-melittin (1 μmol) is reacted with 1.6 μmol of the polyacridine peptide (**6**) at pH 7.5 for 48 hrs to yield the reducible polyacridine-melittin (**7**) gene transfer peptide.

(1828.4 *m/z*) charged positive ions corresponding to the desired mass (Figure 2-3B, inset). It is interesting to note that reactions attempted with the N-terminal cysteine containing peptide **5** resulted in no formation of the disulfide linked polyacridine-melittin peptide, perhaps due to steric hindrance generated between the two acridine moieties flanking the cysteine residue, where the C-terminal placement of cysteine was amendable to directed disulfide formation.

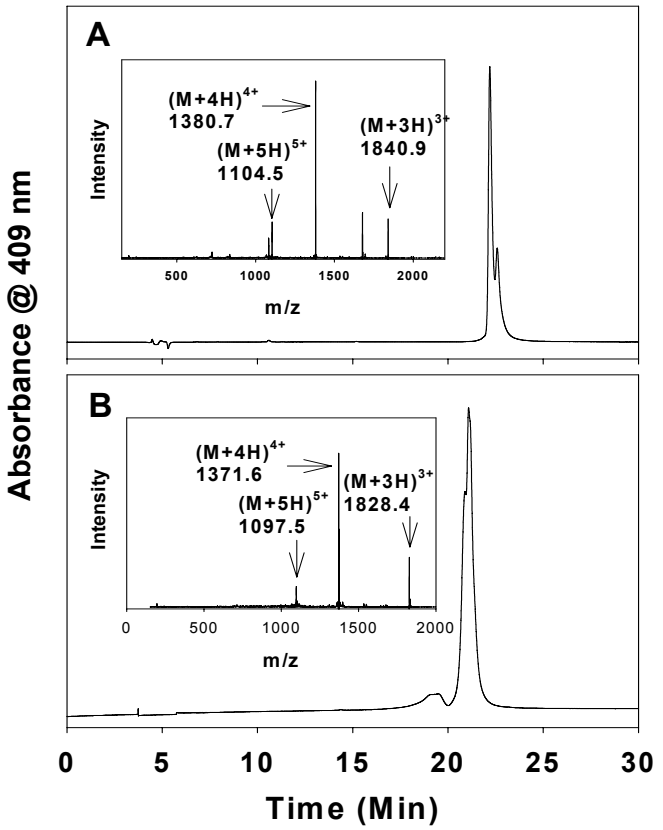


Figure 2-3. *RP-HPLC Analysis of Purified Non-Reducible Polyacridine-Melittin (**8**) and Reducible Polyacridine-Melittin (7).* Rechromatograph of preparatory RP-HPLC purified peptide **8** after a 2 nmol injection eluted with 0.1 v/v % TFA and acetonitrile gradient of 20-45 v/v % over 30 min while monitoring absorbance at 409 nm (Panel A) with ESI-MS analysis of non-reducible polyacridine-melittin (**8**) produced ions at 1104.5, 1380.7, and 1840.9 *m/z*, respectively, corresponding to a mass of 5518.8 amu (Panel A, inset). Panel B demonstrates the RP-HPLC-ESI-MS analysis of reducible polyacridine-melittin (**7**) as described above produces ions of 1097.5, 1371.6, and 1828.4 m/z, all corresponding to a mass of 5482.4 amu (Panel B, inset).

## DNA Binding Properties of Polyacridine-Melittin Peptides

The binding of polyacridine and polyacridine-melittin peptides to pGL3 was investigated using a thiazole orange exclusion assay (*22*). Peptide **5**, **7**, and **8** were found to compete for intercalation and displace thiazole orange, resulting in a decrease in fluorescence intensity. Upon titrating with higher concentrations of peptide, the

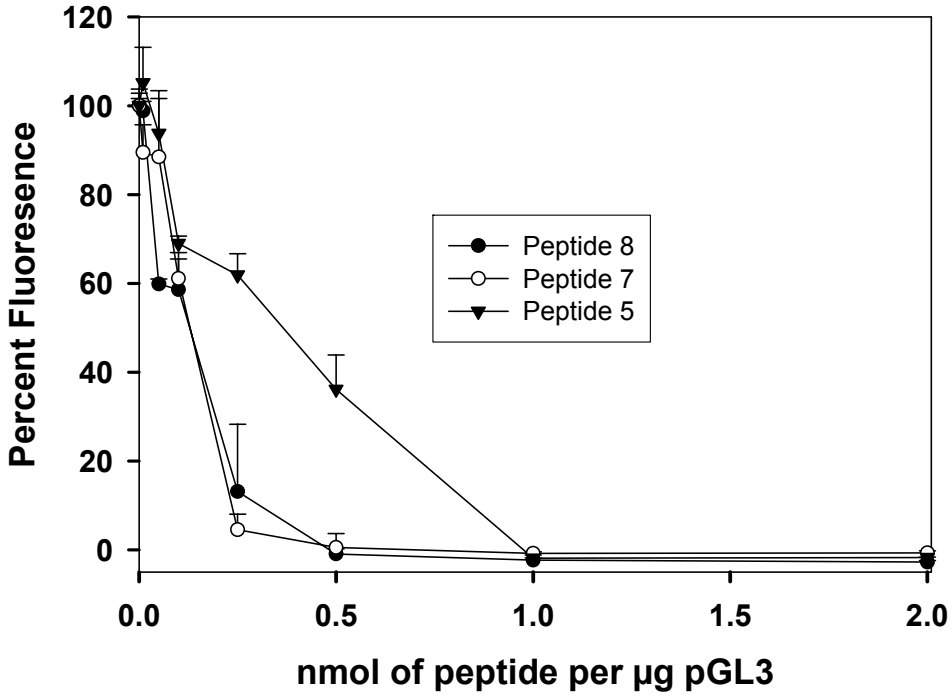


Figure 2-4. *Relative Binding Affinity of Polyacridine-melittin Peptides to DNA*. The concentration dependent displacement of thiazole orange from DNA by polyacridine peptides was used to establish the relative binding affinity. Peptide **5** bound weakly to DNA, resulting in an asymptote in the fluorescence intensity at approximately 1 nmol of peptide per µg of DNA, compared to 0.5 for both peptides **7** and peptide **8**, demonstrating the importance of cationic melittin in regards to DNA affinity of the bioconjugate. The nearly equivalent binding affinities of the reducible and non-reducible polyacridine melittin peptides indicates binding affinity is not affected by nature of linkage between melittin and polyacridine peptide. Results represent the mean (n=3) with the standard deviation.

fluorescence intensity decreased until an asymptote was reached, resulting in an equivalency point (Figure 2-4). Analysis of DNA binding affinity of peptide **5** established an equivalence point of 1 nmol peptide per µg DNA. Comparison of peptide **7** and **8** resulted in a 2-fold increase in binding affinity relative to peptide **5**, with an equivalence point of 0.5 nmol peptide per µg DNA. Additionally, the results demonstrate nearly identical binding properties for peptide **7** and **8** independent of linkage (Figure 2-4).

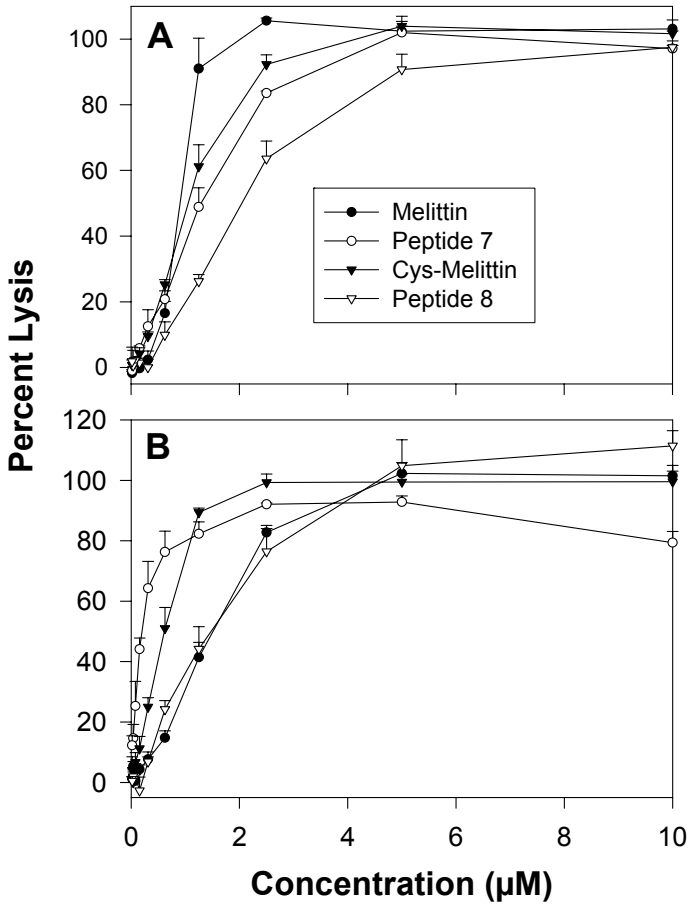


Figure 2-5. *Membrane Lytic Potential of Polyacridine-melittin Peptides.* The hemolytic activity of melittin and polyacridine-melittin peptides were compared at pH 7.4 and 5 using a RBC hemolysis assay. The results establish Cys-melittin is equally potent as natural melittin at pH 7.4 (Panel A), but more potent at pH 5 (Panel B). In comparison, peptide **7** retains nearly full hemolytic potency at pH 7.4 (Panel A) and demonstrates a subtle increase in potency at pH 5. Peptide **8** is less hemolytic overall in comparison to peptide **7** and Cys-melittin, but retains hemolytic potency at lower pH and is comparable to the hemolytic activity of melittin at pH 5.0. Results represent the mean (n=3) with the standard deviation.

## Biological Activity of Polyacridine-Melittin DNA Polyplexes

The membrane lytic potency of polyacridine-melittin peptides were investigated using a RBC hemolysis assay (*42*). Modification of the N-terminus of natural melittin

with Cys-Trp-Lys-Lys and substitution of Leu for Trp 8 to generate Cys-melittin resulted in retention of RBC hemolytic ($HL_{50}$) potency at pH 7.4 relative to natural melittin (Figure 2-5A). Likewise, the hemolytic potency of peptide **7** was comparable to Cys-melittin, indicating the attachment of the polyacridine anchor had a negligible influence on the membrane lytic activity of Cys-melittin. Varying the linkage from a disulfide bond to maleimide thiol-ether resulted in a subtle decrease in hemolytic activity for peptide **8** as compared to Cys-melittin and peptide **7** (Figure 2-5A). As anticipated, polyacridine anchor peptides alone were inactive in membrane lysis ($HL_{50} \geq 10$).

The hemolytic potency of polyacridine melittin peptides was also determined at pH 5 to simulate the pH of the endosome. In contrast to an earlier finding that C and N-terminal modification of natural melittin with Cys-$(Lys)_4$ resulted in the complete loss of hemolytic activity at pH 5 (*42*), Cys-melittin possessed an improved pH 5 RBC lytic potency relative to that of natural melittin (Figure 2-5B). Interestingly, the hemolytic activity of peptide **7** increases at pH 5 as compared to pH 7.4 activity, where the activity of peptide **8** remains constant (Figure 2-5B).

To establish a relationship between reducible or non-reducibly linked melittin to polyacridine, CHO cells were transfected at fixed stoichiometry of 0.5 nmol polyacridine-melittin per μg DNA, which the thiazole orange assay predicts full intercalation and saturation of the plasmid DNA with peptide (Figure 2-4). The reducible polyacridine-melittin peptide **7** produced the highest gene transfection, comparable to levels produced by PEI (9:1 N:P)-pGL3 polyplexes (Figure 2-6). Reducible polyacridine-melittin (**7**) polyplexes were also 1000-fold more active versus the non-reducible counterpart, peptide **8**, indicating the importance of reductive release of melittin from polyacridine anchor. Transfections mediated with Cys-melittin resulted in 100-fold lower expression than peptide **7**, demonstrating the importance of the polyacridine anchor peptide in this gene transfer system. Alternatively, peptide **8** produced gene transfer slightly higher than the control gene delivery peptide $WK_{18}$ and 10-fold lower gene

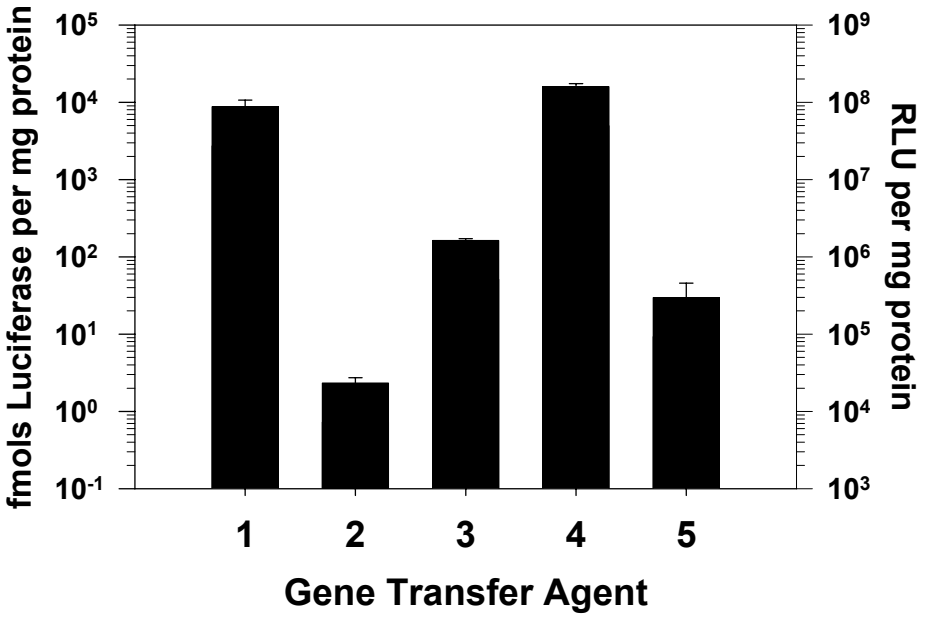


Figure 2-6. *In Vitro Gene Transfer Potency of Polyacridine-melittin Polyplexes.* The relative gene transfer efficiency of DNA polyplexes was determined in CHO cells. Transfections were performed with 10 μg of pGL3 polyplex prepared with 0.5 nmol of peptide per μg of DNA. The gene transfer efficiency mediated by polyacridine-melittin peptides was compared to PEI (N/P 9:1) DNA polyplexes and $WK_{18}$ (0.2 nmol peptide per μg) DNA polyplexes. The bars indicate pGL3 polyplexes combined with **1**) PEI, **2**) $WK_{18}$, **3**) Cys-melittin, **4**) peptide **7**, and **5**) peptide **8**. The luciferase expression was determined at 24 hrs. The results represent the mean (n=3) and standard deviation for three independent transfections.

transfer activity than Cys-melittin. Gene transfections performed with anchor peptide alone, **5** or **6**, produced negligible gene transfer, establishing the importance of a polyacridine peptide reducibly linked to melittin to produce robust gene transfer activity.

## Discussion

The endosome has been proposed as one of the major barriers that limits the gene transfer efficiency of non-viral gene delivery systems (*130*). To increase the endosomal escape of plasmid DNA, prior studies have included fusogenic peptides into experimental delivery systems (*31, 46, 59, 72, 78, 79, 131-133*). Most often, a fusogenic peptide is

linked to a PEI or polylysine to allow for multi-valent reversible ionic binding with the phosphate backbone of DNA (*46-48*). While this approach leads to significant increases in gene transfer efficiency in vitro, ionic interactions are relatively weak leading to premature dissociation of the carrier upon exposure to systemic circulation, with the end result of DNA degradation before the target of interest is reached (*36*). To overcome weak binding, higher molecular weight polycations are used (*26, 33, 40, 41, 134, 135*). However, despite numerous attempts, i.v. dosed polycationic DNA polyplexes are unable to produce therapeutic levels of gene expression (*26*).

We have explored an alternative option of binding fusogenic peptides to DNA. Initial studies including the covalent modification of plasmid DNA with fusogen indicated that method to be destructive to the plasmid transgene. Similar initial studies incorporating a single acridine intercalator could bind reversibly, but with weak affinity. As a consequence, we sought to increase the binding affinity through incorporation of several acridines, which evolved into polyacridine DNA binding peptides that could be incorporated through a bioconjugation reaction with melittin. Considering the pioneering work of Szoka who developed a diacridine glycopeptide, Vierling with a single acridine modified nuclear localizing peptide, Neilson who investigated di and triacridine nuclear localization peptides, and Vinogradov, who most recently developed a triacridine-PEG-NLS dendrimer, we sought to simplify the approach that would allow us to include four or more acridine units with the ability of controlling the charge character of the polyplex without addition of a condensing reagent such as PEI (*7-11, 123*).

The synthetic strategy to obtain multi-valent polyacridine peptides involved the post-synthetic modification of a peptide scaffold containing primary amines in the form of an N-terminal amine and three lysine ε amines available for acridinylation, separated by a spacing amino acid in the form of arginine, which is a modification of a previous report involving the modification of peptides with acridine (*136*). One advantage of the post-synthetic modification strategy is that the DNA binding precursor peptide

C(Acm)W$(KR)_2$K (peptide **1**) and W$(KR)_2$KC(Acm) (peptide **2**) could be obtained in high yield after deprotection and removal from resin. Through the utilization of orthogonal protection of cysteine, this allowed selective functionalization of all primary amines of the DNA binding precursor peptide without risk of unwanted cysteine acylation. Furthermore, synthesis of DNA binding precursor peptides as peptide amides instead of peptide acids prevented cyclization or even polymerization reactions to occur when exposed to the coupling reagents DIC/HOBt (Scheme 2-1). Removal of excess 6-(9-acridinylamino) hexanoic acid presented a synthetic challenge as usage of equal equivalents of acridine and coupling reagent to available amines often resulted in incomplete functionalization. Partial removal of excess reagents and DMF solvent was accomplished with a precipitation step in ice cold diethyl-ether, with the complete removal of 6-(9-acridinylamino) hexanoic acid and DIC/HOBt accomplished by gel filtration chromatography (Figure 5-1B), which afforded a nearly quantitative recovery of a semi-purified product capable (Figure 2-1C) of undergoing Acm deprotection without further preparatory RP-HPLC purification.

Final deprotection of Cys(Acm) was accomplished with modification of the standard protocol using $AgBF_4$/anisole in which neat TFA was replaced with a 40/60 v/v % methanol and TFA solution to completely solvate the Acm protected polyacridine peptide. Polyacridine peptides were obtained as a semi purified product (Figure 2-2B) after G-10 gel filtration with 34.3 to 54.7% recovery of Acr-W$(K(Acr)R)_2$K(Acr)C-$NH_2$ (peptide **6**) and Acr-CW$(K(Acr)R)_2$K(Acr)-$NH_2$ (peptide **5**), respectively. Due to the level of heterogeneity of the G-10 purified material after Acm deprotection, this required the inclusion of a preparatory RP-HPLC step, which afforded a pure product while sacrificing yield, ranging from 8 to 14.5% for peptide **6** and **5**, respectively.

Fortunately, the bioconjugation reactions to produce both non-reducible (peptide **8**) and reducible polyacridine-melittin (peptide **7**) were vigorous enough to produce an acceptable amount of peptide to conduct a series of experiments investigating these

peptides as non-viral gene transfer agents. Polyacridine peptides were investigated for their ability to bind to DNA through an intercalator exclusion assay in which both reported polyacridine-melittin peptides (**7** and **8**) bound at nearly equal affinity and 2-fold higher affinity as compared to polyacridine anchor peptide **5** (Figure 2-4). The equivalency point identified using the thiazole orange assay gave a reference point to conduct biological evaluation.

The design of polyacridine melittin peptides took into account the linkage between melittin and polyacridine anchor, as exemplified in Figure 2-6. Gene transfer mediated by peptide **8** demonstrates a 1000-fold decrease in activity as compared to the reducible peptide **7**, despite nearly equivalent membrane lysis potency against RBCs (Figure 2-5). These results indicate a strong relation on the nature of linkage between anchor peptide and melittin in regard to gene transfer activity. A reducible disulfide bond provided a means for the triggered release of melittin either at or inside the cell. The released melittin apparently enhances gene transfer by lysis of endosomal membranes that then allows the DNA to more efficiently reach the cytosol and the nucleus, resulting in gene expression that equals or surpasses that of PEI (Figure 2-6). These results agree with previously observed improved gene transfer mediated by a reductively triggered release of a fusogenic peptide from a gene delivery system (*47, 91*).

This study discusses the development of a novel gene transfer system relying upon a mixed intercalative ionic interaction to bind and deliver plasmid DNA in vitro. Additionally, the in vitro gene transfer results provide proof of principle data to warrant further advancement to address the multitude of barriers that exist in vivo that limit efficient gene transfer. Possible applications include incorporation of "stealthing" reagents such as poly(ethyleneglycol) to increase the metabolic stability of DNA in the blood and functionalization of polyacridine with targeting ligands to efficiently deliver nucleic acids to specific organs or cell types (*26, 35, 41, 43, 44, 124*). Before these polyacridine bioconjugates can be synthesized, several issues regarding the post-synthetic

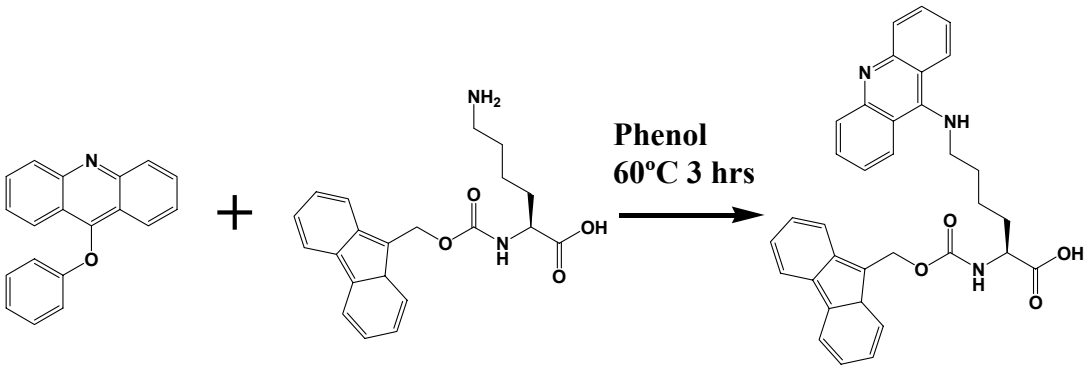


Scheme 2-4. *Synthesis of Fmoc-Lys(Acr)-OH.* Fmoc-Lys(Acr)-OH is prepared by the method reported by Tung et al (*121*). Fmoc-Lys-OH is added to 9-phenoxy-acridine in molten phenol under an argon atmosphere and heated at 60ºC for 3 hrs to obtain the desired product.

modification methodology to generate polyacridine peptides must be addressed. First and foremost, the current method involves several purification steps to yield a polyacridine peptide capable of participating in a bioconjugation reaction, resulting in suboptimal yields and limited reagent for further functionalization. Secondly, the choices for viable spacing amino acid are limited to either neutrally charged side chains or those that cannot participate in coupling reactions. This limitation theoretically eliminates lysine, histidine, aspartic, and glutamic acid as potential choices without further incorporation of orthogonal protection schemes. Taken as a whole, these aspects severely limit SAR studies aimed at optimizing the polyacridine DNA binding system to produce therapeutic levels of gene expression in vivo by a non-viral gene delivery system.

In an effort to address the limitations of post-synthetic modification, I became interested in the possibility of incorporating acridine within the peptide backbone during solid phase peptide synthesis. Previous reports demonstrate the successful incorporation of acridine in the form of a modified Fmoc protected lysine derivative in which the ε amine is functionalized directly with acridine (Scheme 2-4), eliminating the need to incorporate acridine after peptide synthesis and the linker generated by 6-aminocaproic

acid (*120, 121, 137, 138*). The inclusion of acridine during SPPS promises to increase yields and present limitless opportunities to conduct SAR studies.

# CHAPTER 3

# OPTIMIZED SYNTHESIS AND BIOLOGICAL ACTIVITY OF POLYACRIDINE-MELITTIN GENE DELIVERY PEPTIDES


## Abstract

The combination of a polyacridine peptide modified with a melittin fusogenic peptide results in a potent gene transfer agent (comparable to PEI) as demonstrated in Chapter 2. However, the post-synthetic acridinylation of DNA binding precursor peptides severely limits peptide yields and the ability to conduct SAR studies related to the design of polyacridine anchor peptides. To overcome this limitation, the amino acid Fmoc-Lys(Acr)-OH was prepared, allowing the synthesis of structurally diverse polyacridine peptides of the general formula $(Acr\text{-}X)_n$-Cys by solid phase peptide synthesis, where Acr is Lys modified on its ε-amine with acridine, X is Arg, Leu or Lys and n is 2, 3 or 4 repeats. The Cys residue was modified by either a maleimide-melittin or a thiolpyridine-Cys-melittin resulting in reducible or non-reducible polyacridine-melittin peptides. Hemolysis assays established that polyacridine-melittin peptides retained their membrane lytic potency relative to melittin at pH 7.4 and 5. When combined with plasmid DNA, the membrane lytic potency of polyacridine-melittin peptides was neutralized. Gene transfer experiments in multiple cell lines established polyacridine-melittin peptides mediate expression as efficiently as PEI. The expression was very dependent upon a disulfide bond linking polyacridine to melittin. The gene transfer was most efficient when X is Arg and n is 3 or 4 repeats. These studies establish polyacridine peptides as a novel DNA binding anchor peptide.


## Introduction

The results of Chapter 2 demonstrated the potential utility polyacridine anchor peptides have as non-viral gene delivery systems. Polyacridine reducibly linked to melittin was capable of transfecting CHO cells with similar efficiency as PEI pGL3

polyplexes. Furthermore, polyacridine-melittin formed by a non-reducible thiol ether linkage was 1000-fold less active (Figure 2-6), demonstrating the importance of a reducible linkage between polyacridine and melittin. The results of chapter 2 provided evidence in support of the hypothesis that incorporating a fusogenic peptide reducibly linked to a multi-valent polyacridine peptide generates a vector capable of producing robust in vitro gene transfer due to the strong, but reversible binding affinity of polyacridine for DNA. Even with the robust gene transfer afforded by polyacridine-melittin in cell culture, the methodology involving the post-synthetic modification of DNA binding precursor peptides to produce polyacridine anchoring peptides is somewhat limited. The limitations include factors such as low yields afforded by several purification steps and number of synthetic steps, which ultimately limits SAR opportunities.

To address the limitations of post-synthetic modification and efficiently produce polyacridine peptides, this chapter discusses the incorporation of acridine within the peptide backbone during solid phase peptide synthesis. Previous reports demonstrate the successful incorporation of acridine in the form of a modified Fmoc protected lysine derivative in which the ε amine is substituted directly with acridine, yielding Fmoc-Lys(Acr)-OH (Scheme 2-4), eliminating the need to incorporate acridine after peptide synthesis and subsequent orthogonal deprotection and purification steps to isolate the polyacridine peptide (*120, 121, 137, 138*). Following incorporation of Fmoc-Lys(Acr)-OH during SPPS, the resulting polyacridine peptide had the general sequence of $(Acr\text{-}X)_n$-Cys. The peptide synthesis approach resulted in an increased yield and offers limitless opportunities to conduct SAR studies.

The new strategy described herein demonstrates the synthesis of polyacridine-melittin as a DNA binding peptide and reaffirms its efficacy as a potent in vitro gene transfer agent as observed in Chapter 2. The results demonstrate that SPPS derived polyacridine anchor peptides bind to plasmid DNA with sufficient affinity to deliver

polyacridine-melittin polyplexes in vitro with the potential to control DNA polyplex charge for improved in vivo gene delivery. We also describe the synthesis of polyacridine PEG and glycopeptides to form targeted multi-component complexes with polyacridine-melittin to enable gene expression and evaluate polyacridine as a gene transfer vector in vivo (*26, 36, 41*).

## Materials and Methods

Unsubstituted Wang resin for peptide synthesis, 9-hydroxybenzotriazole, Fmoc-protected amino acids, O-(Benzotriazole-N,N,N',N'-tetramethyluronium hexafluorophosphate (HBTU), 1,3-Diisopropylcarbodiimide (DIC), Fmoc-Lysine-OH, and N-Methyl-2-pyrrolidinone (NMP) were obtained from Advanced ChemTech (Lexington, KY). N, N-Dimethylformamide (DMF), trifluoroacetic acid (TFA), and acetonitrile were purchased from Fisher Scientific (Pittsburgh, PA). Diisopropylethylamine (DIPEA), piperdine, acetic anhydride, Tris (2-carboxyethyl)-phosphine hydrochloride (TCEP), 9-chloroacridine, maleic anhydride, 2-2'dithiodipyridine (DTDP), and thiazole orange were obtained from Sigma Chemical Co. (St. Louis, MO). Triisopropylsilane (TIS) and polyethylene amine (PEI 25 KDa) was purchased from Aldrich (Milwaukee, WI). mPEG-maleimide (5,000 Da) was purchased from Laysen Bio (Avab, AL). D-Luciferin and luciferase from *Photinus pyralis* were obtained from Roche Applied Science (Indianapolis, IN). HepG2, CHO, and 3T3 cells were acquired from the American Type Culture Collection (Manassas, VA). Inactivated qualified fetal bovine serum (FBS) was from Life Technologies, Inc. (Carlsbad, CA). BCA reagent was purchased from Pierce (Rockford, IL). pGL3 control vector, a 5.3 kb luciferase plasmid containing a SV40 promoter and enhancer, was obtained from Promega (Madison, WI). pGL3 was amplified in a DH5α strain of *Escherichia coli* and purified according to manufacturer's instructions.

## Synthesis of 9-phenoxyacridine and Fmoc Lysine(Acridine)-OH

9-phenoxyacridine was synthesized with modification from the methods of Tung et al (*121*). Briefly, 12 g of phenol (127.5 mmol) and 0.72 g of sodium hydroxide (18 mmol) were heated to 100ºC. To the liquified phenol, 2.8 g of 9-chloroacridine (13.105 mmol) was added and stirred vigorously for 1.5 hrs. The reaction was quenched by the addition of 100 ml of 2 M sodium hydroxide, and then allowed to sit at RT overnight. A yellow precipitate was filtered, washed with water and dried in vacuo over $CaSO_4$ (3.4822g, 12.835 mmol, 97.9%, M.P. 123 – 124 º C, TLC, 15 : 5 : 1 : 0.5, ethyl acetate / methanol / hexane / acetic acid, $R_f = 0.18$). $^1$H NMR (DMSO-$d_6$) δ 8.23 (d, 2H), 8.04 (d, 2H), 7.88 (t, 2H), 7.59 (t, 2H), 7.32 (t, 2H), 7.08 (t, 1H), 6.88 (d 2H).

Fmoc-Lysine(Acridine)-OH was prepared by adding 2.18 g of Fmoc-Lys-OH (5.91 mmol) in liquid phenol (6.781 g, 73.01 mmol) to 9-phenoxyacridine (3 g, 11.06 mmol) then heated at 60 ºC for 4 hrs under an argon atmosphere. Diethyl ether (80 ml) was then added while stirring vigorously until a yellow precipitate formed that was immediately recovered by filtration and washed repeatedly with diethyl ether. The product was allowed to dry overnight ($CaSO_4$) under vacuum (2.90 g, 5.32 mmol, 90%), M.P. 135-140ºC**,** TLC: 1:1, 0.1 v/v % TFA / acetonitrile, $R_f = 0.75$). MS: $(M + H^+)^{1+}$= 545.5 m/z. $^1$H NMR (DMSO-$d_6$) δ 6.7-7.8 (m, 17H), 3.6-3.95 (m, 2H), 3.25-3.53 (br, 3H), 2,06 (m, 1H), 0.8-1.5 (m, 6H).

## Synthesis of Maleimide Glycine (Mal-Gly-OH)

Glycine (5 g, 66.6 mmol) and maleic anhydride (6.6 g, 66.6 mmol) were suspended in 80 ml of acetic acid and allowed to react for 3 hrs at RT. The resulting white precipitate was collected by filtration, washed with cold water, and dried (10.95 g, 63.3 mmol, 95 %, M.P. 187-189ºC**,** TLC: 2:1:1:1 isopropyl alcohol / acetic acid / ethyl acetate / water, $R_f = 0.5$). The glycine maleic acid intermediate was characterized by

proton NMR (300 MHz, DMSO-d6): δ = 9.2 (s, 1H) 6.397 (d, 1H, j = 8.57 Hz), 6.310 (d, 2H, j = 12.86 Hz), 2.0 (d, 2H j = 6.86 Hz).

Glycine maleamic acid (5.2 g, 30.04 mmol) and 2.1 equivalents of triethylamine (6.37 g, 63 mmol) were refluxed for 3 hrs in 500 ml toluene with removal of water with a Dean-Stark apparatus. Upon reaction completion, the toluene solution was decanted and dried over $CaSO_4$. The resulting solid was acidified with 2 M HCl, extracted with ethyl acetate, dried with $MgSO_4$ and evaporated to yield Mal-Gly-OH (1.7 g, 11 mmol, 36.5%, M.P. 99-110ºC**,** TLC: 2:1:1:1 isopropyl alcohol / acetic acid / ethyl acetate / water, $R_f$ = 0.72). The product was characterized by proton NMR (300 MHz, DMSO-d6): δ = 7.108 (s, 2H), 4.105 (s, 2H) (*126*).

## Synthesis and Characterization of Polyacridine-Melittin Analogues

Melittin analogues, polyacridine peptides, and control peptides were prepared by solid phase peptide synthesis using standard Fmoc procedures with 9-hydroxybenzo-triazole and HBTU double couplings on a 30 µmol scale on an Advanced ChemTech APEX 396 synthesizer. Mal-melittin was prepared by coupling Mal-Gly-OH to the N-terminus of side-chain protected full-length melittin on resin utilizing a 6-fold excess of Mal-Gly-OH, DIC and HOBt, reacted for 4 hrs while stirring. The resin was filtered, washed with DMF, DCM and methanol, and then dried. Peptides were removed from resin and side chain deprotected using a cleavage cocktail of TFA/triisopropylsilane/ water (95:2.5:2.5 v/v/v) for 3 hrs followed by precipitation in cold ether. Precipitates were centrifuged for 10 min at 4000 rpm at 4ºC and the supernatant decanted. Peptides were then reconstituted with 0.1 v/v % TFA and purified to homogeneity on RP-HPLC by injecting 0.5-2 µmol onto a Vydac C18 semipreparative column (2 x 25 cm) eluted at 10 ml/min with 0.1 v/v % TFA with an acetonitrile gradient of 20-45 v/v % over 30 min while monitoring tryptophan (Abs 280 nm) or acridine (Abs 409 nm). The major peak

was collected and pooled from multiple runs, concentrated by rotary evaporation, lyophilized, and stored at -20ºC.

Purified peptides were reconstituted in 0.1 v/v % TFA and quantified by absorbance (tryptophan $\varepsilon_{280\ nm}$ = 5600 $M^{-1}$ $cm^{-1}$, thiolpyridine and tryptophan $\varepsilon_{280\ nm}$ =10915 $M^{-1}$ $cm^{-1}$, or acridine $\varepsilon_{409\ nm}$ =9266 $M^{-1}$ $cm^{-1}$) to determine isolated yield. Purified peptides were characterized by LC-MS by injecting 2 nmol onto a Vydac C18 analytical column (0.47 x 25 cm) eluted at 0.7 ml/min with 0.1 v/v % TFA and an acetonitrile gradient of 10-55 v/v % over 30 min while acquiring ESI-MS in the positive ion mode.

Cys-melittin was reacted with 10-eq of DTDP in 2-propanol/2 N acetic acid (10:3) for 8 hrs at RT to generate the thiolpyridine protected peptide (*127*). The reaction mixture was concentrated by rotary evaporation and applied to a Sephadex G-10 column eluted (2.5 x 50 cm) with 0.1 v/v % TFA while monitoring absorbance at 280 nm to remove excess DTDP. The peptide peak fractions were pooled, concentrated, lyophilized, and purified to homogeneity by RP-HPLC as described previously.

$(Acr\text{-}X)_n$-SS-melittin and $(Acr\text{-}X)_n$-Mal-melittin peptides were synthesized on a 2 μmol scale based on melittin, using 1.7 equivalents (3.4 μmol) of the reduced $(Acr\text{-}X)_n$-Cys, where X equals Arg, Lys, or Leu. Mal-melittin (2 μmol) was prepared in 8 ml of 10 mM ammonium acetate pH 5 and added to $(Acr\text{-}X)_n$-Cys and 2 ml of methanol to facilitate solubility. The reaction occurred over 12 hrs at RT as determined by analyzing aliquots by LC-MS. At completion the reaction mixture was concentrated by rotary evaporation and lyophilized prior to purification of $(Acr\text{-}X)_n$-Mal-melittin by RP-HPLC eluted with 0.1 v/v % TFA and acetonitrile gradient (35-45% over 30 min) while detecting at 409 nm.

Alternatively, thiolpyridine-Cys-melittin (2 μmol) was prepared in 8 ml of 10 mM ammonium acetate pH 6 and added to 3.4 μmol $(Acr\text{-}X)_n$-Cys in 2 ml of methanol. After

24 hrs, $(Acr\text{-}X)_n$-SS-melittin was purified and characterized by LC-MS as described above.

## Synthesis and Characterization of PEGylated Polyacridine Peptides

PEGylation of the Cys residue on $(Acr\text{-}Arg)_4$-Cys was achieved by reacting with 1 μmol of peptide with 1.1 μmol of $PEG_{5000\ Da}$–maleimide in 4 ml of 10 mM ammonium acetate buffer pH 7 for 12 hrs at RT. PEGylated peptides were purified by semipreparative HPLC as previously described and eluted with 0.1 v/v % TFA with an acetonitrile gradient of 25-65 v/v % while monitoring acridine at 409 nm. The major peak was collected and pooled from multiple runs, concentrated by rotary evaporation, lyophilized, and stored at -20ºC. PEG-peptides were reconstituted in water and quantified by $Abs_{409nm}$ to determine isolated yield (Table 3-3). PEG-peptides were characterized by MALDI-TOF MS by combining 1 nmol with 10 μl of 2 mg per ml α-cyano-4-hydroxycinnamic acid (CHCA) in 50 v/v % acetonitrile and 0.1 v/v % TFA. Samples were spotted onto the target and ionized on a Bruker Biflex III Mass Spectrometer operated in the positive ion mode.

## Synthesis and Characterization of Polyacridine $(Acr\text{-}Arg)_4$-Cys-Triantennary Glycopeptide

Glycosylation of the Cys residue on $(Acr\text{-}Arg)_4$-Cys was achieved by reacting 500 nmol of iodoacetamide-triantennary N-glycan (I-TRI) with 625 nmol of $(Acr\text{-}Arg)_4$-Cys in 2.5 ml of 100 mM Tris buffer pH 8 for 12 hrs at RT. The polyacridine glycopeptide was purified by semipreparative HPLC as previously described and eluted with 0.1 v/v % TFA with an acetonitrile gradient of 15-25 v/v % at 10 ml/min while monitoring acridine at 409 nm. The major peak was collected and pooled from multiple runs, concentrated by rotary evaporation, lyophilized, stored at -20ºC, and reconstituted in water and quantified by $Abs_{409nm}$ to determine isolated yield (Table 3-3). Glycopeptides were characterized by

LC-MS by injecting 1 nmol and eluted 0.7 ml per min with 0.1 v/v % TFA and an acetonitrile gradient of 5-40 v/v % over 30 min while acquiring ESI-MS in the positive mode.

## Polyacridine-Melittin Hemolysis Assay

Whole blood was obtained from male ICR mice by heart puncture with heparinized 22G needles and collected in conical tubes containing 10 ml of 0.15 M PBS (pH 7.4) prewarmed to 37ºC. Erythrocytes were immediately separated from plasma by centrifugation at 2000 rpm for 2 min, washed three times with 10 ml of PBS, and then diluted to 1.5 x $10^8$ cells/ml. Peptides were prepared at 15 μM and serially diluted to 10-0.01 μM, after which 100 μl was pipetted in triplicate into a MultiScreenHTS BV 96 well plate. Erythrocytes (50 μl, 7.5 x $10^6$ cells) were added to the peptides and incubated at 37ºC for 1 h followed by filtration on a Multiscreen vacuum manifold (Millipore Corporation, Billerica, MA). The filtrate was measured for $Abs_{410nm}$ on a BioTEK plate reader (BioTEK Instruments Incorporated., Winooski, VT) and compared to the 100% hemolysis caused by replacing PBS with water. Peptide DNA polyplexes (1.5 nmol and 7.5 μg pGL3) were also assayed for hemolysis as described above.

## Formulation and Characterization of Polyacridine-Melittin Polyplexes

The relative binding affinity of peptides for DNA was determined by a fluorophore exclusion assay (*22*). pGL3 (200 μl of 4 μg/ml in 5 mM Hepes pH 7.5 containing 0.1 μM thiazole orange) was combined with 0, 0.05, 0.1, 0.25, 0.35, 0.5, 1, and 2 nmol of peptide in 300 μl of Hepes and allowed to bind at RT for 30 min. Thiazole orange fluorescence was measured using an LS50B fluorometer (Perkin-Elmer, U.K.) by exciting at 498 nm while monitoring emission at 546 nm with the slit widths set at 10 nm. A fluorescence blank of thiazole orange in the absence of DNA was subtracted from all values before data analysis. The data are presented as nmol of peptide per μg of DNA

versus the percent fluorescence intensity ± the standard deviation determined by three independent measurements.

Particle size and zeta potential were determined by preparing 2 ml of polyplex in 5 mM Hepes pH 7.5 at a DNA concentration of 30 μg/ml with 15 nmol/ml of peptide (0.5 nmol of peptide per μg of DNA). Particle size was measured by quasi-elastic light scattering (QELS) at a scatter angle of 90º on a Brookhaven ZetaPlus particle sizer (Brookhaven Instruments Corporation, NY). The zeta potential was determined as the mean of ten measurements immediately following acquisition of the particle size.

## Atomic Force Microscopy (In collaboration with Christian Fernandez)

Polyacridine-melittin DNA polyplexes were prepared at 0.5 nmol of peptide per μg of DNA at a concentration of 100 μg per ml of DNA and directly deposited on a freshly cleaved mica surface and allowed to bind for 10 min prior to washing with deionized water. Alternatively, naked DNA (100 μg pGL3 per ml) was prepared in 10 mM Tris, 1 mM EDTA pH 8, then diluted to 1 μg per ml in 40 mM Hepes 5 mM nickel chloride pH 6.7, and deposited on a fresh cleaved mica surface for 10 min followed by washing with deionized water. An Asylum atomic force microscope (AFM) MFP3D (Santa Barbara, CA) was operated in the AC-mode in order to image either naked DNA or DNA polyplexes using a silicon cantilever (Ultrasharp NSC15/AIBS, MikroMasch).

## Polyacridine-melittin Polyplex Toxicity

The in vitro toxicity of polyacridine-melittin polyplexes was evaluated by MTT assay (*139*). CHO, HepG2 and 3T3 cells were plated on 6 x 35 mm wells at 5 x $10^5$ cells/well and grown to 40-70% confluency. The media was replaced with 2 ml of fresh MEM supplemented with 2% FBS, and the cells treated with 0.5 nmol peptide per μg DNA polyplexes. After 6 hrs, the media was replaced with fresh culture media and grown an additional 18 hrs. The media was replaced with 2 ml of fresh media and 500 μl of

0.5% (w/v) 3-(4,5-dimethylthiazole-2-yl)-2,5-diphenyl tetrazolium bromide (MTT) in PBS solution and allowed to incubate at 37ºC for 1 hr to let formazan crystals form. The media containing MTT was removed, and the crystals dissolved by the addition of 2 ml of dimethyl sulfoxide (DMSO) and 250 µl Sorenson's Glycine Buffer, then measured by absorbance 595 nm on a microplate reader. The percent viability was determined relative to untreated cells.

### In Vitro Gene Transfer of Polyacridine-melittin DNA Polyplexes

HepG2 cells ($5 \times 10^5$) were plated on 6 x 35 mm wells and grown to approximately 50% confluency. Transfections were performed in MEM supplemented with 2% FBS, sodium pyruvate (1 mM), and penicillin and streptomycin (100 U and 100 µg/ml). Polyplexes were prepared at a DNA concentration of 30 µg/ml and a stoichiometry of 0.5 nmol peptide per µg of DNA in Hepes buffered mannitol (HBM). Polyplexes (10 µg of DNA in 0.3 ml of HBM) were added drop wise to wells in triplicate and incubated 24 hrs. After 24 hrs, the cells were washed twice with 2 ml of ice-cold phosphate-buffered saline ($Ca^{2+}$ - and $Mg^{2+}$ - free) and then treated with 0.5 ml of lysis buffer (25 mM Tris Chloride, pH 7.8, 1 mM EDTA, 8 mM magnesium chloride, and 1% Triton X-100) for 10 min at 4ºC. Cell lysates were scraped, transferred to 1.5 ml microcentrifuge tubes, and centrifuged for 10 min at 13,000 g at 4ºC to pellet cell debris. Lysis buffer (300 µl), sodium-ATP (4.3 µl of a 165 mM solution at pH 7, 4ºC) were combined in a test tube, mixed briefly, and immediately placed in the luminometer. Luciferase relative light units were measured by a Lumat LB 9501 (Berthold Systems, Germany) with 10 s integration after automatic injection of 100 µl of 0.5 mM D-luciferin. The relative light units were converted to fmol using a standard curve generated by adding a known amount of luciferase to 35 mm wells containing 50% confluent HepG2 cells. The resulting standard curve had an average slope of $2.6 \times 10^4$ relative light

units/fmol enzyme. Protein concentrations were measured by a BCA assay using bovine serum albumin as a standard (*128*). The amount of luciferase recovered in each sample was normalized to mg of protein and reported as the mean and standard deviation obtained from triplicate transfections. PEI pGL3 polyplexes were prepared by mixing 35 µg of DNA in 525 µl of HBM with 43.8 µg PEI in 525 µl of HBM while vortexing to create DNA complexes possessing a charge ratio ($NH_4^+/PO_4^-$) of 9:1. Cells were transfected with 10 µg PEI-DNA polyplexes as previously described. CHO and 3T3 (5 x $10^5$) cells were plated on 6 x 35 mm wells and grown to ca. 50% confluency and then transfected as described above.

## Hydrodynamic Stimulation and Bioluminescence Imaging (In collaboration with Christian Fernandez and Jason Duskey)

pGL3 (5 µg) was prepared in 50 µl of HBM (5 mM Hepes, 0.27 M mannitol, pH 7.4) and dosed by i.v. tail vein. Mice (n=3) were also dosed via tail vein with 5 µg of 0.5 nmol per µg of multi-component polyacridine polyplex (90% PEG and TRI 10% or 45% PEG, 45% melittin, and 10% TRI) in 50 µl of HBM (5 mM Hepes, 0.27 M mannitol, pH 7.4). At 5 min after polyplex dosing, a stimulatory hydrodynamic dose of normal saline (9 wt/vol% of the body weight; 1.8 – 2.25 ml based on 20-25 g mice) was administered over 5 sec according to a published procedure (*140, 141*). At 24 hrs post-DNA dose, mice were anesthetized by 3% isofluorane, then administered an i.p. dose of 80 µl (2.4 mg) of D-luciferin (30 µg/µl in phosphate-buffered saline). At 5 min following the D-luciferin dose, mice were imaged for bioluminescence (BLI) on an IVIS Imaging 200 Series (Xenogen). BLI was performed in a light-tight chamber on a temperature-controlled, adjustable stage while isofluorane was administered by a gas manifold at a flow rate of 3%. Images were acquired at a 'medium' binning level and a 20 cm field of view. Acquisition times were varied (1 sec - 1 min) depending on the intensity of the

luminescence. The Xenogen system reported bioluminescence as photons/sec/$cm^2$/ seradian in a 2.86 cm diameter region of interest covering the liver.

## Results

### Synthetic Strategy for Polyacridine-Melittin

Polyacridine and melittin peptides were synthesized using HBTU/HOBt with increased coupling efficiency compared to DIC mediated coupling. Early attempts to synthesize polyacridine peptides using DIC resulted in heterogeneous mixtures of truncated peptides with minimal recovery of full length peptide. The identity of the spacing amino acid between Lys-acridine residue significantly influenced the synthetic yield. Bulky amino acid side chains and protecting groups such as Lys-Boc, Phe, Gln-Trt, Leu, Glu-OBut and Arg-Pbf were well tolerated, whereas Gly surprisingly was not. Polyacridine peptides possess a C-terminal Cys to accommodate bioconjugation to Cys-melittin or Mal-melittin. Polyacridine peptides possessing an alternating Lys-Acr (Acr) spaced by either Arg, Lys, or Leu were designed to influence the charge character of the anchor peptide (Scheme 3-1 illustrates $(Acr\text{-}Arg)_4$-melittin synthesis). The lengths of polyacridine peptides were systematically varied to possess 2-4 Acr-Arg repeats to examine the influence of affinity. Polyacridine nona-peptides were routinely obtained in 30-35% purified yield with >95% purity (Table 3-1).

Polyacridine-melittin peptides were designed to possess either a reducible disulfide or a non-reducible maleimide linkage (Scheme 3-1). The most expedient synthetic route proved to be cleavage of Cys-melittin from the resin, followed by modification with dithiol dipyridine to produce a thiolpyr-melittin. The RP-HPLC monitoring of the reaction of thiolpyr-melittin with $(Acr\text{-}Arg)_4$-Cys is illustrated in Figure 3-1A and B. The desired $(Acr\text{-}Arg)_4$-SS-melittin product is formed with complete consumption of thiolpyr-melittin, along with formation of a $(Acr\text{-}Arg)_4\text{-}Cys_2$ by-product (Figure 3-1B). This synthetic route resulted in $(Acr\text{-}X)_n$-SS-melittin in 35-50% purified

Table 3-1. Sequence and Hemolytic Potency of Peptide Conjugates

| | | Mass[a] (calc/obs) | $HL_{50}$ (μM)[b] pH 7.4 : 5.0 |
|---|---|---|---|
| **Polyacridine Anchor Peptides (Acr)= Lys-ε-acridine, Ac=acylated ε-amine)** | | | |
| $(Acr\text{-}Arg)_2$-Cys | | 1044.3 / 1044.2 | N.D.[c] |
| $(Acr\text{-}Arg)_3$-Cys | | 1505.8 / 1505.6 | N.D. |
| $(Acr\text{-}Arg)_4$-Cys | | 1967.4 / 1967.0 | > 10 / > 10 |
| $(Acr\text{-}Lys)_4$-Cys | | 1855.3 / 1855.0 | N.D. |
| $(Acr\text{-}Leu)_4$-Cys | | 1795.3 / 1795.1 | N.D. |
| Trp-$(Lys(Ac)\text{-}Arg)_4$-Cys | | 1612.9 / 1612.7 | N.D. |
| **Melittin Analogues (thiolpyr= thiol pyridine, Mal =maleimide)** | | | |
| Melittin | GIGAVLKVLTTGLPALISWIKRKRQQ | 2847.5 / 2847.4 | 0.9/ 2.3 |
| Cys-melittin | CWKKGIGAVLKVLTTGLPALISLIKRKRQQ | 3320.1 / 3320.4 | 1.0 / 0.7 |
| Dimeric-melittin | $(CWKKGIGAVLKVLTTGLPALISLIKRKRQQ)_2$ | 6638.2 / 6637.6 | 1.0 / 1.2 |
| Thiolpyr-melittin | C(tp)WKKGIGAVLKVLTTGLPALISLIKRKRQQ | 3429.2 / 3428.4 | N.D. |
| Mal-melittin | (m)GWKKGIGAVLKVLTTGLPALISLIKRKRQQ | 3354.0 / 3454.0 | 3.84 / 4.8 |
| **Polyacridine-Melittin (SS = reducible, Mal=non-reducible)** | | | |
| $(Acr\text{-}Arg)_2$-SS-melittin | $(Acr\text{-}Arg)_2$-C-WKKGIGAVLKVLTTGLPALISLIKRKRQQ | 4359.5 / 4362.3 | 2.5 / 3.9 |
| $(Acr\text{-}Arg)_3$-SS-melittin | $(Acr\text{-}Arg)_3$-C-WKKGIGAVLKVLTTGLPALISLIKRKRQQ | 4823.9 / 4823.2 | 1.4 / 2.2 |
| $(Acr\text{-}Arg)_4$-SS-melittin | $(Acr\text{-}Arg)_4$-C-WKKGIGAVLKVLTTGLPALISLIKRKRQQ | 5285.5 / 5285.2 | 1.7 / 1.9 |
| $(Acr\text{-}Arg)_4$-Mal-melttin | $(Acr\text{-}Arg)_4$-C(m)GWKKGIGAVLKVLTTGLPALISLIKRKRQQ | 5321.4 / 5320.8 | 2.1 / 1.7 |
| $(Lys(Ac)\text{-}Arg)_4$-SS-melttin | W$(Lys(Ac)\text{-}Arg)_4$-C-CWKKGIGAVLKVLTTGLPALISLIKRKRQQ | 4931.0 / 4930.4 | 5.6 / 7.7 |
| $(Acr\text{-}Lys)_4$-SS-melittin | $(Acr\text{-}Lys)_4$-C-CWK KG IGAVLKVLTTGLPALISLIKRKRQQ | 5173.4 / 5173.2 | 1.0 / 2.8 |
| $(Acr\text{-}Lys)_4$-Mal-melittin | $(Acr\text{-}Lys)_4$-C(m)GWKKGIGAVLKVLTTGLPALISLIKRKRQQ | 5209.4 / 5208.8 | 1.5 / 1.9 |
| $(Acr\text{-}Leu)_4$-SS-melittin | $(Acr\text{-}Leu)_4$-C-CWK KG IGAVLKVLTTGLPALISLIKRKRQQ | 5113.4 / 5112.8 | 2.2 / 1.6 |
| $(Acr\text{-}Leu)_4$-Mal-melittin | $(Acr\text{-}Leu)_4$-C(m)GWKKGIGAVLKVLTTGLPALISLIKRKRQQ | 5149.3 / 5149.2 | 2.4 / 1.2 |

[a] Calculated and observed mass as determined by ESI LC-MS.

[b] RBC hemolysis at pH 7.4 and 5.0. Results represent the mean (n =3) with the standard deviation.

[c] N.D. = not determined.

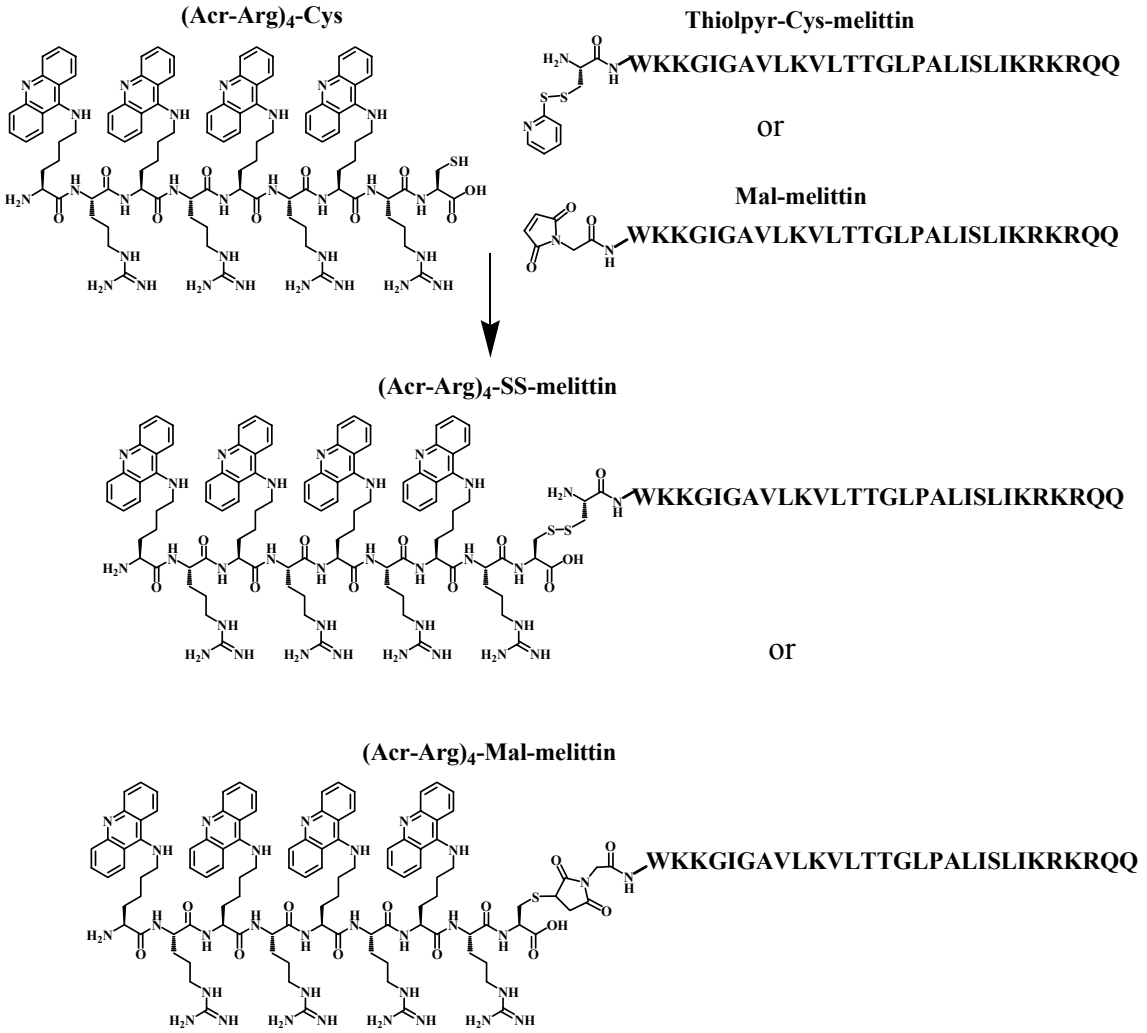


Scheme 3-1. *Synthesis of Polyacridine-Melittin Peptides.* Thiolpyr-melittin is reacted with the DNA binding anchor peptide (Acr-Arg)$_4$-Cys at pH 6 to yield (Acr-Arg)$_4$-SS-melittin as a reducible gene transfer polyacridine melittin peptide. Alternatively, Mal-melittin is reacted with (Acr-Arg)$_4$-Cys at pH 5 to yield a non-reducible (Acr-Arg)$_4$-Mal-melittin gene transfer peptide. In each case, Acr refers to a Lys substituted on its ε-amine with acridine. The Arg was substituted with Lys and Leu to produce DNA binding anchor peptides with different affinity. The (Acr-Arg)$_n$ was also varied from n=2-4 repeats.

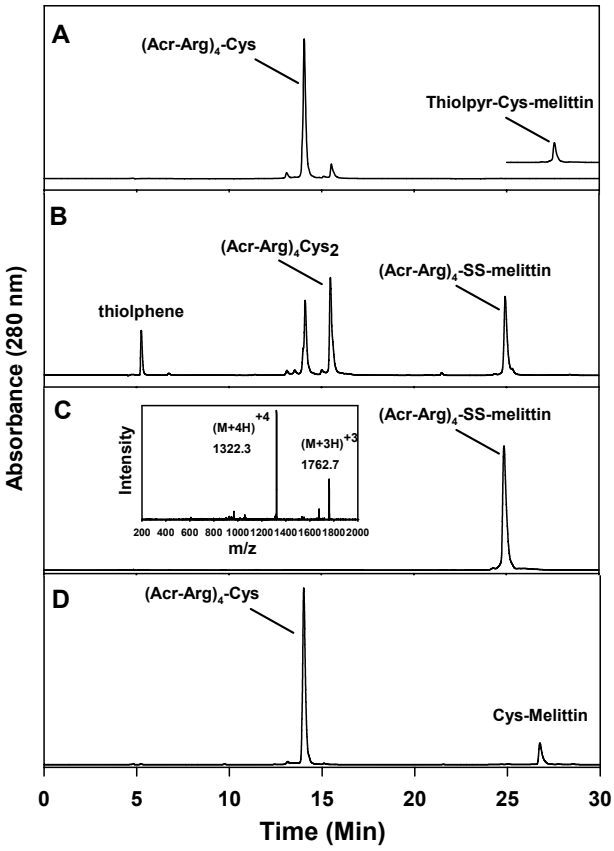


Figure 3-1. *RP-HPLC Analysis of Polyacridine-Melittin Peptide Synthesis.* The reaction monitoring of $(Acr\text{-}Arg)_4$-Cys with thiolpyr-Cys-melittin at time 0 at 1.7:1 mol ratio is illustrated in panel A. The RP-HPLC chromatograms were produced by injecting 2 nmol then eluting with 0.1 v/v % TFA and an acetonitrile gradient of 10-55 v/v % over thirty minutes while monitoring absorbance at 280 nm. The reaction monitoring at 12 hrs established the complete consumption of thiolpyr-Cys-melittin with formation of the product $(Acr\text{-}Arg)_4$-SS-melittin and by-products of dimeric $(Acr\text{-}Arg)_4$-$Cys_2$ and thiolphene (panel B). LC-ESI-MS of purified $(Acr\text{-}Arg)_4$-SS-melittin produced ions of 1762.7 *m/z* and 1322.3 *m/z*, respectively (inset), corresponding to a mass of 5285.2 amu (panel C). Reduction of $(Acr\text{-}Arg)_4$-SS-melittin with TCEP resulted in formation of equi-mol amounts of $(Acr\text{-}Arg)_4$-Cys and Cys-melittin (panel D).

yield at >95% purity as illustrated by LC-MS analysis of purified $(Acr\text{-}Arg)_4$-SS-melittin (Figure 3-1C). ESI-MS was used to establish structure based on the triply and quadruply

charged positive ions corresponding to the calculated mass of the desired polyacridine-melittin peptide (Figure 3-1C, inset). The release of melittin from $(Acr\text{-}Arg)_4$-SS-melittin was established by reaction with TCEP to regenerate $(Acr\text{-}Arg)_4$-Cys and Cys-melittin peptide peaks (Figure 3-1D). $(Acr\text{-}X)_4$-Mal-melittin peptides, where X is Lys or Leu, were synthesized to compare their gene transfer properties with $(Acr\text{-}Arg)_4$-SS-melittin. The synthetic strategy utilized Gly-maleimide that was coupled to the N-terminus of the fully protected melittin peptide on resin (Scheme 3-1). On work-up and purification, this yielded Mal-melittin that was then directly conjugated to $(Acr\text{-}X)_n$-Cys peptides. The conjugation of Mal-melittin with $(Acr\text{-}Arg)_4$-Cys was monitored by RP-HPLC resulting in the complete consumption of Mal-melittin and the formation of $(Acr\text{-}Arg)_4$-Mal-melittin. Purification of $(Acr\text{-}Arg)_4$-Mal-melittin was achieved with a final yield of 35% and >95% purity. Reducible and non-reducible polyacridine-melittin peptides with Acr-Arg repeat of 2 and 3 were synthesized with similar yield and purity, and characterized by LC-MS (Table 3-1).

To target the ASGP-R located on hepatocytes, $(Acr\text{-}Arg)_4$-Cys-TRI (Figure 3-2) was synthesized by displacement of iodide by the nucleophilic cysteine of $(Acr\text{-}Arg)_4$-Cys to produce the non-reducible thiol-ether linkage. Following preparatory HPLC, the peptide was obtained with an isolated yield of 60% (Table 3-2) and characterized by LC-ESI-MS to produce a single peak upon rechromatograph (Figure 3-3A). The ESI-MS produced a triply charged ion of 1393.1, corresponding to an observed mass of 4176.3 amu (Figure 3-3A, inset), agreeing closely with the calculated mass of 4176.4 amu (Table 3-2).

$(Acr\text{-}Arg)_4$-Cys-Mal-PEG (Figure 3-2) was synthesized to produce the shielding component to enable systemic administration of polyacridine-melittin based polyplexes for liver specific gene expression. $(Acr\text{-}Arg)_4$-Cys-Mal-PEG was obtained in good yield after preparatory HPLC of 53% (Table 3-2). RP-HPLC analysis after purification

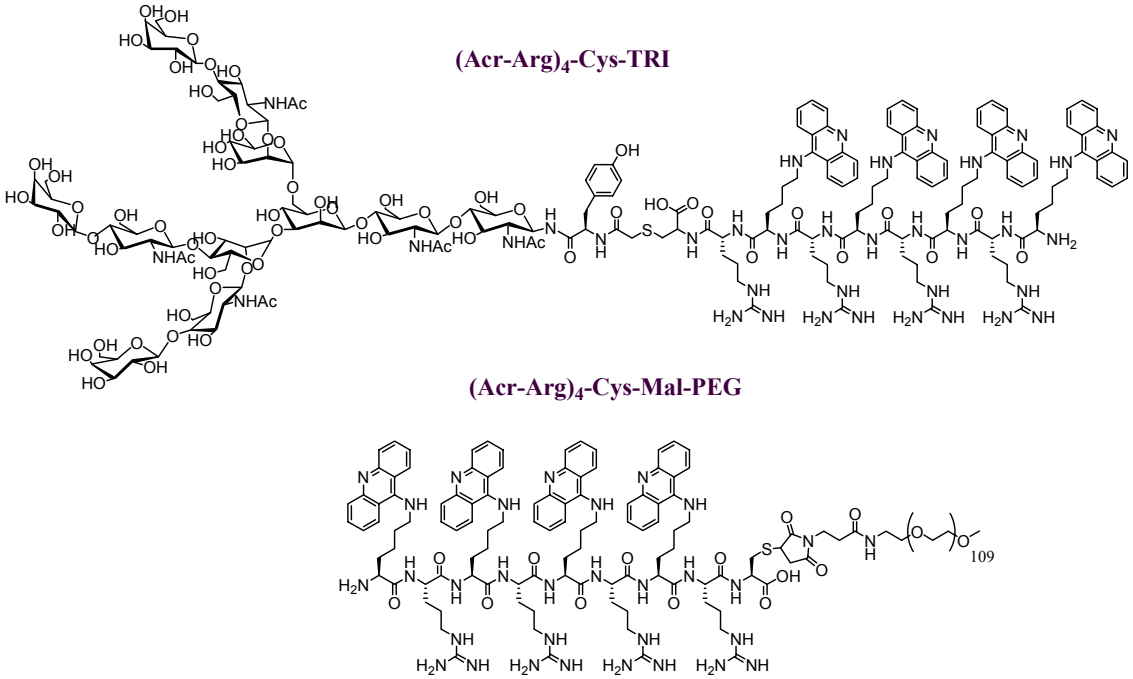


Figure 3-2. *Structures of Hepatocyte Targeting Ligand and Shielding Polyacridine Peptides.* Representative structures of the polyacridine triantennary glycopeptide (Acr-Arg)$_4$-Cys-TRI targeting ligand specific for the ASGP-R located on hepatocytes and the shielding peptide, (Acr-Arg)$_4$-Cys-Mal-PEG.

Table 3-2. *Polyacridine PEG and Targeting Glycopeptides*

| **Polyacridine Targeting Ligand** | **Mass (calc / obs)[a]** | **%Yield[c]** |
|---|---|---|
| (Acr-Arg)$_4$-Cys-TRI | 4176.4 / 4176.3 | 60 |
| **PEGylated Polyacridine Peptides** | **Mass (calc / obs)[b]** | **%Yield[c]** |
| (Acr-Arg)$_4$-Cys-Mal-PEG | 7467 / 7218 | 53 |

a. Determined by ESI-MS.

b. Determined by MALDI-TOF MS.

c. Yields based on acridine absorbance at 409 nm.

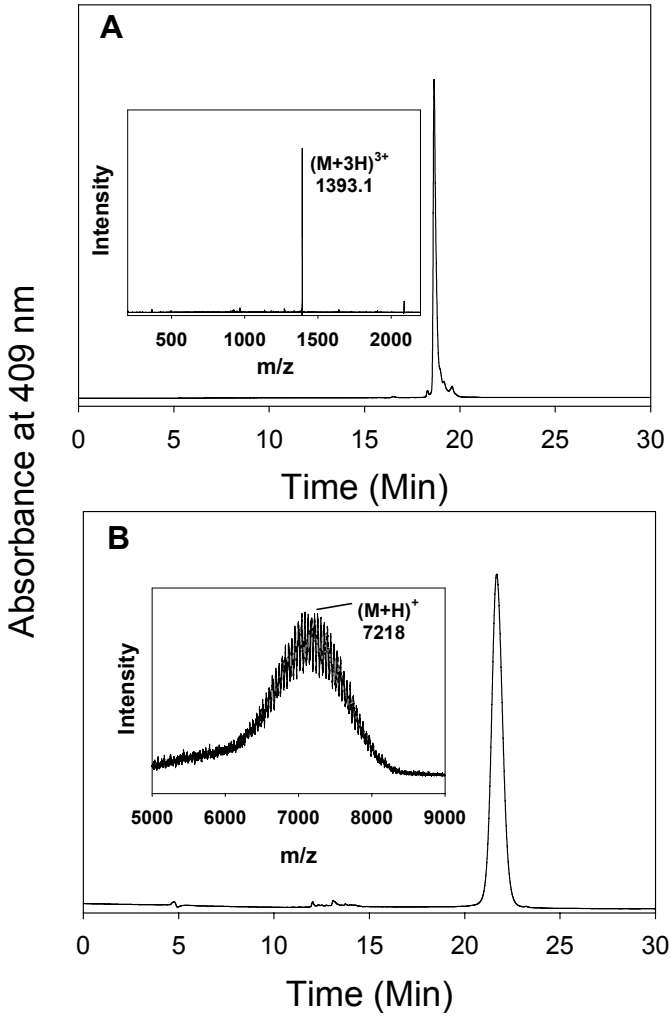


Figure 3-3. *Characterization of (Acr-Arg)$_4$-Cys-TRI and (Acr-Arg)$_4$-Cys-Mal-PEG.* RP-HPLC ESI-MS characterization following a 1 nmol injection of (Acr-Arg)$_4$-Cys-TRI and eluting with 0.1 v/v % TFA and an acetonitrile gradient of 5-40 v/v % ACN reveals a single peak (Panel A) and ESI-MS reveals a triple charged ion at 1393.1 *m/z* resulting in the observed mass of 4176.3 amu (Panel A, inset) corresponding to the calculated mass (Table 3-3). A 1 nmol injection of (Acr-Arg)$_4$-Cys-Mal-PEG on RP-HPLC results as a single peak (panel B) eluted with 0.1 v/v % TFA and acetonitrile gradient of 10-60 v/v % over thirty minutes and is characterized by MALDI-TOF MS (panel B, inset), resulting in an observed *m/z* of 7218 amu, corresponding to the calculated mass (Table 3-3).

produced a single peak (Figure 3-3B) and characterization by MALDI-TOF MS resulted in a broad distribution of masses due to mal-PEG's polydispersity, with an average

observed mass of 7218 amu (Figure 3-3B, inset), agreeing closely with the calculated mass of 7467 amu (Table 3-2).

## Physical Properties of Polyacridine-Melittin DNA Polyplexes

The binding of polyacridine-melittin peptides to pGL3 was investigated using a thiazole orange exclusion assay (*22*). Polyacridine-melittin peptides were found to compete for intercalation and displace thiazole orange resulting in a decrease in fluorescence intensity. When titrated at increasing concentration, the fluorescence decreased until an asymptote is reached at an equivalence point (Figure 3-4A). Analysis of the DNA binding affinity of $(Acr\text{-}Arg)_4$-Cys established an equivalence point at approximately 0.4 nmol peptide per μg of DNA. By comparison, Cys-melittin demonstrated weaker binding and was not able to fully exclude thiazole orange, only approaching an equivalence point at approximately 0.5 nmol of peptide per μg of DNA (Figure 3-4A). A similar result to Cys-melittin was obtained for the reactive intermediates thiolpyr-melittin and Mal-melittin, respectively. Both thiolpyr-melittin and Mal-melittin demonstrated weak binding by generating an equivalency point of 0.5 nmol per μg of DNA (Unpublished observations by N. Baumhover). Alternatively, $(Acr\text{-}Arg)_4$-SS-melittin demonstrated higher affinity resulting in an equivalence point at approximately 0.25 nmol of peptide per μg of DNA. This affinity is comparable to that afforded by a Cys-Trp-$Lys_{18}$ peptide using the same assay (*22*).

Comparison of $(Acr\text{-}Arg)_{2\text{-}4}$-SS-melittin demonstrated nearly equivalent affinity for Acr-Arg repeats of 3 and 4, but less affinity afforded for a repeat of 2 (Figure 3-4B). Direct comparison of the DNA binding affinity of $(Acr\text{-}Arg)_4$-SS-melittin with $(Acr\text{-}Lys)_4$-SS-melittin and $(Acr\text{-}Leu)_4$-SS-melittin established there was a negligible difference, with each producing fully complexed polyplexes at 0.3 nmol per μg of pGL3 (Figure 3-4C).

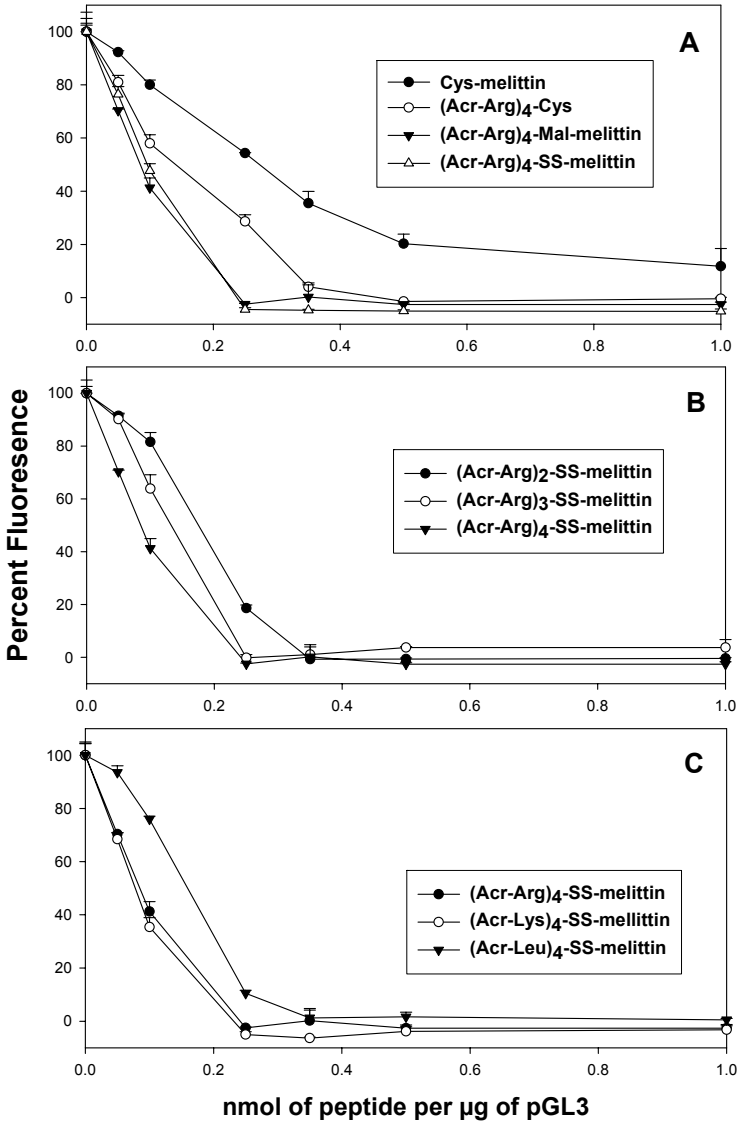


Figure 3-4. *Relative Binding Affinity of Polyacridine-Melittin Peptides to DNA.* The concentration dependent displacement of thiazole orange from DNA by polyacridine-melittin peptides was used to establish relative affinity. Cys-melittin bound weakly to DNA resulting in an asymptote in the fluorescence intensity at approximately 0.5 nmol of peptide per µg of DNA, compared to 0.35 for $(Acr\text{-}Arg)_4$-Cys and 0.25 for $(Acr\text{-}Arg)_4$-SS-melittin (panel A). Comparison of $(Acr\text{-}Arg)_{2\text{-}4}$-SS-melittin established $(Acr\text{-}Arg)_2$-SS-melittin was the weakest binding resulting in an asymptote at 0.35 nmol of peptide per µg of DNA whereas $(Acr\text{-}Arg)_{3 \text{ and } 4}$-SS-melittin were nearly equivalent in displacing thiazole orange (panel B). An equal DNA binding affinity was demonstrated for $(Acr\text{-}Arg)_4$-SS-melittin, $(Acr\text{-}Leu)_4$-SS-melittin and $(Acr\text{-}Lys)_4$-SS-melittin, each resulting in polyplex formation at 0.25 nmol of peptide per µg of DNA (panel C). Results represent the mean (n=3) with the standard deviation.

Table 3-3. *Physical Properties and Toxicity of DNA Polyplexes*

| **Peptide** | **Particle Size (nm)[a]** | **Zeta Potential (+ mV)[b]** | **MTT Assay[c]** | | |
|---|---|---|---|---|---|
| | | | **CHO** | **HepG2** | **3T3** |
| $(Acr\text{-}Arg)_2$-SS-melittin | 737 ± 46.8 | 25 ± 2.2 | 99 ± 7 | 92 ± 7 | 85 ± 2 |
| $(Acr\text{-}Arg)_3$-SS-melittin | 126 ± 4.5 | 29 ± 4.5 | 103 ± 7 | 97 ± 13 | 91 ± 2 |
| $(Acr\text{-}Arg)_4$-SS-melittin | 84 ± 2.0 | 29 ± 2.6 | 70 ± 5 | 67 ± 9 | 58 ± 4 |
| $(Acr\text{-}Arg)_4$-Mal-melittin[d] | 79 ± 1.3 | 28 ± 2.5 | 69 ± 5 | 88 ± 13 | 82 ± 1 |
| $(Lys(Ac)\text{-}Arg)_4$-SS-melittin[d] | 177 ± 6.2 | 20 ± 2.9 | 55 ± 4 | 64 ± 9 | 33 ± 4 |
| $(Acr\text{-}Lys)_4$-SS-melittin | 89 ± 3.5 | 23 ± 1.6 | 76 ± 5 | 66 ± 5 | 72 ± 6 |
| $(Acr\text{-}Lys)_4$-Mal-melittin | 86 ± 2.4 | 26 ± 2.0 | 87 ± 8 | 79 ± 6 | 82 ± 2 |
| $(Acr\text{-}Leu)_4$-SS-melittin | 119 ± 1.4 | 20 ± 2.9 | 46 ± 4 | 49 ± 4 | 50± 4 |
| $(Acr\text{-}Leu)_4$-Mal-melittin | 121 ± 2.5 | 22 ± 2.1 | 90 ± 3 | 117 ± 5 | 74 ± 3 |

[a]Mean particle size of peptide-DNA polyplex (0.5 nmol peptide per μg DNA) as determined by QELS.

[b]Mean zeta potential determined in 5 mM Hepes, pH 7.4.

[c]Percent viability of peptide-DNA polyplexes determined by MTT assay in CHO, HepG2, and 3T3 cells (0.5 nmol of peptide per μg DNA) at 10 μg DNA dose applied to $5x10^5$ cells for 6 hours.

[d]MTT assay of select peptide-DNA polyplexes revealed an insignificant increase in toxicity following 24 hour incubation with polyacridine melittin polyplexes.

The particle size and zeta potential of polyacridine-melittin polyplexes were determined by QELS analysis (Table 3-3). $(Acr\text{-}Arg)_4$-SS-melittin and $(Acr\text{-}Arg)_4$-Mal-melittin produced polyplexes of 79-84 nm average diameter, respectively. Comparison of the size of polyplexes prepared with $(Acr\text{-}Arg)_3$-SS-melittin (126 nm) and $(Acr\text{-}Arg)_2$-SS-melitin (737 nm) established that shorter repeats produced larger particle size (Table 3-3). This result is consistent with earlier findings that indicated that shorter, low affinity polylysine peptides (<13 residues) produced larger polyplexes, whereas polylysine of 18 repeats or longer produced polyplexes of approximately 80 nm in diameter (*29*).

Substitution of the spacing Arg for Lys or Leu in Acr-Arg repeats resulted in a minimal change in particle size (Table 3-3). This supports the hypothesis that polyintercalation, and not ionic binding, is primarily responsible for the binding affinity to DNA. To test this hypothesis, an analogue was prepared that replaced the acridine modified Lys with an acetyl on the ε-amine of lysine resulting in $(Lys(Ac)\text{-}Arg)_4$-SS-melittin. This analogue produced polyplexes of average diameter of 177 nm, suggesting a significantly lower affinity (Table 3-3).

To further validate the change in particle size determined by QELS, polyplexes were analyzed by atomic force microscopy (AFM). Analysis of pGL3 by AFM demonstrated an open structure occupying from 0.5 to 1 μm without a single morphology (Figure 3-5A). Polyplexes prepared with $(Acr\text{-}Arg)_2$-SS-melittin appeared to form clusters composed of several individual particles that account for the larger size determined by QELS (Figure 3-5B). In contrast, the AFM images for polyplexes prepared with $(Acr\text{-}Arg)_4$-SS-melttin (Figure 3-5C), $(Acr\text{-}Leu)_4$-SS-melittin (Figure 3-5D), $(Acr\text{-}Lys)_4$-SS-melittin (Figure 3-5E) all appeared to be less aggregated resulting in overall smaller particle size. It is interesting to note that the zeta potentials of polyacridine-melittin polyplexes containing a spacing Arg, Lys or Leu were approximately +25 mV (Table 3-3). This result indicated that the charge on melittin strongly influenced the overall charge of polyplexes prepared with different anchoring peptides.

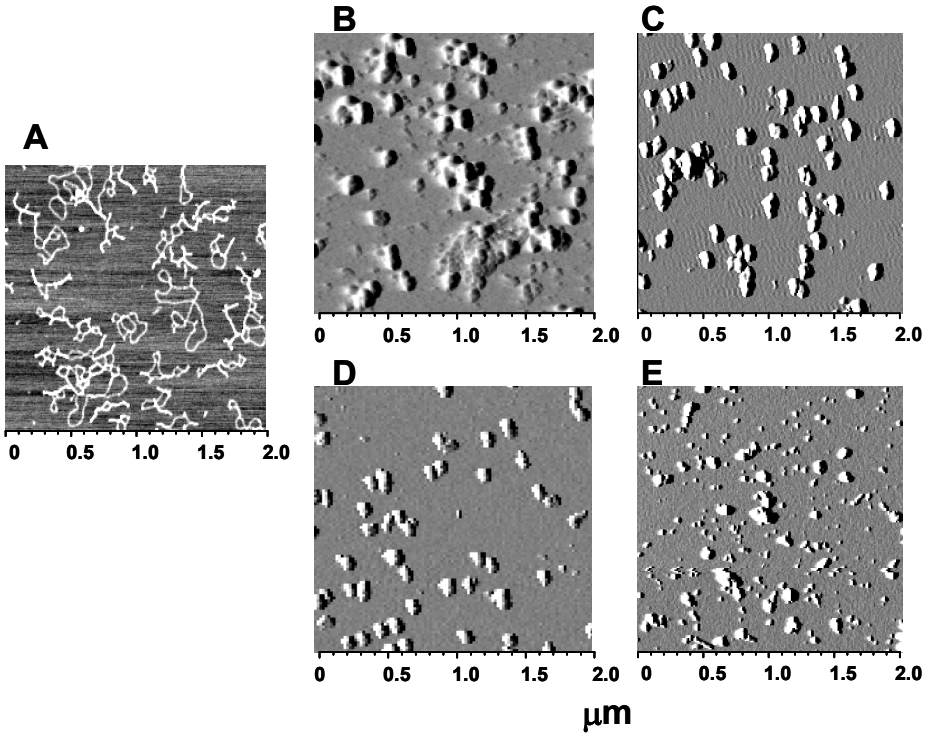


Figure 3-5. *Atomic Force Microscopy of Polyacridine-melittin Polyplexes*. The size and shape of pGL3 (**A**) or polyacridine-melittin DNA polyplexes (**B**-**E**) were determined by atomic force microscopy. $(Acr\text{-}Arg)_2$-SS-melttin (**B**), $(Acr\text{-}Leu)_4$-SS-melttin (**C**), $(Acr\text{-}Arg)_4$-SS-melttin (**D**), and $(Acr\text{-}Lys)_4$-Mal-melttin (**E**) pGL3 polyplexes are compared. The results establish that the weaker DNA binding of $(Acr\text{-}Arg)_2$-SS-melittin results in aggregated polyplexes.

## Biological Activity of Polyacridine-Melittin DNA Polyplexes

The membrane lytic potency of polyacridine-melittin peptides were investigated using a RBC hemolysis assay (*42*). As anticipated, $(Acr\text{-}X)_4$-Cys anchor peptides alone were inactive in membrane lysis. Alternatively, modification of the N-terminus of natural melittin with Cys-Trp-Lys-Lys and substitution of Leu for Trp 8 to generate Cys-melittin, resulted in retention of RBC hemolytic ($HL_{50}$) potency at pH 7.4 relative to natural

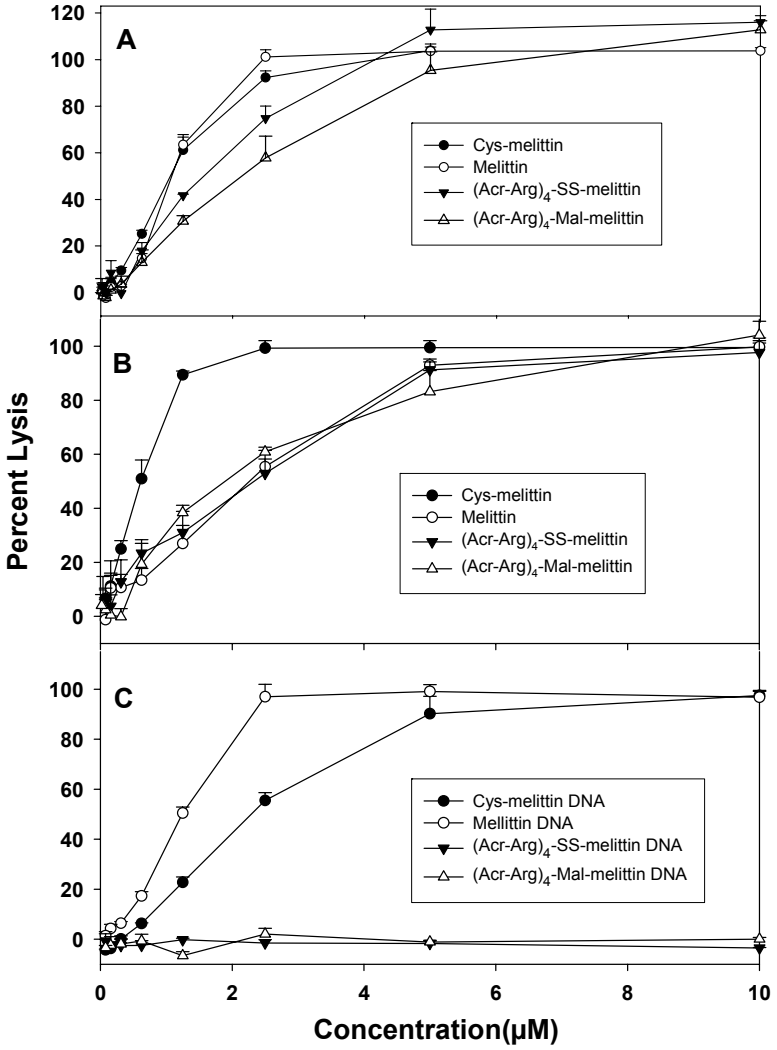


Figure 3-6. *Membrane Lytic Potency of Polyacridine-melittin Peptides.* The hemolytic activity of melittin and polyacridine-melittin peptides were compared at pH 7.4 and 5 using a RBC hemolysis assay. The results establish Cys-melittin is equally potent as natural melittin at pH 7.4 (panel A), but more potent at pH 5 (panel B). In comparison, $(Acr\text{-}Arg)_4$-SS-melittin retains nearly full hemolytic potency at pH 7.4 (panel A) but is less potent at pH 5. However, when combined with pGL3, the pH 7.4 hemolytic activity of both Cys-melittin and melittin is nearly unchanged, whereas $(Acr\text{-}Arg)_4$-SS-melittin is non hemolytic (panel C). These results establish the masking of $(Acr\text{-}Arg)_4$-SS-melittin membrane lytic activity while bound to DNA. Results represent the mean (n=3) with the standard deviation.

melittin (Figure 3-6A). Likewise, the hemolytic potency of $(Acr\text{-}Arg)_4$-SS-melittin was comparable to Cys-melittin, indicating the attachment of the polyacridine anchor had a

negligible influence on the membrane lytic activity of Cys-melittin. The results for polyacridine-melittin peptides possessing either a reducible or non-reducible linkage are summarized in Table 3-1, establishing their nearly equivalent hemolytic potency at pH 7.4.

The hemolytic potency of polyacridine-melittin peptides was also determined at pH 5 to simulate the pH of the endosome. In contrast to an earlier finding that C and N-terminal modification of natural melittin with Cys-$(Lys)_4$ resulted in the complete loss of hemolytic activity at pH 5 (*42*), Cys-melittin possessed an improved pH 5 RBC lytic potency relative to that of natural melittin (Figure 3-6B). Consequently, $(Acr\text{-}Arg)_4$-SS-melittin and $(Acr\text{-}Arg)_4$-Mal-melittin both possess potent hemolytic activity at pH 7.4 and 5 (Table 3-1). When combined with pGL3, Cys-melittin and Mal-melittin maintained their hemolytic activity at pH 7.4, demonstrating their weak association with DNA (Figure 3-6C). In contrast, the hemolytic activity of $(Acr\text{-}Arg)_4$-SS-melittin DNA polyplexes was completely neutralized due to the strong binding of the polyacridine peptide with DNA (Figure 3-6C). Reduction of the disulfide bond would decrease the binding affinity to DNA and thereby release hemolytic Cys-melittin.

To establish a relationship between peptide anchor length, reducibility, and peptide DNA stoichiometry, CHO cells were transfected with polyplexes formed with $(Acr\text{-}Arg)_2$-SS-melittin, $(Acr\text{-}Arg)_3$-SS-melittin, $(Acr\text{-}Arg)_4$-SS-melittin, and $(Acr\text{-}Arg)_4$-Mal-melittin while varying the peptide to DNA ratio from 0.1, 0.35, 0.5, and 0.75 nmol of peptide per μg of DNA (Figure 3-7). Luciferase reporter gene expression for polyplexes formed with 0.1 nmol of peptide per μg DNA resulted in expression comparable to a $WK_{18}$ / DNA control polyplex. Increasing the stoichiometry to 0.35 nmol of peptide per μg of DNA or higher increased the gene expression approximately 100-fold relative to 0.1 nmol of peptide per μg of DNA. Within this series, $(Acr\text{-}Arg)_4$-SS-melittin produced the highest expression at a stoichiometry of 0.3 and 0.5. The expression mediated by $(Acr\text{-}Arg)_4$-SS-melittin was approximately 1000-fold greater than that of

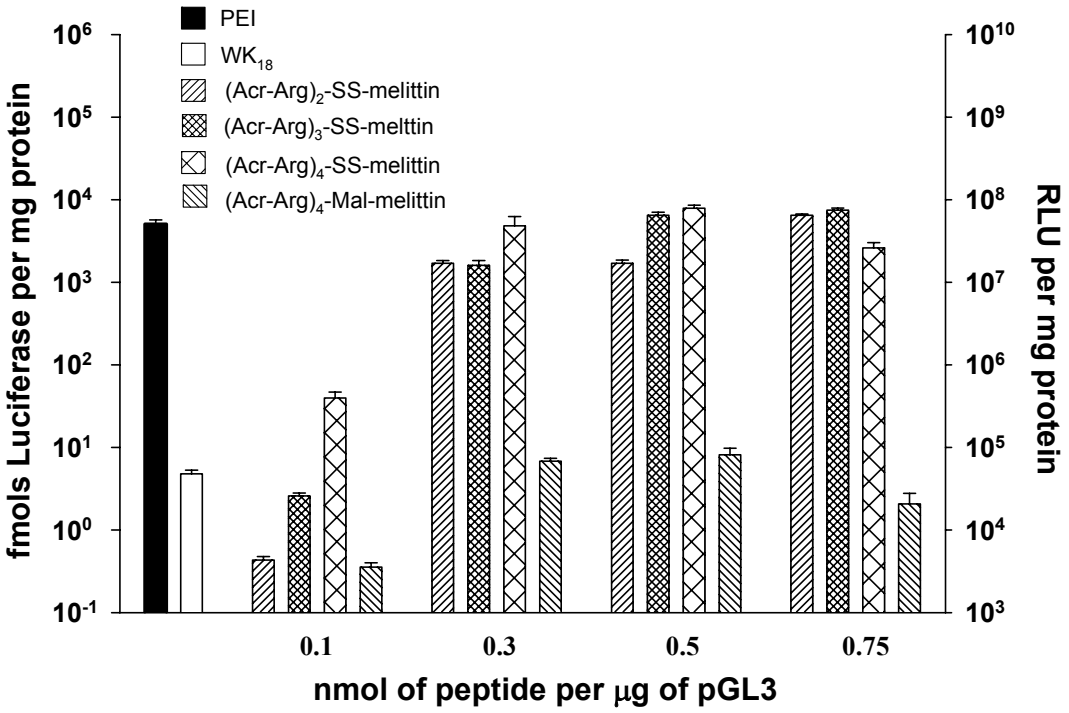


Figure 3-7. *Comparative In Vitro Gene Transfer Potency of Polyacridine-melittin Polyplexes.* CHO cells were transfected with increasing amounts of peptide (0.1, 0.35, 0.5, and 0.75 nmol peptide per μg DNA) combined with 10 μg pGL3. The luciferase expression determined at 24 hrs represents the mean (n=3) and standard deviation for three independent transfections.

$(Acr\text{-}Arg)_4$-Mal-melittin which differed only by the reducibility of the linkage between the anchor and melittin (Figure 3-7). Transfections conducted with 10% serum revealed a 2-fold increase in expression mediated by $(Acr\text{-}Arg)_4$-SS-melittin versus 2% serum (Figure 3-8A).

A broader panel of polyacridine-melittin peptides were combined with pGL3 at a fixed stoichiometry of 0.5 nmol per μg of pGL3 and used to mediate gene expression in HepG2, 3T3, and CHO cells. As illustrated in Figure 3-9, polyacridine-melittin peptides of the $(Acr\text{-}Arg)_{2\text{-}4}$-SS-melittin series produced the highest gene transfection in all three cell lines, with levels similar to that of PEI (9:1 N:P). By comparison, $(Acr\text{-}Lys)_4$-SS-

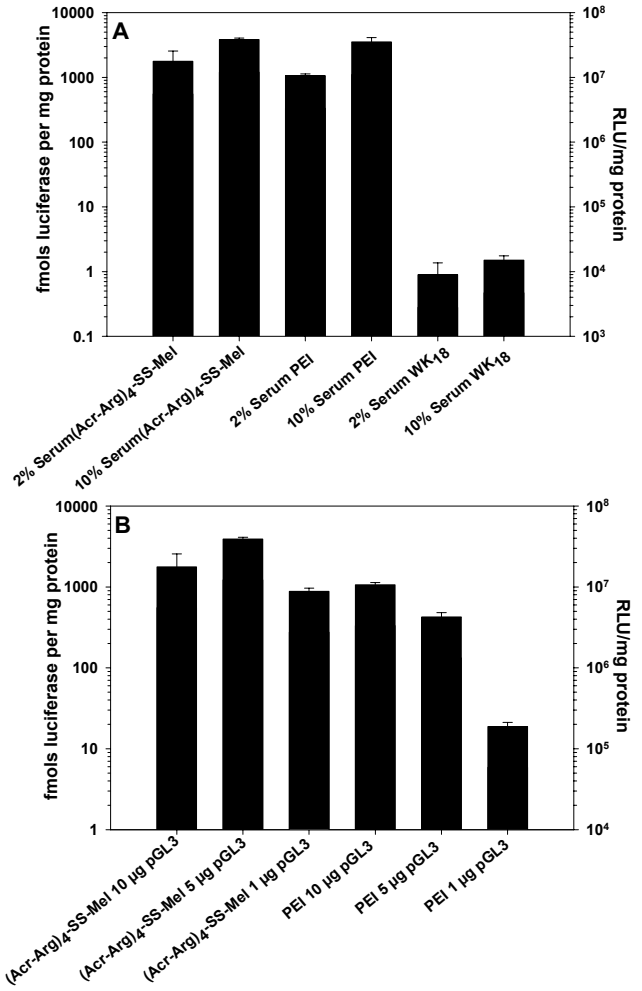


Figure 3-8. *pGL3 dose response and Serum Effects on (Acr-Arg)$_4$-SS-Mel Mediated Transfection.* (Acr-Arg)$_4$-SS-melittin transfections were conducted by varying the percentage of serum contained within the transfect media, supplemented with 2% or 10% FBS. The overall results demonstrate a subtle increase in gene transfection efficiency for 10 µg pGL3 polyplexes formed with 0.5 nmol per µg of (Acr-Arg)$_4$-SS-melittin, PEI, and 0.2 nmol per µg of $WK_{18}$ when comparing transfections conducted with media containing 10% serum versus 2% serum (Panel A). Plasmid dose response using 1, 5, and 10 µg of pGL3 were investigated in CHO cells with polyplexes formed with 0.5 nmol per µg of (Acr-Arg)$_4$-SS-melittin and compared to PEI polyplexes (Panel B). The luciferase expression determined at 24 hrs represents the mean (n=3) and standard deviation for three independent transfections.

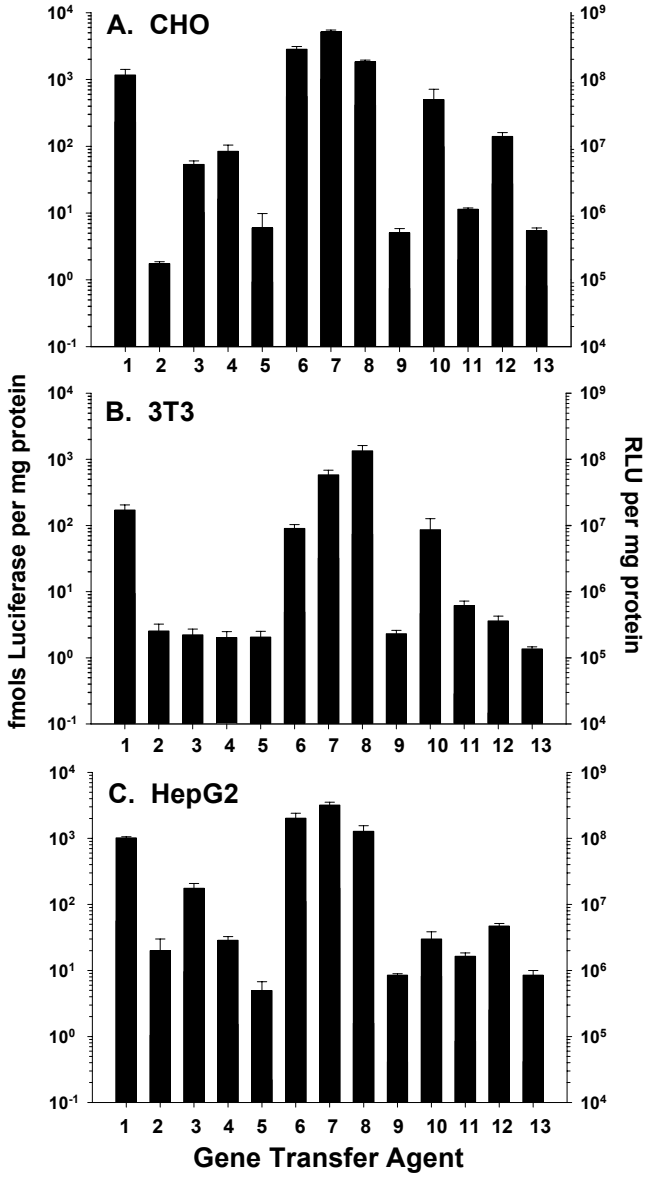


Figure 3-9. *Cell Dependent In Vitro Gene Transfer Potency of Polyacridine-melittin Polyplexes.* The relative gene transfer efficiency of DNA polyplexes was determined in CHO (A), 3T3 (B), and HepG2 (C) cells. Transfections were performed with 10 µg of pGL3 polyplex prepared with 0.5 nmol of peptide per µg of DNA. The gene transfer efficiency mediated by polyacridine-melittin peptides was compared to PEI (N/P 9:1) DNA polyplexes and $WK_{18}$ DNA polyplexes. The bars indicate transfection pGL3 combined with **1**) PEI, **2**)$WK_{18}$, **3**)Dimeric-melittin, **4**) Cys-melittin, **5**) $(Lys(Ac)\text{-}Arg)_4$-SS-melittin, **6**) $(Acr\text{-}Arg)_2$-SS-melittin, **7**) $(Acr\text{-}Arg)_3$-SS-melittin, **8**) $(Acr\text{-}Arg)_4$-SS-melittin, **9**) $(Acr\text{-}Arg)_4$-Mal-melittin, **10**) $(Acr\text{-}Lys)_4$-SS-melittin, **11**) $(Acr\text{-}Lys)_4$-Mal-melittin, **12**) $(Acr\text{-}Leu)_4$-SS-melittin, and **13**) $(Acr\text{-}Leu)_4$-Mal-melittin. The luciferase expression was determined at 24 hrs. The results represent the mean and standard deviation for three independent transfections.

melittin and (Acr-Leu)$_4$-SS-melittin were approximately 10-100 fold less active in gene transfer than (Acr-Arg)$_4$-SS-melittin in all three cell lines. Reducible (Acr-Arg)$_{2-4}$-SS-melittin peptides were 100-1000 fold more active in gene transfer compared to (Acr-Arg)$_4$-Mal-melittin in all three cell lines. The importance of the reductive release of melittin was also determined for (Acr-Lys)$_4$-SS-melittin and (Acr-Leu)$_4$-SS-melittin in all three cell lines. DNA dose response studies in CHO cells of 10, 5, and 1 μg of (Acr-Arg)$_4$-SS-melittin polyplexes revealed a linear response from 1 μg to 5 μg, however the 5 μg dose demonstrated a 2-fold increase in gene transfer efficiency versus the 10 μg dose (Figure 3-8B).

To establish the contribution of polyacridine to DNA binding affinity and gene transfer, the ε-amine of lysine was modified with an acetyl group to prepare (Lys(Ac)-Arg)$_4$-SS-melittin. Gene transfer mediated by (Lys(Ac)-Arg)$_4$-SS-melittin wasapproximately 100-1000 fold less relative to (Acr-Arg)$_4$-SS-melittin in all three cell lines (Figure 3-9). To further establish the importance of the anchor peptides, Cys-melittin and Dimeric-melittin were used to mediate gene transfer (Figure 3-9). Both mediated gene transfer that was 10-100 fold lower than (Acr-Arg)$_{2-4}$-SS-melittin, demonstrating the importance of the polyacridine anchor in this gene transfer system. Gene transfer efficiency mediated by (Acr-X)$_n$Cys peptides were similar to the control peptide WK$_{18}$.

The toxicity of polyacridine DNA polyplexes was assessed by MTT assay on CHO, HepG2 and 3T3 cells (Table 3-3). (Acr-Arg)$_{2-3}$-SS-melittin DNA polyplexes display no toxicity relative to control. However, (Acr-Arg)$_4$-SS-melittin and (Acr-Arg)$_4$-Mal-melittin polyplexes resulted in 70% cell viability while (Lys(Ac)-Arg)$_4$-SS-melittin polyplex was more toxic producing 55% viability. CHO cells treated with (Acr-Lys)$_4$-SS-melittin and (Acr-Lys)$_4$-Mal-melittin polyplexes were 75-86% viable, respectively. Whereas, (Acr-Leu)$_4$-SS-melittin polyplexes were compared to (Acr-Leu)$_4$-Mal-melittin polyplexes that were minimally toxic (Table 3-3).

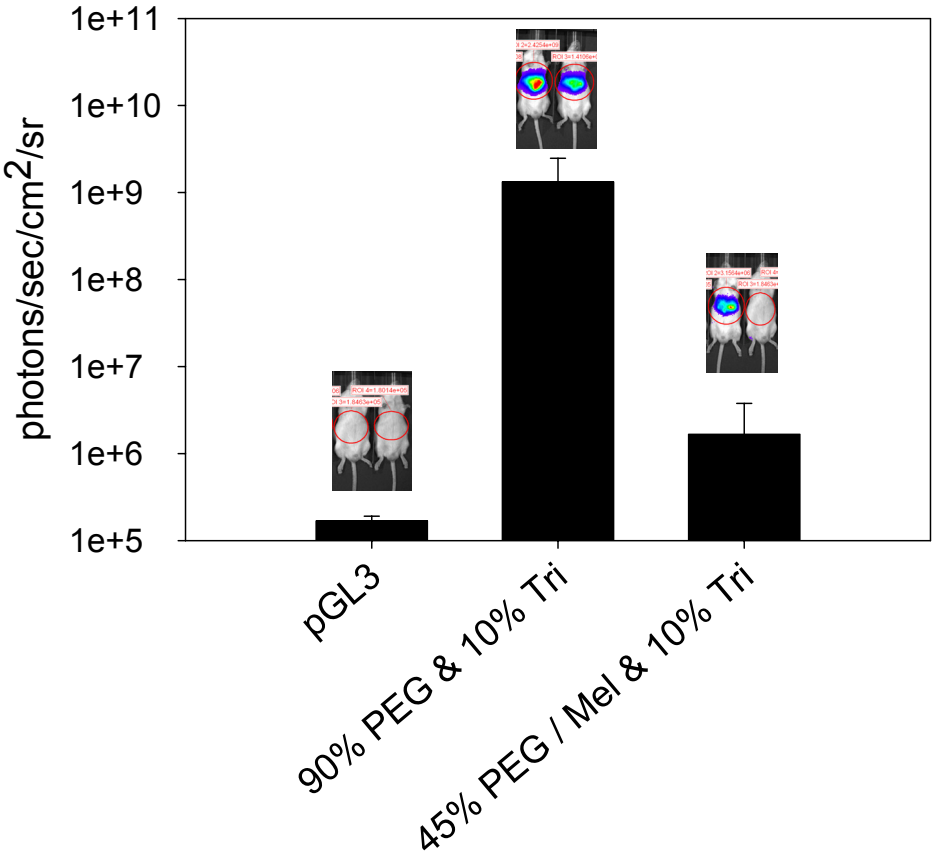


Figure 3-10. *Hydrodynamically Stimulated In Vivo Gene Expression with Melittin Polyplexes.* Polyplexes formed with 5 µg pGL3 and 90% $(Acr\text{-}Arg)_4$-Cys-Mal-PEG (PEG) and 10% $(Acr\text{-}Arg)_4$-Cys-TRI (TRI) or 45% $(Acr\text{-}Arg)_4$-Cys-Mal-PEG, 45% $(Acr\text{-}Arg)_4$-SS-melittin (Mel), and 10% $(Acr\text{-}Arg)_4$-Cys-TRI at 0.5 nmol per µg are dosed by i.v. tail vein injection. Following a 5 min delay, a stimulatory hydrodynamic dose of normal saline (9 wt/vol% of the body weight; 1.8 – 2.25 ml based on 20-25 g mice) was administered over 5 sec according to a published procedure (*140, 141*). After 24 hrs, luciferase expression was evaluated by BLI. The results establish transfection efficiencies for 45% PEG, 45% melittin, and 10% TRI polyplexes of $10^6$ photons/sec/$cm^2$/sr, similar to the levels previously observed with a polymerizable melittin system (*26*). Stimulated luciferase expression with 90% PEG and 10% TRI polyplexes produces $10^9$ photons/sec/$cm^2$/sr, surprisingly similar to expression observed with a direct 5 µg pGL3 hydrodynamic dose (*26, 142*). A delay of 5 min following tail vein administration of 5 µg pGL3 results in a BLI response near background of $10^5$ photons/sec/$cm^2$/sr due to plasmid degradation in the systemic circulation. The luciferase expression determined at 24 hrs represents the mean (n=3) and standard deviation for three independent transfections.

In vivo gene transfer was investigated following formulation of pGL3 (5 μg) polyplexes with either 45% $(Acr\text{-}Arg)_4$-Cys-Mal-PEG, 45% $(Acr\text{-}Arg)_4$-SS-melittin, and 10% $(Acr\text{-}Arg)_4$-Cys-TRI or 90% $(Acr\text{-}Arg)_4$-Cys-Mal-PEG and 10% $(Acr\text{-}Arg)_4$-Cys-TRI and dosed by i.v. tail vein injection followed by a stimulatory hydrodynamic dose with a dwell time of 5 min (*26*). A control consisting of tail vein dose of 5 μg pGL3 followed by a 5 min delayed hydrodynamic dose resulted in $10^5$ photons/sec/$cm^2$/sr due to circulatory degradation, while a stimulated formulation of 45% PEG, 45% melittin, and 10% TRI produced a BLI response of $10^6$ photons/sec/$cm^2$/sr, similar to transgene expression observed with a targeted polymerizable melittin system (Figure 3-10) (*26*). However, a stimulated dose consisting of 90% PEG and 10% TRI produced a BLI response of $10^9$ photons/sec/$cm^2$/sr, surprisingly similar to a direct hydrodynamic dose of 5 μg of pGL3 (*26, 142*), suggesting a stabilization and protection of plasmid DNA while in the blood (Figure 3-10). It should be noted that a non-stimulated standard tail vein dose of 5 μg of pGL3 polyplexed with 45% PEG, 45% melittin, and 10% TRI dose not produce measurable luciferase expression as observed by BLI (data not shown).

## Discussion

The endosome has been proposed as one of the major barriers that limits the gene transfer efficiency of non-viral gene delivery systems (*130*). To increase the endosomal escape of plasmid DNA, many prior studies have incorporated fusogenic peptides into experimental delivery systems (*31, 46, 59, 72, 78, 79, 131-133*). Most often, a fusogenic peptide is linked to a PEI or polylysine to allow for multi-valent reversible ionic binding with the phosphate backbone of DNA (*46-48*). While this approach often leads to significant increases in gene transfer efficiency in vitro, ionic interactions are relatively weak leading to premature dissociation of the carrier in vivo and degradation of the DNA (*36*). To overcome weak binding, higher molecular weight polycations are used. These can be prepared with reducible linkages that revert to low molecular weight, lower

affinity polycations and trigger the release of DNA inside the cell (*26, 33, 40, 41, 134, 135*). However, despite numerous attempts, i.v. dosed polycationic DNA polyplexes are unable to produce therapeutic levels of gene expression (*26*).

We have therefore explored an alternative method of binding fusogenic peptides to plasmid DNA by reversible intercalation. Preliminary studies suggested that a single acridine binds to DNA through intercalation but with relatively weak affinity. Consequently, we sought to increase the binding affinity by preparing polyacridines. Considering the pioneering studies of Szoka who developed a synthetic scheme to prepare a diacridine glycopeptide (*123*), Vierling with a single acridine modified nuclear localizing peptide (*11*), Vinogradov with a tri-acridine dendrimer functionalized with PEG-NLS chimera (*7-9*), and Nielsen who prepared and tested di and triacridine nuclear localization peptides (*10*), we sought to simplify the post-synthetic modification approach of Chapter 2 that would allow us to extend the valency of polyacridine to four or more acridine units and control the charge of polyacridine DNA polyplexes. We therefore adopted a strategy reported by Ueyama et al. (*120*), who demonstrated that polyacridine peptides could be prepared from Fmoc-Lys(Acr) using solid phase synthesis. Several early attempts at synthesis established that polyacridine peptides could be prepared in good yield (>30%) provided that coupling was conducted with HBTU and that a spacing amino acid was used that had a bulky side chain or protecting group. Using Gly as a spacing amino acid resulted in poor yields.

The synthetic design of polyacridine peptides took into account the relative DNA binding affinity by varying polyacridine repeat, the influence of the spacing amino acid on gene transfer, and linkage between polyacridine and a melittin fusogenic peptide. As indicated in Figures 3-7 and 3-9, there is a strong dependency on the nature of the linkage between polyacridine and melittin in relationship to the gene transfer efficiency. A reducible disulfide bond provided a means for the triggered release of melittin either at or inside the cell. The reduction of the disulfide bond greatly diminishes the affinity of

melittin for DNA, releasing it and unmasking its membrane lytic activity (Figure 3-6C). The released melittin apparently enhances gene transfer by lysis of endosomal membranes that then allows the DNA to more efficiently reach the cytosol and the nucleus, resulting in gene expression that equals or surpasses that of PEI in multiple cell lines (Figure 3-9). In support of this mechanism, polyacridine linked to melittin by a non-reducible maleimide is 1000-fold less active in gene transfer, despite its equivalent membrane lysis potency against RBCs (Table 3-1). These results agree with previously observed improved gene transfer mediated by a reductively triggered release of a fusogenic peptide from a gene delivery system (*47, 91*).

The length of the polyacridine repeat appears to be less important for in vitro gene transfer, since repeats of 2, 3 and 4 (Acr-Arg)-SS-melittin all produced nearly equivalent gene transfer in three cell lines (Figure 3-9). However, it is clear that $(Acr\text{-}Arg)_2$-SS-melittin has lower affinity for DNA as indicated by its ability to displace an intercalator dye (Figure 3-4B). The lower affinity results in larger DNA polyplexes as determined by QELS (Table 3-3) and AFM (Figure 3-5B). However, larger polyplexes also sediment more efficiently, facilitating in vitro gene transfer.

The spacing amino acid of Arg, Lys or Leu within a $(Acr\text{-}X)_4$-SS-melittin only slightly influences their affinity for binding DNA (Figure 3-4C). Each of the resulting polyplexes possessed comparable size, charge and shape as determined by QELS, zeta potential and AFM (Table 3-3, Figure 3-5). However, the gene transfer efficiency was influenced significantly by the identity of the spacing amino acid in the order of Arg > Lys > Leu (Figure 3-9). In each case, and in each cell line, the reducible polyacridine-melittin peptide mediated greater expression than the non-reducible analogue. The mechanism by which the spacing amino acid influences gene transfer efficiency is unclear. However, it is clear that polyacridine is necessary to mediate significant gene transfer. A control peptide, $(Lys(Ac)\text{-}Arg)_4$-SS-melittin, was fully active in membrane

lysis but proved to be approximately 1000-fold less active than $(Acr\text{-}Arg)_4$-melittin in mediating gene transfer (Figure 3-9).

The lytic potency of melittin on cells in culture has been well documented (*81, 82*). However, this toxicity can be overcome by polymerization of melittin through disulfide bonds resulting in its neutralization due to high affinity binding to DNA (*42*). It is apparent that even dimeric-melittin can bind to DNA and mediate moderate gene transfer (Figure 3-9). The MTT assay did establish that polyacridine-melittin peptides are moderately toxic (approx 50-70% viable) when added to DNA at 0.5 nmol of peptide per μg of DNA or higher (Table 3-3). However, this toxicity is the result of saturation of the DNA with polyacridine peptide resulting in unbound peptide that can lyse cells.

In vivo transfer capabilities afforded by polyacridine-melittin based polyplexes followed by hydrodynamic stimulation produced by a BLI response similar to a previously reported study from our lab (Figure 3-10) (*26*). Unfortunately the formulation of polyacridine-melittin within a multi-component complex with targeting ligand and PEG peptide do not represent an overall improvement in stimulated gene expression. However, the experiment does provide the first step towards creating complex gene delivery systems composed of individual characterizable components, all incorporated with the desire to fulfill a specialized purpose of achieving targeted gene expression in a specific organ or tissue.

Surprisingly, a multi-component complex composed of 90% PEG and 10% TRI produced robust gene expression following a 5 minute delayed stimulatory HD dose (Figure 3-10), suggesting the $(Acr\text{-}Arg)_4$-Cys peptide scaffold is capable of stabilizing plasmid DNA from degradation while in the blood, where naked DNA is almost immediately degraded (*143*). The stimulated gene expression observed after tail vein i.v. dosing offers the opportunity to conduct several structure activity relationships in respect to the polyacridine DNA binding peptide in an effort to increase expression levels after a stimulatory HD dose and to increase polyplex stability in vivo. The HD stimulatory

phenomenon may allow the investigation of hepatocyte targeting effects with regard to expression levels following synthesis of control glycopeptide targeting ligands.

In conclusion, we have described an optimized polyacridine DNA binding anchor that, when linked with melittin through disulfide bond, produces potent in vitro gene transfer. The polyacridine anchor is designed to be optimized for either in vitro or in vivo gene transfer by controlling the binding affinity to DNA and charge of resulting DNA polyplexes. Furthermore, we have demonstrated the modularity of the Cys residue as it allows coupling of fusogenic peptides, targeting ligands, and PEG. These attributes should allow polyacridine several unique advantages compared to other polycationic DNA binding peptides and polymers.

# CHAPTER 4

# METABOLICALLY STABILIZED LONG-CIRCULATING PEGYLATED POLYACRIDINE PEPTIDE POLYPLEXES RESULT IN HYDRODYNAMICALLY STIMULATED GENE EXPRESSION IN LIVER


## Abstract

To advance the observation of stimulated expression in Chapter 3, a new panel of PEGylated polyacridine peptides were developed and tested in mice. The peptides of the general structure $(Acr\text{-}X)_n$, possessed from 2-6 repeats of Lys(Acr), spaced by amino acid X. The number of Acr repeats and the identity of the spacing amino acid were studied in relation to the DNA binding affinity, metabolic stability, pharmacokinetic half-life and in vivo gene transfer efficiency. Each peptide possessed a C-terminal Cys that was modified either reducibly or non-reducibly with polyethylene glycol ($PEG_{5000\ Da}$). PEGylated polyacridine peptides were examined for DNA binding affinity by dye displacement and gel band shift, for particle size and zeta potential using QELS, and for shape using atomic force microscopy (AFM). Substitution of $(Acr\text{-}X)_4$-Cys-PEG, with X as either Lys, Arg, Leu or Glu, established that polyacridine peptides possessing a Lys and Arg bind with higher affinity than peptides possessing Leu and Glu. Increasing the number of Acr-Lys repeats from 2 to 6 resulted in increased DNA binding affinity and greater protection of DNA from DNase. Pharmacokinetic analysis of $(Acr\text{-}Lys)_6$-PEG polyplexes established the metabolic stability of plasmid DNA with a long-circulatory half-life of 3 hrs in blood. A high level of luciferase expression was stimulated in the liver following a tail vein dose of PEGylated polyacridine peptide pGL3 polyplexes (1 μg in 50 μl). Administration of the stimulatory hydrodynamic dose of normal saline at times ranging from 5-60 min post-DNA administration, resulted in liver expression that was equal or greater than the level mediated by direct hydrodynamic dosing of pGL3 (1 μg). The results establish the unique

properties of PEGylated polyacridine peptides that facilitate reversible binding to plasmid DNA, protect it from DNase in vivo, allow it to circulate for hours, and release transfection-competent DNA into the liver to mediate high-level gene expression.

## Introduction

New gene delivery agents are needed that function by efficiently mediating targeted non-viral gene delivery in vivo. Some of the most successful delivery agents developed to date, such as PEI and cationic lipids, produce robust gene transfer in vitro, but fail to mediate significant gene expression in vivo (*43, 144-150*). In contrast, hydrodynamic (HD) dosing and electroporation are proven physical methods that are highly efficient in delivering plasmid DNA to animals and may find utility in humans (*140, 151-156*). However, due to the invasiveness of HD dosing, there is a need for new gene delivery agents that produce gene expression at levels comparable to HD dosing, but without the requirement of high-volume administration.

Most i.v. dosed non-viral gene delivery systems are cationic polyplexes or lipoplexes, the primary exception being anionic liposomes with encapsulated DNA (*157*). To increase their compatibility with blood, cationic polyplexes are modified with polyethylene glycol (PEG) to block albumin binding and to "stealth" their rapid endocytosis by cells of the reticuloendothelial system (RES) (*41, 43, 158-160*). Despite these attempts, most PEGylated cationic polyplexes still quickly biodistribute to the liver, and are taken-up primarily by Kupffer cells (*36, 39*). Few, if any, of these experimental i.v. dosed gene delivery systems have produced appreciable gene expression in the liver (*131, 132*), especially when compared to the level of luciferase expression from an equivalent dose of DNA delivered hydrodynamically (*140, 141*).

To develop non-viral gene delivery agents that function with greater efficiency in vivo following i.v. dosing, it is necessary to control the size, charge and metabolic stability of polyplexes (*44*). The cationic surface charge of most polyplexes results from

residual unpaired amines on the cationic polymer used to condense DNA. Anionic polyplexes may be more blood-compatible, but would require a new mode of binding polymers to DNA, not based on electrostatic interaction.

The use of polyintercalation has been shown to increase the binding affinity of small polymers and peptides to DNA (*7-11, 123, 137*). The results of Chapters 2 and 3 have demonstrated that polyacridine peptides possessing four Lys(Acr) residues (ε amine of Lys is modified with acridine), spaced by either a Lys or Arg, produce high affinity binding for plasmid DNA (*161*). Modification of polyacridine peptides with either a fusogenic peptide (melittin) or an N-glycan (high-mannose) produced gene transfer agents that formed cationic polyplexes resulting in high level selective gene transfer in vitro (*161, 162*). PEGylated polyacridine peptides have been shown to bind to plasmid DNA and produce unique, metabolically stable, anionic open-polyplexes that are capable of mediating gene transfer in vivo when delivered by intramuscular-electroporation (*163*).

Given the observation of potent gene transfer of a formulation hydrodynamically simulated (Figure 3-10) in chapter 3, this has led to the hypothesis that polyacridine peptide chain length and subsequent DNA binding affinity is vitally important for providing protection from premature vector dissociation and plasmid DNA degradation in vivo. Furthermore, we predict that polyacridine peptides of longer chain lengths will provide superior plasmid DNA protection, which in turn will allow for longer delay times between primary and stimulatory dose while producing robust gene expression in vivo. In this chapter we prepared a panel of PEGylated polyacridine peptides beginning with the core sequence $(Acr\text{-}X)_4$-Cys to establish their utility in mediating gene expression following i.v. dosing. The results establish a clear structure-activity relationship by which protection of the DNA in blood and liver by a PEGylated polyacridine peptide results in the ability to stimulate high level gene expression in liver with a delayed hydrodynamic dose of saline. The results also establish the ability to extend the circulatory half-life of a

significant percentage of i.v. dosed DNA, which is an important prerequisite of achieving targeted gene delivery to organs and tissues. The synthetic adaptability of polyacridine peptides, along with the ability to prepare either anionic-open or cationic-closed-polyplexes that mediate gene transfer in vivo, demonstrate the unique importance of polyintercalative binding to achieve gene delivery.

## Materials and Methods

Unsubstituted Wang resin, 9-hydroxybenzotriazole, Fmoc-protected amino acids, O-(7-Azabenzo-triazol-1-yl)-N,N,N’,N’-tetramethylurionium hexafluorophosphate (HATU), O-(Benzotriazole)-N,N,N',N'-tetramethyluronium hexafluorophosphate (HBTU), Fmoc-Lysine-OH, and N-Methyl-2-pyrrolidinone (NMP) were obtained from Advanced ChemTech (Lexington, KY). N,N-Dimethylformamide (DMF), trifluoroacetic acid (TFA), and acetonitrile were purchased from Fisher Scientific (Pittsburgh, PA). Diisopropylethylamine, piperidine, acetic anhydride, Tris(2-carboxyethyl)-phosphine hydrochloride (TCEP), 9-chloroacridine, and thiazole orange were obtained from Sigma Chemical Co. (St. Louis, MO). Triisopropylsilane (TIS), 1, 2-ethanedithiol (EDT) was from Aldrich (Milwaukee, WI). Agarose was obtained from Gibco-BRL. mPEG-maleimide and mPEG-OPSS (5,000 Da) were purchased from Laysen Bio (Avab, AL). D-Luciferin and luciferase from *Photinus pyralis* were obtained from Roche Applied Science (Indianapolis, IN). pGL3 control vector, a 5.3 kb luciferase plasmid containing a SV40 promoter and enhancer, was obtained from Promega (Madison, WI). pGL3 was amplified in a DH5α strain of *Escherichia coli* and purified according to manufacturer’s instructions.

### Synthesis of 9-phenoxyacridine and Fmoc Lysine(Acridine)-OH

9-phenoxyacridine was synthesized with modification from the methods of Tung et al (*121*). Briefly, 12 g of phenol (127.5 mmol) and 0.72 g of sodium hydroxide (18

mmol) were heated to 100ºC. To the liquified phenol, 2.8 g of 9-chloroacridine (13.105 mmol) was added and stirred vigorously for 1.5 hrs. The reaction was quenched by the addition of 100 ml of 2 M sodium hydroxide then allowed to sit at RT overnight. A yellow precipitate was filtered, washed with water and dried in vacuo over $CaSO_4$ (3.4822g, 12.835 mmol, 97.9%, M.P. 123 – 124 º C, TLC, 15 : 5 : 1 : 0.5, ethyl acetate / methanol / hexane / acetic acid, $R_f = 0.18$). $^1H$ NMR (DMSO-$d_6$) δ 8.23 (d, 2H), 8.04 (d, 2H), 7.88 (t, 2H), 7.59 (t, 2H), 7.32 (t, 2H), 7.08 (t, 1H), 6.88 (d 2H).

Fmoc-Lysine(Acridine)-OH was prepared by adding 2.18 g of Fmoc-Lys-OH (5.91 mmol) in liquid phenol (6.781 g, 73.01 mmol) to 9-phenoxyacridine (3 g, 11.06 mmol), and then heated at 60 ºC for 4 hrs under an argon atmosphere. Diethyl ether (80 ml) was then added while stirring vigorously until a yellow precipitate formed that was immediately recovered by filtration and washed repeatedly with diethyl ether. The product was allowed to dry ($CaSO_4$) overnight under vacuum (2.90 g, 5.32 mmol, 90%), M.P. 135-140ºC**,** TLC: 1:1, 0.1 v/v % TFA / acetonitrile, $R_f = 0.75$). MS: $(M + H^+)^{1+}$= 545.5 m/z. $^1H$ NMR (DMSO-$d_6$) δ 6.7-7.8 (m, 17H), 3.6-3.95 (m, 2H), 3.25-3.53 (br, 3H), 2,06 (m, 1H), 0.8-1.5 (m, 6H).

## Synthesis and Characterization of Polyacridine Peptides

Preparation of the polyacridine peptides reported in Table 4-1 were initially prepared by solid phase peptide synthesis using standard Fmoc procedures with 9-hydroxybenzotriazole and HBTU double couplings on a 30 µmol scale on an Advanced ChemTech APEX 396 synthesizer. Peptides were removed from resin and side chain deprotected using a cleavage cocktail of TFA/triisopropylsilane/water (95:2.5:2.5 v/v/v) for 3 hrs followed by precipitation in cold ether. Precipitates were centrifuged for 10 min at 4000 rpm at 4ºC and the supernatant decanted. Peptides were then reconstituted with 0.1 v/v % TFA and purified to homogeneity on RP-HPLC by injecting 0.5-2 µmol onto a Vydac C18 semipreparative column (2 x 25 cm) eluted at 5 ml/min with 0.1 v/v % TFA

with an acetonitrile gradient of 10-30 v/v % over 30 min while monitoring acridine absorbance at 409 nm. The major peak was collected and pooled from multiple runs, concentrated by rotary evaporation, lyophilized, and stored at -20ºC. Purified peptides were reconstituted in 0.1 v/v % TFA and quantified by absorbance (acridine $\varepsilon_{409\ nm}$ = 9266 $M^{-1}$ $cm^{-1}$ assuming additivity of ε for multiple acridines) to determine isolated yield (Table 4-1). Purified peptides were characterized by LC-MS by injecting 2 nmol onto a Vydac C18 analytical column (0.47 x 25 cm) eluted at 0.7 ml per min with 0.1 v/v % TFA and an acetonitrile gradient of 10-55 v/v % over 30 min while acquiring ESI-MS in the positive mode.

## Optimization of Synthetic Conditions for Polyacridine (Acr-Lys)$_2$-Cys Peptides.

Due to the low yields afforded by standard HBTU/HOBt coupling for (Acr-Lys)$_{6\ and\ 8}$–Cys peptides (Table 4-1), the more robust aminium coupling reagent HATU was investigated as a replacement for HBTU and coupling efficiency was investigated qualitatively by the Kaiser test (presence of blue resin beads indicate incomplete coupling) (*164, 165*). Coupling of Fmoc-Lys(Acr)-OH was judged complete after two coupling cycles, while the spacing amino acid Fmoc-Lys(Boc)-OH was judged complete after three cycles using HATU as the coupling reagent. To improve the solubility of Fmoc-Lys(Acr)-OH in DMF, Fmoc-Lys(Acr)-OH was preactivated by addition of 0.4 mol equivalents of HATU relative to amino acid to generate the DMF soluble reactive intermediate Fmoc-Lys(Acr)-OBt ester. The aforementioned optimization steps improved the crude yields of (Acr-Lys)$_2$-Cys to 93.2% from an initial yield of 58.9% using HBTU/HOBt double coupling, resulting in the final synthetic protocol including 9-hydroxybenzotriazole and HATU activation while employing double coupling of Fmoc-Lys(Acr)-OH and triple coupling for the spacing amino acid while using a 5-fold excess of amino acid over resin and omitting N-capping of truncated peptide species.

Conditions for the removal of $(Acr\text{-}Lys)_2$-Cys from resin and side chain deprotection were also investigated by varying the percentage and identity of the side chain scavenger included in the cleavage cocktail (Figure 4-3). Cleavage cocktails investigated include: TFA/water (95:5 v/v), TFA/water/triisopropylsilane (TIS) (95:4.5:0.5 v/v/v), TFA/water/TIS (95:2.5:2.5 v/v/v), TFA/water/TIS (90:5:5 v/v/v), TFA/water/ethanedithiol (EDT) (95:4:1 v/v/v), and TFA/water/EDT (95:2:3 v/v/v). Peptides were most successfully removed from resin and side chain deprotected using a cleavage cocktail of TFA/water/EDT (93:3:4 v/v/v) for 3 hrs as judged by analytical RP-HPLC by injecting 2.5 nmol on an analytical Vydac C18 analytical column and eluted at 0.7 ml per min with 0.1 v/v % TFA and an acetonitrile gradient of 10-45 v/v % over 30 min (Figure 4-3). Combined, the improvements in synthetic methodology and cleavage and deprotection protocols discovered by modeling the $(Acr\text{-}Lys)_2$-Cys synthesis afforded higher yields when applied to $(Acr\text{-}Lys)_{6 \text{ and } 8}$–Cys peptides (Table 4-1).

## Synthesis and Characterization of PEGylated Polyacridine Peptides

PEGylation of the Cys residue on $(Acr\text{-}X)_n$-Cys was achieved by reacting with 1 mol equivalent of peptide with 1.1 mol equivalent of $PEG_{5000\ Da}$–maleimide or $PEG_{5000\ Da}$-OPSS in 4 ml of 10 mM ammonium acetate buffer pH 7 for 12 hrs at RT. PEGylated peptides were purified by semipreparative HPLC as previously described and eluted with 0.1 v/v % TFA with an acetonitrile gradient of 25-65 v/v % while monitoring acridine at 409 nm. The major peak was collected and pooled from multiple runs, concentrated by rotary evaporation, lyophilized, and stored at -20ºC. Counter-ion exchange was accomplished by chromatography on a G-25 column (2.5 x 50 cm) equilibrated with 0.1 v/v % acetic acid to obtain the peptide in an acetate salt form. The major peak corresponding to the PEG-peptide eluted in the void volume (100 ml) was pooled, concentrated by rotary evaporation, and freeze-dried. PEG-peptides were reconstituted in

water and quantified by $Abs_{409nm}$ to determine isolated yield (Table 4-1). PEG-peptides were characterized by MALDI-TOF MS by combining 1 nmol with 10 µl of 2 mg per ml α-cyano-4-hydroxycinnamic acid (CHCA) in 50 v/v % acetonitrile and 0.1 v/v % TFA. Samples were spotted onto the target and ionized on a Bruker Biflex III Mass Spectrometer operated in the positive ion mode.

## Synthesis and Characterization of Polyacridine-(Acr-Lys)$_6$-Cys-Mal-PEG

PEGylation of the Cys residue on (Acr-Lys)$_6$-Cys was achieved by reacting 1 mol equivalent of peptide with 1.2 mol equivalents of $PEG_{5000\ Da}$–maleimide in 10 mM ammonium acetate buffer pH 7 for 14 hr at RT. Reactions were monitored with analytical RP-HPLC by taking aliquots at time points of t=0, 1, and 14 hrs by injecting 1.2 nmol (relative to (Acr-Lys)$_6$-Cys) of the reaction mixture and eluting with 0.1 v/v % TFA with an acetonitrile gradient of 10-55% over 30 min while monitoring absorbance at 280 nm. Once the reaction was judged complete, PEGylated peptides were purified by semipreparative HPLC as previously described and eluted with 0.1 v/v % TFA with an acetonitrile gradient of 25-65 v/v % while monitoring acridine at 409 nm. The major peak was collected and pooled from multiple runs, concentrated by rotary evaporation, lyophilized, and stored at -20ºC. Counter-ion exchange and characterization were done as previously described.

## Formulation and Characterization of PEGylated Polyacridine Peptide Polyplexes (In Collaboration with Christian Fernandez)

The relative binding affinity of PEGylated polyacridine peptides for DNA was determined by a fluorophore exclusion assay (*22*). pGL3 (200 µl of 4 µg/ml in 5 mM Hepes pH 7.5 containing 0.1 µM thiazole orange) was combined with 0, 0.05, 0.1, 0.25, 0.35, 0.5, or 1 nmol of PEGylated polyacridine peptide in 300 µl of Hepes and allowed to

bind at RT for 30 min. Thiazole orange fluorescence was measured using an LS50B fluorometer (Perkin-Elmer, U.K.) by exciting at 498 nm while monitoring emission at 546 nm with the slit widths set at 10 nm. A fluorescence blank of thiazole orange in the absence of DNA was subtracted from all values before data analysis. The data are presented as nmol of peptide per μg pGL3 versus the percent fluorescence intensity ± the standard deviation determined by three independent measurements.

The particle size and zeta potential were determined by preparing 2 ml of polyplex in 5 mM Hepes pH 7.5 at a DNA concentration of 30 μg per ml and a PEGylated polyacridine peptide stoichiometry of 0, 0.2, 0.3, 0.4, 0.5, 0.6, 0.8 or 1 nmol per μg of DNA. The particle size was measured by quasi-elastic light scattering (QELS) at a scatter angle of 90º on a Brookhaven ZetaPlus particle sizer (Brookhaven Instruments Corporation, NY). The zeta potential was determined as the mean of ten measurements immediately following acquisition of the particle size.

The shape of PEGylated polyacridine polyplexes were determined using atomic force microscopy (AFM). pGL3 alone, or anionic PEGylated polyacridine polyplexes at 0.2 nmol of peptide per μg of DNA, were prepared at a concentration of 100 μg per ml of DNA in 10 mM Tris, 1 mM EDTA pH 8. Polyplexes were diluted to 1 μg per ml in 40 mM Hepes, 5 mM nickel chloride at pH 6.7 and deposited on a fresh cleaved mica surface (cationic mica) for 10 min followed by washing with deionized water. Cationic PEGylated polyacridine polyplexes prepared at 0.8 nmol of PEGylated $(Acr\text{-}Lys)_6$ per μg of DNA, at 100 μg per ml of DNA in 10 mM Tris, 1 mM EDTA pH 8 were deposited directly on a freshly cleaved mica surface (anionic mica) and allowed to bind for 10 min prior to washing with deionized water. Images were captured using an Asylum AFM MFP3D (Santa Barbara, CA) operated in the AC-mode using a silicon cantilever (Ultrasharp NSC15/AIBS, Mikro Masch).

## Gel Band Shift and DNase Protection Assay (In collaboration with Christian Fernandez)

pGL3 (1 μg), or pGL3 polyplexes (1 μg) at either 0.2 or 0.8 nmol of $(Acr\text{-}Lys)_{2,\ 4,\ or\ 6}$-PEG, were prepared in 20 μl of 5 mM Hepes buffer pH 7.4. The ability of polyplexes to resist digestion with DNase was determined by incubation with 0.06 U of DNase I for 10 min. Polyplexes were prepared into 500 μl of 0.5 mg per ml proteinase K (in 100 mM sodium chloride, 1% SDS and 50 mM Tris pH 8.0) and incubated at 37°C for 30 min to deactivate DNase. The polyplexes were extracted with 500 μl of phenol/chloroform /isoamyl alcohol (24:25:1) to remove PEGylated peptides, followed by precipitation of DNA with the addition of 1 ml of ethanol. The precipitate was collected by centrifugation at 13,000 g for 10 min, and the DNA pellet was dried and dissolved in 5 mM Hepes buffer pH 7.4. DNA samples were combined with 2 μl of loading buffer and applied to a 1% agarose gel (50 ml) and electrophoresed in TBE buffer at 80 V for 90 min (*32*). The gel was post-stained with 0.1 μg per ml ethidium bromide at 4°C overnight then imaged on a UVP Biospectrum Imaging System (Upland, California).

## Pharmacokinetic Analysis of PEGylated Polyacridine Polyplexes (In collaboration with Christian Fernandez and Sanjib Khargharia)

Radioiodinated pGL3 was prepared as previously described (*143*). Triplicate mice were anesthetized by i.p. injection of ketamine hydrochloride (100 mg per kg) and xylazine hydrochloride (10 mg per kg) then underwent a dual cannulation of the right and left jugular veins. An i.v. dose of $^{125}$I-DNA (3 μg in 50 μl of HBM, 1.2 μCi) or $^{125}$I-DNA polyplex (3 μg) was administered via the left catheter, and blood samples (10 μl) were drawn from the right catheter at 1, 3, 6, 10, 20, 30, 60, 90 and 120 min and immediately frozen, then replaced with 10 μl of normal saline. The amount of radioactivity in each blood time point was quantified by direct γ-counting followed by extraction of the DNA

and separation by gel electrophoresis as described above. The gel was dried on a zeta probe membrane and autoradiographed on a Phosphor Imager (Molecular Devices, Sunnyvale CA) following a 15 hr exposure.

## Biodistribution Analysis of PEGylated Polyacridine Polyplexes (In collaboration with Christian Fernandez and Sanjib Khargharia)

Triplicate mice were anesthetized and a single catheter was placed in the left jugular vein. $^{125}$I-DNA (1.5 μg in 50 μl of HBM, 0.6 μCi) or $^{125}$I-DNA polyplexes (1.5 μg) were dosed i.v. followed by vein ligation. After 5, 15, 30, 60, or 120 min, mice were sacrificed by cervical dislocation and the major organs (liver, lung, spleen, stomach, kidney, heart, large intestine, and small intestine) were harvested, and rinsed with saline. The radioactivity in each organ was determined by direct γ-counting and expressed as the percent of the dose in the organ.

## Hydrodynamic Stimulation and Bioluminescence Imaging (In collaboration with Christian Fernandez and Jason Duskey)

pGL3 (1 μg) was prepared in a volume of normal saline corresponding to 9 wt/vol % of the mouse's body weight (1.8 – 2.25 ml based on 20-25 g mice). The DNA dose was administered by tail vein to 4-5 mice in 5 sec according to a published procedure (*140, 141*). Mice (4-5) were also dosed via tail vein with 1 μg of PEGylated polyacridine polyplex in 50 μl of HBM (5 mM Hepes, 0.27 M mannitol, pH 7.4). At times ranging from 5-120 min, a stimulatory hydrodynamic dose of normal saline (9 wt/vol % of the body weight) was administered over 5 sec. At 24 hrs post-DNA dose, mice were anesthetized by 3% isofluorane, then administered an i.p. dose of 80 μl (2.4 mg) of D-luciferin (30 μg/μl in phosphate-buffered saline). At 5 min following the D-luciferin dose, mice were imaged for bioluminescence (BLI) on an IVIS Imaging 200 Series

(Xenogen). BLI was performed in a light-tight chamber on a temperature-controlled, adjustable stage while isofluorane was administered by a gas manifold at a flow rate of 3%. Images were acquired at a 'medium' binning level and a 20 cm field of view. Acquisition times were varied (1 sec - 1 min) depending on the intensity of the luminescence. The Xenogen system reported bioluminescence as photons/sec/$cm^2$/ seradian in a 2.86 cm diameter region of interest covering the liver. The integration area was transformed to pmols of luciferase in the liver using a previously reported standard curve (*142*). The results were determined to be statistically significant ($p \leq 0.05$) based on a two-tailed unpaired t-test.

## Results

A panel of PEGylated polyacridine peptides were prepared and tested for their ability to bind and transport DNA in vivo. The peptides were designed to test the influence of DNA binding affinity on gene transfer efficiency. To examine the influence of spacing amino acid, four peptides of the general structure $(Acr\text{-}X)_4$-Cys were prepared, where X is either Lys, Arg, Leu or Glu (Table 4-1). As discussed in more detail below, a Lys spacing amino acid proved most efficient in gene transfer, which warranted an expansion of $(Acr\text{-}Lys)_n$ to include repeats of 2, 6 and 8 (Table 4-1). Each polyacridine peptide also possessed a C-terminal Cys residue to allow modification with PEG. During the course of synthesis using $(Acr\text{-}Lys)_2$-Cys as a model peptide, the synthetic yields of polyacridine peptides were improved by substituting HATU for HBTU to activate amino acids during coupling. Preactivation of Fmoc-Lys(Acr)-OH with HATU resulted in formation of the reactive intermediate Fmoc-Lys(Acr)-OBt ester and increased the solubility of the amino acid monomer in DMF, eliminating a common precipitation problem that was observed to occur during longer polyacridine peptide synthesis. The Kaiser test also revealed incomplete coupling of the spacing amino acid after two cycles; addition of a third cycle resulted in a negative Kaiser test, indicating complete coupling

Table 4-1. *PEGylated Polyacridine Peptides*

| **Polyacridine Peptides** | **Mass (calc / obs)[a]** | **%Yield** |
|---|---|---|
| (Acr-Lys)$_2$-Cys | 988.5 / 988.3 | 37 |
| (Acr-Lys)$_4$-Cys | 1855.3 / 1855.1 | 26 |
| (Acr-Lys)$_6$-Cys | 2722.4 / 2722.0 | 1.6 (20)* |
| (Acr-Lys)$_8$-Cys | 3589.5 / 3588.2 | NR (2.5)* |
| (Acr-Arg)$_4$-Cys | 1967.4 / 1967.2 | 30 |
| (Acr-Leu)$_4$-Cys | 1795.3 / 1795.1 | 31 |
| (Acr-Glu)$_4$-Cys | 1859.1 / 1859.0 | 22 |
| **PEGylated Polyacridine Peptides** | **Mass (calc / obs)[b]** | **%Yield** |
| (Acr-Lys)$_2$-Cys-Mal-PEG | 6488 / 6531 | 64 |
| (Acr-Lys)$_4$-Cys-Mal-PEG | 7355 / 7218 | 55 |
| (Acr-Lys)$_6$-Cys-Mal-PEG | 8222 / 8116 | 66 |
| (Acr-Lys)$_8$-Cys-Mal-PEG | 9090 / 8967 | 59 |
| (Acr-Arg)$_4$-Cys-Mal-PEG | 7467 / 7218 | 53 |
| (Acr-Arg)$_4$-SS-PEG | 7467 / 7450 | 44 |
| (Acr-Leu)$_4$-Cys-Mal-PEG | 7295 / 7110 | 46 |
| (Acr-Glu)$_4$-Cys-Mal-PEG | 7359 / 7262 | 35 |

a. Determined by ESI-MS.

b. Determined by MALDI-TOF MS.

NR: Not recoverable by preparatory HPLC

* Yields after optimization of (Acr-Lys)$_x$-Cys peptide synthesis.

of the unprotected N-terminus to the incoming amino acid. The Kaiser test revealed complete coupling of Fmoc-Lys(Acr)-OH to the protected peptide resin. N-capping of un-reacted N-terminal amines was omitted to avoid a side reaction with acridine. The optimization steps taken together increased crude yields of (Acr-Lys)$_2$-Cys from 58.9 to 93.2%.

Cleavage cocktails were also optimized and quality of crude peptide was analyzed by RP-HPLC (Figure 4-1). Figure 4-1A demonstrates a dramatic effect of omitting a scavenger from the cleavage cocktail, resulting in minimal product recovery. Addition of 0.5% TIS improves the quality of crude peptide, resulting in a 47/53% mixture of

product/by-product by comparison of HPLC peak areas (Figure 4-1B). Increasing the amount of TIS in the cleavage cocktail to 2.5% resulted in a peak area ratio of 71/29% for product/by-product (Figure 4-1C). Increasing the amount of TIS to 5% did not result in an appreciable change in peak area ratio of product/by-product (Figure 4-1D). Substitution of TIS with 1% EDT revealed a dramatic improvement in the crude quality of $(Acr\text{-}Lys)_2$-Cys, with a peak area ratio of 89/11% product/by-product (Figure 4-1E). Inclusion of 3% EDT in the cleavage cocktail resulted in the optimal workup protocol, resulting in a peak area ratio of 92/8% product/by-product (Figure 4-1F).

Application of the optimization steps discovered from the synthesis of $(Acr\text{-}Lys)_2$-Cys to the synthesis $(Acr\text{-}Lys)_6$-Cys resulted in a dramatic improvement in crude peptide quality as observed with RP-HPLC (Figure 4-2). The initial synthesis of $(Acr\text{-}Lys)_6$-Cys resulted in a highly heterogeneous crude peptide utilizing HBTU/HOBt double couplings using a cleavage cocktail of TFA:TIS:water (95:5:5 v/v/v)(Figure 4-2A). Employing HATU as the coupling agent while double coupling Fmoc-Lys(Acr)-OH and triple coupling Fmoc-Lys(Boc)-OH and a cleavage cocktail include EDT resulted in a dramatic improvement of crude quality (Figure 4-2B). Pre-activation of Fmoc-Lys(Acr)-OH with HATU to increase DMF solubility during peptide synthesis resulted in a further improvement in crude peptide quality (Figure 4-2C). LC-MS analysis of all crude peptides resulted in positive identification of the product (Figure 4-2C, inset). Under these conditions, $(Acr\text{-}Lys)_n$–Cys with repeats ranging from 2 to 6 were prepared in 20-37% isolated yield, with exception of $(Acr\text{-}Lys)_8$–Cys isolated in 2.5% yield (Table 4-1). Each polyacridine peptide produced an ESI-MS consistent with the calculated mass (Table 4-1).

Conjugation of each polyacridine peptide with PEG was accomplished by reaction of the Cys residues with either PEG-maleimide or PEG-OPSS, resulting in PEGylated polyacridine peptides with a reducible disulfide or a non-reducible maleimide linkage (Scheme 4-1). The reaction was monitored by analytical RP-HPLC in which the

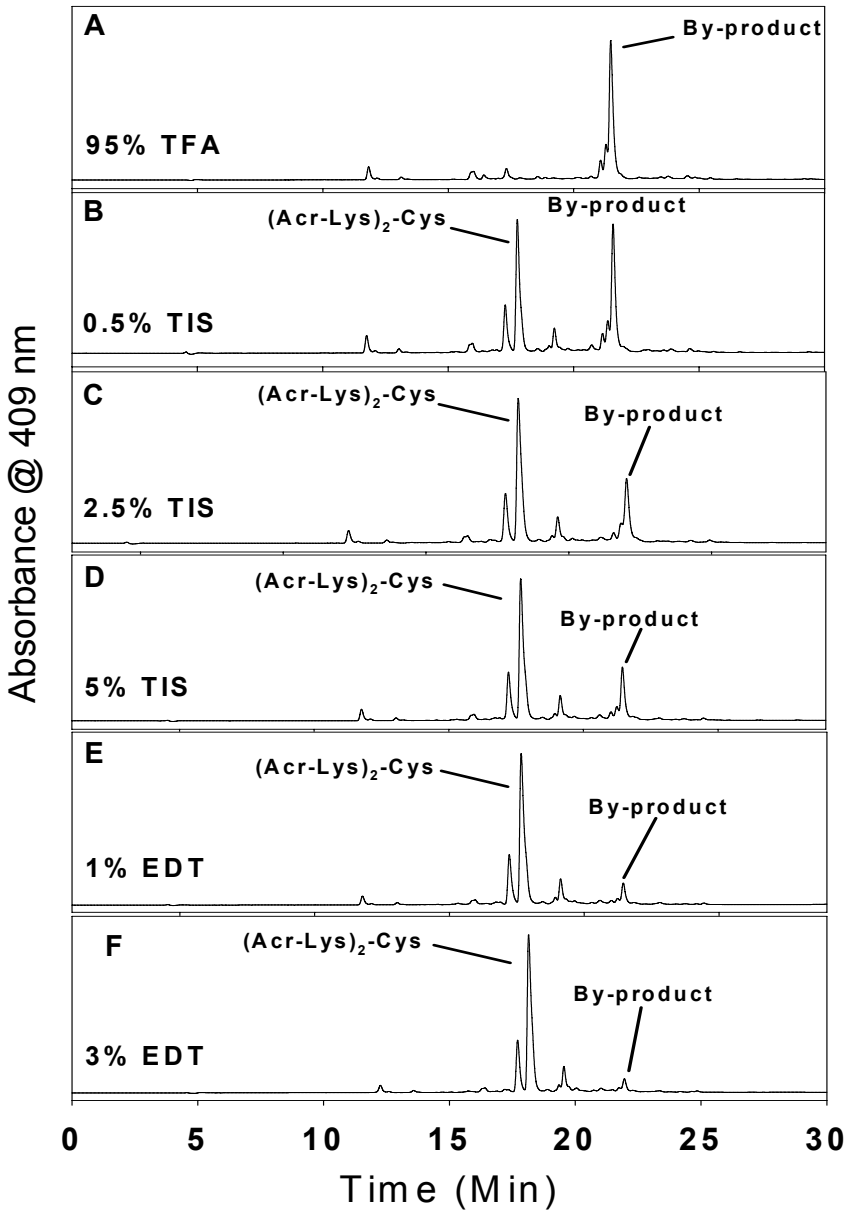


Figure 4-1. *RP-HPLC Analysis of (Acr-Lys)$_2$-Cys Workup Conditions.* Following the synthesis of (Acr-Lys)$_2$-Cys as a model peptide for optimizing synthetic conditions, small aliquots of resin were cleaved from resin and side chain deprotected with varying cleavage cocktails and analyzed by injection of 2.5 nmol of crude peptide with 0.1 v/v % TFA and eluted with a 10-30 v/v % ACN gradient over 30 minutes. Cleavage cocktails tested included; TFA/$H_2O$ (95:5 v/v) (Panel A), TFA/$H_2O$/TIS (95:4.5:0.5 v/v/v) (Panel B), TFA/$H_2O$)/TIS (95:2.5:2.5 v/v/v) (Panel C), TFA/$H_2O$/TIS (90:5:5 v/v/v) (Panel D), TFA/$H_2O$/EDT (95:4:1 v/v/v) (Panel E), and TFA/$H_2O$/EDT (95:2:3 v/v/v) (Panel F). Cleavage cocktails including EDT (Panels E and F) produced the higher quality crude peptide as judged by RP-HPLC analysis.

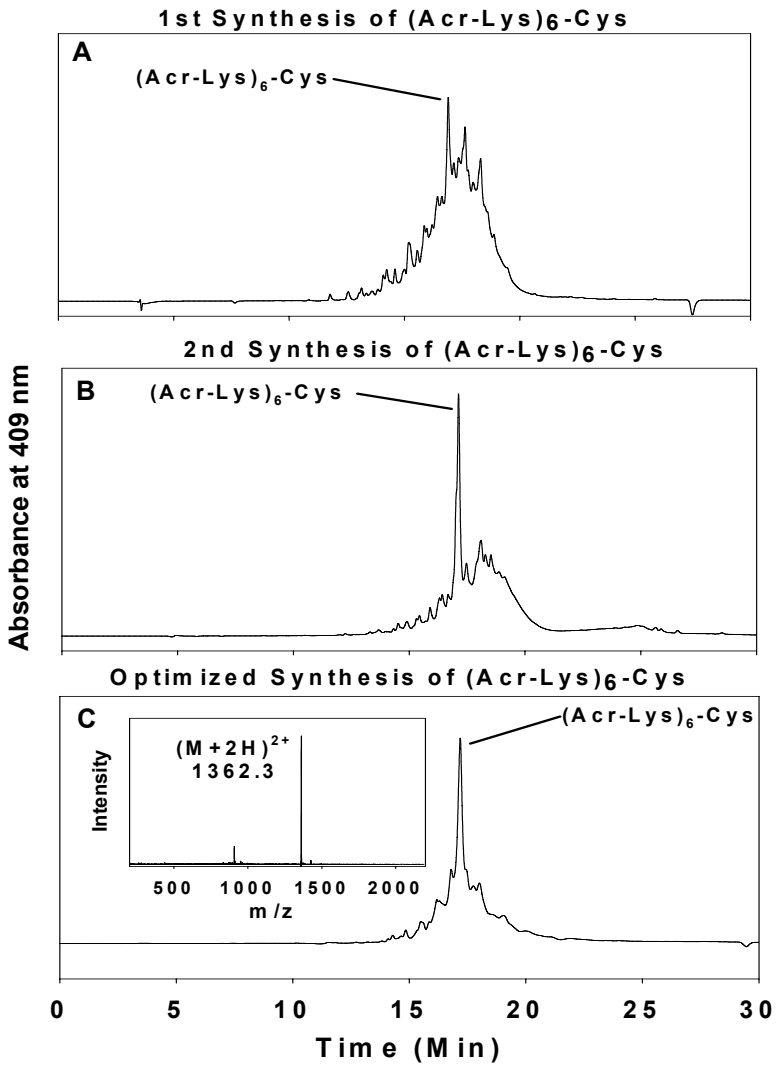


Figure 4-2. *RP-HPLC Analysis of (Acr-Lys)$_6$-Cys Crude Peptide Quality Following Iterative Improvements Discovered by Modeling (Acr-Lys)$_2$-Cys Peptide Synthesis.* Following completion of peptide synthesis, 2.5 nmol of crude peptide was analyzed by RP-HPLC with 0.1 v/v % TFA and an ACN gradient of 10-45 v/v % over 30 minutes. The first synthesis of (Acr-Lys)$_6$-Cys using standard HBTU/HOBt coupling chemistry employing double couplings deprotected with 95% TFA/$H_2O$/TIS (95:2.5:2.5 v/v/v) (Panel A). Second synthesis employing HATU/HOBt double couplings for Fmoc-Lys(Acr)-OH and triple couplings for the spacing amino acid (Fmoc-Lys(Boc)-OH), followed by cleavage and deprotection with TFA/$H_2O$/EDT (95:2:3 v/v/v) (Panel B). Further optimization incorporating pre-activation of Fmoc-Lys(Acr)-OH with HATU to improve amino acid solubility during coupling reactions (Panel C). Mass spectral analysis of crude peptide produces a doubly charged ion of 1362.3 *m/z*, corresponding to an observed mass of 2722.6 amu, agreeing with the calculated mass of 2722.3 amu (Panel C, inset).

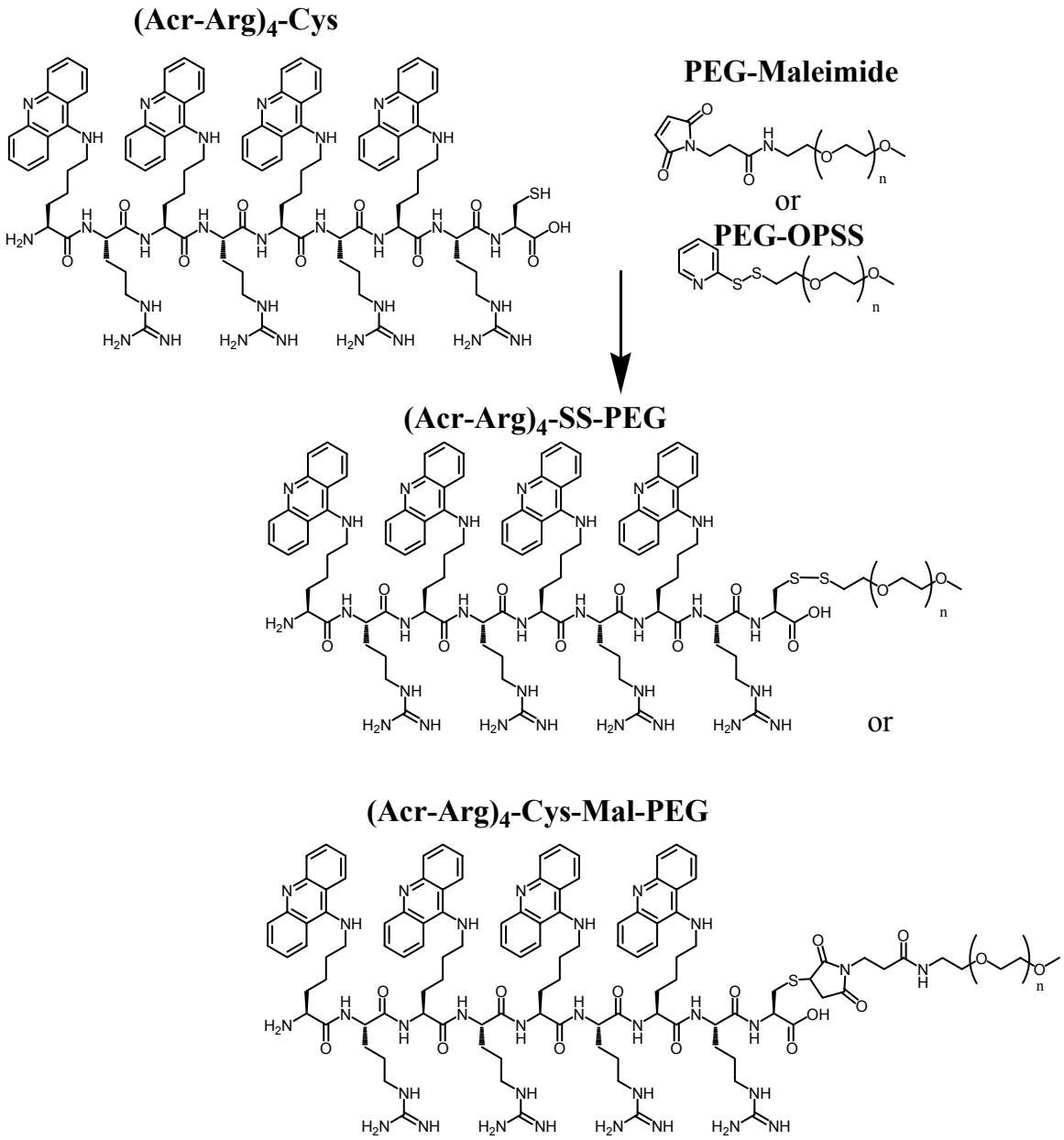


Scheme 4-1. *Synthetic Strategy for PEGylated Polyacridine Peptides.* The approach used to prepare $(Acr\text{-}Arg)_4$-Cys-Mal-PEG and $(Acr\text{-}Arg)_4$-SS-PEG is demonstrated as an example of how all other polyacridine PEG-peptides described in Table 4-1 were prepared. $(Acr\text{-}Arg)_4$-Cys (where Acr is Lys modified on the ε-amine with an acridine) was prepared by solid phase peptide synthesis. The Cys thiol was then reacted with either 5 KDa PEG-maleimide or PEG-OPSS (n = 109), resulting in $(Acr\text{-}Arg)_4$-Cys-Mal-PEG or $(Acr\text{-}Arg)_4$-SS-PEG.

polyacridine peptide (Figure 4-3A) was mostly consumed, resulting in formation of a later eluting PEG-peptide (Figure 4-3B). Preparative RP-HPLC purification produced PEG peptides free of unreacted polyacridine peptide and PEG as established by analytical RP-HPLC and MALDI-TOF analysis (Figure 4-3C).

In addition, the reaction of PEG-maleimide with $(Acr\text{-}Lys)_6$-Cys was monitored by RP-HPLC following injection of an aliquot at a reaction time point of 0 hrs (Figure 4-4A). At a time point of 1 hr, the chromatograph demonstrates consumption of monomeric $(Acr\text{-}Lys)_6$-Cys, formation of the later eluting dimer $((Acr\text{-}Lys)_6\text{-}Cys))_2$ and the much later eluting $(Acr\text{-}Lys)_6$-Cys-Mal-PEG peptide (Figure 4-4B). An aliquot of the reaction analyzed at 12 hrs confirms reaction completion (Figure 4-4C). Preparative RP-HPLC purification followed by analytical RP-HPLC rechromatograph produced a $(Acr\text{-}Lys)_6$-Cys-Mal-PEG peptide as a single peak free of unreacted polyacridine peptide and PEG (Figure 4-4D). MALDI-TOF MS was used to establish identity of the PEGylated peptide (Figure 4-4D, inset). Each PEGylated polyacridine peptide produced a MALDI-TOF MS with multiple peaks due to the polydispersity of $PEG_{5000\ Da}$, with average mass closely correlated to the calculated mass for the PEGylated peptide (Table 4-1).

The relative binding affinity of PEGylated polyacridine peptides for pGL3 was compared by determining the concentration of peptide that displaces a thiazole orange intercalator dye, resulting in decreased fluorescence. Comparison of $(Acr\text{-}X)_4$-PEG (X is either Arg, Lys, Leu or Glu) established the importance of cationic amino acids to increased binding affinity. Both the Lys and Arg analogue demonstrated high affinity by completely displacing thiazole orange at 0.4 nmol of peptide per μg of DNA. Conversely, the Leu analogue demonstrated weaker binding, resulting in full displacement at 1 nmol, and the Glu analogue was the weakest, by only achieving 40% displacement at 1 nmol (Figure 4-5).

A similar comparison of the binding affinities for $(Acr\text{-}Lys)_{2,\ 4\ and\ 6}$–PEG peptides established a relationship of increasing affinity with increasing number of Acr, such that

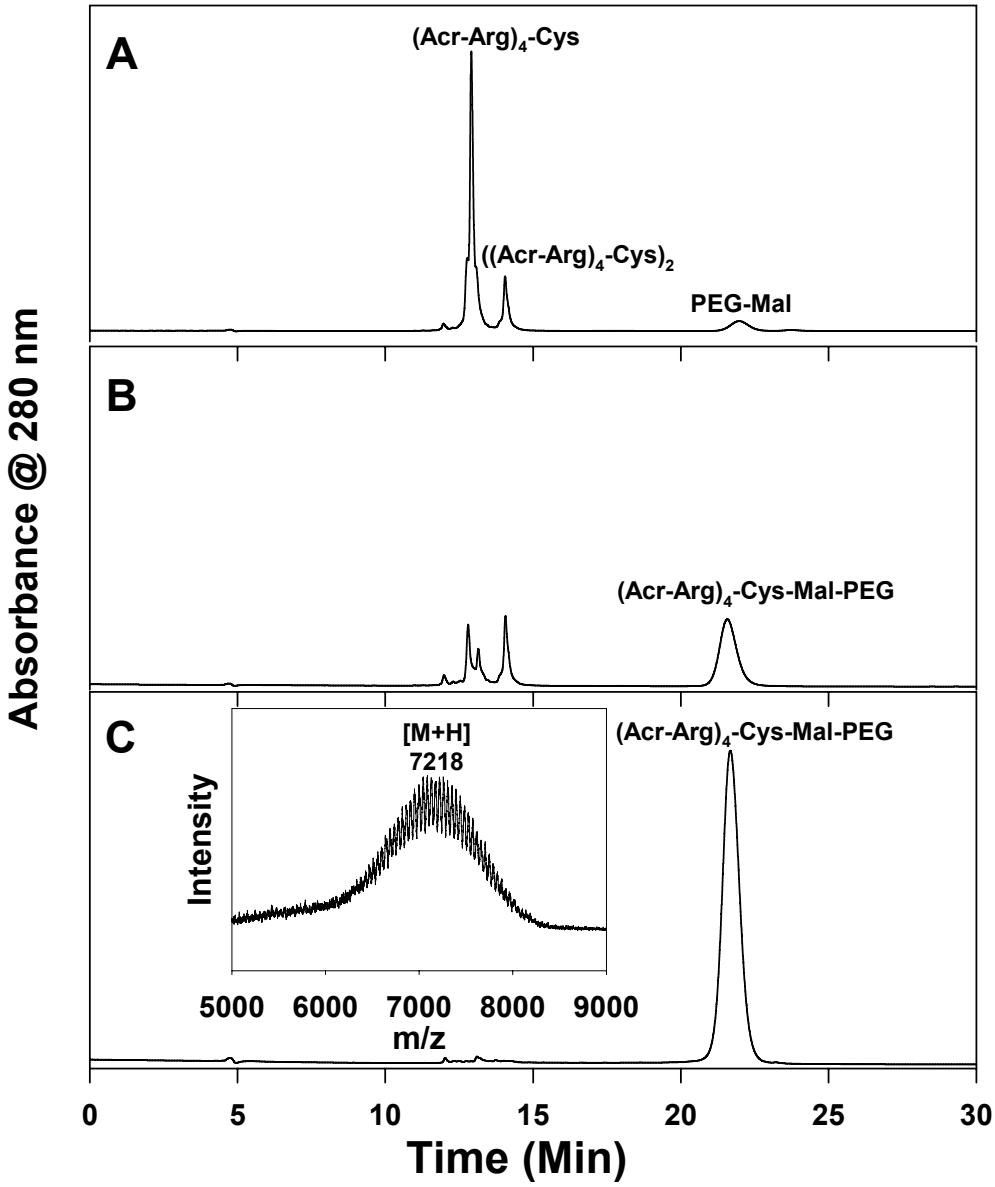


Figure 4-3. *RP-HPLC Analysis of Polyacridine PEG-Peptide Synthesis.* Reaction of $(Acr\text{-}Arg)_4$-Cys with 1.1 mol equivalents of PEG-Mal (panel A), results in the formation of $(Acr\text{-}Arg)_4$-Cys-Mal-PEG detected at 280 nm with simultaneous consumption of $(Acr\text{-}Arg)_4$–Cys and formation of dimeric peptide $((Acr\text{-}Arg)_4\text{-}Cys)_2$ (Panel B). The HPLC purified product $(Acr\text{-}Arg)_4$-Cys-Mal-PEG rechromatographed on RP-HPLC as a single peak (Panel C) and is characterized by MALDI-TOF MS (Panel C, inset), resulting in an observed *m/z* corresponding to the calculated mass (Table 4-1). The preparation of $(Acr\text{-}X)_n$–Cys-Mal-PEG and $(Acr\text{-}X)_n$–Cys-SS-PEG peptides described in Table 4-1 produced equivalent chromatographic evidence.

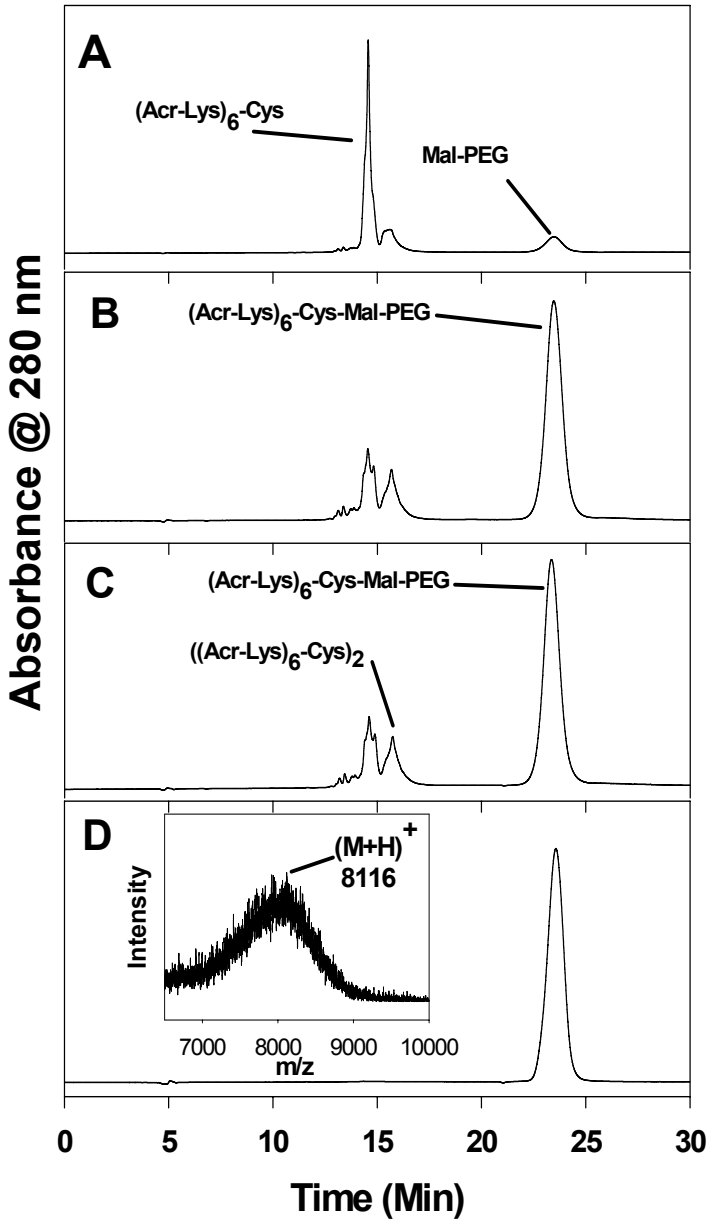


Figure 4-4. *RP-HPLC Analysis of (Acr-Lys)$_6$-Cys-Mal-PEG After Reaction Optimization.* Reaction of (Acr-Lys)$_6$-Cys with 1.2 mol equivalents of Mal-PEG (Panel A), results in the formation of (Acr-Lys)$_6$-Cys-Mal-PEG detected at 280 nm with simultaneous consumption of (Acr-Lys)$_6$-Cys and formation of dimeric peptide ((Acr-Lys)$_6$-Cys)$_2$ at 1 hr (Panel B). Reaction is judged complete by 12 hrs (Panel C). The HPLC purified product (Acr-Lys)$_6$-Cys-Mal-PEG rechromatographed on RP-HPLC as a single peak (Panel D) and is characterized by MALDI-TOF MS (Panel D, inset), resulting in an observed *m/z* corresponding to the calculated mass (Table 4-1).

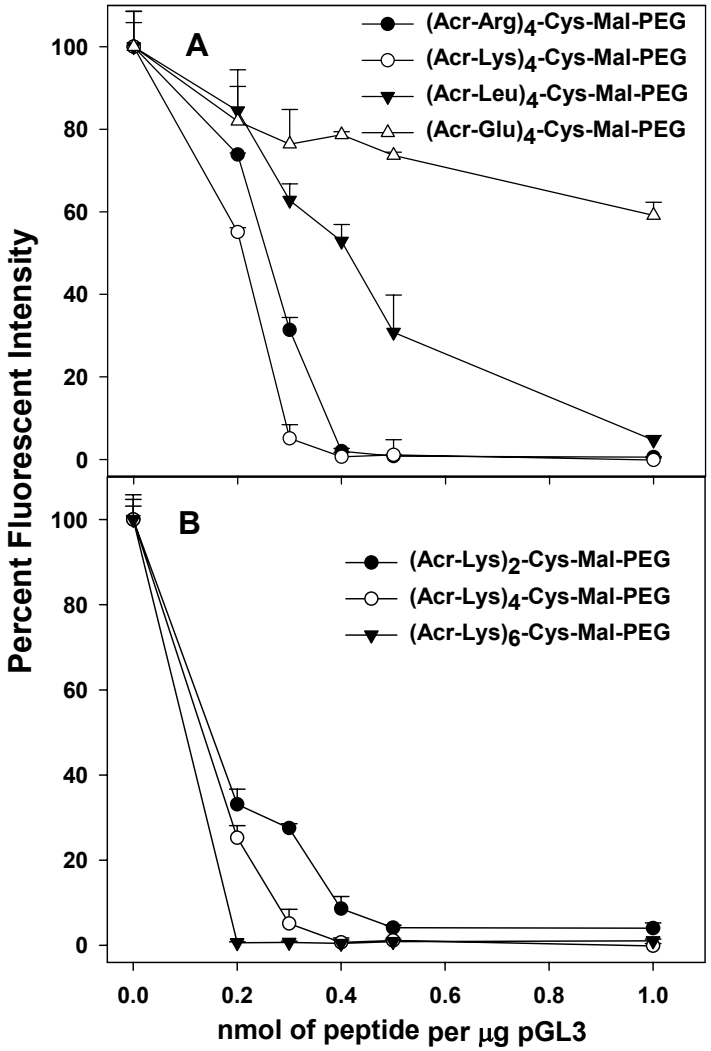


Figure 4-5. *DNA Binding Affinity of PEGylated Polyacridine Peptides.* A thiazole orange displacement assay was used to determine the relative binding affinity of polyacridine PEG peptides for DNA. Polyacridine PEG peptides when titrating 0.2 to 1 nmol of $(Acr\text{-}Arg)_4$-Cys-Mal-PEG (●), $(Acr\text{-}Lys)_4$-Cys-Mal-PEG (○), $(Acr\text{-}Leu)_4$-Cys-Mal-PEG (▼), or $(Acr\text{-}Glu)_4$-Cys-Mal-PEG (Δ), with 1 μg of pGL3 and 0.1 μM thiazole orange in 0.5 ml of 5 mM Hepes pH 7.0 prior to measuring thiazole fluorescence intensity. The results in Panel A established that $(Acr\text{-}Arg)_4$-Cys-Mal-PEG and $(Acr\text{-}Lys)_4$ possessed higher affinity for DNA compared to $(Acr\text{-}Glu)_4$-Cys-Mal-PEG and $(Acr\text{-}Leu)_4$-Cys-Mal-PEG. In Panel B the relative affinity of $(Acr\text{-}Lys)_2$-Cys-Mal-PEG, $(Acr\text{-}Lys)_4$-Cys-Mal-PEG, and $(Acr\text{-}Lys)_6$-Cys-Mal-PEG are compared. The results establish that both the number of Acr and the spacing amino acid contribute to the DNA binding affinity.

$(Acr\text{-}Lys)_6$-Cys-Mal-PEG completely displaced thiazole orange at 0.2 nmol of peptide per μg of DNA (Figure 4-5B). The importance of spacing amino acid was further established by $(Acr\text{-}Lys)_2$-Cys-Mal-PEG which possessed greater DNA binding affinity than $(Acr\text{-}Glu)_4$-Cys-Mal-PEG (Figure 4-5 A and B).

The size and charge of DNA polyplexes are often a function of the stoichiometry of peptide bound to DNA. To examine this relationship for PEGylated polyacridine polyplexes, QELS particle size and zeta potential were measured as a function of peptide to DNA ratio. One unusual property of PEGylated polyacridine polyplexes was their QELS mean diameter remained constant throughout the titration (Figure 4-6A-F). Each of the polyplexes had an apparent mean diameter of approximately 100-200 nm, with the exception of $(Acr\text{-}Leu)_4$–Cys-Mal-PEG and $(Acr\text{-}Glu)_4$–Cys-Mal-PEG which produced polyplexes of a 200-400 nm mean diameter (Figure 4-6B and C).

A second unusual property of PEGylated polyacridine polyplexes was the observed zeta potential at each peptide stoichiometry (Figure 4-6). Titration with $(Acr\text{-}Arg)_4$–Cys-Mal-PEG resulted in an increase in zeta potential from -15 mV to a maximum of -2 mV at 0.4 nmol of peptide per μg of DNA or higher (Figure 4-6A). Similar zeta potential titration curves were determined for $(Acr\text{-}Leu)_4$–Cys-Mal-PEG, $(Acr\text{-}Lys)_2$–Cys-Mal-PEG and $(Acr\text{-}Lys)_4$–Cys-Mal-PEG, each of which resulted in polyplexes with a negative zeta potential when fully titrated (Figure 4-6B, D and E). In contrast, $(Acr\text{-}Glu)_4$–Cys-Mal-PEG produced no change in zeta potential during the titration (Figure 4-6C), and titration with $(Acr\text{-}Lys)_6$–Cys-Mal-PEG produced zeta potentials that increased from -5 mV to a maximum of +5 mV during the titration (Figure 4-6F). These data suggested that, unlike polylysine or PEI polyplexes that condense DNA into smaller polyplexes of 50-100 nm with charge of +25 mV (*166, 167*), polyacridine peptides bind without dramatically changing DNA size and can be, in certain cases, titrated to completion while maintaining a negative zeta potential.

The shape and relative charge of PEGylated polyacridine polyplexes was further examined by atomic force microscopy (AFM) (Figure 4-7). Polyplexes prepared at 0.8 nmol per μg of DNA using (Acr-Arg)$_4$–Cys-Mal-PEG, (Acr-Lys)$_4$–Cys-Mal-PEG, (Acr-Leu)$_4$–Cys-Mal-PEG and (Acr-Glu)$_4$–Cys-Mal-PEG, each produced anionic open-polyplexes that bound to cationically charged mica (Figure 4-7A-D). The relative size and shape appeared as open-polyplexes of approximately 0.2-0.3 μm, relative to naked plasmid DNA which also bound to cationic mica to produce a more open coiled structure of approximately 0.5 μm diameter (Figure 4-7E). Examination of AFM images of (Acr-Lys)$_6$–Cys-Mal-PEG polyplexes revealed anionic open-polyplexes that bound to cationic mica at 0.2 nmol per μg of DNA (Figure 4-7F). Alternatively, 0.8 nmol per μg of DNA produced cationic closed-polyplexes of slightly smaller size that bound to anionic mica (Figure 4-7G). Cationic closed-polyplexes were only observed on anionic mica, whereas an attempt to bind to cationic mica resulted in images devoid of visible polyplexes (Figure 4-7H). These results illustrate the unique shape of anionic open-polyplexes as well as the ability to manipulate the charge of (Acr-Lys)$_6$–Cys-Mal-PEG polyplexes to be either cationic or anionic and change shape from open to closed-polyplexes depending on peptide stoichiometry.

The unique shape and charge of anionic PEGylated open-polyplexes should minimize binding to serum proteins and extend the pharmacokinetic half-life of plasmid DNA, provided that the DNA remains protected from premature metabolism. To investigate the metabolic stability of DNA polyplexes, (Acr-Lys)$_{2,\ 4,\ \text{and}\ 6}$–Cys-Mal-PEG polyplexes were digested with DNase, followed by phenol-chloroform extraction to remove peptide and gel electrophoresis to determine the status of the plasmid DNA (Figure 4-8). Unique band shifts occurred for (Acr-Lys)$_{2,\ 4,\ \text{and}\ 6}$–Cys-Mal-PEG polyplexes prepared at either 0.2 or 0.8 nmol of peptide per μg of plasmid DNA (Figure 4-8, lane 2 and 3 of Panels A, B, C). However, phenol-chloroform extraction removed the PEG-peptide allowing recovery of the DNA which migrated coincident with control (Figure 4-

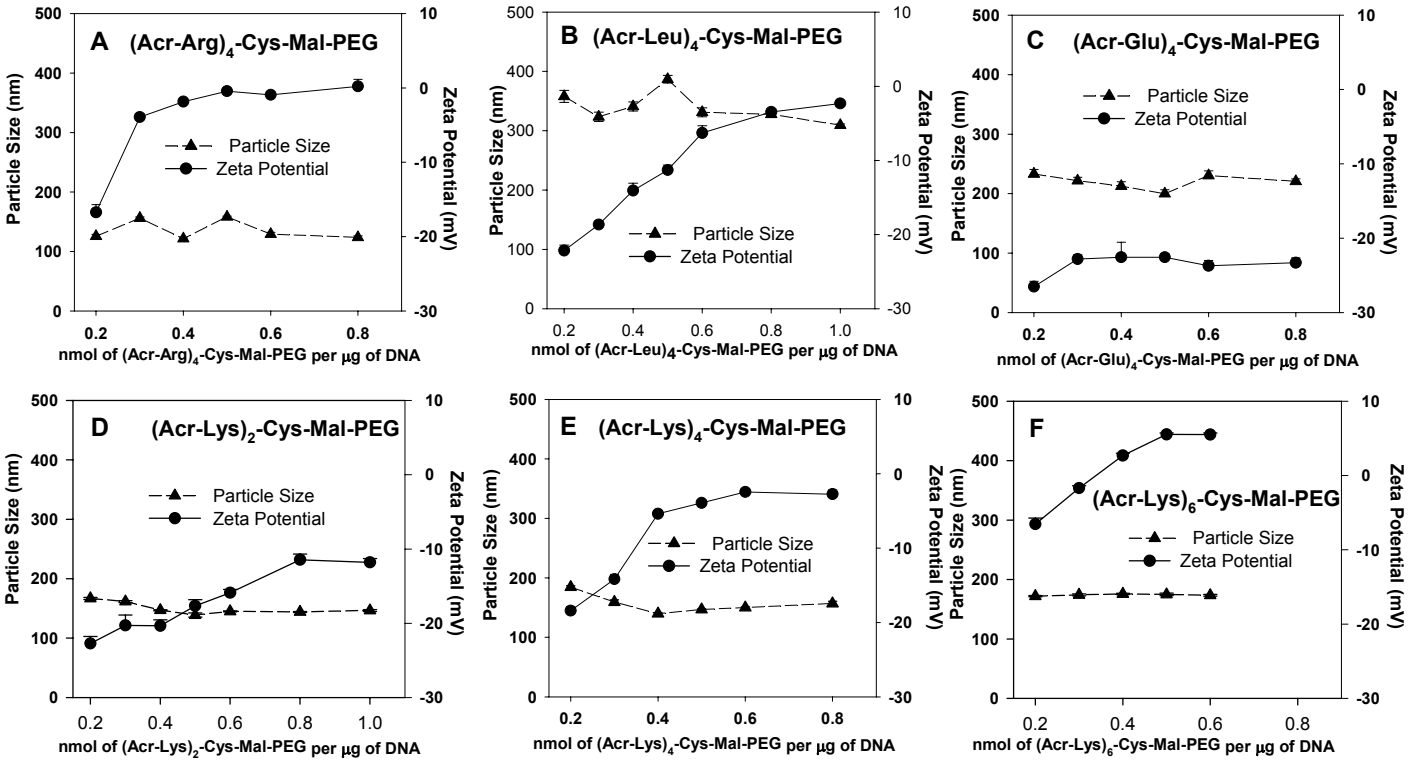


Figure 4-6. *Size and Charge of PEGylated Polyacridine Polyplexes.* The QELS particle size (--▲--) and zeta potential (-●-) of polyplexes, prepared at concentrations ranging from 0.2-1 nmol of peptide per µg of DNA, are illustrated for $(Acr\text{-}Arg)_4$-Cys-Mal-PEG (A), $(Acr\text{-}Leu)_4$-Cys-Mal-PEG (B), $(Acr\text{-}Glu)_4$-Cys-Mal-PEG (C), $(Acr\text{-}Lys)_2$-Cys-Mal-PEG (D), $(Acr\text{-}Lys)_4$-Cys-Mal-PEG (E) or $(Acr\text{-}Lys)_6$-Cys-Mal-PEG (F). The results establish no significant change in particle size throughout the titration, whereas the zeta potential increases from -20 to 0 mV when titrating with peptides containing spacing amino acids Arg, Lys or Leu (panels A, B, D). Comparison of $(Acr\text{-}Lys)_n$-Cys-Mal-PEG repeats of n = 2, 4 and 6 (panel D, E and F) results in polyplexes that titrate to final zeta potential of -10, -2 and 5 mV, respectively.

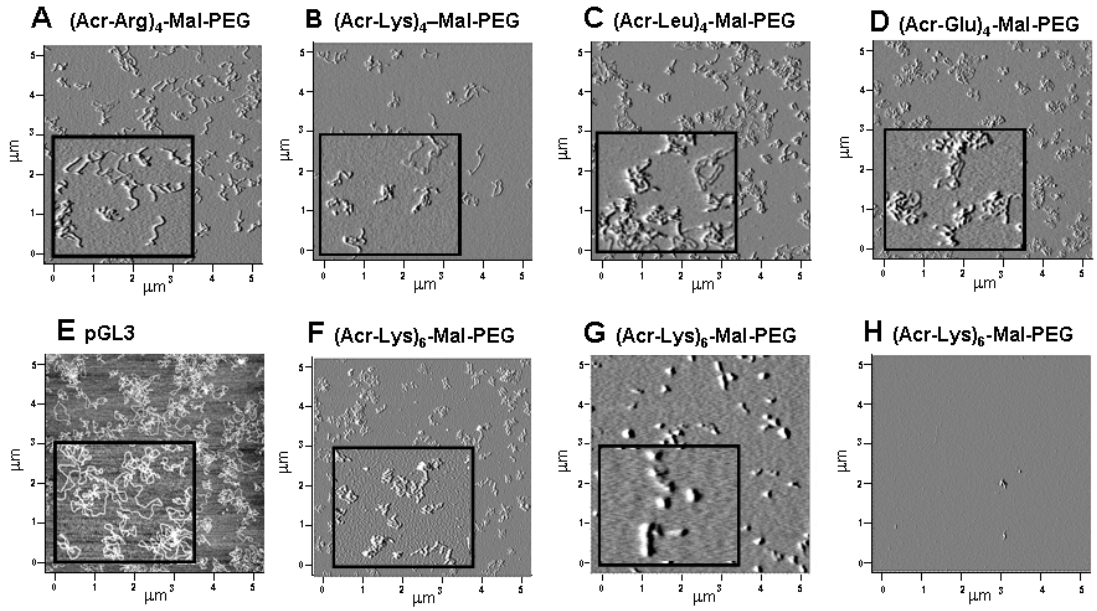


Figure 4-7. *Shape of PEGylated Polyacridine Polyplexes.* Atomic force microscopy (AFM) was used to analyze the shape of DNA polyplexes prepared at 0.8 nmol per µg of DNA with (A) $(Acr\text{-}Arg)_4$-Cys-Mal-PEG (+) mica, (B) $(Acr\text{-}Lys)_4$-Cys-Mal-PEG (+) mica, (C) $(Acr\text{-}Leu)_4$-Cys-Mal-PEG (+) mica, (D) $(Acr\text{-}Glu)_4$-Cys-Mal-PEG (+) mica, or (E) pGL3 (+) mica, (F) 0.2 nmol of $(Acr\text{-}Lys)_6$-Cys-Mal-PEG (+) mica, (G) 0.8 nmol of $(Acr\text{-}Lys)_6$-Cys-Mal-PEG (-) mica, and (H) 0.8 nmol of $(Acr\text{-}Lys)_6$-Cys-Mal-PEG (+) mica. Anionic PEGylated polyacridine polyplexes produced open polyplex structures (A-D, F) that appeared slightly more coiled than plasmid DNA (E), where cationic PEGylated polyacridine polyplexes produced closed polyplex structures (G). Panel H demonstrates that cationic polyplexes do not bind to cationic mica. Each inset represents a 1 x 1 µm enlargement.

8, lane 4 of Panels A, B and C). When challenged with a DNase digestion, $(Acr\text{-}Lys)_{2\text{ or }4}$–Cys-Mal-PEG polyplexes prepared at 0.2 nmol per µg of DNA failed to protect DNA from metabolism (Figure 4-8, Panel A and B, lane 5 and 6). In contrast, polyplexes formed at 0.2 nmol $(Acr\text{-}Lys)_6$–Cys-Mal-PEG, protected the DNA from DNase resulting in the recovery of bands following extraction (Figure 4-8, Panel C, lanes 5 and 6). At a higher stoichiometry of 0.8 nmol, $(Acr\text{-}Lys)_{2,\ 4\text{ and }6}$–Cys-Mal-PEG each protected DNA from metabolism (Figure 4-8, Panel A-C, lanes 7 and 8). These results establish a clear correlation between polyacridine DNA binding affinity (Figure 4-5) and metabolic

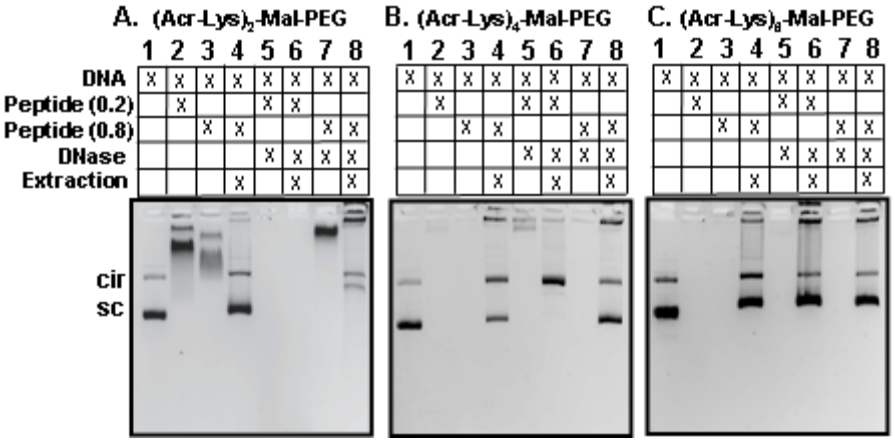


Figure 4-8. *Metabolic Stability of PEGylated Polyacridine Polyplexes.* Agarose gel electrophoresis of (1) plasmid DNA, (2) (Acr-Lys)$_n$-Cys-Mal-PEG polyplex (n =2, 4 or 6) at 0.2 nmol of peptide per μg of DNA, (3) (Acr-Lys)$_n$-Cys-Mal-PEG polyplex at 0.8 nmol of peptide per μg of DNA, (4) release of DNA from (Acr-Lys)$_n$-Cys-Mal-PEG polyplex at 0.8 nmol per μg of DNA, (5) (Acr-Lys)$_n$-Cys-Mal-PEG polyplex at 0.2 nmol per μg of DNA following DNase digest, (6) released (Acr-Lys)$_n$-Cys-Mal-PEG polyplex at 0.2 nmol per μg of DNA following DNase digest, (7) (Acr-Lys)$_n$-Cys-Mal-PEG polyplex at 0.8 nmol per μg of DNA following DNase digest, (8) released (Acr-Lys)$_n$-Cys-Mal-PEG polyplex at 0.8 nmol per μg of DNA following DNase digest. The results establish the partial or complete protection of DNA from DNase at 0.8 nmol of (Acr-Lys)$_2$-Cys-Mal-PEG (Panel A lane 8) and (Acr-Lys)$_4$-Cys-Mal-PEG (Panel B lane 8), and the complete protection of DNA from DNase at 0.2 and 0.8 nmol of (Acr-Lys)$_6$-Cys-Mal-PEG (panel C lane 6 and 8).

stability of polyplexes. Most importantly, (Acr-Lys)$_6$–Cys-Mal-PEG is able to form DNase stable anionic open-polyplexes when prepared at 0.2 nmol, as well as cationic closed-polyplexes prepared at 0.8 nmol per μg of DNA.

PEGylated polyacridine peptides were also subjected to trypsin digestion to determine if they could be digested by a common serine protease, suggesting perhaps they could also be more easily cleared from cells *(In collaboration with Mark Ericson)*. The results established that even as little as 100 mU of trypsin catalyzed the formation of a dipeptide of Lys-Lys(Acr) with mass of 451 g/mol, to a reaction completion within 1

hr. Thereby, the high-affinity DNA binding of PEGylated polyacridine peptides is greatly reduced upon proteolytic digestion.

To determine if polyacridine peptides would also mediate gene transfer, we chose to examine the ability of PEGylated DNA polyplexes to produce luciferase expression in the liver of mice, 24 hrs following a 1 μg dose of pGL3. Hydrodynamic dosing of 1 μg of pGL3 produced $10^8$ photon/sec/cm$^2$/sr determined using a calibrated bioluminescence assay (Figure 4-9A, HD DNA). When pGL3 (1 μg in 50 μl) was dosed via the tail vein without hydrodynamic delivery, there was no detectable luciferase expression (not shown). In an attempt to stimulate gene expression, PEGylated polyacridine peptide polyplexes were administered via the tail vein (1 μg of pGL3 in 50 μl) and after a 30 min delay, a hydrodynamic dose (2 ml) of saline was used to stimulate liver uptake and gene expression (Figure 4-9A). In the subsequent studies described below, stimulated expression produced $10^7$-$10^9$ photon/sec/cm$^2$/sr, the magnitude being dependent on the structure of the PEGylated polyacridine peptide, the time delay between primary dose and stimulation dose, the charge ratio at which the polyplex was prepared, and the amount of DNA dosed.

At a fixed dose of 1 μg of pGL3 and time delay of 30 min between primary and stimulatory dose, polyplexes prepared at 0.5 nmol of (Acr-Arg)$_4$-PEG, in which the PEG was attached by a maleimide (Mal) or a reducible disulfide (SS) linkage, were administered to mice and analyzed by BLI after 24 hrs. Approximately 5-fold higher luciferase expression was observed for Mal versus SS, indicating that a reducible linkage offered no advantage for stimulated expression (Figure 4-9A). Comparison of the Mal peptide prepared as either an acetate or TFA salt form (ion paired with Arg) resulted in an approximately 10-fold loss of gene transfer for the TFA form (Figure 4-9A). These results justified the use of Mal peptides in the acetate salt form for further comparisons.

Several controls were applied to further establish that PEGylated polyacridine peptides were necessary to achieve stimulated expression. The administration of a 1 μg

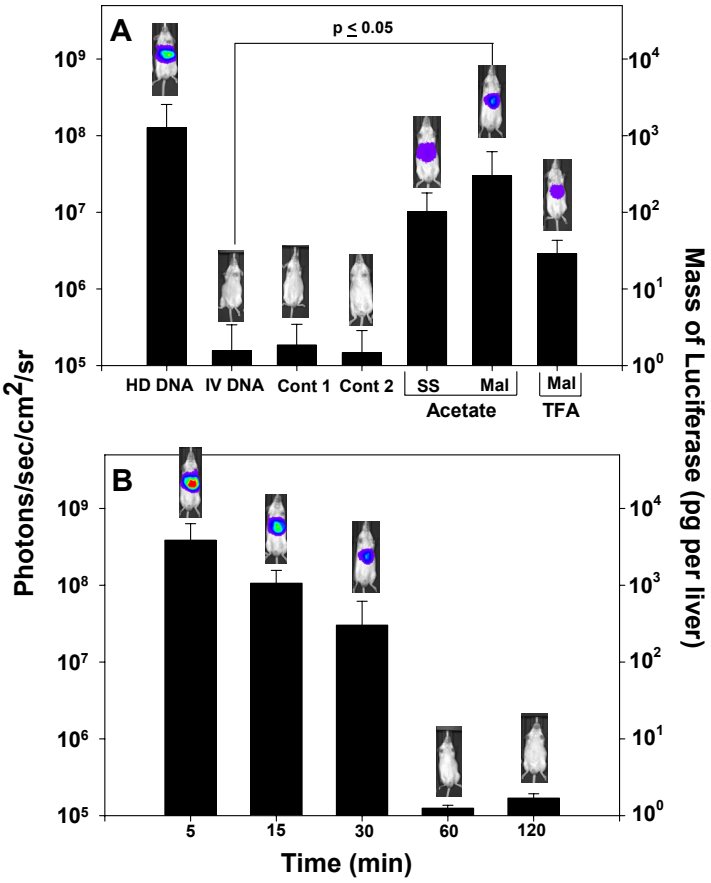


Figure 4-9. *Stimulated In Vivo Gene Expression Using PEGylated Polyacridine Polyplexes.* Direct HD dosing of 1 μg of pGL3 in multiple mice results in a mean BLI response of $10^8$ photons/sec/cm$^2$/sr at 24 hrs following dosing (Panel A, HD DNA). Alternatively, a 24 hr BLI analysis of mice tail vein dosed with pGL3 (1 μg in 50 μl) in complex with 0.5 nmol of either (Acr-Arg)$_4$-Cys-Mal-PEG (Panel A, Mal) or (Acr-Arg)$_4$-SS-PEG (Panel A, SS) followed by hydrodynamic stimulation with 2 ml of saline delivered 30 min after DNA delivery, results in approximately $10^7$ photons/sec/cm$^2$/sr (panel A). Omission of HD stimulation (not shown) or PEGylated polyacridine peptide (Panel A, i.v. DNA) results in no expression ($10^5$ photons/sec/cm$^2$/sr). Likewise, HD stimulation after 30 min failed to produce measurable expression from a 1 μg pGL3 dose in complex with PEG-Cys-Trp-Lys$_{18}$ (Panel A, Cont 1) or a PEGylated glycoprotein described previously (*26*) (Panel A, Cont 2). An acetic acid counter ion on (Acr-Arg)$_4$-Cys-Mal-PEG resulted in nearly 10-fold increase in expression relative to a TFA counter ion (panel A). Varying the dwell time of the HD stimulation from 5-120 min following a 1 μg dose of pGL3 in complex with 0.5 nmol of (Acr-Arg)$_4$-Cys-Mal-PEG established a maximum of 30 min to retain expression at $10^7$ photons/sec/ cm$^2$/sr or higher measured at 24 hrs post administration (panel B). Analysis was performed using a two-tailed unpaired t-test (*p ≤0.05).

dose of pGL3 followed by a stimulatory dose of saline after 30 min resulted in no detectable luciferase expression at 24 hrs (Figure 4-9A, IV DNA). Likewise, there was no detectable luciferase expression with a 1 μg dose of pGL3 prepared as a PEGylated-Cys-Trp-$Lys_{18}$ polyplex (*35*) (Figure 4-9A, cont 1), or PEGylated glycoprotein polyplex (*26*) (Figure 4-9A, cont 2). These controls confirmed that naked DNA was not responsible for the observed expression and also established that not all gene formulations were capable of mediating stimulated expression.

The stimulated expression mediated by $(Acr\text{-}Arg)_4$–Cys-Mal-PEG polyplexes (1 μg) was examined to determine the influence of the delay time between primary and stimulatory dose. Varying the delay from 5-120 min established a 10-fold loss in luciferase expression between 5 and 30 min, followed by a complete loss of stimulated expression at 60 min and longer (Figure 4-9B). Interestingly, the magnitude of stimulated gene expression at a delay time of 5 min was approximately 5-fold greater than direct hydrodynamic dosing of 1 μg of pGL3 (Figure 4-9A and B).

To determine how the spacing amino acid influences stimulated gene expression, PEGylated peptides of general structure $(Acr\text{-}X)_4$, possessing X as either Lys, Arg, Leu or Glu were used to prepare polyplexes that were dosed in mice and stimulated to express luciferase. While the DNA dose was fixed at 1 μg, and the delay time was 30 min, the stoichiometry of PEGylated peptide to DNA was adjusted, based on the results of zeta potential titration (Figure 4-6), to favor complete polyplex formation. The results established that only PEGylated peptides possessing an Arg or Lys spacing amino acid produced appreciable levels of luciferase expression (Figure 4-10A), whereas peptides with Glu and Leu spacers were essentially inactive.

The stoichiometry of both Lys and Arg spaced PEGylated polyacridine peptide were varied from 0.2-1 nmol of peptide per μg of DNA, then dosed via tail vein and stimulated after 30 min. A 1 μg open polyplex prepared with 0.6 nmol of $(Acr\text{-}Arg)_4$–Cys-Mal-PEG or 0.8 nmol of $(Acr\text{-}Lys)_4$–Cys-Mal-PEG mediated maximal luciferase

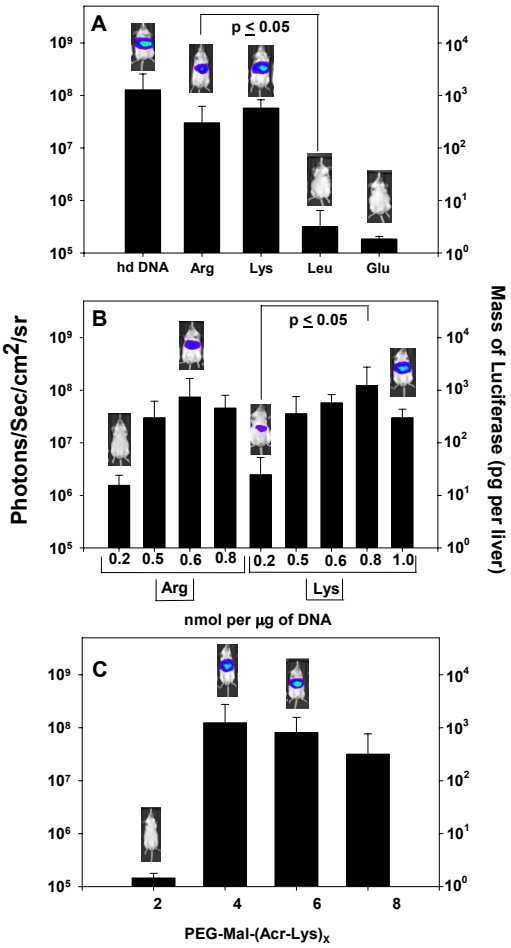


Figure 4-10. *Structure-Activity Relationships for Stimulated Gene Expression.* The BLI analysis at 24 hrs following tail vein dosed and HD stimulated (30 min post-DNA administration) pGL3 (1 µg in 50 µl) in complex with 0.5 nmol of either $(Acr\text{-}Arg)_4$-Cys-Mal-PEG (Panel A, Arg), 0.6 nmol of $(Acr\text{-}Lys)_4$-Cys-Mal-PEG (Panel A, Lys), 1 nmol of $(Acr\text{-}Leu)_4$-Cys-Mal-PEG (panel A, Leu), or 0.8 nmol of $(Acr\text{-}Glu)_4$-Cys-Mal-PEG (Panel A, Glu) are compared with direct HD delivery of 1 µg of pGL3. The results establish polyacridine PEG-peptides with Arg and Lys spacing amino acids mediate $10^7$-$10^8$ photons/sec/ $cm^2$/sr whereas substitution with Leu and Glu results in negligible expression. Varying only the stoichiometry of PEGylated polyacridine peptide to DNA for $(Acr\text{-}Arg)_4$-Cys-Mal-PEG (Panel B, Arg) and $(Acr\text{-}Lys)_4$-Cys-Mal-PEG (Panel B, Lys), established a maximal expression at 0.6 for Arg and 0.8 for Lys (Panel B). Direct comparison of HD stimulated gene expression using $(Acr\text{-}Lys)_n$-Cys-Mal-PEG (where n = 2, 4, or 6) in complex with 1 µg of pGL3 established the equivalency of 0.8 of $(Acr\text{-}Lys)_4$-Cys-Mal-PEG with 0.2 nmol of $(Acr\text{-}Lys)_6$-Cys-Mal-PEG, respectively (Panel C), relative to $(Acr\text{-}Lys)_2$-Cys-Mal-PEG which mediated negligible expression. Analysis was performed using a two-tailed unpaired t-test (*$p \leq 0.05$).

expression when assayed by BLI at 24 hrs (Figure 4-10B). Both the Lys and Arg spaced PEGylated peptide mediated approximately 100-fold lower gene expression at 0.2 nmol of peptide compared to the stoichiometry of maximal expression (Figure 4-10B). Likewise, at stoichiometries greater than maximal expression, a decline in expression was observed. These results suggested that a Lys spacer may have a slight advantage over Arg, which then prompted an investigation into varying the number of (Acr-Lys) repeats.

Comparison of the stimulated gene expression (30 min) mediated by PEGylated $(Acr\text{-}Lys)_{2,\ 4,\ 6\ and\ 8}$ polyplexes (1 μg pGL3) prepared at an optimized stoichiometry of 1, 0.8, 0.2 nmol and 0.2 nmol of peptide respectfully (based on zeta potential, Figure 4-6), established that $(Acr\text{-}Lys)_2$–Cys-Mal-PEG was completely inactive. In contrast, $(Acr\text{-}Lys)_6$–Cys-Mal-PEG at 0.2 nmol matched the activity of $(Acr\text{-}Lys)_4$–Cys-Mal-PEG at 0.8 nmol while lengthening the polyacridine chain length by 2 Acr-Lys subunits with $(Acr\text{-}Lys)_8$-Cys-Mal-PEG results in a decrease in activity (Fig. 4-10C). These results correlate with $(Acr\text{-}Lys)_6$–Cys-Mal-PEG having a higher binding affinity for DNA (Figure 4-6), with a greater ability to protect DNA from metabolism (Figure 4-8), and with the ability to mediate stimulated gene expression even at a low stoichiometry of 0.2 nmol per μg of DNA (Figure 4-10).

When $(Acr\text{-}Lys)_6$–Cys-Mal-PEG polyplexes were administered to mice to determine how changing stoichiometry influenced gene expression, the results established that a 1 μg dose of pGL3 polyplex, stimulated at 30 min, produced equivalent gene expression across the range of 0.2-0.8 nmol of peptide (Figure 4-11A). These results are in sharp contrast to those determined for $(Acr\text{-}Lys)_4$-Cys-Mal-PEG (Figure 4-10B), in which the gene expression was highly dependent on the stoichiometry of peptide to DNA. Furthermore, since $(Acr\text{-}Lys)_6$–Cys-Mal-PEG was the only peptide to produce a zeta potential titration that started anionic (-5 mV) at 0.2 nmol and titrated to cationic (+5 mV) at 0.6 nmol (Figure 4-6F), it appeared that the stimulated gene expression mediated by

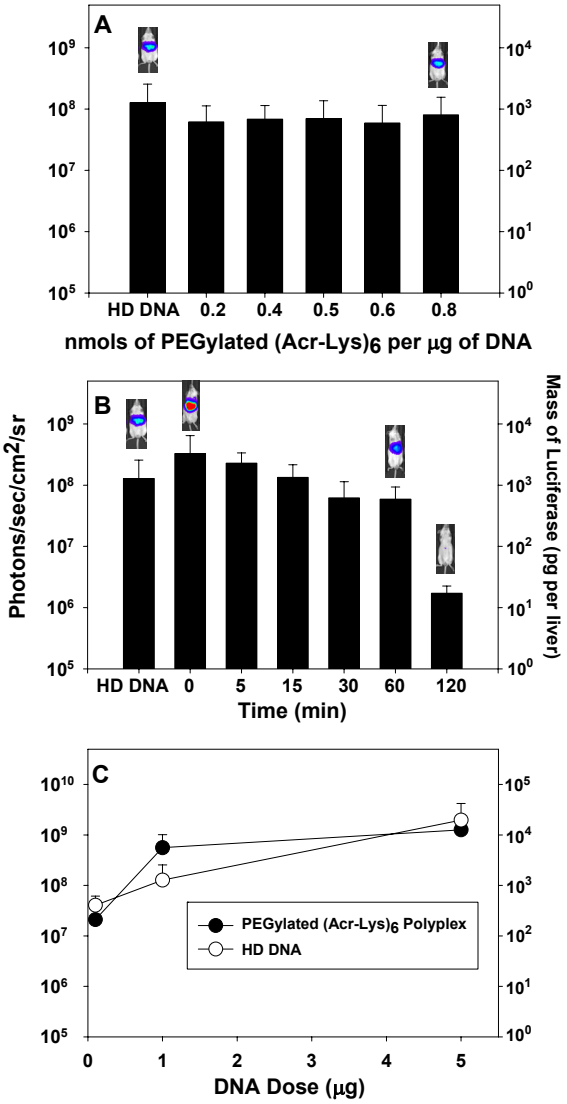


Figure 4-11. *Optimal Parameters for Stimulated Gene Expression of Polyacridine PEG-peptide DNA Polyplexes.* In panel A, the level of expression measured at 24 hrs, following HD stimulation 30 min after DNA dosing, remains nearly constant when delivering $(Acr\text{-}Lys)_6$-Cys-Mal-PEG pGL3 polyplexes prepared at stoichiometries ranging from 0.2-0.8 nmol of peptide per μg of DNA (Panel A). The results in panel B illustrate that varying the HD stimulation delay-time following delivery of $(Acr\text{-}Lys)_6$-Cys-Mal-PEG pGL3 polyplexes results in expression of approximately $10^8$ photons/sec/cm$^2$/sr up to 60 min, whereas the expression decreased nearly 100-fold when delaying HD stimulation to 120 min (Panel B). The dose-response curve for in vivo gene expression mediated delivery of $(Acr\text{-}Lys)_6$-Cys-Mal-PEG pGL3 polyplexes with 5 min delay in stimulation (●) is compared with direct HD of pGL3 (○). The luciferase expression at 24 hrs determined by BLI established that HD delivery of 1 μg of $(Acr\text{-}Lys)_6$-Cys-Mal-PEG polyplex is approximately 5-fold more efficient than the HD delivery of pGL3 (Panel C).

$(Acr\text{-}Lys)_6$–Cys-Mal-PEG is fully functional as both an anionic open polyplex (Figure 4-7F), and as an cationic closed polyplex (Figure 4-7G).

To determine if the unique DNA binding properties of $(Acr\text{-}Lys)_6$–Cys-Mal-PEG would also extend the delay time allowed between primary and stimulatory dose, polyplexes (1 μg) were prepared with 0.2 nmol of peptide and administered with a delay time of 0 to 120 min. Delaying the stimulation from 5 to 60 min resulted in only a slight 2-3 fold decrease in expression, whereas with a 120 min delay the expression decreased 100-fold (Figure 4-11B). Using a zero delay time resulted in a nearly 5-fold increase in gene expression relative to dose equivalent direct HD administration of pGL3 (Figure 4-11B). These results demonstrate that $(Acr\text{-}Lys)_6$–Cys-Mal-PEG mediates significant high-level gene expression, even with a 60 min delay time, compared to $(Acr\text{-}Arg)_4$–Cys-Mal-PEG which failed to mediate detectable expression following a 60 min delay in stimulation (Figure 4-9B).

To establish the dose-equivalency of direct HD administration of DNA, relative to the stimulated expression of PEGylated polyacridine polyplexes, a dose-response experiment was performed (Figure 4-11C). The BLI detected expression at 24 hrs post-DNA delivery was determined for direct HD delivered pGL3, dosed at 0.1, 1 and 5 μg of DNA (Figure 4-11C). This was compared with the 24 hr luciferase expression from identical DNA doses of $(Acr\text{-}Lys)_6$–Cys-Mal-PEG polyplexes prepared with 0.2 nmol of peptide and administered with a 5 min delay in stimulation. A nearly linear dose-response curve was identified for direct HD dosing of pGL3, whereas $(Acr\text{-}Lys)_6$–Cys-Mal-PEG polyplexes showed an increase from 0.1-1 μg, followed by a plateau at 5 μg dose (Figure 4-11C). At a dose of 1 μg of DNA, $(Acr\text{-}Lys)_6$–Cys-Mal-PEG mediated approximately 5-fold greater gene expression (Figure 4-11C).

To gain further mechanistic insight into the reason that PEGylated polyacridine polyplexes mediate stimulated gene expression, pharmacokinetic and biodistribution studies were performed. Following i.v. dosing of $^{125}$I-DNA or $(Acr\text{-}Lys)_2$–Cys-Mal-PEG

polyplexes resulted in a rapid 10-fold loss of radioactivity from the blood within 20-30 min, followed by an apparent long half-life (Figure 4-12A). Isolation of $^{125}$I-DNA from blood time points, followed by gel electrophoresis and autoradiography demonstrated that plasmid DNA was rapidly degraded to fragments within 1 min (Figure 4-12C). Likewise, electrophoretic analysis of blood time points following dosing of $(Acr\text{-}Lys)_2$–Cys-Mal-PEG $^{125}$I-DNA polyplexes demonstrated complete loss of plasmid DNA within 20 min (Figure 4-12D), suggesting that the modest binding from $(Acr\text{-}Lys)_2$–Cys-Mal-PEG leads to slightly delayed metabolism.

The pharmacokinetic profile for $(Acr\text{-}Lys)_{4 \text{ and } 6}$–Cys-Mal-PEG $^{125}$I-DNA polyplexes were both very similar and distinct from those of $^{125}$I-DNA and PEGylated $(Acr\text{-}Lys)_2$ $^{125}$I-DNA polyplexes (Figure 4-12A). The radioactivity in blood only decreased 3-4 fold in the first 20 min and proceeded with an apparent long half-life (Figure 4-12A). Recovery of $^{125}$I-DNA from $(Acr\text{-}Lys)_{4 \text{ and } 6}$–Cys-Mal-PEG polyplexes resulted in an agarose gel autoradiographic analysis that established the blood stability of plasmid DNA up to 30 min for $(Acr\text{-}Lys)_4$–Cys-Mal-PEG (Figure 4-12E), and up to 120 min for $(Acr\text{-}Lys)_6$–Cys-Mal-PEG (Figure 4-12F). Non-linear least squares analysis of the radioactivity in blood over time was used to calculate an apparent $\alpha$-half-life of 2-3 min and a $\beta$-half-life of 65 min for $(Acr\text{-}Lys)_4$–Cys-Mal-PEG and 120 min for $(Acr\text{-}Lys)_6$–Cys-Mal-PEG (Table 4-2). For the purpose comparison, complete metabolic stability of plasmid DNA was assumed in the pharmacokinetic calculation, even though the autoradiographic gel analysis for $(Acr\text{-}Lys)_2$–Cys-Mal-PEG and $(Acr\text{-}Lys)_4$–Cys-Mal-PEG proved otherwise. The apparent clearance rate decrease and the mean residence time increased as the $\beta$-half-live increased, whereas the apparent volume of distribution remained nearly constant.

The unique long pharmacokinetic $\beta$-half-life for $(Acr\text{-}Lys)_{4 \text{ and } 6}$–Cys-Mal-PEG polyplexes and the nearly coincident volume of distribution suggested there would be similar biodistribution to the organs. The experimental result established that the liver

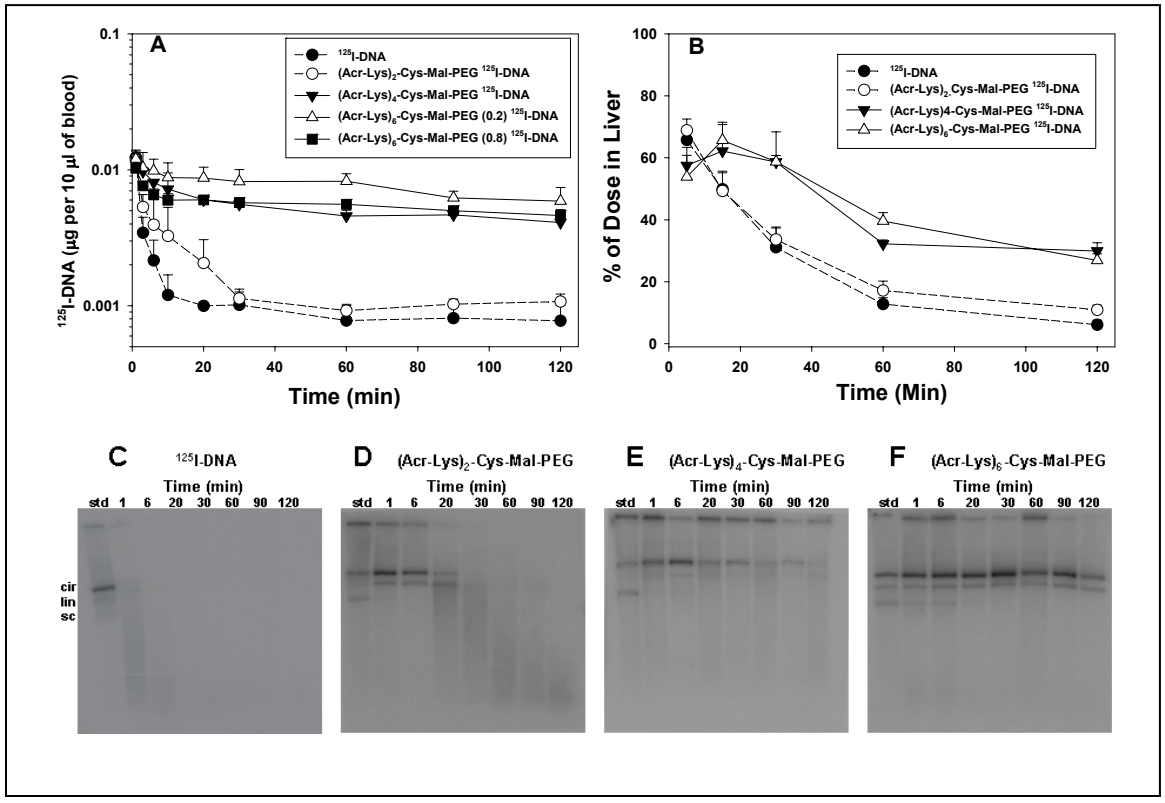


Figure 4-12. *Pharmacokinetic and Biodistribution Analysis of PEGylated Polyacridine Polyplexes.* The pharmacokinetic profile for (Acr-Lys)$_2$-Cys-Mal-PEG, (Acr-Lys)$_4$-Cys-Mal-PEG, and (Acr-Lys)$_6$-Cys-Mal-PEG $^{125}$I-DNA polyplexes is compared with $^{125}$I-DNA (panel A). Extraction of the $^{125}$I-DNA from blood time points followed by agarose electrophoresis and autoradiography produced the images in C-F. Biodistribution analysis of PEGylated polyplexes resulted in comparison of the liver accumulation and elimination over time (panel B). The results establish that (Acr-Lys)$_6$-Cys-Mal-PEG stabilizes DNA in the blood for up to two hours.

was the major site of biodistribution for (Acr-Lys)$_{2,\ 4\ \text{and}\ 6}$–Cys-Mal-PEG $^{125}$I-DNA polyplexes (Table 4-3). In each of these experiments, it was not possible to extract $^{125}$I-DNA from the liver or other tissues to determine its metabolic status, as was performed for DNA in blood. The biodistribution of $^{125}$I-DNA and (Acr-Lys)$_2$–Cys-Mal-PEG $^{125}$I-DNA polyplexes both reached a maximum of approximately 65% in the liver at 5 min,

Table 4-2. *Pharmacokinetic Parameters for PEGylated Polyacridine Polyplexes*

| Polyacridine Peptide Polyplex | $t_{1/2}\alpha$ [a] (min) | $t_{1/2}\beta$ [b] (min) | Vol Dis[c] (ml) | CL[d] (ml/min) | MRT[e] (min) |
|---|---|---|---|---|---|
| $(Acr\text{-}Lys)_2$-Mal-PEG $^{125}$I-DNA[f] | 0.7+/- 0.0 | 15.2+/-0.8 | 42.8+/-0.1 | 2.3+/-0.0 | 18.9+/-0.1 |
| $(Acr\text{-}Lys)_4$-Mal-PEG $^{125}$I-DNA[g] | 2.3+/-0.3 | 65.6+/-13.5 | 37.4+/-1.9 | 0.4+/-0.1 | 92.2+/-19 |
| $(Acr\text{-}Lys)_6$-Mal-PEG $^{125}$I-DNA[h] | 1.8+/-0.9 | 182+/-33 | 31.6+/-1.3 | 0.1+/-0.0 | 261+/-48 |

a. Calculated α-half-life.

b. Calculated β-half-life.

c. Volume of distribution.

d. Total body clearance rate.

e. Mean residence time.

f. Calculated using cpm values over 20 min, assuming complete DNA stability.

g. Calculated using cpm values over 60 min, assuming complete DNA stability.

h. Calculated using cpm values over 120 min, assuming complete DNA stability.

followed by a decrease to less than 10% by 120 min (Figure 4-12B). In contrast, when dosing $(Acr\text{-}Lys)_{4 \text{ and } 6}$–Cys-Mal-PEG $^{125}$I-DNA polyplexes the percent of radioactive dose in liver was approximately 55% at 5 min, which accumulated to over 60% at 15 min, followed by a decline to 30-40% at 120 min (Figure 4-12B). By comparison, a maximum of 1-2% of the total radioactive dose distributed to lungs, heart, kidneys and intestine at all time points (Table 4-3). The exception was the spleen which showed a steady accumulation over time to reach 18% at 2 hrs when dosing $(Acr\text{-}Lys)_6$–Cys-Mal-PEG polyplexes. In addition to the liver and spleen, the blood accounted for the majority of the radioactive dose, which ranged from 65-40% in the circulation during 2 hrs following dosing of $(Acr\text{-}Lys)_6$–Cys-Mal-PEG polyplexes.

## Discussion

PEGylated polyacridine peptides were designed to bind to plasmid DNA for the purpose of making polyplexes more blood compatible. This is the first step toward ultimately adding a targeting ligand and sub-cellular targeting peptides needed to complete the delivery system and achieve significant in vivo gene expression following i.v. dosing, without the requirement of an additional stimulation. To accomplish this goal, an optimal polyacridine peptide would need to bind to DNA with sufficient affinity to protect from DNase metabolism in the circulation, while being able to release the DNA inside the cell to gain access to the nucleus.

It is likely there are many unique sequences of polyacridine peptides that accomplish this goal. The aim of the structure-activity study described was to determine a relationship between the number of Acr, the binding affinity for DNA, the polyplex pharmacokinetic half-life, and the magnitude of stimulated expression in mice. Initially, a nine amino acid peptide allowed the incorporation of four Acr spaced by a hydrophobic (Leu), anionic (Glu), or cationic (Lys and Arg) residues, along with a C-terminal Cys for modification. Prior studies from our group established that spacing amino acids that lacked a bulky side-chain or protecting group (Gly or Ala) resulted in low peptide yields. During the course of this study it was necessary to further optimize peptide yield to prepare $(Acr\text{-}Lys)_6$-Cys. While it is possible to prepare even longer polyacridine peptides of this design, we found the yields begin to diminish, as demonstrated by the case of $(Acr\text{-}Lys)_8$-Cys. Each of the polyacridine peptides was coupled to $PEG_{5000\ Da}$, resulting in PEGylated polyacridine peptide that produced a single symmetrical peak on RP-HPLC and a MALDI-TOF MS that verified the structure.

The primary structural features that influence the level of gene expression mediated by PEGylated polyacridine peptides was the presence of at least four Acr residues combined with cationic (Lys or Arg) spacing amino acid. PEGylated polyacridine peptides possessing four Acr residues spaced by either Glu or Leu

Table 4-3. Biodistribution Parameters for PEGylated Polyacridine Polyplexes

| Polyacridine Peptide Polyplex | Time min) | Blood[a] | Liver[b] | Lung[b] | Spleen[b] | Stomach[b] | Kidney[b] | Heart[b] | LI[b] | SI[b] | Total[c] |
|---|---|---|---|---|---|---|---|---|---|---|---|
| $^{125}$I-DNA | 5 | 14.4± 5.8 | 65.7±2.5 | 6.1±2.2 | 2.8±0.3 | 0.2±0.0 | 0.9±0.2 | 0.1±0.0 | 0.2±0.1 | 0.4±0.1 | 84.7±11.2 |
| | 30 | 6.8±1.7 | 31.1±6.2 | 1.4±0.1 | 2.1±0.6 | 1.6±1.3 | 3.5±1.0 | 0.2±0.0 | 1.6±0.7 | 2.8±0.3 | 51.1±11.9 |
| | 60 | 5.2±1.6 | 12.7±2.0 | 0.9±0.2 | 1.3±0.2 | 4.5±1.0 | 3.5±0.6 | 0.2±0.0 | 1.1±0.2 | 2.1±0.3 | 31.5± 6.2 |
| | 120 | 5.2±1.5 | 6.1±1.5 | 0.5±0.2 | 0.8±0.2 | 9.4±3.2 | 1.6±0.9 | 0.1±0.1 | 1.9±0.8 | 2.6±0.5 | 28.2±8.9 |
| (Acr-Lys)$_2$Cys-Mal-PEG $^{125}$I-DNA | 5 | 26.4±14.0 | 68.9±3.6 | 1.9±0.1 | 5.3±1.8 | 0.2±0.0 | 0.8±0.5 | 0.1±0.1 | 0.3±0.2 | 0.4±0.1 | 104.2±20.5 |
| | 30 | 7.6±1.3 | 33.6±4.0 | 1.0±0.3 | 1.7±0.4 | 1.5±0.3 | 2.8± 0.6 | 0.2±0.1 | 1.9 ±0.5 | 2.5±0.5 | 52.8±8.1 |
| | 60 | 6.2±0.6 | 17.1±3.1 | 0.7±0.2 | 0.7±0.5 | 6.1±2.0 | 2.6± 1.1 | 0.2±0.1 | 2.3±0.5 | 3.1±1.1 | 39.1±9.3 |
| | 120 | 7.2±1.0 | 10.9±1.5 | 0.8±0.2 | 1.0 ±0.4 | 8.3±1.7 | 2.3± 0.4 | 0.2±0.0 | 1.9±0.4 | 3.6±0.7 | 36.2±6.4 |
| (Acr-Lys)$_4$Cys-Mal-PEG $^{125}$I-DNA | 5 | 54.1±2.7 | 57.5±5.8 | 2.2±0.9 | 2.1±0.5 | 0.3±0.2 | 0.9±0.5 | 0.2±0.1 | 0.3±0.2 | 0.5±0.2 | 118.0±11.1 |
| | 30 | 37.3±4.4 | 58.6±9.7 | 1.0±0.1 | 4.5±2.3 | 0.5±0.1 | 1.4± 0.9 | 0.1±0.1 | 0.5±0.1 | 0.9±0.5 | 104.8±18.3 |
| | 60 | 31.2±2.2 | 32.2±1.2 | 0.8±0.3 | 4.7±0.3 | 2.6±0.4 | 2.1 ±0.8 | 0.2±0.0 | 1.1±0.2 | 2.7±0.7 | 77.6± 6.1 |
| | 120 | 27.4±3.2 | 29.9±2.7 | 1.0±0.2 | 4.1±2.4 | 5.3±2.4 | 2.7± 1.5 | 0.2±0.1 | 1.5±0.6 | 1.7±0.1 | 73.9±13.3 |
| (Acr-Lys)$_6$Cys-Mal-PEG $^{125}$I-DNA | 5 | 65.8±14.3 | 53.8±7.0 | 1.3±0.5 | 6.8±3.1 | 0.4±0.2 | 0.7±0.1 | 0.2±0.0 | 0.2±0.1 | 0.5±0.0 | 129.6±25.3 |
| | 30 | 54.9±12.3 | 58.7±2.0 | 0.9±0.2 | 11.7±1.1 | 0.7±0.2 | 1.1± 0.1 | 0.2±0.1 | 0.5±0.3 | 0.9±0.2 | 129.6±16.5 |
| | 60 | 55.2±7.6 | 39.6±2.8 | 0.6±0.1 | 15.4±0.1 | 1.3±0.3 | 1.3 ±0.4 | 0.1±0.1 | 0.8±0.3 | 1.5±0.2 | 115.9±11.8 |
| | 120 | 39.4±10.2 | 26.8±2.1 | 0.8±0.2 | 18.0±1.4 | 3.2±2.8 | 1.5 ±0.2 | 0.1±0.0 | 1.1±0.7 | 2.2±0.3 | 93.2±17.9 |

a. Percent of dose base on pharmacokinetic analysis. Results represent the mean (n=3) and standard deviation.

b. Percent of dose based on gamma counting of tissue. Results represent the mean (n=3) and standard deviation.

c. Total percent of dose recovered.

demonstrated weak binding to DNA (Figure 4-5A), resulting in no stimulated gene expression (Figure 4-10A), presumably due to the inability to protect DNA from metabolism in vivo. Conversely, $(Acr\text{-}Lys)_4$–Cys-Mal-PEG or $(Acr\text{-}Arg)_4$–Cys-Mal-PEG possessed higher affinity for binding with DNA (Figure 4-5A), which correlated with their ability to produce stimulated expression (Figure 4-10A), due to their ability to stabilize DNA from premature metabolism in vivo (Figure 4-12E). We previously reported that PEGylated Cys-Trp-$Lys_{18}$ formed polyplexes that readily dissociate in the blood, resulting in rapid DNA metabolism (*36*). It was therefore anticipated that stimulation of i.v. dosed PEGylated Cys-Trp-$Lys_{18}$ polyplexes would not produce gene expression (Figure 4-9A, cont 1). Thus, a combination of polyintercalation and ionic binding to plasmid DNA results in improved affinity and stable polyplexes, where either functionality alone is insufficient.

One of the more unique aspects of PEGylated polyacridine polyplexes is their open polyplex structures that resemble naked DNA. These structures appear to form at all stoichiometries of peptide to DNA that remain anionic (Figure 4-6). $(Acr\text{-}Lys)_4$–Cys-Mal-PEG and $(Acr\text{-}Arg)_4$–Cys-Mal-PEG produced anionic open-polyplexes across the titration range of 0.2-0.8 nmol of peptide (Figure 4-6A and E). When i.v. dosed and allowed to circulate for 30 min, the level of stimulated expression was dependent upon the stoichiometry of peptide to DNA, resulting in a parabolic peptide dose-response curve (Figure 4-10B). These results suggested that the DNA stability afforded by $(Acr\text{-}Lys)_4$–Cys-Mal-PEG and $(Acr\text{-}Arg)_4$–Cys-Mal-PEG, was dependent on peptide stoichiometry, with higher stoichiometries required to stabilize DNA from metabolism (Figure 4-8B) that also resulted in nearly charge neutral polyplexes (Figure 4-6A) with diminished gene transfer efficiency.

$(Acr\text{-}Lys)_6$–Cys-Mal-PEG binds to DNA with higher affinity compared to all other peptides studied (Figure 4-5B). It also possessed an unusual zeta potential titration curve that produced anionic open-polyplexes at 0.2 nmol of peptide, which convert to

cationic closed-polyplexes at 0.8 nmol and higher (Figure 4-6F and Figure 4-7F & G). The DNase stability afforded to $(Acr\text{-}Lys)_6$–Cys-Mal-PEG polyplexes at both 0.2 and 0.8 nmol of peptide (Figure 4-8C) resulted in equivalent, high-level stimulated gene expression at each stoichiometry from 0.2-0.8 nmol (Figure 4-11A). The greater affinity also led to greater stimulated expression for longer delay times compared to $(Acr\text{-}Arg)_4$–Cys-Mal-PEG polyplexes, such that following the administration of 1 μg of DNA, a 1 hour delayed stimulation produced high-level gene expression, and at a 2 hour delay measurable expression was still detected (Figure 4-11B). These results established that $(Acr\text{-}Lys)_6$–Cys-Mal-PEG polyplexes mediated equal gene expression as either closed or open-polyplex structures, and suggest that enhanced binding affinity translates to higher expression at longer delay times due to postponing metabolism.

Pharmacokinetic and biodistribution studies were used to gain insight into the underlying mechanism of how delayed hydrodynamic stimulation caused $(Acr\text{-}Lys)_6$–Cys-Mal-PEG polyplexes to mediate gene expression in the liver. The most striking result was the apparent long pharmacokinetic half-life of $(Acr\text{-}Lys)_4$–Cys-Mal-PEG and $(Acr\text{-}Lys)_6$–Cys-Mal-PEG polyplexes, compared to the rapid loss of $^{125}$I-DNA and $(Acr\text{-}Lys)_2$–Cys-Mal-PEG polyplexes (Figure 4-12A). Electrophoretic analysis of the $^{125}$I-DNA recovered from blood clearly established that $(Acr\text{-}Lys)_6$–Cys-Mal-PEG stabilized DNA in the circulation for 2 hrs (Figure 4-12F), whereas $(Acr\text{-}Lys)_4$–Cys-Mal-PEG stabilized open circular DNA bands for at least 30 min (Figure 4-12E), and $(Acr\text{-}Lys)_2$–Cys-Mal-PEG for no more than 20 min (Figure 4-12D). Most importantly, approximately 40% of the radioactive dose remained in the blood after 2 hrs when dosing $(Acr\text{-}Lys)_6$–Cys-Mal-PEG $^{125}$I-DNA polyplexes (Table 4-3). This unique feature suggests that $(Acr\text{-}Lys)_6$–Cys-Mal-PEG polyplexes may find application in targeting DNA to tissues outside the liver. These results cannot be directly compared with other studies that developed long circulating DNA formulations. In each of these prior studies, the pharmacokinetics of the carrier system was analyzed by incorporating either a radiolabel or fluorophore into the

carrier, whereas the metabolic status of DNA recovered from blood time points was not determined.

Analysis of the tissue distribution of $^{125}$I-DNA polyplexes over time established the liver as the major site of distribution accounting for approximately 54-69% of the dose within the first 5 min, with only minor (<1%) distribution to other organs. (Acr-Lys)$_4$–Cys-Mal-PEG and (Acr-Lys)$_6$–Cys-Mal-PEG polyplexes produced a distinct liver distribution and metabolism profile, with maximal accumulation of 60% at 20 min followed by a decrease to 30% over two hrs (Figure 4-12A). The liver biodistribution profile of $^{125}$I-DNA and (Acr-Lys)$_2$–Cys-Mal-PEG $^{125}$I-DNA polyplexes were coincident with maximal accumulation of 65% at 5 min, followed by a decrease to 10% over 2 hrs. Taken together, the pharmacokinetic and biodistribution data support a hypothesis in which the DNA that distributes to the liver is primarily responsible for the stimulated expression. However, liver distribution is not sufficient; the DNA must also be sufficiently metabolically stabilized to mediate significant stimulated expression with delay times up to 1 hr. The hypothesis that liver associated DNA, and not the DNA in blood, is responsible for stimulated expression is deduced by comparison of the level of stimulated expression from (Acr-Lys)$_6$–Cys-Mal-PEG polyplexes (Figure 4-11B), which decrease by nearly 100-fold between 60 and 120 min while the level of intact DNA in the blood remains constant over that time period (Figure 4-12F).

In conclusion, this is the first report of high-level stimulated gene expression from a non-viral delivery system that mirrors the level of expression produced by the same dose administered by direct hydrodynamic dosing. The unique attributes of PEGylated polyacridine peptides establish their ability to form open or closed polyplex structures that stabilize DNA from metabolism in mice and allow a stimulation of a high volume rapid dose of saline to complete the gene transfer, even after a 1 hour delay following the primary dose. This is still only a starting point toward the development of a non-viral delivery system that produces high level expression in animals without physical

stimulation to produce gene expression. However, given the modularity of polyacridine peptides, it should be possible to build multi-component gene delivery systems that drive the DNA further toward the nucleus, to ultimately achieve this aim.

# CHAPTER 5

# THE SYNTHESIS AND DEVELOPMENT OF NOVEL MULTI-COMPONENT POLYACRIDINE GENE DELIVERY SYSTEMS


## Abstract

An integrated approach is necessary to successfully target i.v. dosed plasmid DNA to the nucleus of specific cells in animals. Previous chapters have reported the development of polyacridine peptides as novel anchor peptides that reversibly bind to plasmid DNA. We initially tested this concept by preparing polyacridine-melittin peptides that demonstrate potent in vitro gene expression and with PEGylated-polyacridine peptides mediating potent in vivo stimulated gene transfer.

In the present chapter, we report the synthesis of a triantennary N-glycan hepatocyte targeting ligand peptide based upon the $(Acr\text{-}Lys)_6$-Cys scaffold. As a hepatocyte targeting control, an agalactosyl triantennary polyacridine peptide was synthesized. Furthermore, PEG was reducibly conjugated to the polyacridine peptide $(Acr\text{-}Lys)_6$-Cys to provide the shielding component. An alternative endosomal escape mechanism afforded by the endosomal buffering capacity of histidine was investigated with $(Acr\text{-}His)_6$-SS-PEG and $(Acr\text{-}His)_6$-Cys-TRI. In an attempt to overcome the delivery barrier presented by the nuclear envelope, we have synthesized polyacridine NLS and NLS-fusogen constructs.

Ternary polyacridine DNA polyplexes were formed by simultaneous incorporation of PEGylated polyacridine peptide, polyacridine-fusogen, and polyacridine -triantennary glycopeptide. Pharmacokinetic and biodistribution experiments established liver specific uptake of ternary polyplexes. Gene transfer experiments evaluating the transfection of multi-component complexes demonstrated low level liver gene expression without biophysical stimulation at a 25 μg pGL3 dose. The results establish the ability to

deliver i.v. dosed plasmid DNA in vivo using a novel and modular polyacridine gene delivery system.

## Introduction

The ultimate aim of non-viral gene delivery involves the efficient and targeted delivery of DNA polyplexes to specific cells in vivo. Additionally, the carrier system must incorporate multiple components to overcome the various barriers to efficient delivery and subsequent therapeutic protein expression. A notable impediment that exists is the undesirable non-specific interaction between blood components and DNA nanoparticles or proteins such as DNases that can degrade plasmid DNA to nucleotides (*44, 124*). A common method of overcoming or shielding polyplexed nucleic acids is through PEGylation of the vehicle and stability to DNase degradation being a property of the vehicle itself (*41, 43, 158-160*). A second barrier that exists is delivering the plasmid to the intended cells, which can be accomplished through incorporation of targeting ligands such as peptides or N-glycans (*26, 36, 38*). In this study, the intended targets are hepatocytes located within the liver. The ligand used is the triantennary-N-glycan to target the endocytosing ASPG-R to cross the cell membrane (*26, 38, 40, 41*).

Once inside the endosome, the vehicle must provide means of escape or risk degradation within the endosome, perhaps one of the greatest barriers to overcome (*12, 46, 73, 125*). Our attempts to address this barrier have been the incorporation of fusogenic peptides, such as melittin, JTS-1, and the charge neutral peptide PC-4 (*26, 31, 42, 46-48, 80, 92, 93, 161*). In addition to incorporating fusogenic peptides, we have investigated the incorporation of endosomal buffering agents within the backbone of polyacridine peptides in the form of histidine as an alternative strategy of providing an endosomal escape mechanism (*57-61, 63, 168, 169*).

Another major barrier exists in the efficient translocation of plasmid DNA from the cytosol to the nucleus as it has been well documented that senescent or primary cells

are very difficult to transfect due to a relatively non-permeable nuclear membrane (*94-100*). This has been attempted previously with polyplex incorporation of nuclear localization sequences in a covalent or reversible fashion, resulting often in controversial in vitro data (*10, 11, 13*). To overcome the nuclear localization barrier, we have synthesized a panel of fusogenic peptide analogues based upon PC-4 or melittin incorporating the SV40 NLS sequence PKKKRKV (*101*) to generate NLS-fusogen chimeras. We hypothesize that these NLS-fusogen chimeras will be translocated to the nuclear membrane, and upon interaction with the membrane, generate pores large enough for plasmid DNA to transiently migrate through to enhance transgene expression in vivo. We have also synthesized an NLS peptide conjugated to the polyacridine peptide scaffold to examine NLS activity.

As discussed in the previous chapter, $(Acr\text{-}Lys)_6$-Cys was identified as the lead polyacridine DNA anchor peptide that offers stronger affinity for DNA versus polycationic vehicles (PEI or poly-lysine) due to a mixed ionic-intercalation phenomenon. Therefore, $(Acr\text{-}Lys)_6$-Cys will serve as the common anchoring peptide in this study on which PEG, TRI, and fusogenic peptides will be attached. Upon synthesis of all components, DNA nanoparticle multi-component complexes formed with shielding peptide, glycopeptide, and fusogenic peptide will be characterized and evaluated in vivo using bioluminescence imaging (BLI) to quantify luciferase expression after plasmid delivery.

## Materials and Methods

Unsubstituted Wang resin for peptide synthesis, 9-hydroxybenzotriazole, Fmoc-protected amino acids, and 1,3-Diisopropylcarbodiimide (DIC), were obtained from Advanced ChemTech (Lexington, KY). O-(7-Azabenzo-triazol-1-yl)-N,N,N’,N’-tetramethyluronium hexafluorophosphate (HATU), and O-(Benzotriazol-1-yl)-N,N,N',N'-tetramethyluronium hexafluorophosphate (HBTU), and Fmoc-Lysine-OH were

purchased from AAPPTEC (Louisville, KY). N,N-Dimethylformamide (DMF), trifluoroacetic acid (TFA), and acetonitrile were purchased from Fisher Scientific (Pittsburgh, PA). Diisopropylethylamine, piperdine, acetic anhydride, Tris (2-carboxyethyl)-phosphine hydrochloride (TCEP), 9-chloroacridine, maleic anhydride, 2-2'dithiodipyridine (DTDP), and thiazole orange were obtained from Sigma Chemical Co. (St. Louis, MO). Triisopropylsilane (TIS), 1, 2-ethanedithiol (EDT) and polyethylene amine (PEI 25 KDa) were purchased from Aldrich (Milwaukee, WI). D-Luciferin and luciferase from *Photinus pyralis* were obtained from Roche Applied Science (Indianapolis, IN). CHO cells were acquired from the American Type Culture Collection (Manassas, VA). Inactivated qualified fetal bovine serum (FBS) was from Life Technologies, Inc. (Carlsbad, CA). BCA reagent was purchased from Pierce (Rockford, IL). pGL3 control vector, a 5.3 kb luciferase plasmid containing a SV40 promoter and enhancer, was obtained from Promega (Madison, WI). pGL3 was amplified in a DH5α strain of *Escherichia coli* and purified according to manufacturer's instructions.

## Synthesis of 9-Phenoxyacridine and Fmoc Lysine(Acridine)-OH

9-phenoxyacridine was synthesized with modification from the methods of Tung et al (*121*). Briefly, 12 g of phenol (127.5 mmol) and 0.72 g of sodium hydroxide (18 mmol) were heated to 100ºC. To the liquified phenol, 2.8 g of 9-chloroacridine (13.105 mmol) was added and stirred vigorously for 1.5 hrs. The reaction was quenched by the addition of 100 ml of 2 M sodium hydroxide then allowed to sit at RT overnight. A yellow precipitate was filtered, washed with water and dried in vacuo (3.4822g, 12.835 mmol, 97.9%, M.P. 123 – 124 º C, TLC, 15 : 5 : 1 : 0.5, ethyl acetate / methanol / hexane / acetic acid, $R_f = 0.18$). $^1$H NMR (DMSO-$d_6$) δ 8.23 (d, 2H), 8.04 (d, 2H), 7.88 (t, 2H), 7.59 (t, 2H), 7.32 (t, 2H), 7.08 (t, 1H), 6.88 (d 2H).

The synthesis of Fmoc-Lysine(Acridine)-OH was conducted as previously described in Chapters 3 and 4 with modification of the method to substitute the reaction solvent phenol with methanol (*122*). Fmoc-Lysine(Acr)-OH was prepared by adding 6.5 g of Fmoc-Lys-OH (17.64 mmol) in 100 ml of molecular sieve filtered methanol to 9-phenoxyacridine (6.63 g, 24.4 mmol), then heated at 50 ºC for 24 hrs with a condenser in place to prevent evaporation of the reaction solvent (*122*). Following reaction completion, excess methanol was removed by rotary evaporation until 10 ml remained; diethyl ether (250 ml) was then added while stirring vigorously until a yellow precipitate formed that was immediately recovered by filtration and washed repeatedly with diethyl ether. The product was allowed to dry overnight under vacuum (9.55 g, 17.5 mmol, 99.2%), M.P. 135-140ºC**,** TLC: 1:1, 0.1 v/v % TFA / acetonitrile, $R_f = 0.75$). MS: $(M + H^+)^{1+}$= 545.5 m/z. $^1$H NMR (DMSO-$d_6$) δ 6.7-7.8 (m, 17H), 3.6-3.95 (m, 2H), 3.25-3.53 (br, 3H), 2,06 (m, 1H), 0.8-1.5 (m, 6H).

Synthesis of Maleimide Glycine (Mal-Gly-OH)

Glycine (5 g, 66.6 mmol) and maleic anhydride (6.6 g, 66.6 mmol) were suspended in 80 ml of acetic acid and allowed to react for 3 hrs at RT. The resulting white precipitate was collected by filtration, washed with cold water, and dried (10.95 g, 63.3 mmol, 95 %, M.P. 187-189ºC**,** TLC: 2:1:1:1 isopropyl alcohol / acetic acid / ethyl acetate / water, $R_f = 0.5$). The glycine maleic acid intermediate was characterized by proton NMR (300 MHz, DMSO-d6): δ = 9.2 (s, 1H) 6.397 (d, 1H, j = 8.57 Hz), 6.310 (d, 2H, j = 12.86 Hz), 2.0 (d, 2H j = 6.86 Hz).

Glycine maleamic acid (5.2 g, 30.04 mmol) and 2.1 equivalents of triethylamine (6.37 g, 63 mmol) were refluxed for 3 hrs in 500 ml toluene with removal of water with a Dean-Stark apparatus. Upon reaction completion, the toluene solution was decanted and dried. The resulting solid was acidified with 2 M HCl, extracted with ethyl acetate, dried with $MgSO_4$ and evaporated to yield Mal-Gly-OH (1.7 g, 11 mmol, 36.5%, M.P. 99-

110ºC**,** TLC: 2:1:1:1 isopropyl alcohol / acetic acid / ethyl acetate / water, $R_f = 0.72$). The product was characterized by proton NMR (300 MHz, DMSO-d6): $\delta = 7.108$ (s, 2H), 4.105 (s, 2H) (*126*).

## Synthesis and Characterization of Polyacridine and Fusogenic Peptide Analogues

Melittin analogues, PC-4, and JTS-1 peptides were prepared by solid phase peptide synthesis using standard Fmoc procedures with 9-hydroxybenzotriazole and HBTU double couplings on a 30 μmol scale on an Advanced ChemTech APEX 396 synthesizer (Table 5-1). Polyacridine peptide $(Acr\text{-}Lys)_6$-Cys, $(Acr\text{-}Lys)_8$-Cys, and $(Acr\text{-}His)_6$-Cys were synthesized using double coupling for Fmoc-Lys(Acr)-OH and triple coupling for the spacing amino acid Fmoc-Lys(Boc)-OH or Fmoc-His(Trt)-OH using HATU and 9-hyrdoxybenzotriazole. Fmoc-Lys(Acr)-OH was preactivated by addition of 0.4 mol equivalents HATU relative to amino acid to generate DMF soluble reactive intermediate Fmoc-Lys(Acr)-OBt ester. Mal-K-melittin, Mal-PC-4, and Mal-NLS were prepared by coupling Mal-Gly-OH to the N-terminus of side-chain protected full-length peptide on resin utilizing a 6-fold excess of Mal-Gly-OH, DIC and HOBt, and reacted for 4 hrs while stirring. The resin was filtered, washed with DMF, DCM and methanol, and then dried. Mal-Gly containing peptides were removed from resin and side chain deprotected using a cleavage cocktail of TFA/triisopropylsilane/water (95:2.5:2.5 v/v/v) for 3 hrs followed by precipitation in cold ether.

Peptides containing a cysteine residue were removed from resin and side chain deprotected using a cleavage cocktail of TFA/ethandithiol/water (93:3:4 v/v/v) for 3 hrs followed by precipitation in cold ether. Precipitates were centrifuged for 10 min at 4000 rpm at 4ºC and the supernatant decanted. Peptides were then reconstituted with 0.1 v/v % TFA and purified to homogeneity on RP-HPLC by injecting 0.5-2 μmol onto a Vydac C18 semipreparative column (2 x 25 cm) eluted at 8 ml/min with 0.1 v/v % TFA with an

acetonitrile gradient of 20-45 v/v % (melittin and PC-4 analogues), 75-100 v/v % (Cys-JTS-1 and TP-Cys-JTS-1), or 15-25 v/v % (polyacridine peptides) over 30 min while monitoring tryptophan (Abs 280 nm) or acridine (Abs 409 nm). The major peak was collected and pooled from multiple runs, concentrated by rotary evaporation, lyophilized, and stored at -20ºC. Purified peptides were reconstituted in 0.1 v/v % TFA and quantified by absorbance (tryptophan $\varepsilon_{280\ nm} = 5600\ M^{-1}\ cm^{-1}$(K-melittin and Cys-JTS-1 analogues), thiolpyridine and tryptophan $\varepsilon_{280\ nm} = 10915\ M^{-1}\ cm^{-1}$(TP-Cys-K-melittin and TP-Cys-JTS-1 analogues), $\varepsilon_{280\ nm} = 18130\ M^{-1}cm^{-1}$ (PC-4 analogues), $\varepsilon_{280\ nm} = 23445\ M^{-1}cm^{-1}$ (TP-Cys-PC-4 analogues), or acridine $\varepsilon_{409\ nm} = 9266\ M^{-1}\ cm^{-1}$ per acridine, assuming additivity of ε for multiple acridines) to determine isolated yield. Purified peptides were characterized by LC-MS by injecting 2 nmol onto a Vydac C18 analytical column (0.47 x 25 cm) eluted at 0.7 ml/min with 0.1 v/v % TFA and an acetonitrile gradient of 10-55 v/v% over 30 min while acquiring ESI-MS in the positive ion mode. JTS-1 peptides (Cys-JTS-1 and TP-Cys-JTS-1) were eluted with 0.1 v/v % TFA with an acetonitrile gradient of 45-99 v/v % over 30 min while acquiring ESI-MS in the negative mode.

Cys-melittin, Cys-JTS-1, and Cys-PC-4 analogues were reacted with 10-eq of DTDP in 2-propanol/2 N acetic acid (10:3) for 8 hrs at RT to generate the thiolpyridine protected peptide (*127*). The reaction mixture, with exception to TP-Cys-JTS-1, was concentrated by rotary evaporation and applied to a Sephadex G-10 column eluted (2.5 x 50 cm) with 0.1 v/v % TFA while monitoring absorbance at 280 nm to remove excess DTDP. The peptide peak fractions were pooled, concentrated, lyophilized, and purified to homogeneity by RP-HPLC as described previously. TP-Cys-JTS-1 was purified to homogeneity after thiolpyridine reaction by preparatory RP-HPLC and eluted at 8 ml/min with 0.1 v/v % TFA and an acetonitrile gradient of 75-100 v/v % due to the peptides' hydrophobic nature.

$(Acr\text{-}Lys)_6$-Mal-fusogen (Mal-K-melittin or Mal-PC-4) or Mal-NLS peptide analogues were synthesized on a 1 μmol scale based on fusogen or NLS peptide, using

1.4 equivalents (1.4 μmol) of the reduced $(Acr\text{-}Lys)_6$-Cys. One μmol of Mal-fusogen (Mal-K-melittin and Mal-PC-4) or Mal-NLS were prepared in 5 ml of 10 mM ammonium acetate pH 5 and added to $(Acr\text{-}Lys)_6$-Cys. The reaction occurred over 12 hrs at RT as determined by analyzing aliquots by LC-MS. At reaction completion, the reaction mixture was concentrated by rotary evaporation and lyophilized prior to purification of $(Acr\text{-}Lys)_6$-Mal-fusogen by RP-HPLC eluted at 8 ml/min with 0.1 v/v % TFA and acetonitrile gradient of 35-45 v/v % over 30 min while detecting at 409 nm. The counter-ion was exchanged by repetitive freeze drying cycles with 0.5 M acetic acid to obtain the peptide in an acetate salt form and reconstituted in water and quantified by $Abs_{409nm}$ to determine isolated yield (Table 5-2).

Alternatively, 1 μmol of thiolpyridine-Cys-fusogenic peptide (TP-Cys-K-melittin, TP-Cys-PC-4, TP-Cys-NLS-PC-4, TP-Cys-control-NLS-PC-4, TP-PC-4-NLS, and TP-Cys-NLS-K-melittin) was prepared in 5 ml of 10 mM ammonium acetate pH 6 and added to 1.4 μmol $(Acr\text{-}Lys)_6$-Cys. After 24 hrs, $(Acr\text{-}Lys)_6$-SS-fusogenic peptides were purified and characterized by LC-MS as described above.

Synthesis of $(Acr\text{-}Lys)_6$-SS–JTS-1, $(Acr\text{-}Lys)_8$-SS–JTS-1, and $(Acr\text{-}Lys)_6$-SS-NLS-QL-melittin were synthesized with modification as described above. One μmol of TP-Cys-JTS-1 or TP-Cys-NLS-QL-melittin were prepared in 2.5 ml methanol to facilitate peptide solubility and added to 1.4 μmol $(Acr\text{-}Lys)_6$-Cys or $(Acr\text{-}Lys)_8$-Cys in 2.5 ml of 10 mM ammonium acetate pH 6. After 24 hrs, $(Acr\text{-}Lys)_6$-SS–JTS-1, $(Acr\text{-}Lys)_8$-SS–JTS-1, and $(Acr\text{-}Lys)_6$-SS-NLS-QL-melittin peptides were purified and characterized by LC-MS as described above.

## Synthesis and Characterization of PEGylated Polyacridine Peptides

PEGylation of the Cys residue on $(Acr\text{-}X)_6$-Cys, where X is the spacing amino acid Lys or His, was achieved by reacting 1 μmol of peptide with 1.1 μmol of $PEG_{5000\ Da}$-

OPSS in 4 ml of 10 mM ammonium acetate buffer pH 7 for 12 hrs at RT. PEGylated peptides were purified by semipreparative HPLC as previously described and eluted at 8 ml/min with 0.1 v/v % TFA and acetonitrile gradient of 25-55 v/v % over 30 min while monitoring acridine at 409 nm. The major peak was collected and pooled from multiple runs, concentrated by rotary evaporation, lyophilized, and stored at -20ºC. The counter-ion was exchanged as previously described and reconstituted in water and quantified by $Abs_{409nm}$ to determine isolated yield (Table 5-3). PEG-peptides were characterized by MALDI-TOF MS by combining 1 nmol with 10 μl of 2 mg per ml α-cyano-4-hydroxycinnamic acid (CHCA) in 50 v/v % acetonitrile and 0.1 v/v % TFA. Samples were spotted onto the target and ionized on a Bruker Biflex III Mass Spectrometer operated in the positive ion mode.

## Synthesis and Characterization of Polyacridine $(Acr\text{-}X)_6$-Cys-Triantennary Glycopeptides

Glycosylation of the Cys residue on $(Acr\text{-}Lys)_6$-Cys or $(Acr\text{-}His)_6$-Cys was achieved by reacting with 1 mol equivalent of iodoacetamide-triantennary N-glycan (I-TRI) with 1.125 mol equivalent of $(Acr\text{-}Lys)_6$-Cys or $(Acr\text{-}His)_6$-Cys in 5 ml of 100 mM Tris buffer pH 8 for 12 hrs at RT (Scheme 5-1). The polyacridine glycopeptide was purified by semipreparative HPLC as previously described and eluted with 0.1 v/v % TFA with an acetonitrile gradient of 15-30 v/v % at 8 ml/min while monitoring acridine at 409 nm. The major peak was collected and pooled from multiple runs, concentrated by rotary evaporation, lyophilized, and stored at -20ºC. The counter-ion was exchanged as previously described and reconstituted in water and quantified by $Abs_{409nm}$ to determine isolated yield (Table 5-3). Glycopeptides were characterized by LC-MS by injecting 1 nmol and eluted 0.7 ml/min with 0.1 v/v % TFA and an acetonitrile gradient of 10-40 v/v % over 30 min while acquiring ESI-MS in the positive mode.

## Synthesis and Characterization of $(Acr\text{-}Lys)_6$-Cys-Agalactose Triantennary Glycopeptides

Removal of the terminal galactose residues was performed according to an established literature procedure (*38*). Prior to removal of terminal galactose residues on $(Acr\text{-}Lys)_6$-Cys-TRI, 100 nmol of the glycopeptide was freeze dried. The lyophilized peptide was reconstituted in 450 µl of 50 mM citrate phosphate buffer, pH 4.3. The reaction was initiated upon addition of 60 mU of β-galactosidase from bovine testes (0.6 mU of enzyme per nmol peptide in 50 µl of citrate phosphate buffer) allowed to proceed in a 37ºC water bath for 6 hrs. The reaction was terminated by freezing the reaction mixture at -70ºC.

The agalactose polyacridine glycopeptide was purified by semipreparative HPLC as previously described and eluted with 0.1 v/v % TFA with an acetonitrile gradient of 15-30 v/v % at 8 ml/min while monitoring acridine at 409 nm. The major peak was collected and pooled from multiple runs, concentrated by rotary evaporation, lyophilized, and stored at -20ºC. The counter-ion was exchanged as previously described and reconstituted in water and quantified by $Abs_{409nm}$ to determine isolated yield (Table 5-3). Glycopeptides were characterized by LC-MS by injecting 1 nmol and eluted at 0.7 ml/min with 0.1 v/v % TFA and an acetonitrile gradient of 10-40 v/v % over 30 min while acquiring ESI-MS in the positive mode.

## Formulation and Characterization of Polyacridine Peptide Polyplexes

The relative binding affinity of peptides for DNA was determined by a fluorophore exclusion assay (*22*). pGL3 (200 µl of 4 µg/ml in 5 mM Hepes pH 7.5 containing 0.1 µM thiazole orange) was combined with 0, 0.05, 0.1, 0.25, 0.35, 0.5, 1, and 2 nmol of peptide in 300 µl of Hepes and allowed to bind at RT for 30 min. Thiazole orange fluorescence was measured using an LS50B fluorometer (Perkin-Elmer, U.K.) by

exciting at 498 nm while monitoring emission at 546 nm with the slit widths set at 10 nm. A fluorescence blank of thiazole orange in the absence of DNA was subtracted from all values before data analysis. The data is presented as nmol of peptide per μg of pGL3 versus the percent fluorescence intensity ± the standard deviation determined by three independent measurements.

Multi-component complex DNA polyplexes were prepared at 0.5 nmol of peptide per μg of DNA with 100% (Acr-Lys)$_6$-SS-PEG, 90% (Acr-Lys)$_6$-SS-PEG and 10% (Acr-Lys)$_6$-SS-TRI, with 70% (Acr-Lys)$_6$-SS-PEG, 20% (Acr-Lys)$_6$-SS-K-melittin or (Acr-Lys)$_6$-SS-PC-4 at a concentration of 100 μg per ml of DNA and directly deposited on a freshly cleaved mica surface and allowed to bind for 10 min prior to washing with deionized water. An Asylum atomic force microscope (AFM) MFP3D (Santa Barbara, CA) was operated in the AC-mode in order to image either naked DNA or DNA polyplexes using a silicon cantilever (Ultrasharp NSC15/AIBS, MikroMasch).

### Multi-Component Integration Analysis through Spin Assay

Polyacridine peptide components were added together in a 1.5 ml centrifuge tube at the appropriate ratios (70% -3.5 nmol (Acr-Lys)$_6$-SS-PEG, 20%-1.0 nmol (Acr-Lys)$_6$-SS-K-Melittin, and 10% -0.5 nmol (Acr-Lys)$_6$-Cys-TRI) and freeze dried. Once dry, 25 μl $H_2O$ was added to reconstitute the peptides. pGL3 (10 μg in 25 μl $H_2O$) was added dropwise while vortexing. Multi-component complexes containing variable amounts of PEG, NLS, and fusogen component were prepared accordingly while maintaining the 0.5 nmol of peptide per μg DNA ratio. Polyplexes were allowed 30 minutes at room temperature to form ternary complexes. As a multi-component peptide sample control, pGL3 was omitted and 25 μl $H_2O$ was added to the peptide mixture. All samples were prepared in triplicate.

Once peptides were allowed to form polyplexes, 500 μl of $H_2O$ was added to the polyplex solution and then transferred to a Corning Spin-X UF 500 Concentrator

equipped with a 50 KDa molecular weight cutoff membrane. Samples were then centrifuged for 10 min at 13,000 g. As recommended by the manufacturer, a second round of centrifugation was employed immediately following addition of 500 µl of $H_2O$ and centrifugation repeated for 10 min at 13,000 g. After centrifugation, the filtrate was pooled (total volume is 1 ml). Multi-component peptide sample controls without DNA were also subjected to similar centrifugation procedures.

An aliquot of the filtrate (100 µl) was then analyzed by RP-HPLC with 0.1 v/v % TFA and a gradient of 10-55 v/v % acetonitrile over 30 min while monitoring absorbance at 409 nm. Percent individual component incorporation was calculated as the peak area percent difference between the peptide/DNA containing samples versus the peak area of multi-component peptide controls containing peptide only and results reported as the mol percent output ratio ± the standard deviation of the mean.

### In Vitro Gene Transfer of Polyacridine-melittin DNA Polyplexes

CHO cells ($2 \times 10^5$) were plated on 6 x 35 mm wells and grown to approximately 50% confluency. Transfections were performed in DMEM supplemented with 2% FBS, sodium pyruvate (1 mM), and penicillin and streptomycin (100 U and 100 µg/ml). Polyplexes were prepared at a DNA concentration of 30 µg per ml and a stoichiometry of 0.5 nmol peptide per µg of DNA in Hepes buffered mannitol (HBM). Polyplexes (2 µg of DNA in 0.06 ml of HBM) were added drop wise to wells in triplicate and incubated 24 hrs. After 24 hrs, the cells were washed twice with 2 ml of ice-cold phosphate-buffered saline ($Ca^{2+}$ - and $Mg^{2+}$ - free) and then treated with 0.5 ml of lysis buffer (25 mM Tris Chloride, pH 7.8, 1 mM EDTA, 8 mM magnesium chloride, and 1% Triton X-100) for 10 min at 4ºC. Cell lysates were scraped, transferred to 1.5 ml microcentrifuge tubes, and centrifuged for 10 min at 13,000 g at 4ºC to pellet cell debris. Lysis buffer (300 µl), sodium-ATP (4.3 µl of a 165 mM solution at pH 7, 4ºC) were combined in a test tube,

mixed briefly, and immediately placed in the luminometer. Luciferase relative light units were measured by a Lumat LB 9501 (Berthold Systems, Germany) with 10 s integration after automatic injection of 100 µl of 0.5 mM D-luciferin. The relative light units were converted to fmol using a standard curve generated by adding a known amount of luciferase to 35 mm wells containing 50% confluent CHO cells. The resulting standard curve had an average slope of 2.6 x $10^4$ relative light units/fmol enzyme. Protein concentrations were measured by a BCA assay using bovine serum albumin as a standard (*128*). The amount of luciferase recovered in each sample was normalized to mg of protein and reported as the mean and standard deviation obtained from triplicate transfections. PEI pGL3 polyplexes were prepared by mixing 7 µg of DNA in 105 µl of HBM with 8.8 µg PEI in 105 µl of HBM while vortexing to create DNA complexes possessing a charge ratio ($NH_4^+/PO_4^-$) of 9:1. $WK_{18}$ pGL3 polyplexes were prepared by mixing 7 µg of DNA in 105 µl of HBM with 1.4 nmol $WK_{18}$ in 105 µl of HBM while vortexing to create DNA complexes possessing a peptide/DNA ratio of 0.2 nmol peptide per µg DNA and transfected with 2 µg $WK_{18}$ DNA polyplexes as previously described.

### In Vivo Gene Transfer and Bioluminescence Imaging (In Collaboration with Sanjib Khargharia and Christian Fernandez)

pGL3 (1 µg) was prepared in volume of normal saline corresponding to 9 wt/vol % of the mouse's body weight (1.8 – 2.25 ml based on 20-25 g mice). The DNA dose was administered by tail vein to 4-5 mice in 5 sec according to a published procedure (*140, 141*). Mice (n≥3) were also dosed tail vein with 1, 5, or 25 µg of multi-component polyacridine polyplex formulations prepared at peptide to DNA ratio of 0.5 nmol peptide per µg of DNA in 100 µl of HBM (5 mM Hepes, 0.27 M mannitol, pH 7.4). For hydrodynamically dosed control formulations, a stimulatory hydrodynamic dose of normal saline (9 wt/vol% of the body weight) was administered over 5 sec with a 15 min

dwell time post formulation administration. At 24 hrs post-DNA dose, mice were anesthetized by 3% isofluorane, then administered an i.p. dose of 80 μl (2.4 mg) of D-luciferin (30 μg/μl in phosphate-buffered saline). At 5 min following the D-luciferin dose, mice were imaged for bioluminescence (BLI) on an IVIS Imaging 200 Series (Xenogen). BLI was performed in a light-tight chamber on a temperature-controlled, adjustable stage while isofluorane was administered by a gas manifold at a flow rate of 3%. Images were acquired at a 'medium' binning level and a 20 cm field of view. Acquisition times were varied (1 sec - 1 min) depending on the intensity of the luminescence. The Xenogen system reported bioluminescence as photons/sec/$cm^2$/ seradian in a 2.86 cm diameter region of interest covering the liver.

### Pharmacokinetic Analysis of Multi-Component Polyacridine Polyplexes (In Collaboration with Sanjib Khargharia)

Radioiodinated pGL3 was prepared as previously described (*143*). Triplicate mice were anesthetized by i.p. injection of ketamine hydrochloride (100 mg per kg) and xylazine hydrochloride (10 mg per kg) then underwent a dual cannulation of the right and left jugular veins. An i.v. dose of $^{125}$I-DNA (3 μg in 50 μl of HBM, 1.2 μCi) or $^{125}$I-DNA polyplex (3 μg) was administered via the left catheter, and blood samples (10 μl) were drawn from the right catheter at 1, 3, 6, 10, 20, 30, 60, 90 and 120 min and immediately frozen, then replaced with 10 μl of normal saline. The amount of radioactivity in each blood time point was quantified by direct γ-counting.

### Biodistribution Analysis of Multi-Component Polyacridine Polyplexes (In Collaboration with Sanjib Khargharia)

Mice were anesthetized and a single catheter was placed in the left jugular vein. $^{125}$I-DNA (1.5 μg in 50 μl of HBM, 0.6 μCi) or $^{125}$I-DNA polyplexes (1.5 μg) were dosed i.v. followed by vein ligation. After 5, 15, 30, 60, or 120 min, mice were sacrificed by

cervical dislocation and the major organs (liver, lung, spleen, stomach, kidney, heart, large intestine, and small intestine) were harvested, and rinsed with saline. The radioactivity in each organ was determined by direct γ-counting and expressed as the percent of the dose in the organ.

## Results

### Synthetic Strategy for Polyacridine Peptides.

In addition to the synthetic optimization steps outlined in the previous chapters to obtain polyacridine peptides in high yield and purity, we have further adjusted the synthetic conditions for the SPPS reagent Fmoc-Lys(Acr)-OH. By adjusting the synthetic methodologies by Chiu et al to substitute phenol with methanol as the reaction solvent (*122*), we have increased the purity of Fmoc-Lys(Acr)-OH by eliminating residual phenol from the final product. Figure 5-1 demonstrates the quality of Fmoc-Lys(Acr)-OH by RP-HPLC. The chromatographs corresponding to amino acid produced with phenol as the solvent were analyzed by monitoring absorbance at 280 nm and 409 nm (Figure 5-1A and C, respectively) and these are compared to amino acid prepared in methanol (Figure 5-1B and D, respectively). Upon integration of peak areas, the product purity is improved considerably from 61% to 92% while monitoring at 280 nm (Figure 5-1 A and B) while a similar purity of approximately 92% is obtained when comparing the 409 nm chromatographs (Figure 5-1C and D) with both methods producing an ESI-MS consistent with the calculated mass (Figure 5-1D, inset).

The fusogenic peptide analogues based upon melittin, PC-4, and JTS-1 were synthesized using standard Fmoc solid phase peptide chemistry employing HBTU/HOBt coupling methodology (Table 5-1 and 5-2). Isolated peptide yields after preparatory HPLC for melittin analogues varied from 6.3% to 10.5% (Table 5-2). The chimeric peptides Cys-NLS-K-melittin and the charge neutralized analogue Cys-NLS-QL-melittin were obtained in good yield considering these are peptides with a linear length of 36

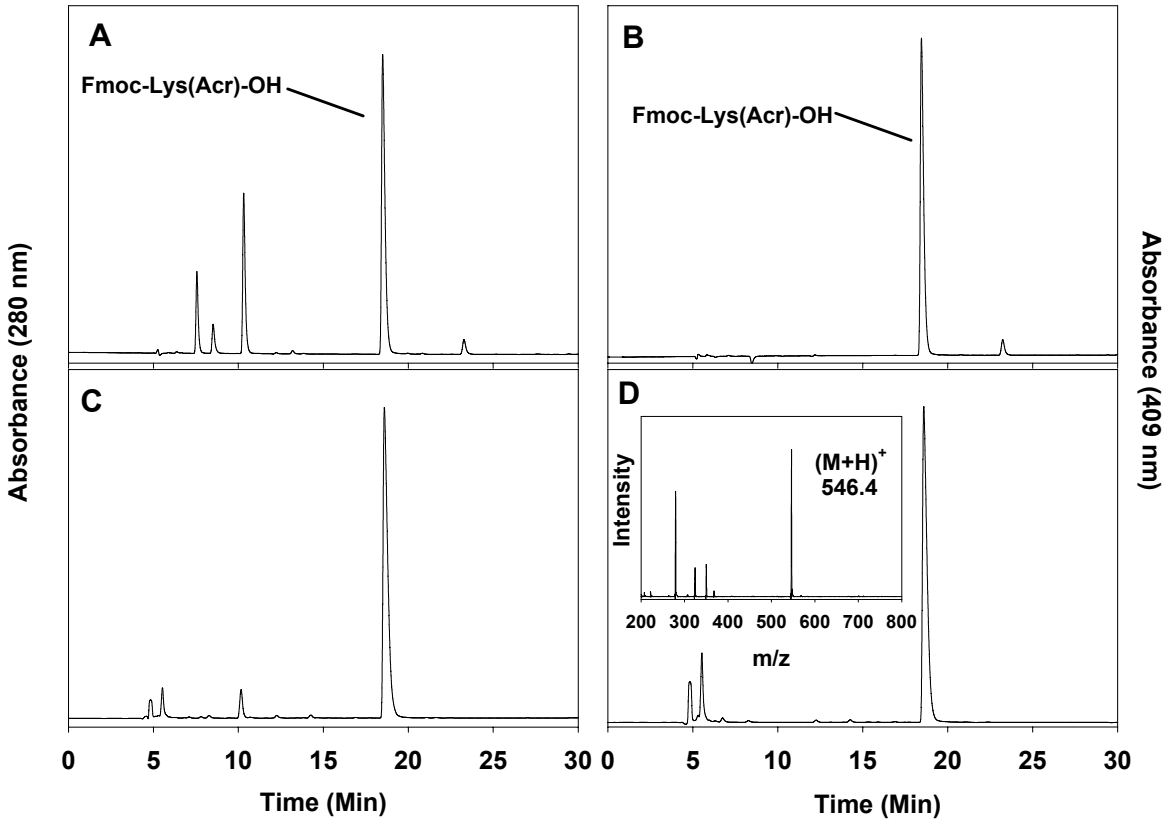


Figure 5-1. *RP-HPLC Comparison of Fmoc-Lys(Acr)-OH Prepared in Phenol or Methanol.* HPLC analysis of Fmoc-Lys(Acr)-OH after synthesis by injecting 5 nmol and eluting with a 0.1 v/v % TFA with a 30-60 v/v % acetonitrile gradient while monitoring absorbance at 280 nm and at 409 nm. Fmoc-Lys(Acr)-OH prepared using phenol (A) as the solvent is compared to the methanol prepared amino acid monomer (C) while observing 280 nm absorbance. Purity as judged by peak area integration at 280 nm is improved from 61% to 92% for Fmoc-Lys(Acr)-OH prepared in methanol. Purity judged at 409 nm is nearly equivalent for either phenol (92.6%) or methanol (92.0%) prepared Fmoc-Lys(Acr)-OH, demonstrating the importance of monitoring multiple wavelengths when judging purity by analytical RP-HPLC. ESI-MS analysis of phenol or methanol prepared Fmoc-Lys(Acr)-OH produced a positively charged ion of 546.4 *m/z* (Panel D, inset), corresponding to a mass of 545.4 amu.

Table 5-1. *Peptide Nomenclature and Sequence Information for Polyacridine Fusogenic Peptides*

| Peptide Nomenclature | Sequence |
|---|---|
| **Polyacridine Anchor Peptide (Acr) = Lys-ε-acridine** | |
| $(Acr\text{-}Lys)_6$-Cys | Acr-K-Acr-K-Acr-K-Acr-K-Acr-K-Acr-K-C |
| $(Acr\text{-}Lys)_8$-Cys | Acr-K-Acr-K-Acr-K-Acr-K-Acr-K-Acr-K-Acr-K-Acr-K-Acr-K-C |
| $(Acr\text{-}His)_6$-Cys | Acr-H-Acr-H-Acr-H-Acr-H-Acr-H-Acr-H-C |
| **Fusogenic Peptide Analogues (TP = thiol pyridine, m = maleimide)** | |
| Cys-K-Melittin | CWGIGAVLKVLTTGLPALISLIKKKKQQ |
| TP-Cys-K-Melittin | C(tp)WGIGAVLKVLTTGLPALISLIKKKKQQ |
| Mal-K-Melittin | (m)GWGIGAVLKVLTTGLPALISLIKKKKQQ |
| Cys-K-NLS-Melittin | CGPKKKRKVWGIGAVLKVLTTGLPALISLIKKKKQQ |
| Mal-NLS | (m)GGPKKKRKVG |
| TP-Cys-NLS-Melittin | C(tp)GPKKKRKVWGIGAVLKVLTTGLPALISLIKKKKQQ |
| Cys-QL-NLS-Melittin | CGPK KKRKVWGIGAVLQVLTTGLPALISLIQLQLQL |
| TP-Cys-QL-NLS-Melittin | C(tp)GPKKKRKVWGIGAVLQVLTTGLPALISLIQLQLQL |
| Cys-PC-4 | CSSA WWSYWPPVA |
| TP-Cys-PC-4 | C(tp)SSAWWSYWPPVA |
| Mal-PC-4 | (m)GSSAWWSYWPPVA |
| Cys-NLS-PC-4 | CGGPKKKRKVGSSAWWSYWPPVA |
| TP-Cys-NLS-PC-4 | C(tp)GGPKKKRKVGSSAWWSYWPPVA |
| Cys-conNLS-PC-4 | CGGPKTKRKVGSSAWWSYWPPVA |
| TP-Cys-conNLS-PC-4 | C(tp)GGPKTKRKVGSSAWWSYWPPVA |
| Cys-PC-4-NLS | CSSAWWSYWPPVAGGPKKKRKVG |
| TP-Cys-PC-4-NLS | C(tp)SSAWWSYWPPVAGGPKKKRKVG |
| Cys-JTS-1 | CGLFEALLELLESLWELLLEA |
| TP-Cys-JTS-1 | C(tp)GLFEALLELLESLWELLLEA |
| **Polyacridine Fusogens (SS = reducible, Mal = non reducible** | |
| $(Acr\text{-}Lys)_6$-SS-K-Mel | $(Acr\text{-}Lys)_6$-C-CWGIGAVLKVLTTGLPALISLIKKKKQQ |
| $(Acr\text{-}Lys)_6$-Mal-K-Mel | $(Acr\text{-}Lys)_6$-C(m)GWGIGAVLKVLTTGLPALISLIKKKKQQ |
| $(Acr\text{-}Lys)_6$-SS-NLS-K-Mel | $(Acr\text{-}Lys)_6$-C-CGPKKKRKVWGIGAVLKVLTTGLPALISLIKKKKQQ |
| $(Acr\text{-}Lys)_6$-Mal-NLS | $(Acr\text{-}Lys)_6$-C-(m)GGPKKKRKVG |
| $(Acr\text{-}Lys)_6$-SS-NLS-QL-Mel | $(Acr\text{-}Lys)_6$-C-CGPKKKRKVWGIGAVLQVLTTGLPALISLIQLQLQL |
| $(Acr\text{-}Lys)_6$-SS-PC-4 | $(Acr\text{-}Lys)_6$-C-CSSAWWSYWPPVA |
| $(Acr\text{-}Lys)_6$-Mal-PC-4 | $(Acr\text{-}Lys)_6$-C-(m)GSSAWWSYWPPVA |
| $(Acr\text{-}Lys)_6$-SS-NLS-PC-4 | $(Acr\text{-}Lys)_6$-C-CGGPKKKRKVGSSAWWSYWPPVA |
| $(Acr\text{-}Lys)_6$-SS-conNLS-PC-4 | $(Acr\text{-}Lys)_6$-C-CGGPKTKRKVGSSAWWSYWPPVA |
| $(Acr\text{-}Lys)_6$-SS-PC-4-NLS | $(Acr\text{-}Lys)_6$-C-CSSAWWSYWPPVAGGPKKKRKVG |
| $(Acr\text{-}Lys)_6$-SS-JTS-1 | $(Acr\text{-}Lys)_6$-C-CGLFEALLELLESLWELLLEA |
| $(Acr\text{-}Lys)_8$-SS-JTS-1 | $(Acr\text{-}Lys)_8$-C-CGLFEALLELLESLWELLLEA |

amino acid residues (Table 5-2). The neutrally charged fusogenic peptide PC-4 and NLS-PC-4 chimera's produced isolated peptide yields ranging from 23 to 38%. The anionic Cys-JTS-1 produced a yield of 5%, suggesting on-resin secondary structure formation and subsequent aggregation, resulting in a variety of truncated peptide species and an

Table 5-2. *ESI-MS Characterization and Synthetic Yield Data for Polyacridine Peptides and Polyacridine Fusogens*

| Peptide | Mass[a] (Obs/Calc) | Yield[b] |
|---|---|---|
| **Polyacridine Anchor Peptide (Acr) = Lys-ε-acridine** | | |
| $(Acr\text{-}Lys)_6$-Cys | 2722.6 / 2722.4 | 40.10% |
| $(Acr\text{-}Lys)_8$-Cys | 3588.9 / 3589.5 | 9.03% |
| $(Acr\text{-}His)_6$-Cys | 2776.24 / 2776.0 | 23.36% |
| **Fusogenic Peptide Analogues (TP = thiol pyridine, m = maleimide)** | | |
| Cys-K-Melittin | 3007.4 / 3007.7 | 10.46% |
| TP-Cys-K-Melittin | 3116.6 / 3116.9 | 27.30% |
| Mal-K-Melittin | 3041.4 / 3041.6 | 10.31% |
| Mal-NLS | 1135.0 / 1134.3 | 55.21% |
| Cys-K-NLS-Melittin | 3928.8 / 3929.8 | 8.30% |
| TP-Cys-NLS-Melittin | 4038.3 / 4039.0 | 23.20% |
| Cys-QL-NLS-Melittin | 3884.0 / 3884.7 | 6.30% |
| TP-Cys-QL-NLS-Melittin | 3993.0/ 3993.9 | 59.02% |
| Cys-PC-4 | 1538.4 / 1538.7 | 30.10% |
| TP-Cys-PC-4 | 1647.4 / 1647.8 | 46.90% |
| Mal-PC-4 | 1572.2 / 1572.6 | 35.10% |
| Cys-NLS-PC-4 | 2577.0 / 2575.9 | 24.25% |
| TP-Cys-NLS-PC-4 | 2685.2 / 2684.1 | 58.30% |
| Cys-conNLS-PC-4 | 2547.8 / 2547.4 | 37.90% |
| TP-Cys-conNLS-PC-4 | 2656.8 / 2657.1 | 35.61% |
| Cys-PC-4-NLS | 2577.0 / 2576.0 | 23.17% |
| TP-Cys-PC-4-NLS | 2686.0 / 2685.1 | 45.26% |
| Cys-JTS-1 | 2404.6 / 2404.8 | 5.10% |
| TP-Cys-JTS-1 | 2513.8 / 2514.0 | 28.48% |
| **Polyacridine Fusogens (SS = reducible, Mal = non reducible** | | |
| $(Acr\text{-}Lys)_6$-SS-K-Mel | 5728.8 / 5728.1 | 42.50% |
| $(Acr\text{-}Lys)_6$-Mal-K-Mel | 5764.8 / 5764.1 | 31.34% |
| $(Acr\text{-}Lys)_6$-SS-NLS-K-Mel | 6649.5 / 6650.1 | 25.91% |
| $(Acr\text{-}Lys)_6$-Mal-NLS | 3858.0 / 3856.8 | 25.06% |
| $(Acr\text{-}Lys)_6$-SS-NLS-QL-Mel | 6604.4 / 6605.2 | 3.60% |
| $(Acr\text{-}Lys)_6$-SS-PC-4 | 4261.2 / 4259.1 | 52.43% |
| $(Acr\text{-}Lys)_6$-Mal-PC-4 | 4295.4 / 4295.1 | 47.20% |
| $(Acr\text{-}Lys)_6$-SS-NLS-PC-4 | 5296.2 / 5295.2 | 23.00% |
| $(Acr\text{-}Lys)_6$-SS-conNLS-PC-4 | 5268.0 / 5267.4 | 26.00% |
| $(Acr\text{-}Lys)_6$-SS-PC-4-NLS | 5297.2 / 5296.4 | 23.23% |
| $(Acr\text{-}Lys)_6$-SS-JTS-1 | 5125.8 / 5125.2 | 18.6% |
| $(Acr\text{-}Lys)_8$-SS-JTS-1 | 5992.8 / 5992.3 | 23.26% |

[a]Observed and calculated masses as determined by ESI-MS in the positive mode with exception to JTS-1 analogues in the negative mode.

[b]Yields based on acridine absorbance at 409 nm or tryptophan and/or thiolpyridine absorbance at 280 nm.

overall decrease in yield (Table 5-2) (*28*). Synthesis of reactive intermediates to accommodate conjugation to the polyacridine anchors was accomplished through selective protection of the N-terminal Cys residue with thiolpyridine to direct disulfide formation for reducible polyacridine-fusogen peptides. Typical yields for thiolpyridine protected peptides varied from 23 to 58% (Table 5-2). Maleimide containing analogues used to generate non-reducible polyacridine-fusogenic or NLS containing peptides were synthesized by coupling Mal-Gly-OH to the N-terminus of the side chain protected peptide on resin using DIC/HOBt coupling. Once removed from resin, side-chain deprotected, and purified, Mal-K-melittin, Mal-NLS, and Mal-PC-4 produced yields of 10.3, 55.2, and 35%, respectively (Table 5-2).

Polyacridine peptide $(Acr\text{-}Lys)_6$-Cys, $(Acr\text{-}Lys)_8$-Cys, and $(Acr\text{-}His)_6$-Cys were synthesized through an optimized protocol consisting of double coupling of Fmoc-Lys(Acr)-OH and triple coupling of the spacing amino acid (Fmoc-Lys(Boc)-OH or Fmoc-His(Trt)-OH). Additionally, upon optimization of the Fmoc-Lys(Acr)-OH synthesis through replacement of phenol with methanol as the reaction solvent, the amino acid became significantly less soluble in common peptide synthesis solvents such as DMF and NMP, which contributed to lower overall yields and poor crude peptide quality as observed by RP-HPLC analysis. To counteract the solubility issue of Fmoc-Lys(Acr)-OH in DMF, the amino acid was pre-activated to the corresponding OBt-ester by addition of HATU and HOBt to the amino acid during synthesis preparation. Upon addition of DMF and vortexing, the amino acid was immediately solvated and precipitation was not observed during the course of peptide synthesis. Before employing this countermeasure, crude yields for the peptide $(Acr\text{-}Lys)_6$-Cys maximally reached 50% based upon acridine absorbance at 409 nm and now are routinely between 75 to 95% with a highly improved quality of crude peptide as judged by RP-HPLC analysis. The purified polyacridine peptides $(Acr\text{-}Lys)_6$-Cys and $(Acr\text{-}His)_6$-Cys were obtained in 40.1 and 23.4% yields, respectively (Table 5-2). The aforementioned optimization steps allowed the synthetically

difficult peptide $(Acr\text{-}Lys)_8$-Cys to be synthesized and isolated in a 9% yield versus previous attempts that failed to isolate the peptide in appreciable yield (Table 4-1). The improved yields allowed for further modulation and DNA binding abilities of a polyacridine peptide, an important prospect for anionic species, such as the fusogen JTS-1.

The polyacridine-fusogenic peptides $(Acr\text{-}Lys)_6$-K-melittin and $(Acr\text{-}Lys)_6$-PC-4 were designed to possess either a reducible disulfide bond or non-reducible maleimide linkage as previous in vitro gene transfer studies demonstrated a 1000-fold improvement in activity for the reducible polyacridine-melittin analogue $(Acr\text{-}Arg)_4$-SS-melittin versus the non-reducible analogue (Chapter 2 and 3) (*161*). Subsequent polyacridine NLS-fusogen chimeras were synthesized through disulfide bond formation due to the observed improvement in gene transfer efficiency observed in vitro. Following the coupling reaction of polyacridine to fusogenic peptide, the polyacridine-fusogens were purified by preparatory HPLC and isolated yields of 18% to 52% with > 95% purity with one exception of a 3.6% yield for $(Acr\text{-}Lys)_6$-SS-NLS-QL-melittin, which resulted due to a non-reactive thiolpyridine protected cysteine and limited aqueous solubility of the reactive precursor, TP-Cys-NLS-QL-melittin (Table 5-2). Representative LC-MS evidence of purity and identity is presented in Figure 5-2A for $(Acr\text{-}Lys)_6$-SS-K-melittin producing triply and quadruply charged ions corresponding to the calculated mass (Figure 5-2A inset). Similar evidence is presented for $(Acr\text{-}Lys)_6$-SS-PC-4 (Figure 5-2B) and the chimeric peptide $(Acr\text{-}Lys)_6$-SS-PC-4-NLS (Figure 5-1C). Mass spectral analysis reveals the presence of a triply charged ion for $(Acr\text{-}Lys)_6$-SS-PC-4 (Figure 5-1B inset) and doubly and triply charged ions for $(Acr\text{-}Lys)_6$-SS-PC-4-NLS (Figure 5-1C inset), all corresponding to the desired calculated mass.

PEGylated-polyacridine peptides composed of a 5 KDa poly(ethylene)glycol were synthesized with a reducible disulfide bond through reaction with a 1.1 mol excess of the

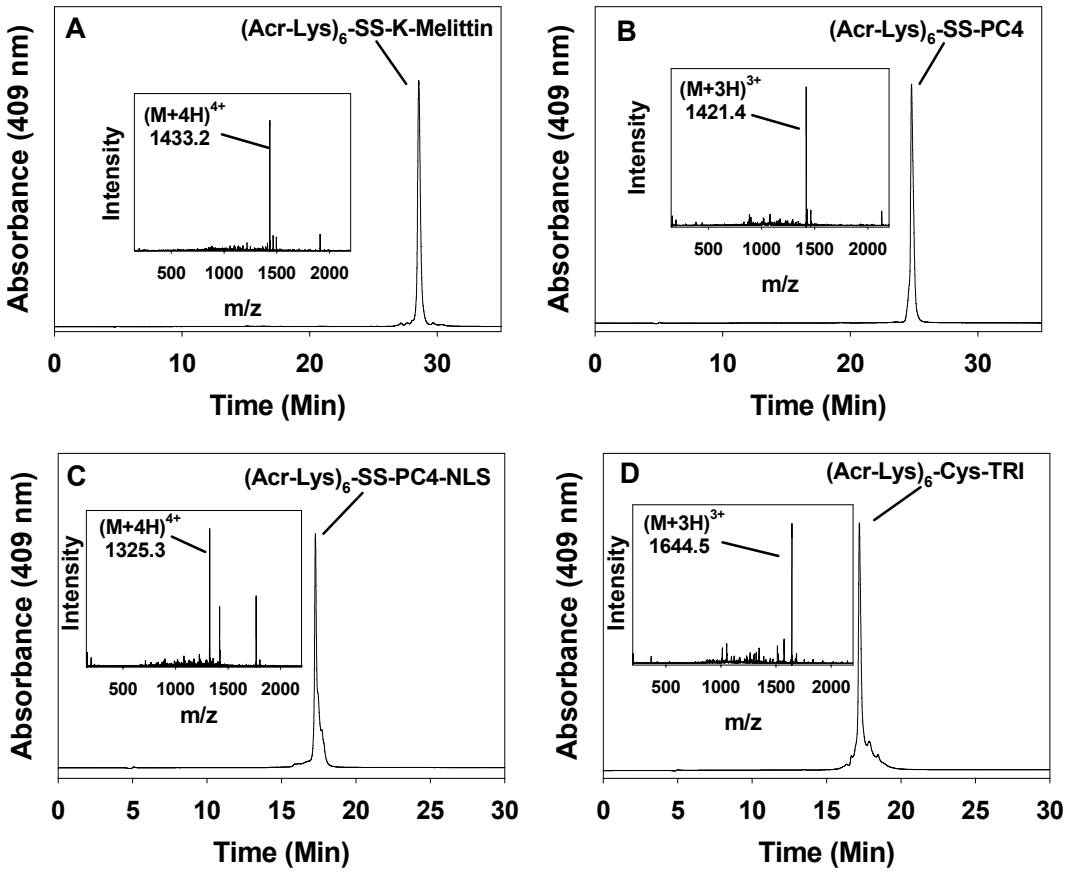


Figure 5-2. *RP-HPLC and ESI-MS Analysis of Polyacridine Peptides after Preparatory HPLC.* Panel A is a representative LC-MS chromatograph of $(Acr\text{-}Lys)_6$-SS-K-melittin produced after injection of 1 nmol while eluting with a 0.1 v/v % TFA and an acetonitrile gradient of 10-55 v/v % over 30 min while monitoring absorbance at 409 nm, while producing an intense ion of 1433.2 *m/z* (Panel A, inset) corresponding to the mass of 5728.8 amu. Panel B represents the LC-MS chromatograph after 1 nmol injection of $(Acr\text{-}Lys)_6$-SS-PC-4 eluted with the same gradient as mentioned above to produce a dominant ion of 1421.4 *m/z* (Panel B, inset) corresponding to a mass of 4261.2 amu. Panel C represents a 1 nmol injection of $(Acr\text{-}Lys)_6$-SS-PC-4-NLS chimera producing a major ion of 1325.3 *m/z* corresponding to a mass of 5296.2 amu (Panel C, inset). Panel D represents the rechromatograph after purification of $(Acr\text{-}Lys)_6$-Cys-TRI eluted with a 0.1 v/v % TFA and an acetonitrile gradient of 10-40 v/v % over 30 min while monitoring absorbance at 409 nm while producing a major ion of 1644.5 *m/z* (Panel A, inset) corresponding to the mass of 4930.5 amu.

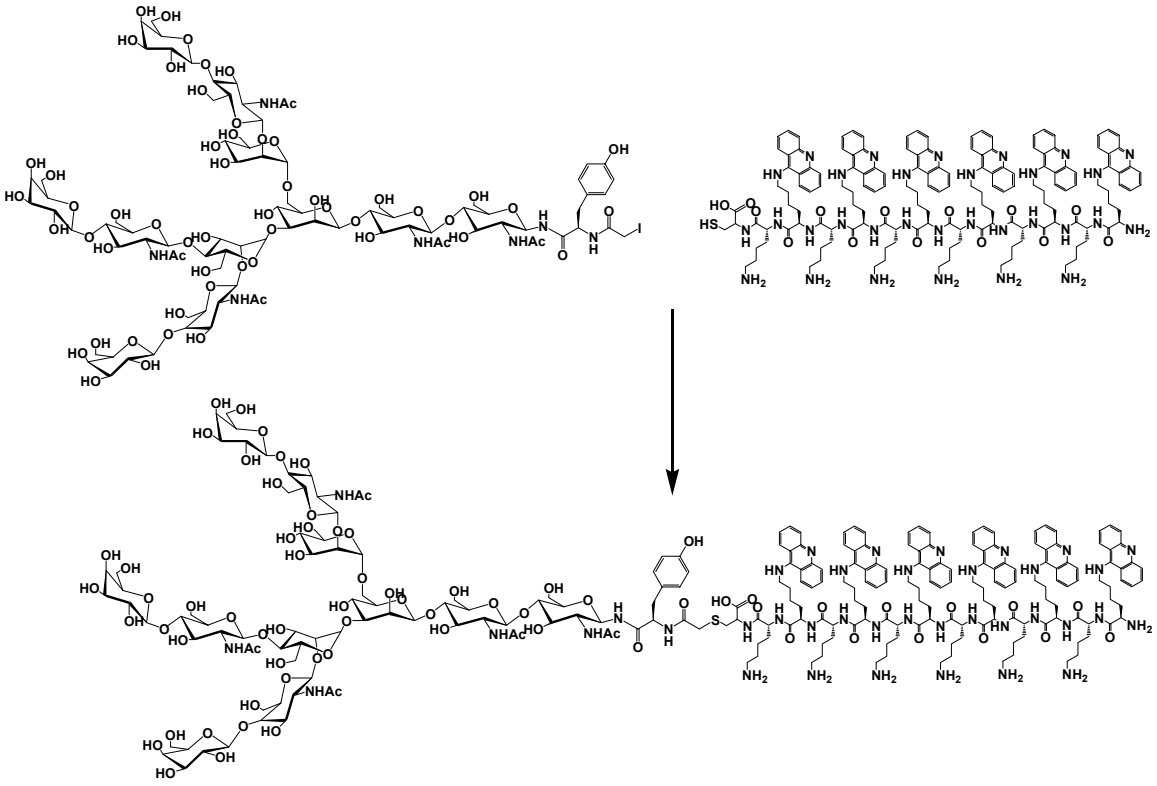

Scheme 5-1. *Synthesis of (Acr-Lys)$_6$-Cys-TRI Glycopeptide Targeting Ligand.* Iodoacetamide triantennary N-Glycan (I-TRI) is reacted with a 1.25 mol excess of (Acr-Lys)$_6$-Cys polyacridine peptide overnight to generate the thiol ether linked glycopeptide (Acr-Lys)$_6$-Cys-TRI.

commercially available OPSS-mPEG$_{5000\ D}$ with either (Acr-Lys)$_6$-Cys or the endosomal buffering polyacridine peptide (Acr-His)$_6$-Cys to generate (Acr-Lys)$_6$-SS-PEG or (Acr-His)$_6$-SS-PEG in yields of 62% and 55% at >95% purity, respectively (Table 5-3). Identity was confirmed by MALDI-TOF MS to yield an observed average molecular weight of 8189.5 amu for (Acr-Lys)$_6$-SS-PEG and 8276.2 amu for (Acr-His)$_6$-SS-PEG, which agreed closely with the calculated average mass (Table 5-3).

Polyacridine-triantennary glycopeptides were synthesized through reaction of the reactive N-glycan I-TRI with the C-terminal cysteine of either 1.2 mol equivalents of

Table 5-3. *Characterization Data for Polyacridine PEG and Targeting Ligands*

| **PEGylated Polyacridine Peptides** | **Mass[a] (Obs/Calc)** | **Yield[c]** |
|---|---|---|
| $(Acr\text{-}Lys)_6$-SS-PEG | 8169.5 / 8222.6 | 61.83% |
| $(Acr\text{-}His)_6$-SS-PEG | 8308.9 / 8276.2 | 54.65% |
| **Polyacridine Glycopeptides** | **Mass[b] (Obs/Calc)** | **Yield[c]** |
| $(Acr\text{-}Lys)_6$-Cys-TRI | 4930.5 / 4933.48 | 47.34% |
| $(Acr\text{-}Lys)_6$-Cys-agalactose-TRI | 4446.0 / 4447.06 | 87.02% |
| $(Acr\text{-}His)_6$-Cys-TRI | 4984.8 / 4987.28 | 13.52% |

[a]Observed and calculated masses as determined by MALDI-TOF MS in the positive mode.

[b]Observed and calculated masses as determined by ESI-MS in the positive mode.

[c]Yields based on acridine absorbance at 409 nm.

$(Acr\text{-}Lys)_6$-Cys or $(Acr\text{-}His)_6$-Cys to displace iodide and generate the non-reducible thiol-ether linkage to form $(Acr\text{-}Lys)_6$-Cys-TRI (Scheme 5-1) or $(Acr\text{-}His)_6$-Cys-TRI. Upon purification, LC-MS analysis revealed a >95% pure polyacridine glycopeptide (Figure 5-2D). Mass spectral analysis of $(Acr\text{-}Lys)_6$-Cys-TRI reveals a triply charged ion of 1644.5 *m/z* producing an observed mass of 4930.5 Da corresponding to the calculated mass of 4933.48 Da (Figure 5-2D, inset) with a yield of 47% for $(Acr\text{-}Lys)_6$-Cys-TRI and 13.5% for $(Acr\text{-}His)_6$-Cys-TRI (Table 5-3). Similar characterization data of $(Acr\text{-}His)_6$-Cys-TRI is presented in Table 5-3.

The hepatocyte targeting control peptide $(Acr\text{-}Lys)_6$-Cys-Agal-TRI was synthesized by reacting $(Acr\text{-}Lys)_6$-Cys-TRI with β-galactosidase isolated from bovine testes (*38*). Following a 6 hr reaction at 37ºC, the enzyme was quenched by freezing at -70 ºC overnight and purified by preparatory HPLC with a yield of 87% and characterized by ESI-MS to produce a triply charged ion of 1483.0 *m/z* that yielded an observed mass of 4446.0 Da that corresponded to the calculated mass of 4447.03 Da (Table 5-3).

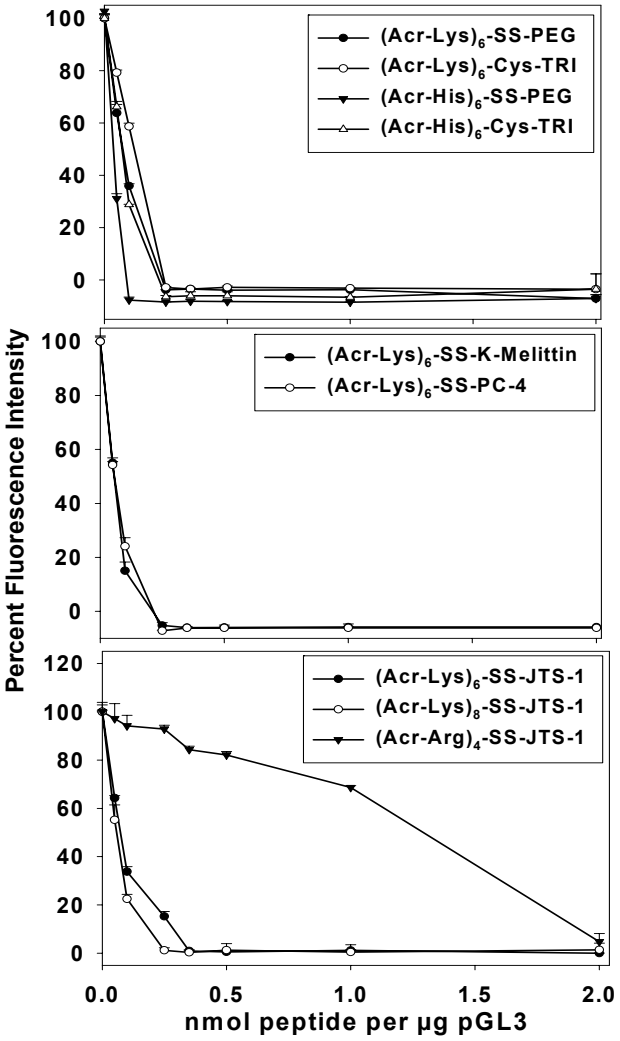


Figure 5-3. *Relative Binding Affinity of Polyacridine Peptides for pGL3.* The concentration dependent displacement of thiazole orange established relative affinity of polyacridine peptides for DNA. $(Acr\text{-}Lys)_6$-SS-PEG, $(Acr\text{-}Lys)_6$-Cys-TRI, and $(Acr\text{-}His)_6$-Cys-TRI display nearly equivalent binding resulting in an asymptote of 0.25 nmol peptide per µg of DNA where $(Acr\text{-}His)_6$-SS-PEG displayed the strongest binding with an asymptote of 0.1 nmol peptide per µg of DNA (Panel A). The fusogenic polyacridine peptides $(Acr\text{-}Lys)_6$-SS-PC-4 and $(Acr\text{-}Lys)_6$-SS-K-melittin produced nearly equivalent binding with an asymptote of 0.25 nmol peptide per µg of DNA (Panel B). Conversely, an $(Acr\text{-}Arg)_4$-SS-JTS-1 analogue of the negatively charged fusogen JTS-1 was unable to fully displace thiazole orange out to 2 nmol peptide per µg of DNA. Upon functionalization of JTS-1 with either $(Acr\text{-}Lys)_6$-Cys or $(Acr\text{-}Lys)_8$-Cys to form $(Acr\text{-}Lys)_6$-SS-JTS-1 and $(Acr\text{-}Lys)_8$-SS-JTS-1 produced an asymptote of 0.35 and 0.25 nmol peptide per µg of DNA, respectively (Panel C), demonstrating nearly equivalent DNA binding affinity to $(Acr\text{-}Lys)_6$-SS-PC-4 and $(Acr\text{-}Lys)_6$-SS-K-melittin.

## Physical Properties of Polyacridine-Peptides and Polyplexes.

The binding properties of polyacridine fusogens, PEG peptides, and targeting glycopeptides were investigated by a thiazole orange exclusion assay (*22*). Polyacridine peptides regardless of their biological purpose were found to compete for intercalation and displace thiazole orange, resulting in a decrease in fluorescence intensity. When titrated at increasing peptide/DNA ratios, the fluorescence decreased until an asymptote was reached to establish an equivalence point (Figure 5-3). Analysis of DNA binding affinity for the $(Acr\text{-}Lys)_6$-Cys-TRI and $(Acr\text{-}His)_6$-TRI reveal nearly equivalent binding profiles resulting in an equivalency point of 0.25 nmol peptide per μg of DNA while the shielding peptides reveal stronger binding by $(Acr\text{-}His)_6$-SS-PEG with an asymptote of 0.1 nmol peptide per μg of DNA versus the equivalency point of 0.25 nmol peptide per μg of DNA for $(Acr\text{-}Lys)_6$-SS-PEG (Figure 5-3A). The polyacridine-fusogenic peptides, $(Acr\text{-}Lys)_6$-SS-K-melittin and $(Acr\text{-}Lys)_6$-SS-PC-4, display equivalent DNA binding with an asymptote of 0.25 nmol peptide per μg of DNA (Figure 5-3B). An anionic JTS-1 peptide conjugated to the polyacridine anchor $(Acr\text{-}Arg)_4$-Cys displays poor DNA binding properties, unable to fully displace thiazole orange at a peptide to DNA ratio of 2 nmol peptide per μg of DNA. DNA binding affinity is restored upon synthesis of $(Acr\text{-}Lys)_{6 \text{ and } 8}$-SS-JTS-1, resulting in an asymptote of 0.35 and 0.25 nmol peptide per μg of DNA, respectively (Figure 5-3C). As a whole, the thiazole binding data suggest nearly equivalent binding affinities for polyacridine PEGylated, fusogenic, and targeting peptides based on $(Acr\text{-}Lys)_6$-Cys, enabling multiple component integration, formulation, and co-delivery of targeted multi-component complexes in vivo.

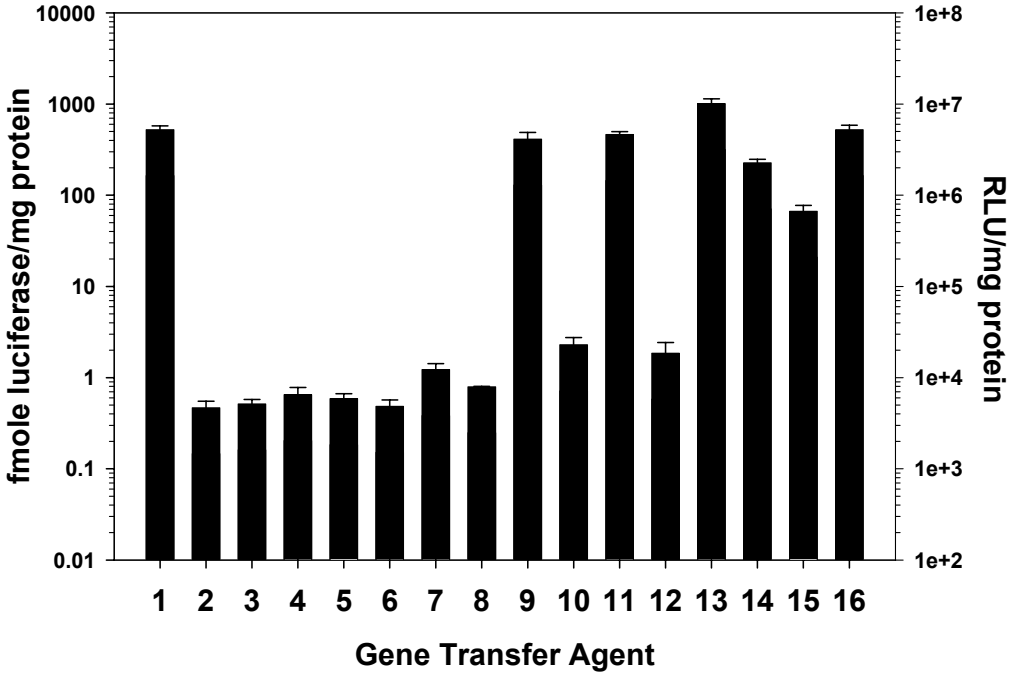


Figure 5-4. *In Vitro Gene Transfection of Polyacridine Fusogen Polyplexes in CHO Cells.* Transfections were performed with 2 µg pGL3 polyplex prepared with 0.5 nmol of total peptide per µg DNA on 2 x $10^5$ CHO cells/well. The gene transfer efficiency mediated by polyacridine fusogens, as an add mixture with $(Acr\text{-}Lys)_6$-Mal-NLS, or chimeric NLS-fusogen peptides and compared to PEI (N:P 9:1) and $WK_{18}$-DNA polyplexes. The bars indicate transfection of pGL3 with (**1**) PEI, (**2**) $WK_{18}$, (**3**) $(Acr\text{-}Lys)_6$-SS-PC-4, (**4**) $(Acr\text{-}Lys)_6$-Mal-PC-4, (**5**) 0.4 nmol per µg of $(Acr\text{-}Lys)_6$-SS-PC-4 and 0.1 nmol per µg of $(Acr\text{-}Lys)_6$-Mal-NLS, (**6**) 0.4 nmol per µg of $(Acr\text{-}Lys)_6$-Mal-PC-4 and 0.1 nmol per µg of $(Acr\text{-}Lys)_6$-Mal-NLS, (**7**) $(Acr\text{-}Lys)_6$-SS-PC-4-NLS, (**8**) $(Acr\text{-}Lys)_6$-SS-NLS-PC-4, (**9**) $(Acr\text{-}Lys)_6$-SS-K-melittin, (**10**) $(Acr\text{-}Lys)_6$-Mal-K-melittin, (**11**) 0.4 nmol per µg of $(Acr\text{-}Lys)_6$-SS-K-melittin and 0.1 nmol per µg $(Acr\text{-}Lys)_6$-Mal-NLS, (**12**) 0.4 nmol per µg of $(Acr\text{-}Lys)_6$-Mal-K-melittin and 0.1 nmol per µg $(Acr\text{-}Lys)_6$-Mal-NLS, (**13**) $(Acr\text{-}Lys)_6$-SS-NLS-melittin, (**14**) 0.25 nmol per µg each of $(Acr\text{-}Lys)_6$-SS-K-melittin and $(Acr\text{-}Lys)_6$-SS-NLS-PC-4, (**15**) 0.25 nmol per µg each of $(Acr\text{-}Lys)_6$-SS-NLS-melittin and $(Acr\text{-}Lys)_6$-SS-NLS-PC-4, and (**16**) 0.25 nmol per µg each of $(Acr\text{-}Lys)_6$-SS-NLS-melittin and $(Acr\text{-}Lys)_6$-SS-K-melittin. The luciferase expression was determined at 24 hrs. The results represent the mean (n=3) and standard deviation for three independent transfections.

## In Vitro Gene Transfer Activity of Polyacridine-Fusogenic Peptides.

The endosomal escape activity of fusogenic peptides were evaluated through an in vitro gene transfer assay. CHO cells were transfected with polyplexes formed with polyacridine-fusogenic peptide constructs at a peptide/DNA ratio of 0.5 nmol peptide per μg of DNA (Figure 5-4). The 0.5 nmol peptide per μg of DNA proved to be the optimal peptide/DNA ratio in the previous polyacridine-melittin studies reported in Chapter 2 and 3 (*161*). Expression levels mediated by $(Acr\text{-}Lys)_6$-SS-K-melittin polyplexes are nearly equivalent to that of the positive control PEI polyplexes formed at an N:P ratio of 9:1 and 1000-fold more potent than $(Acr\text{-}Lys)_6$-Mal-K-melittin polyplexes. Formulations of 0.1 nmol per μg of $(Acr\text{-}Lys)_6$-Mal-NLS and 0.4 nmol per μg of $(Acr\text{-}Lys)_6$-SS-K-melittin or $(Acr\text{-}Lys)_6$-Mal-K-melittin is equivalent to polyplexes formed with $(Acr\text{-}Lys)_6$-SS-K-melittin and $(Acr\text{-}Lys)_6$-Mal-K-melittin, indicating no NLS effect based on expression levels (Figure 5-4). Inclusion of NLS on the N-terminus of melittin results in a 4-fold greater gene expression for $(Acr\text{-}Lys)_6$-SS-NLS-K-melittin versus $(Acr\text{-}Lys)_6$-SS-K-melittin polyplexes, indicating transgene delivery and expression is enhanced by inclusion of an NLS sequence, however it cannot be ruled out that the observed increase is due to Cys-NLS-K-melittin's five additional cationic residues.

Polyplexes formed with 0.25 nmol per μg each of $(Acr\text{-}Lys)_6$-SS-K-melittin and $(Acr\text{-}Lys)_6$-SS-NLS-K-melittin results in nearly equivalent transfection mediated by $(Acr\text{-}Lys)_6$-SS-K-melittin alone and a subtle decrease when compared to $(Acr\text{-}Lys)_6$-SS-NLS-melittin expression levels (Figure 5-4). The robust gene transfer efficiency of the reducible polyacridine-K-melittin and NLS-K-melittin peptides offer the ability to accommodate endosomal escape in vivo if properly incorporated into a targeted multi-component gene delivery system.

The gene expression levels mediated by polyacridine-PC-4 analogues and NLS-PC-4 chimeras' were independent of reducibility or NLS placement and were similar to

gene transfer levels generated with polyplexes formed with the control DNA condensing peptide $WK_{18}$ at 0.2 nmol peptide per μg of DNA (Figure 5-4). Additionally, when compared to the luciferase levels mediated by a reducible polyacridine-melittin polyplex, PC-4's fusogenic activity is greatly eclipsed in an in vitro gene transfer arena. Polyplexes were then formed with 0.25 nmol peptide per μg each of $(Acr\text{-}Lys)_6$-SS-K-melittin and $(Acr\text{-}Lys)_6$-SS-NLS-PC-4 or $(Acr\text{-}Lys)_6$-SS-NLS-K-melittin and $(Acr\text{-}Lys)_6$-SS-NLS-PC-4. These formulations resulted in a 5-fold decrease in respect to K-melittin polyplex transfection and a 10-fold decrease in gene transfer when compared to NLS-K-melittin polyplexes (Figure 5-4). While PC-4 based analogues were observed to operate as weak fusogenic peptides upon comparison to melittin, their unique neutrally charged sequence offered the opportunity to modulate polyplex charge properties and reduce non-specific interactions with blood components. These properties justified further investigation of PC-4 as an endosomal escape agent in a multi-component system.

### Determination of Multiple Component Integration by Spin Assay.

pGL3 polyplexes were formed upon addition of PEGylated polyacridine peptide, glycopeptide, and fusogenic peptide at predetermined input ratios of 0.5 nmol peptide per μg of DNA using 10 μg pGL3. Following incubation at room temperature, the non-incorporated peptide was separated by a 50 KDa MWCO membrane from peptide/DNA polyplexes by size exclusion centrifugation. Following multiple wash and centrifugation cycles, an aliquot of the filtrate was analyzed by RP-HPLC and compared to a control omitting pGL3 where the percent difference between control and experimental peak areas represents the percent of each component incorporated, or the output ratio. Polyplexes consisting of an input ratio 70% $(Acr\text{-}Lys)_6$-SS-PEG (PEG), 10% $(Acr\text{-}Lys)_6$-Cys-TRI (TRI), and 20% $(Acr\text{-}Lys)_6$-SS-K-melittin (melittin) were analyzed by spin assay (Figure 5-5 and Table 5-4). The RP-HPLC chromatograph of the control sample demonstrates the

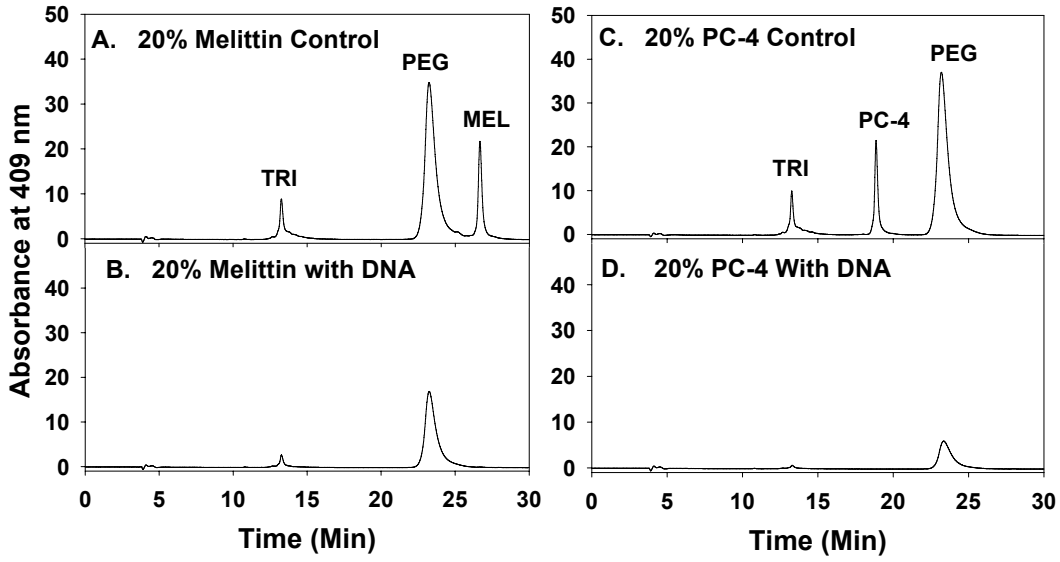


Figure 5-5. *Spin Assay Analysis* by *RP-HPLC of Multi-Component Polyplex Incorporation with 70% PEG, 10% TRI, and 20% Fusogenic Peptide Input Ratio.* The chromatographs in Panels A and C represent controls that have been subjected to size exclusion centrifugation through a 50 KDa MWCO membrane while omitting pGL3 from the formulation and analyzed by RP-HPLC. Panel A represents a 20% input ratio of melittin and Panel C represents a 20% input ratio of PC-4. Experimental samples were formulated with 10 µg pGL3 with input ratios of 70% PEG, 10% TRI, 20% melittin (Panel B) or 70% PEG, 10% TRI, 20% PC-4 (Panel D) to generate output ratios or percent component integration ratios of 53.7% PEG, 12.8% TRI, 33.6% melittin (Table 5-4) and 64.6% PEG, 11.1% TRI, 24.2% PC-4 (Table 5-5). Output ratios are based upon the control and experimental peak area percent differences obtained from RP-HPLC analysis after injection of 100 µl of filtrate eluted with a 0.1 v/v % TFA and an acetonitrile gradient of 10-55 v/v % over 30 min while monitoring 409 nm absorbance.

typical retention characteristics for TRI, PEG, and melittin (Figure 5-5A). Early control experiments established that non-specific binding to the filter membrane is maximally 20%. The experimental RP-HPLC chromatograph demonstrates a dramatic loss of peak area coincident with all components (Figure 5-5B). Upon analysis of the RP-HPLC peak areas; polyplexes were composed of 53.7% PEG, 12.8% TRI, and 33.6% melittin, demonstrating a majority of components were present within the multi-component

Table 5-4. *Spin Assay Results for Melittin Based Formulations*

| Input Ratio (mol % PEG: mol % TRI: mol % Melittin Peptide) | Output Ratio (mol % PEG: mol % TRI: mol % Melittin Peptide) |
|---|---|
| 90 : 10 : 0 (K-Melittin) | 90.3 ± 3 : 9.6 ± 0.2 : 0 |
| 80 : 10 : 10 (K-Melittin) | 75.0 ± 4.4 : 11.8 ± 0.3 : 13.5 ± 0.1 |
| 70 : 10 : 20 (K-Melittin) | 53.7 ± 6.9 : 12.8 ± 0.7 : 33.6 ± 0.0 |
| 60 : 10 : 30 (K-Melittin) | 30.9 ± 1.8 : 11.5 ± 0.5 : 57.5 ± 0.2 |
| 45 : 10 : 45 (K-Melittin) | 18.5 ± 8.4 : 8.8 ± 0.7 : 72.7 ± 3.3 |
| 30 : 10 : 60 (K-Melittin) | 12.1 ± 1.5 : 6.7 ± 0.9 : 81.1 ± 1.7 |
| 10 : 10 : 80 (K-Melittin) | 3.4 ± 3.4 : 4.8 ± 3.4 : 91.4 ± 15.2 |
| 70 : 10 : 20 (NLS-K-Melittin) | 65.4 ± 0.8 : 10.4 ± 0.1 :24.1 ± 0.0 |
| 50:10:20 (NLS-PC-4):20 (K-Melittin) | 31.0±5.3 : 11.0±1.5 : 26.9±1.9 : 31.4±1.6 |

Note: Spin assay results of ternary complexes formed from addition of pGL3 to various ratios of $(Acr\text{-}Lys)_6$-SS-PEG (PEG), $(Acr\text{-}Lys)_6$-Cys-TRI (TRI), and $(Acr\text{-}Lys)_6$-SS-Melittin (K-Melittin) analogue formed at peptide/DNA ratio of 0.5 nmol peptide per μg DNA. The first column represents the input ratio of individual components (mol % PEG: mol % TRI, and mol% melittin analogue) and the second column represents the output ratio or percent component incorporation into the polyplex. The general trend that is observed upon increasing the input ratio of melittin, the output ratios for both PEG and TRI peptides decrease, indicating that a 20% input ratio of melittin will ensure PEG and TRI components are present in the polyplex after formulation. TRI was used at a constant input ratio of 10%. The results represent the mean and standard deviation for three independent experiments.

complex with DNA (Table 5-4). An interesting trend is observed upon increasing the input ratio of melittin that results in an increasing loss of PEG and TRI from the polyplex. This trend is most dramatically illustrated with an input ratio of 80% melittin, which results in an output ratio of 0% for PEG and TRI. Multi-component complexes formed with 70% PEG, 10% TRI, and 20% NLS-K-melittin results in an output ratio of 65.4% PEG, 10.4% TRI, and 24.1% NLS-K-melittin, which represents an improvement over the 20% melittin formulation (Table 5-4).

Multi-component complexes formed with PC-4 analogues demonstrate very similar incorporation behavior when compared to melittin formulations (Figure 5-5C, D, and Table 5-5). The RP-HPLC chromatographs for the control (Figure 5-5C) and experimental sample (Figure 5-5D) containing the filtrate of polyplexes formulated with 70% PEG, 10% TRI, and 20% PC-4 were analyzed and revealed an output ratio of 64.9%

Table 5-5. *Spin Assay Results for PC-4 Based Formulations*

| Input Ratio (mol % PEG: mol % TRI: mol % PC-4 Peptide) | Output Ratio (mol % PEG: mol % TRI: mol % PC-4 Peptide) |
|---|---|
| 90 : 10 : 0 (PC-4) | 90.3 ± 3 : 9.6 ± 0.2 : 0 |
| 80 : 10 : 10 (PC-4) | 78.3 ± 2.5 : 10.6 ± 0.1 :11.0 ± 0.0 |
| 70 : 10 : 20 (PC-4) | 64.6 ± 2.7 : 11.1 ± 0.1 : 24.2 ± 0.0 |
| 60 : 10 : 30 (PC-4) | 31.0 ± 1.4 : 9.9 ± 1.0 : 60.0 ± 0.6 |
| 45 : 10 : 45 (PC-4) | 16.3 ± 3.8 : 7.0 ± 1.3 : 76.6 ± 0.4 |
| 30 : 10 : 60 (PC-4) | 4.6 ± 2.5 : 4.6 ± 1.9 : 91.0 ± 3.3 |
| 10 : 10 : 80 (PC-4) | 0.0 ± 3.7 : 0.7 ± 1.4 : 99.3 ± 39.3 |
| 70 : 10 : 20 (PC-4-NLS) | 69.1 ± 0.8 : 9.7 ± 0.3 : 20.0 ± 0.0 |
| 70 : 10 : 20 (NLS-PC-4) | 69.9 ± 0.2 : 10 ± 0.0 : 20.0 ± 0.0 |

Note: Spin assay results of ternary complexes formed from addition of pGL3 to various ratios of $(Acr\text{-}Lys)_6$-SS-PEG (PEG), $(Acr\text{-}Lys)_6$-Cys-TRI (TRI), and $(Acr\text{-}Lys)_6$-SS-PC-4 (PC-4) analogue formed at peptide/DNA ratio of 0.5 nmol peptide per μg DNA. The first column represents the input ratio of individual components (mol % PEG: mol % TRI, and mol% PC-4 analogue) and the second column represents the output ratio or percent component incorporation into the polyplex. The general trend that is observed upon increasing the input ratio of PC-4, the output ratios for both PEG and TRI peptides decrease, indicating that a 20% input ratio of PC-4 will ensure PEG and TRI components are present in the polyplex after formulation. TRI was used at a constant input ratio of 10%. The results represent the mean and standard deviation for three independent experiments.

PEG, 11.1% TRI, and 24.2% PC-4 (Table 5-5). As is the case with melittin, a similar trend is observed as the input ratio of fusogen is increased, the output ratios for PEG and TRI decrease. Inclusion of NLS on either the N or C-terminus of PC-4 improved the output ratios of PEG to approximately 69%, suggesting the NLS- PC-4 or PC-4-NLS peptides to be more compatible analogues for the formulation of multi-component complexes (Table 5-5). The input ratio of 70% PEG, 10% TRI, and 20% melittin or PC-4 were used in future experiments as it guaranteed the maximal input ratio of all components, especially fusogenic peptide component.

Atomic force microscopy (AFM) was employed to investigate the size and shape of the multi-component complexes deposited on freshly cleaved electronegative mica. Complexes prepared only with 100% $(Acr\text{-}Lys)_6$-SS-PEG at 0.5 nmol peptide per μg of DNA formed a dense, but open coiled polyplex shape with the presence of structures

appearing as a traditional spherical nanoparticle (Figure 5-6A). Complexes formed with 90% $(Acr\text{-}Lys)_6$-SS-PEG and 10% $(Acr\text{-}Lys)_6$-Cys-TRI formed less dense coiled structures (Figure 5-6B). In contrast, complexes formulated with 20% $(Acr\text{-}Lys)_6$-SS-K-melittin (Figure 5-6C) or $(Acr\text{-}Lys)_6$-SS-PC-4 (Figure 5-6D) predominately formed structures reminiscent of traditional spherical nanoparticles with the exception that PC-4 based nanoparticles are slightly larger than those complexes formed with polyacridine-melittin.

## In Vivo Gene Delivery of Multi-Component Complexes.

One of the greatest issues preventing clinical application of non-viral gene therapy is the overall lack of delivery efficiency in an in vivo liver targeted system. These inefficiencies force investigators to increase plasmid dose levels to achieve modest gene expression that will ultimately be unpractical and unachievable if ever to be translated clinically (*170*). To investigate the delivery efficiency of polyacridine multi-component polyplexes, they were initially formulated with 1 μg pGL3 at 0.5 nmol peptide per μg of DNA and administered by i.v. tail vein injection to multiple mice. Following 24 hrs after administration of multi-component complexes formulated with 70% $(Acr\text{-}Lys)_6$-SS-PEG, $(Acr\text{-}Lys)_6$-Cys-TRI or Agal-TRI, and $(Acr\text{-}Lys)_6$-SS-K-melittin or $(Acr\text{-}Lys)_6$-SS-PC-4, luciferase expression was quantified by BLI (Figure 5-7). The results revealed undetectable expression below the limit of detection for BLI for formulations containing PC-4 or melittin and presence of targeting ligand or control targeting ligand. This demonstrated an overall inefficiency of the delivery vehicle based upon luciferase expression (Figure 5-7), when compared to the $10^8$ photons/sec/$cm^2$/sr benchmark level produced by 1 μg HD pGL3. To improve the delivery vehicle through SAR studies relating to component design and function, dosing levels were increased to 25 μg pGL3 per mouse to induce some level of optimizable expression.

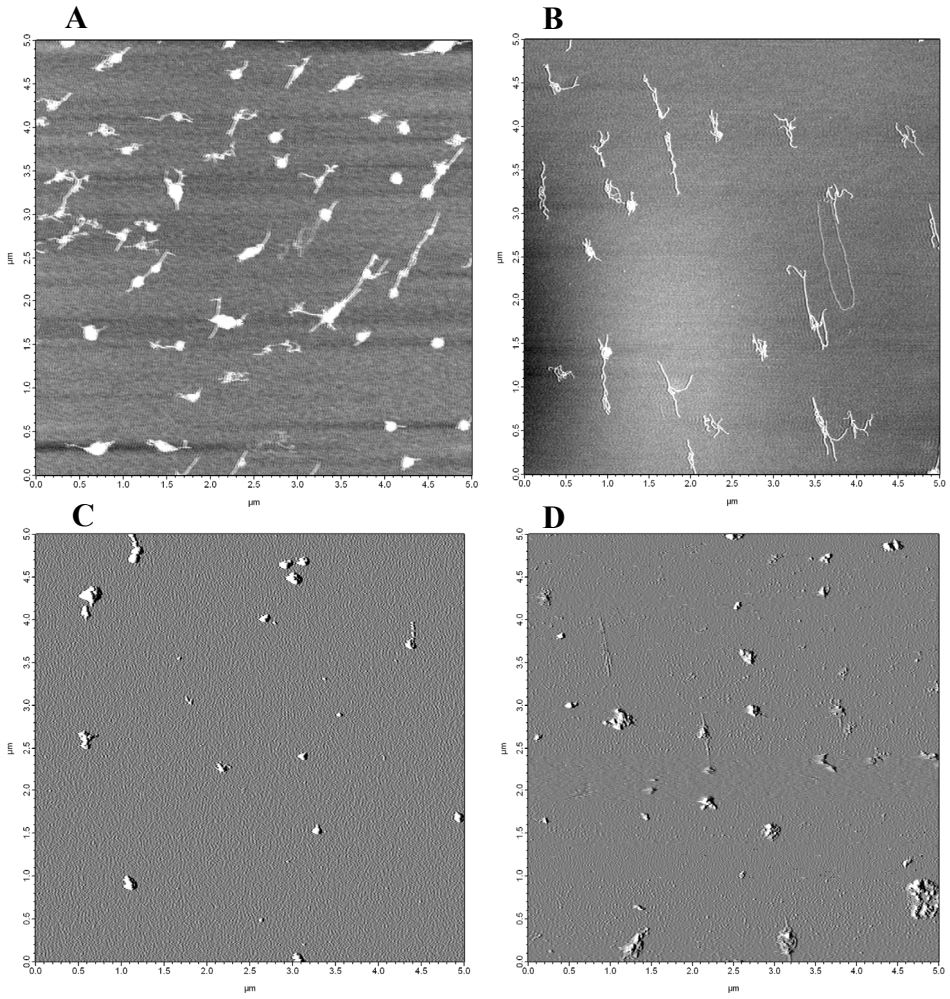


Figure 5-6. *Atomic Force Microscopy of Polyacridine Multi-Component Complexes.* The size and shape of formulations formed at a peptide/DNA ratio of 0.5 nmol peptide per µg of DNA of (Panel A) 100% (Acr-Lys)$_6$-SS-PEG, (Panel B) 90% (Acr-Lys)$_6$-SS-PEG and 10% (Acr-Lys)$_6$-Cys-TRI, (Panel C) 70% (Acr-Lys)$_6$-SS-PEG, 10% (Acr-Lys)$_6$-Cys-TRI, and 20% (Acr-Lys)$_6$-SS-K-melittin, and (Panel D) 70% (Acr-Lys)$_6$-SS-PEG, 10% (Acr-Lys)$_6$-Cys-TRI, and 20% (Acr-Lys)$_6$-SS-PC-4 were determined. The results establish that a formulation consisting of 20% fusogen (Panel C and D) produce shapes consistent with a traditional nanoparticle while formulations containing only PEG (Panel A) or 90% PEG and 10% TRI (Panel B) form the less dense coiled open polyplex shape. Polyplexes were deposited on freshly cleaved electronegative mica.

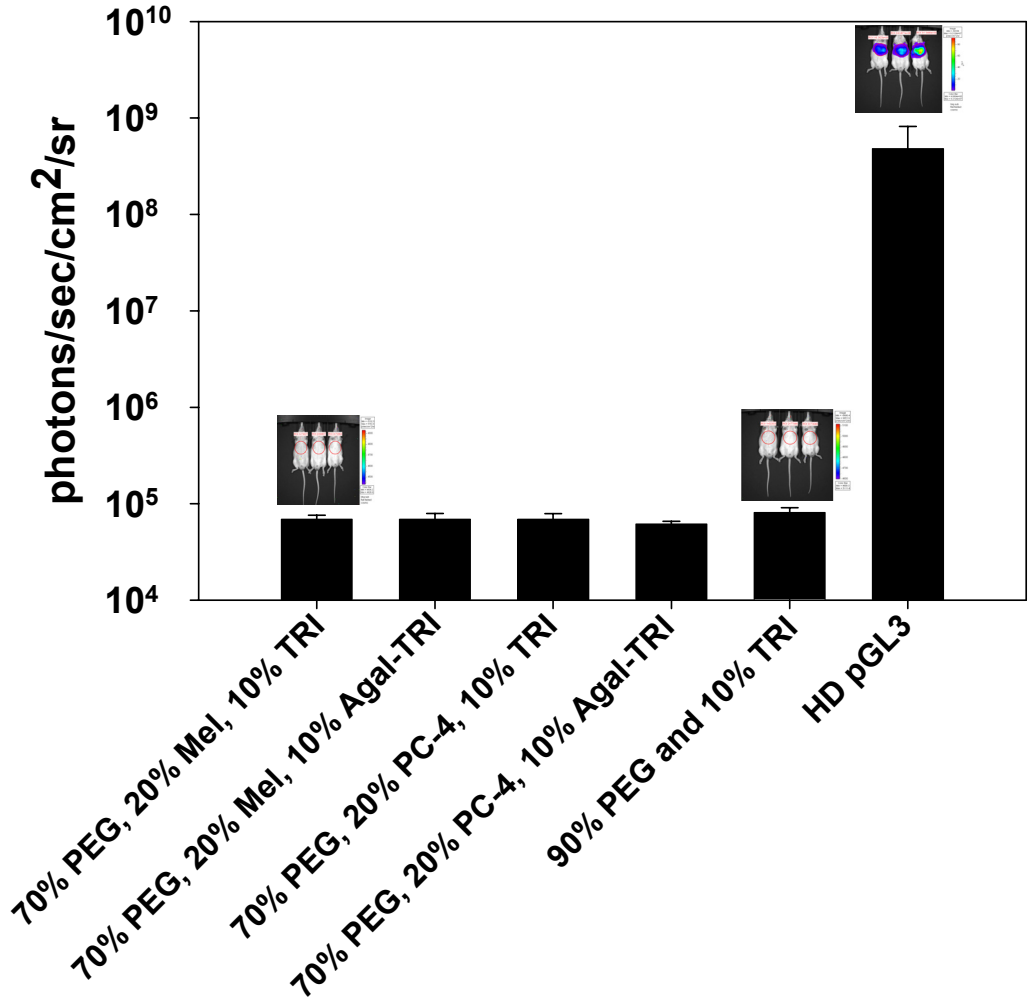


Figure 5-7. *In Vivo Gene Transfer with Multi-Component Complexes After a 1 µg pGL3 Dose Following Standard Tail Vein Injection.* Direct HD dosing of 1 µg pGL3 resulted in a mean BLI response of $10^8$ photons/sec/cm$^2$/sr at 24 hrs following dosing of HD pGL3. In contrast, a 1 µg dose of multi-component polyplexes formed with pGL3 resulted in undetectable luciferase expression. Polyplexes were formed at a peptide to DNA ratio of 0.5 nmol peptide per µg of DNA with 70% (Acr-Lys)$_6$-SS-PEG, 20% (Acr-Lys)$_6$-SS-K-melittin, and 10% (Acr-Lys)$_6$-Cys-TRI; 70% (Acr-Lys)$_6$-SS-PEG, 20% (Acr-Lys)$_6$-SS-K-melittin, and 10% (Acr-Lys)$_6$-Cys-Agal-TRI; 70% (Acr-Lys)$_6$-SS-PEG, 20% (Acr-Lys)$_6$-SS-PC-4, and 10% (Acr-Lys)$_6$-Cys-TRI; 70% (Acr-Lys)$_6$-SS-PEG, 20% (Acr-Lys)$_6$-SS-PC-4, and 10% (Acr-Lys)$_6$-Cys-Agal-TRI; and 90% (Acr-Lys)$_6$-SS-PEG, and 10% (Acr-Lys)$_6$-Cys-TRI. The results demonstrate an overall inefficiency of the delivery vehicle regardless of fusogen incorporated (melittin or PC-4), presence of targeting ligand (TRI versus Agal) at the 1 µg dose level. In an effort to observe detectable gene transfer with BLI, future experiments were conducted at an escalated dose of 25 µg pGL3 per mouse.

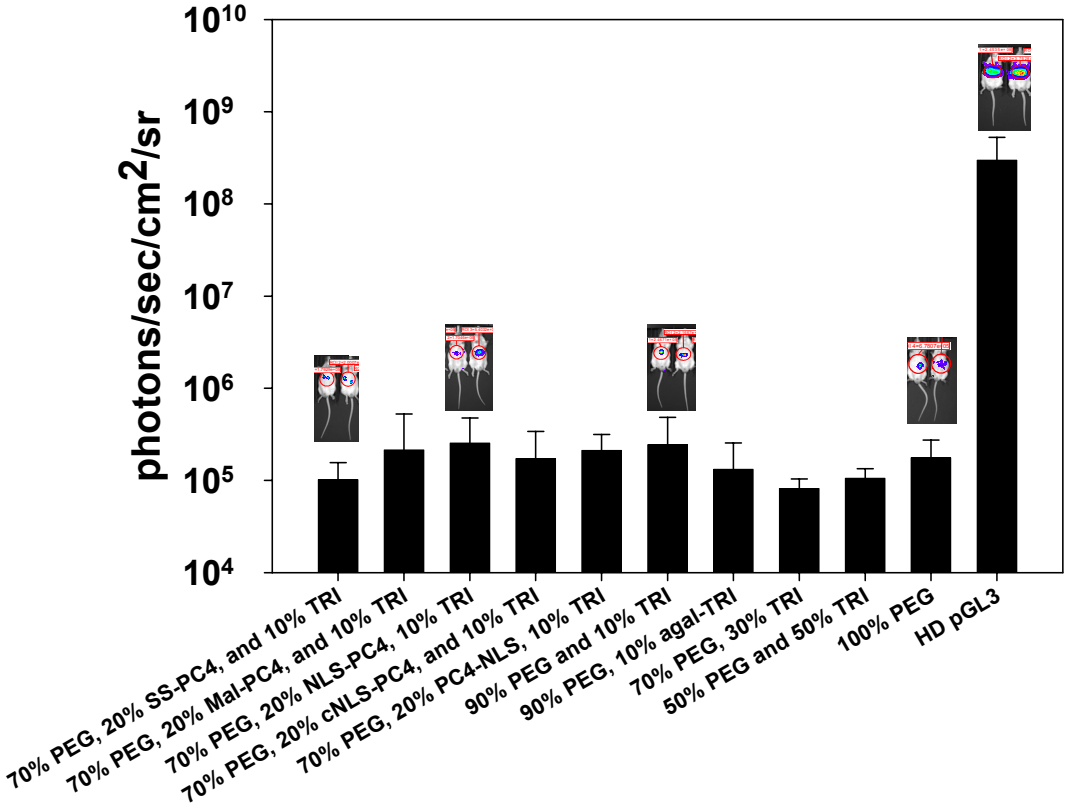


Figure 5-8. *In Vivo Transfer of PC-4 Analogue Based Multi-Component Polyplexes at a 25 µg Dose.* Multi-component polyplexes were formed at total peptide to DNA ratio of 0.5 nmol peptide per µg of DNA and dosed in multiple mice (n≥3) by tail vein injection with 100 µl HBM. At the 25 µg polyplex dose level, gene expression was detectable with BLI 24 hrs after administration with a maximal response observed with formulations consisting of either 20% $(Acr\text{-}Lys)_6$-Mal-PC-4; 20% $(Acr\text{-}Lys)_6$-SS-PC-4-NLS, NLS-PC-4 chimera, 90% $(Acr\text{-}Lys)_6$-SS-PEG and 10% $(Acr\text{-}Lys)_6$-Cys-TRI, or a formulation consisting of 100% $(Acr\text{-}Lys)_6$-SS-PEG with mean BLI results of approximately $2.5 \times 10^5$ photons/sec/cm$^2$/sr. The results demonstrate a non-specific gene expression phenomenon independent of polyacridine-PC-4 linkage (reducible disulfide versus non-reducible maleimide), placement of nuclear localization signal on chimeric fusogens (N-terminus versus C-terminus), nuclear localization (SV40 NLS sequence versus control sequence), and hepatocyte targeting ligand (TRI versus Agal-TRI or omission of targeting ligand in the form of a 100% PEG formulation). In an attempt to observe a hepatocyte specific uptake and expression, the amount of $(Acr\text{-}Lys)_6$-Cys-TRI was varied from 30% and 50%, resulting in a loss of detectible luciferase expression. A direct HD dose of 1 µg of pGL3 was used as a positive control.

Figure 5-8 reveals the results of multi-component complexes formulated with PC-4 or NLS-PC-4 chimeras with an escalated dose of 25 µg pGL3. Gene expression at the 25 µg dosing level was detectable with BLI and maximal gene expression was observed with formulations containing 0.5 nmol per µg of either 20% $(Acr\text{-}Lys)_6$-Mal-PC-4, 20% $(Acr\text{-}Lys)_6$-SS-PC-4-NLS, 90% $(Acr\text{-}Lys)_6$-SS-PEG and 10% $(Acr\text{-}Lys)_6$-Cys-TRI, or a formulation consisting of 100% $(Acr\text{-}Lys)_6$-SS-PEG at an approximate level $2.5 \times 10^5$ photons/sec/$cm^2$/sr (Figure 5-8). Slight differences are demonstrated for formulations consisting of 90% $(Acr\text{-}Lys)_6$-SS-PEG and 10% $(Acr\text{-}Lys)_6$-Cys-TRI or the hepatocyte targeting control Agal-TRI, suggesting that hepatocyte specific uptake is occurring for the targeted multi-component polyplexes. However, due to the low levels of observable expression and nearly equivalent expression for a 100% PEG formulation, it must be concluded that polyplex uptake is non-specific in regards to a receptor mediated pathway based upon BLI measurement. To address this further, the amount of $(Acr\text{-}Lys)_6$-Cys-TRI was increased to 30% and 50% in an attempt to illicit an increase in gene expression that could be correlated to a specific uptake mechanism. The results demonstrate a decrease in luciferase expression upon increasing the input ratio of TRI in the polyplex, suggesting a change in the pharmacokinetic properties, thus leading to enhanced susceptibility of pGL3 to degradation (Figure 5-8). Results also demonstrate a non-specific gene expression phenomenon independent of polyacridine-PC-4 linkage, where a reducible disulfide produces lower expression levels versus non-reducible maleimide (Figure 5-8), which is contrary to in vitro results established with polyacridine-melittin (Chapters 2 and 3). The phenomenon is also independent of nuclear localization sequence placement at the N or C-terminus of chimeric NLS-PC-4 peptides, however the expression levels of both $(Acr\text{-}Lys)_6$-SS-NLS-PC-4 and PC-4-NLS are greater than that of the reducible $(Acr\text{-}Lys)_6$-SS-PC-4. This result suggests that inclusion of the cationic NLS sequence is beneficial for the PC-4 system, perhaps due to greater polyplex solubility afforded by NLS. This solubility phenomenon also translates into greater overall mol %

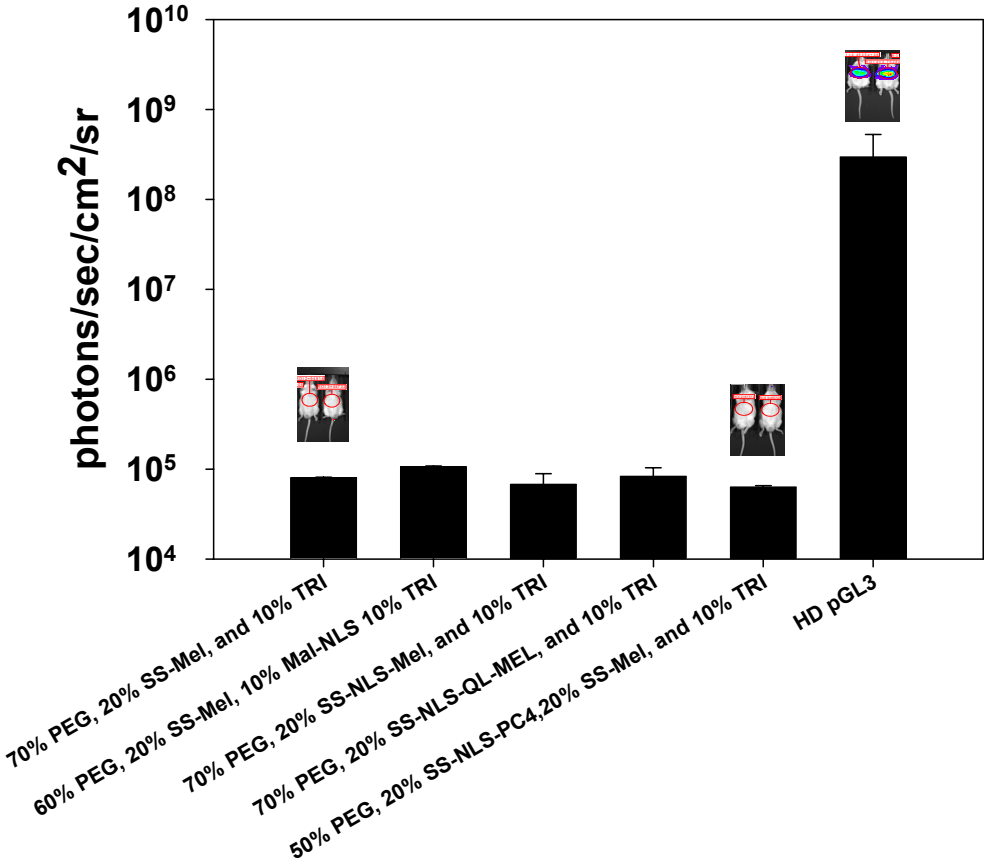


Figure 5-9. *In Vivo Gene Transfer of Melittin Analogue Based Multi-Component Polyplexes at a 25 µg Dose.* Luciferase expression levels remained below detectable levels for all formulations incorporating a melittin analogue in the multi-component complex formulation when dosed (n=3) with 25 µg pGL3 with 0.5 nmol peptide per µg of DNA and measured 24 hrs later by BLI. The results demonstrate the low level expression observed with many PC-4 based formulations is negated upon addition of melittin to the formulation (50% $(Acr\text{-}Lys)_6$-SS-PEG, 20% $(Acr\text{-}Lys)_6$-SS-NLS-PC-4, 20% $(Acr\text{-}Lys)_6$-SS-K-melittin, and 10% $(Acr\text{-}Lys)_6$-Cys-TRI). Neutralization of melittin's cationic residues by replacement with glutamine or leucine residues results in undetectable luciferase expression (70% $(Acr\text{-}Lys)_6$-SS-PEG, 20% $(Acr\text{-}Lys)_6$-SS-NLS-QL-melittin, and 10% $(Acr\text{-}Lys)_6$-Cys-TRI). Furthermore, formulation with 10% $(Acr\text{-}Lys)_6$-Mal-NLS with 20% melittin resulted in undetectable expression, suggesting translocation of plasmid DNA from the cytosol to the nucleus may be limited by the diameter of the nuclear pore complex. The results taken as a whole suggest melittin promotes either polyplex instability or undesirable polyplex-blood component interactions leading to premature degradation or neutralization of melittin's inherent membrane lytic potential.

incorporation and compatibility within a multi-component system as demonstrated by spin assay (Table 5-5).

Finally, the results are independent of NLS effect as demonstrated by inclusion of the control peptide, $(Acr\text{-}Lys)_6$-SS-cNLS-PC-4 and subsequent expression producing nearly equivalent BLI response as afforded by $(Acr\text{-}Lys)_6$-SS-NLS-PC-4 (Figure 5-8). Overall, the results indicate PC-4 is at best operating as a marginal to weak endosomal escape agent and at worst functioning only as a tolerated bystander in the multi-component complex.

In an attempt to increase in vivo gene transfer and present positive evidence to support the endosomal escape hypothesis, multi-component polyplexes based upon the potent cationic fusogenic peptide melittin were formulated at 0.5 nmol peptide per µg of DNA with 25 µg pGL3 and analyzed for luciferase expression 24 hrs after dosing. The results reveal a loss of detectable luciferase expression for formulations containing 20% $(Acr\text{-}Lys)_6$-SS-K-melittin analogue (Figure 5-9). A multi-component complex formed with four components consisting of 60% $(Acr\text{-}Lys)_6$-SS-PEG, 20% $(Acr\text{-}Lys)_6$-SS-K-melittin, 10% $(Acr\text{-}Lys)_6$-Mal-NLS, and 10% $(Acr\text{-}Lys)_6$-Cys-TRI also failed to produce detectable luciferase expression, disproving NLS's ability to translocate cytosolic pGL3 to the nucleus due to nuclear pore size restriction (*94*), assuming efficient endosomal escape is afforded by melittin (Figure 5-9). Polyplexes formulated with 20% $(Acr\text{-}Lys)_6$-SS-NLS-melittin or $(Acr\text{-}Lys)_6$-SS-NLS-QL-melittin were incapable of producing measurable gene expression. This result fails to provide evidence supporting the hypothesis that an NLS-fusogen (melittin or PC-4) can translocate to the nucleus after reductive release from $(Acr\text{-}Lys)_6$-Cys to induce nuclear membrane pore formation that allows passage of plasmid DNA into the nucleus. (Figure 5-8 and 5-9). However, one must also keep in mind the reported physical dimensions of pores formed by melittin (3-5 nm) and the typical particle size reported for polyplexed DNA (75-150 nm) (*86-88*). The undetectable luciferase expression followed by administration of a four component

complex consisting of 50% (Acr-Lys)$_6$-SS-PEG, 20% (Acr-Lys)$_6$-SS-K-melittin, 20% (Acr-Lys)$_6$-SS-NLS-PC-4, and 10% (Acr-Lys)$_6$-Cys-TRI are of interest as well. The result suggests that upon addition of highly cationic components such as melittin, detectable luciferase expression levels are abrogated (Figure 5-9), demonstrating multi-component complexes are intolerant of cationic species. The lack of in vivo expression with NLS-QL-melittin polyplexes suggests there is a limit in regards to allowable peptide sequence length as a shortened NLS-PC-4 sequence produces detectable expression (Figure 5-8 compared to 5-9).

In vivo gene transfer experiments conducted with the anionic fusogen JTS-1 were attempted to offer a complete survey of the various classes of fusogenic peptides as it is widely acknowledged viruses often mediate endosomal escape through utilization of anionic peptides or proteins (*45, 53, 68*). Polyplexes were formulated with 20% (Acr-Lys)$_{6 \text{ or } 8}$–SS-JTS-1 at 0.5 nmol peptide per μg of DNA complexed with 25 μg pGL3. The results demonstrate polyplexes formulated with (Acr-Lys)$_{6 \text{ or } 8}$–SS-JTS-1 are incapable of producing detectable luciferase expression (Figure 5-10). Despite the thiazole orange data supporting strong DNA binding affinity for (Acr-Lys)$_{6 \text{ or } 8}$–SS-JTS-1 (Figure 5-3), it appears strongly anionic species such as JTS-1 are not well tolerated in a multi-component formulation, much like the in vivo gene expression results observed with melittin formulations at a 25 μg dose (Figure 5-9). Further suggesting that any bioactive component must be of a neutrally charged nature, such as PEG, TRI, and PC-4 (with exception to NLS-PC-4 chimeras), to allow for efficient delivery of plasmid DNA in vivo.

As the spin assay suggests there is a physical limit on the amount of fusogenic peptide that can be incorporated into a multi-component delivery system; we attempted an alternative strategy of eliciting endosomal escape through incorporation of an endosomal buffering component within the backbone of the polyacridine DNA binding peptide. The spacing amino lysine was replaced with the imidazole side chain of histidine

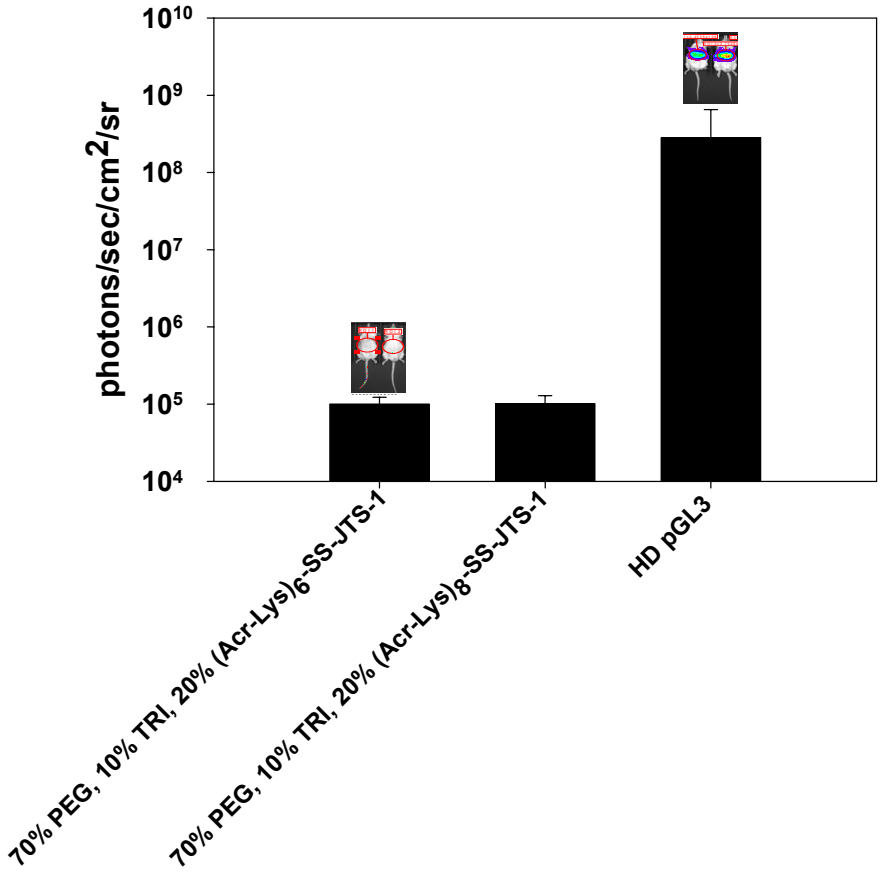


Figure 5-10. *In Vivo Gene Transfer with Multi-Component Complexes Formed with (Acr-Lys)$_x$-SS-JTS-1.* Polyplexes were formed with 25 µg of pGL3 using 70% (Acr-Lys)$_6$-SS-PEG, 20% (Acr-Lys)$_6$-SS-JTS-1 or (Acr-Lys)$_8$-SS-JTS-1, and 10% (Acr-Lys)$_6$-Cys-TRI with a peptide to DNA ratio of 0.5 nmol peptide per µg of DNA. Following BLI analysis, polyplexes formed with either 20% (Acr-Lys)$_{6\text{ or }8}$ SS-JTS-1 are incapable of producing detectable expression offering evidence that strongly anionic (JTS-1) or cationic (melittin) constructs are not well tolerated in a multi-component formulation. The positive control consists of a direct HD dose of 1 µg pGL3. Results represent the mean (n=3) and standard deviation.

(pKa 6.5), resulting in the multifunctional peptide (Acr-His)$_6$-Cys that was further functionalized to generate (Acr-His)$_6$-SS-PEG and the targeting ligand (Acr-His)$_6$-Cys-TRI. Upon acidification of the late endosome, the side chain of histidine becomes protonated, encouraging an additional influx of protons and water, creating a hypertonic

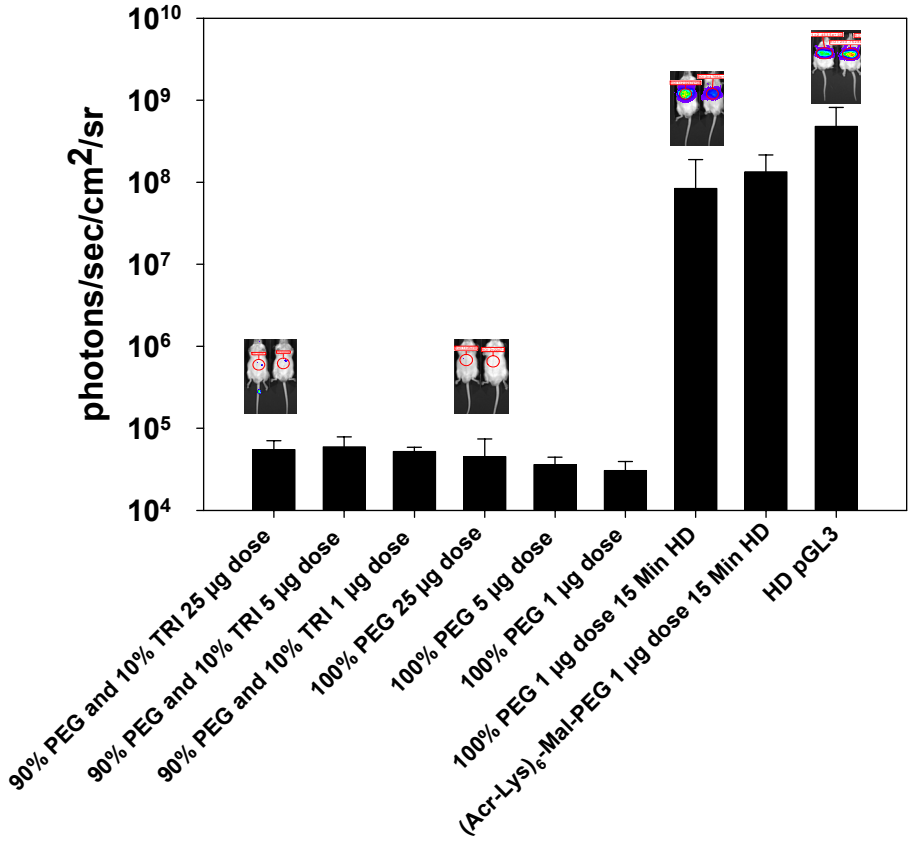


Figure 5-11. *Dose Response of Non-Stimulated Administration of Endosomal Buffering Polyacridine PEG and Glycopeptides.* Multi-component complexes were formed by addition of 90% $(Acr\text{-}His)_6$-SS-PEG and 10% $(Acr\text{-}His)_6$-Cys-TRI or with a single component system of 100% $(Acr\text{-}His)_6$-SS-PEG formed at a peptide to DNA ratio of 0.5 nmol peptide per µg of DNA at doses of 1, 5, and 25 µg pGL3 and delivered by tail vein i.v injection. Luciferase activity was assayed 24 hrs later to reveal that at all dosing levels tested for multi-component polyplexes formed with $(Acr\text{-}His)_6$-SS-PEG and $(Acr\text{-}His)_6$-Cys-TRI or $(Acr\text{-}His)_6$-SS-PEG failed to produce detectible levels of transgene expression which is contrary to results observed at a 25 µg dose with polyplexes formed with $(Acr\text{-}Lys)_6$-SS-PEG and/or $(Acr\text{-}Lys)_6$-Cys-TRI (Figure 5-8). However, upon hydrodynamic stimulation at 15 min, a 1 µg dose of $(Acr\text{-}His)_6$-SS-PEG polyplex displayed expression levels similar to a 1 µg dose of 0.2 nmol peptide per µg of DNA $(Acr\text{-}Lys)_6$-Mal-PEG pGL3 polyplex stimulated at 15 min, demonstrating potential utility as a stimulatable gene delivery system. Results represent the mean (n=3) and standard deviation.

environment inside the endosome forcing it to rupture. This is also the reported mechanism of action for chloroquine and PEI mediated endosomal escape (*54-56*).

Polyplexes formed with 90% (Acr-His)$_6$-SS-PEG and 10% (Acr-His)$_6$-Cys-TRI or 100% (Acr-His)$_6$-SS-PEG were formulated at 0.5 nmol peptide per μg of DNA and dosed with 1, 5, and 25 μg of pGL3 (Figure 5-11). The results reveal an overall inefficiency for the (Acr-His)$_6$-SS-PEG and TRI or (Acr-His)$_6$-SS-PEG based polyplexes to promote detectible luciferase expression by BLI, suggesting that the buffering capacity of (Acr-His)$_6$-Cys is well below the required capacity to force endosomal lysis. Alternatively, a component that encourages translocation of plasmid DNA to the nucleus is missing and has yet to be discovered. It is interesting to note that even for the 25 μg doses that (Acr-His)$_6$-SS-PEG and TRI or (Acr-His)$_6$-SS-PEG alone is incapable of producing expression levels generated by (Acr-Lys)$_6$-Cys based delivery systems (Figure 5-11), demonstrating the potential promise that (Acr-Lys)$_6$-Cys based delivery systems holds for non-viral delivery of plasmid DNA (Figure 5-8). However, a 1 μg dose of 0.5 nmol per μg of pGL3 polyplexed with (Acr-His)$_6$-SS-PEG hydrodynamically stimulated at 15 min produces a BLI response of $10^8$ photons/sec/cm$^2$/sr. This result is comparable to a 15 min stimulation of polyplexes formed with 0.2 nmol per μg of (Acr-Lys)$_6$-SS-Mal-PEG (Figure 5-11), demonstrating the potential utility of (Acr-His)$_6$-Cys as a stimulatable gene delivery system.

Pharmacokinetic (PK) and biodistribution (BD) analysis was conducted for 20% (Acr-Lys)$_6$-SS-K-melittin formulations using $^{125}$I-pGL3 (Figure 5-12). PK analysis demonstrates a rapid decrease of 20% (Acr-Lys)$_6$-SS-K-melittin $^{125}$I-DNA polyplexes from the blood in comparison to long circulating polyplexes formulated with 90% (Acr-Lys)$_6$-SS-PEG and 10% (Acr-Lys)$_6$-Cys-TRI (Figure 5-12A). Melittin polyplexes in which the targeting ligand had been replaced with (Acr-Lys)$_6$-Cys-Agal-TRI or omitted also demonstrate a rapid decrease or clearance from the blood as well. However, unlike the targeted melittin polyplex, the levels of radiation begin to rebound, perhaps indicating degradation and release of nucleotides back into the blood.

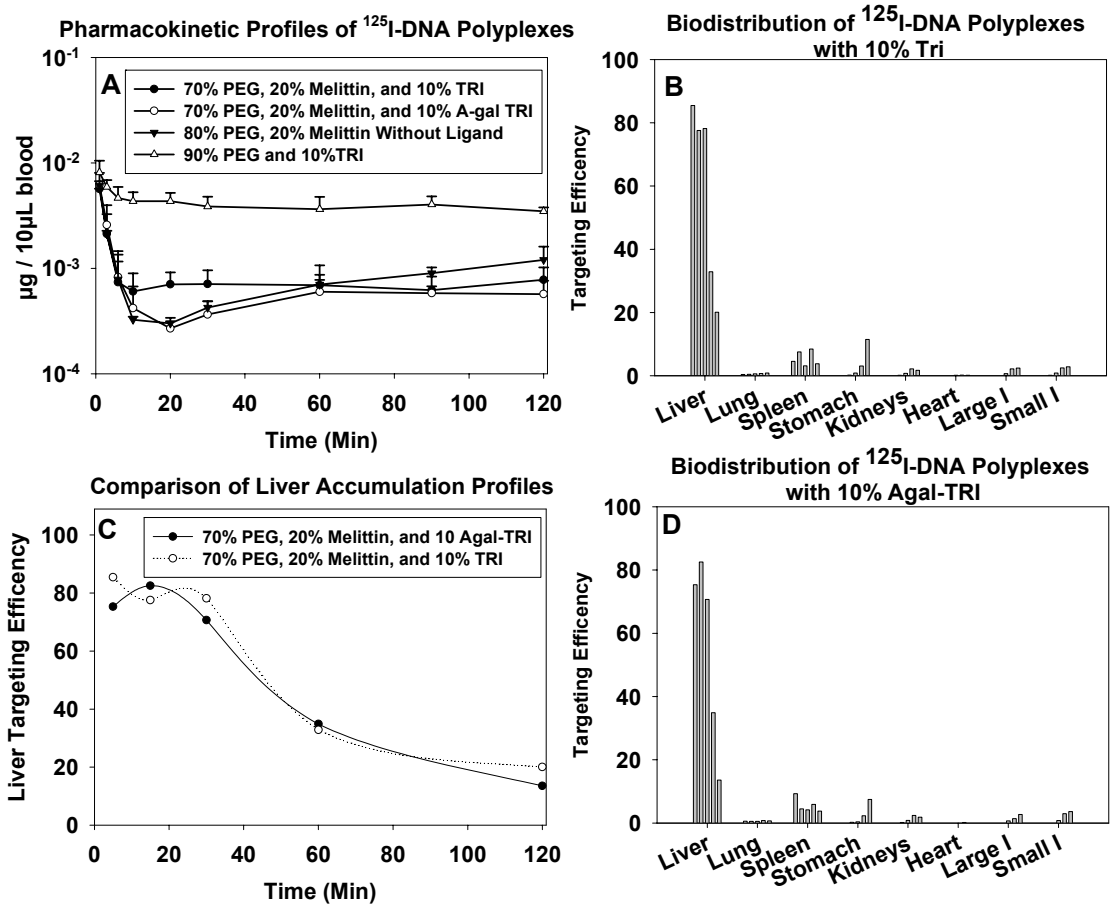


Figure 5-12. *Pharmacokinetic and Biodistribution Analysis of Multi-Component Formulations with 20% (Acr-Lys)$_6$-SS-K-melittin.* The pharmacokinetic profiles for multi-component polyplexes formed at 0.5 nmol peptide per µg of $^{125}$I-DNA consisting of 70% PEG, 20% melittin, 10% TRI; 70% PEG, 20% melittin, 10% Agal-TRI; and 80% PEG, 20% melittin are compared to the long circulating polyplex formed with 90% PEG and 10% TRI (Panel A). Results represent the mean (n = 3) and standard deviation per time point. The biodistribution profiles for formulations consisting of 70% PEG, 20% melittin, and 10% TRI or Agal-TRI demonstrate the liver is the primary organ of accumulation (Panel B and D). Replotting the time course of accumulation for TRI or Agal-TRI containing formulations reveals similar accumulation and elimination profiles for the percent of dose found in the liver (Panel C). The biodistribution results represent a single mouse per time point.

To determine the major organ of accumulation, BD studies were conducted with $^{125}$I-DNA polyplexes formulated with 70% (Acr-Lys)$_6$-SS-PEG, 20% (Acr-Lys)$_6$-SS-K-

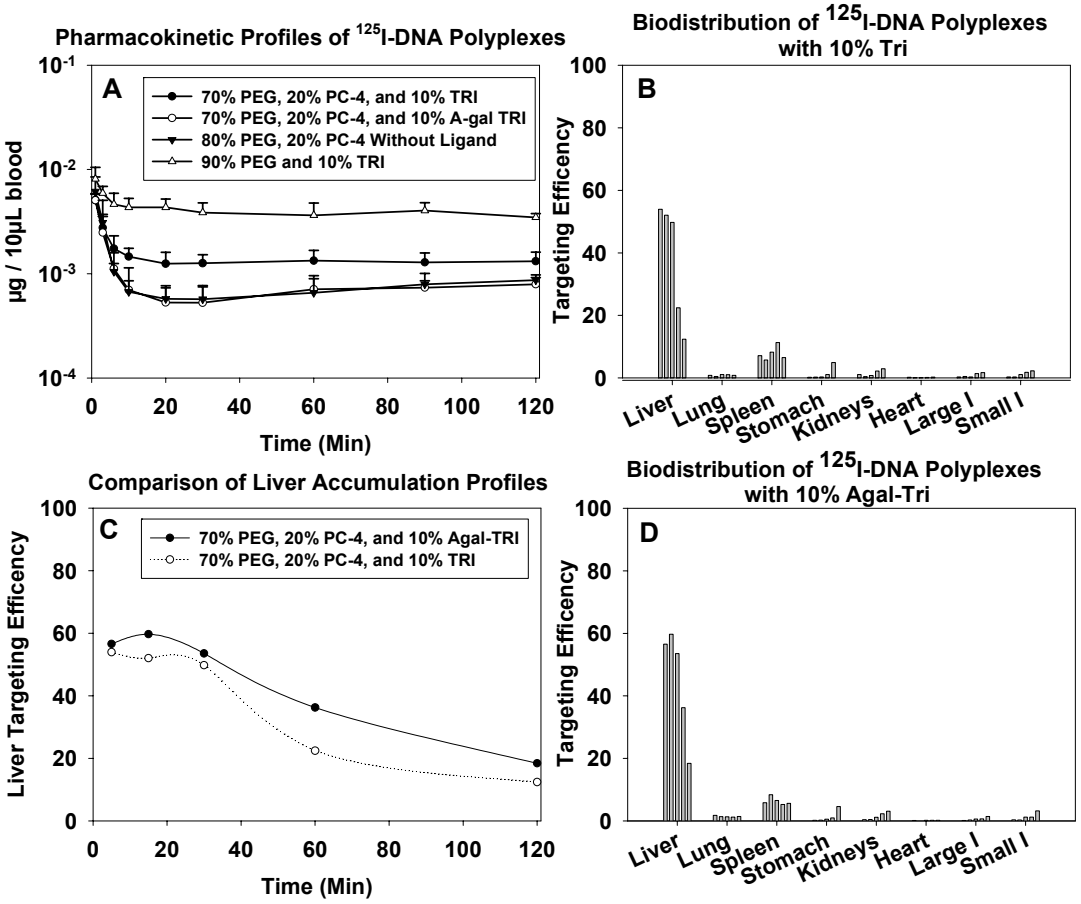


Figure 5-13. *Pharmacokinetic and Biodistribution Analysis of Multi-Component Formulations with 20% (Acr-Lys)$_6$-SS-PC-4.* The pharmacokinetic profiles for multi-component polyplexes formed at 0.5 nmol peptide per µg of $^{125}$I-DNA consisting of 70% PEG, 20% PC-4, 10% TRI; 70% PEG, 20% PC-4, 10% Agal-TRI; and 80% PEG, 20% PC-4 are compared to the long circulating polyplex formed with 90% PEG and 10% TRI (Panel A). Results represent the mean (n = 3) and standard deviation per time point. The biodistribution profiles for formulations consisting of 70% PEG, 20% PC-4, and 10% TRI or Agal-TRI demonstrate the liver is the primary organ of accumulation followed by the spleen (Panel B and D). The replot of the time course of accumulation for TRI or Agal-TRI containing formulations reveals similar accumulation and elimination profiles for the percent of dose found in the liver (Panel C), but approximately 30% lower than multi-component complexes formed with melittin (Figure 5-12C). Overall, the results suggest that formulations containing TRI or Agal-TRI naturally biodistribute to the liver. The biodistribution results represent a single mouse per time point.

melittin, and 10% (Acr-Lys)$_6$-Cys-TRI or control Agal-TRI. The results demonstrate very similar organ distribution patterns for the targeted and control polyplexes over time

(Figure 5-12B and 5-12C) and reveal the liver as the major organ of accumulation followed by the spleen and stomach as minor sites of accumulation. The replot of the time course of liver accumulation reveals maximal accumulation of nearly 80% of dose is observed by 15 min for both TRI and Agal-TRI containing formulations and decreases steadily until it reaches 20% of dose by 2 hrs, suggesting inoperability of the TRI targeting ligand (Figure 5-12C). Alternatively, the liver is the major site for detoxification and metabolism of many entities and is composed of several cell types, such as Kupffer cells and hepatocytes, which hepatocytes outnumber Kupffer cells at a ratio of 10:1 (*41*). It is only after separation of these cells that one could definitively provide evidence of specific cell targeting provided through incorporation of the triantennary-N-glycan versus control. This has been previously demonstrated with poly-lysine based delivery vehicles synthesized and developed within the group and demonstrated hepatocyte specific uptake of polyplexes containing the triantennary-N-glycan (*26, 36, 38, 40*).

Similar PK and BD studies were conducted with 20% (Acr-Lys)$_6$-SS-PC-4 based multi-component polyplexes (Figure 5-13). Upon comparison of complexes containing 70% PEG, 20% PC-4, and 10% TRI to the control 90% PEG and 10% TRI reveals a decrease over time in total radioactivity associated with the blood (Figure 5-13A). A formulation substituting TRI with Agal-TRI or omitting TRI (80% PEG and 20% PC-4) demonstrates a greater overall decrease of radioactivity in the blood when compared to the 70% PEG, 20% PC-4, and 10% TRI and the control formulation containing only PEG and TRI, suggesting formulations lacking TRI are susceptible to elimination. However, the BD results for formulations containing 70% PEG, 20% PC-4, and 10% TRI or Agal-TRI contradict the PK observation as the BD profiles for both formulations are nearly identical, with the liver as the primary organ of distribution, with minor percentages of the dose accumulating in the spleen and stomach (Figure 5-13B and 5-13D). Replotting the time course of liver accumulation reveals maximal accumulation (60% of dose) occurring by 15 min for both TRI and Agal-TRI formulations and decreases steadily until

it reaches nearly 20% of dose by 2 hrs (Figure 5-13C). With exception of a 30% reduction of PC-4 based formulations present in the liver (Figure 5-13C), the results are very similar to those produced with melittin based formulations (Figure 5-12C). An intriguing observation is revealed when comparing PK and BD data (Figure 5-12 and 5-13) to the in vivo gene delivery data (Figure 5-8 and 5-9); the melittin system delivers more plasmid to the liver, though is incapable of producing detectable luciferase activity, conversely a PC-4 system generates detectible luciferase activity by BLI with 30% less pGL3 in the liver. Further investigation is needed to demonstrate whether both melittin and PC-4 formulations are equally stable within the circulation.

## Discussion

There is a tremendous need for a multi-component non-viral gene delivery system capable of delivering plasmid DNA to specific cells and tissues in an efficient manner that is efficacious and cost effective. Polyacridine peptide based systems hold potential to fulfill this need. In this chapter, we have developed a delivery system composed of multiple components, all designed with a specific purpose in an effort to generate in vivo gene expression following a low volume dose administered through i.v. tail vein injection. To overcome delivery barriers presented by systemic circulation, PEGylated polyacridine peptides were synthesized to provide stability and protection from DNases and undesirable non-specific interactions with blood components (Table 5-3). To achieve cell specific targeting, polyacridine peptides were functionalized with a triantennary N-glycan (Table 5-3) targeting the ASGP-R located on hepatocytes to exploit the receptor's internalizing nature. Once the polyplex has gained access to the endosome, an exit strategy must be employed to prevent endosomal maturation and subsequent degradation of delivery vehicle and plasmid within the lysosome. To address the very significant barrier of endosomal escape, several polyacridine peptides were synthesized to incorporate fusogenic peptides such as melittin, PC-4, and JTS-1 (Table 5-1 and 5-2). An

alternative endosomal escape mechanism based on endosomal buffering was explored as well, resulting in the synthesis of (Acr-His)$_6$-Cys to serve as a platform to generate shielding and targeting analogues.

All polyacridine peptides were designed based upon the (Acr-Lys)$_6$-Cys platform that was identified as an optimizable lead gene delivery peptide in Chapter 4. The PEGylated peptide synthesized in this study was a reducible analogue resulting in (Acr-Lys)$_6$-SS-PEG as several in vitro studies have suggested reductive release is important for activity. A PEGylated endosomal buffering polyacridine peptide was synthesized based on the (Acr-Lys)$_6$-Cys design, with substitution of the spacing amino acid for histidine, resulting in the (Acr-His)$_6$-SS-PEG analogue. Both PEGylated polyacridine peptides were obtained in excellent yield (55 to 62%) after preparatory HPLC (Table 5-3).

Targeting peptides based upon (Acr-Lys)$_6$-Cys and (Acr-His)$_6$-Cys were synthesized as well with varying yields, where (Acr-Lys)$_6$-Cys-TRI was obtained in 47% yield and (Acr-His)$_6$-Cys-TRI was obtained at 13.52% yield, due to solubility issues of (Acr-His)$_6$-Cys at the reaction pH of 8.0 in 100 mM Tris buffer (Table 5-3). The targeting control glycopeptide (Acr-Lys)$_6$-Cys-Agal-TRI was obtained in excellent yield of 87% after removal of terminal galactose residues from (Acr-Lys)$_6$-Cys-TRI by β-galactosidase following preparatory HPLC (Table 5-3).

Polyacridine-fusogenic peptides were synthesized through directed disulfide formation or non-reducible thiol ether formation afforded by N-terminus functionalization of fusogenic peptides with a thiolpyridine protected cysteine or with Mal-Gly-OH as previously established in Chapters 2 and 3. Yields of polyacridine-fusogenic peptides containing analogues of melittin, PC-4, or JTS-1 were generally acceptable, ranging from 19% to 52.43%, with the exception of (Acr-Lys)$_6$-SS-NLS-QL-melittin isolated in only 3.6% yield (Table 5-2). The reduced yields may be attributed to a non-reactive thiolpyridine protected cysteine and due to limited solubility of TP-Cys-NLS-QL-melittin in the reaction solvent.

$(Acr\text{-}Lys)_6$-Cys peptides functionalized with PEG, TRI, or fusogenic peptides were confirmed to bind to plasmid DNA by a thiazole orange exclusion assay. Binding affinities were observed to be nearly equivalent for peptides containing PEG, TRI, or fusogenic peptide, an important quality to prevent over incorporation of one component within the polyplex at the sacrifice of other components (Figure 5-3). To overcome the natural repulsion of anionic JTS-1 for DNA, JTS-1 was functionalized with $(Acr\text{-}Lys)_{6\text{-}8}$-Cys as an earlier analogue $(Acr\text{-}Arg)_4$-SS-JTS-1 demonstrated poor binding affinity for DNA (Figure 5-3C). Not surprisingly, the $(Acr\text{-}Lys)_6$-SS-JTS-1 demonstrated slightly weaker binding affinity than $(Acr\text{-}Lys)_6$-SS-PC-4 or melittin, where the $(Acr\text{-}Lys)_8$-SS-JTS-1 demonstrated equivalent affinity, signifying the effect of additional Acr-Lys subunits on the binding affinity and neutralization of JTS-1's overall anionic character (Figure 5-3B and C). More importantly, the improved binding affinity of the JTS-1 analogues allowed for the inclusion and in vivo testing of anionic fusogens within a multi-component complex. Endosomal buffering peptides $(Acr\text{-}His)_6$-SS-PEG and $(Acr\text{-}His)_6$-Cys-TRI demonstrated somewhat stronger binding affinity for pGL3 versus their $(Acr\text{-}Lys)_6$-Cys based counterparts (Figure 5-3A).

Polyacridine melittin and PC-4 analogues were assessed for endosomal escape activity with an in vitro gene transfer assay involving CHO cells. $(Acr\text{-}Lys)_6$-SS-K-melittin demonstrated a 1000-fold higher activity versus the non-reducible $(Acr\text{-}Lys)_6$-Mal-K-melittin analogue (Figure 5-4). Conversely, $(Acr\text{-}Lys)_6$-SS-PC-4 and $(Acr\text{-}Lys)_6$-Mal-PC-4 demonstrated gene transfer activity comparable to the control pGL3-$WK_{18}$ polyplexes, suggesting the mechanism of action is not dependent upon disulfide reduction. Alternatively, due to low transfection levels, PC-4 may function as a very weak fusogen upon comparison to transfection levels produced by $(Acr\text{-}Lys)_6$-SS-K-melittin. However the neutrally charged nature of PC-4 is beneficial when considering a potential reduction of undesirable protein interaction found within the systemic circulation. In regards to NLS-fusogen chimeras and co-incorporation of $(Acr\text{-}Lys)_6$-Mal-

NLS within the formulation with $(Acr\text{-}Lys)_6$-PC-4 or $(Acr\text{-}Lys)_6$-K-melittin, no appreciable improvement of gene transfer was observed, perhaps due to the reported size of the nuclear pore complex and size of pores formed by melittin insertion in membranes versus the size of a typical nanoparticle (Figure 5-4).

To ensure incorporation of multiple components within a polyplex, the spin assay was developed based upon the size exclusion separation of components bound to pGL3 and those free in solution. The assay demonstrates successful incorporation of multiple components within a polyplex with limitation of the fusogen input ratio being maximally 20% without sacrificing amounts of PEG and TRI incorporated (Table 5-4 and 5-5). Upon inclusion of an NLS sequence at the N or C-terminus for PC-4 or the N-terminus for melittin, the output ratio improves to an almost quantitative incorporation of all components involving the NLS-PC4 based system and a 12% increased PEG incorporation with NLS-melittin. The results suggest polyacridine-NLS-fusogen chimeras are much more amendable to a multi-component complex formulation versus their non-NLS containing counterparts (Table 5-4 and 5-5).

AFM was conducted on complexes containing 100% PEG, 90% PEG and 10% TRI, 70% PEG, 20% PC-4 or melittin and 10% TRI (Figure 5-6). The attachment of all formulations to the anionic surface of mica demonstrates the presence of cationic polyplexes. The resulting morphologies are of interest as well, ranging from loosely coiled polyplexes (100% PEG and 90% PEG, 10% TRI) to traditional polyplexes formed upon addition of 20% PC-4 or melittin. Unfortunately, the in vivo biological activity of multi-component polyplexes cannot be correlated to sizes and morphologies observed with AFM as demonstrated for PC-4 (Figure 5-8) and melittin (Figure 5-9) based formulations.

The in vivo gene transfer of polyplexes formed with multi-component complexes at 1 μg demonstrated an overall inefficiency for melittin and PC-4 systems (Figure 5-7). To overcome this inefficiency and to conduct SAR based upon gene expression,

individual dosing levels were escalated to 25 μg to generate luciferase expression detectable by BLI. Expression levels generated based upon a PC-4 system produced low level gene expression that was ultimately observed to be independent of NLS effect, targeting, or fusogenic effect (Figure 5-8). Attempts to increase the amount of targeting ligand resulted in a loss of detectible luciferase expression, suggesting a fine line exists in regards to polyplex PEGylation patterns. Multi-component complexes based upon melittin did not generate a detectible BLI response (Figure 5-9), which is surprising considering the level of gene expression observed in an in vitro system. The results suggest DNA degradation or undesirable melittin-serum protein interactions may be preventing the delivery of transfection competent DNA to the liver. The overall cause may be due to the cationic nature of melittin as the biodistribution studies suggest the majority of dose reaches the liver within 15 min after administration (Figure 5-12C). Further evidence suggesting melittin's incompatibility in vivo is demonstrated upon addition of melittin to a PC-4 formulation, resulting in a loss of detectable gene expression (Figure 5-9).

While cationic fusogens appear to be incompatible with multi-component delivery of plasmid DNA, complexes formulated with the anionic fusogen JTS-1 conjugated to either $(Acr\text{-}Lys)_{6\text{ or }8}$-Cys also fail to promote detectible luciferase expression in vivo (Figure 5-10). This phenomenon may be explained through ionic interactions between JTS-1's glutamic acid residues and polyacridine anchor of TRI and PEG components. This ionic interaction interrupts polyplex incorporation and leads to an increased plasmid susceptibility to premature degradation within the blood. Further PK and BD analysis is needed to confirm this hypothesis.

Formulations dosed with the endosomal buffering peptides $(Acr\text{-}His)_6$-SS-PEG and $(Acr\text{-}His)_6$-Cys-TRI failed to produce detectible luciferase expression as measured with BLI at dosing levels of 1, 5, and 25 μg of pGL3 (Figure 5-11). These results demonstrate the importance of the $(Acr\text{-}Lys)_6$-Cys peptide to future optimization studies

of polyacridine based gene delivery systems. Interestingly enough, formulations polyplexed with $(Acr\text{-}His)_6$-SS-PEG are capable of producing stimulated gene expression comparable to $(Acr\text{-}Lys)_6$-Cys-Mal-PEG at a dwell time of 15 min, suggesting a possible utility for $(Acr\text{-}His)_6$-Cys in these types of gene delivery systems (Figure 5-11).

We have described the first generation of multi-component complexes based upon the $(Acr\text{-}Lys)_6$-Cys or $(Acr\text{-}His)_6$-Cys DNA binding scaffold. The low level in vivo gene expression produced by these non-stimulated systems is approximately 2-fold more efficient (relative to DNA dose) than a recently reported study utilizing a non-stimulated cationic polymer based system (*171*). While a fusogenic effect was not observed, some parameters were discovered in regards to the fusogenic peptide charge character that is allowed. Neither cationic nor anionic fusogens permitted detectable gene expression, where analogues based upon the charge neutral PC-4 fusogen did mediate a BLI response. Furthermore, inclusion of an NLS sequence to generate an NLS-fusogen chimera did not result in increased gene transfer efficiency, exposing a fundamental flaw in the hypothesis involving NLS mediated delivery of nucleic acids to the nucleus; a 100 nm diameter nanoparticle will not easily translocate through the reported 9 nm diameter nuclear pore complex (*94*). In addition to this, the reported 3-5 nm diameter pore formed by melittin cannot mediate transient translocation of plasmid DNA through an NLS-melittin induced pore on the nuclear envelope even if the peptide operated as initially designed (*86-88*). These observations demonstrate the importance of keeping biophysical parameters and limitations in mind when designing biologically active compounds.

In conclusion, we have tested several systems incorporating various endosomal escape mechanisms. While a detectible BLI response was observed with some systems with 25 μg of pGL3, the efficiency is much below that of a 1 μg direct HD dose of pGL3, suggesting the multi-component complex systems is still missing needed components. It has been proposed that many viruses contain enzymes capable of phospholipase-like activity, and it is this phospholipase activity that is responsible for endosomal escape and

robust viral infectivity (*172-174*). While this may boost endosomal escape, it still leaves the fundamental issue of translocation of genetic material to the nucleus. It is conceivable that the means of overcoming the nuclear localization barrier have yet to be discovered. While it may be difficult to observe whether an endosomal escape mechanism is functioning in vivo, it is conceivable to assess the fusogenic activity of melittin, JTS-1, or PC-4 through in vivo silencing RNA (siRNA) delivery as the interfering RNA mechanism is not dependant upon entering the nucleus.

# CHAPTER 6
# RESEARCH SUMMARY

Non-viral gene therapy has made several advances in recent years. However, several barriers must be overcome to generate vectors capable of rivaling viral gene transfer efficiencies before transitioning into clinical applications. The field of peptide mediated non-viral gene therapy offers an excellent opportunity to incorporate a variety of biologically active compounds capable of overcoming the barriers to efficient gene transfer in vivo (Figure 1-1).

One barrier of interest to my thesis project is the integration of fusogenic peptides to enhance endosomal escape and limit lysosomal degradation of gene delivery vectors. Previous efforts have demonstrated the importance of the inclusion of endosomal escape components by either chemically modifying the gene delivery vector with fusogenic peptide or transformation of the fusogenic peptide into a non-viral delivery vehicle (*31, 46-48, 50-52, 71, 73, 125*). Previous work in our lab by Chen and co-workers demonstrated the utility of a polymeric melittin system in an in vitro gene transfer model (*42*) and was able to integrate melittin into a targeted PEGylated glycoprotein disulfide crosslinked vector (*26*). Unfortunately, these efforts did not produce detectable transgene expression in vivo using BLI. However, expression was observed for these formulations after a 5 min delay and subsequent blank HD dose, producing a relatively weak BLI response independent of melittin concentration. The hypotheses regarding the failure of PEGylated glycoprotein vectors to produce non-stimulated gene expression after i.v. tail vein injection are numerous. However, the primary failure may rest in the utilization of a polylysine scaffold on which the PEGylated and targeting glycopeptides were engineered. The deficiencies regarding the use of polylysine or cationic polymer are well documented regarding their use to deliver nucleic acids in vivo (*43, 44*), which

necessitated the development of a novel non-viral delivery vehicle that relies on an alternative to ionic interaction between vehicle and DNA.

Szoka was among the first to utilize the intercalative properties of acridine as an alternative to cationic polymers with the synthesis of trigalactosyl-bisacridine compound (Figure 1-3) used to specifically deliver plasmid DNA in cell culture to hepatocytes targeting the ASGP-R (*123*). Unfortunately, transgene expression was not increased due to formulation with trigalactosyl-bisacridine. Nielsen and Vierling attempted to demonstrate an increase in transgene expression with NLS conjugates containing 1 (Figure 1-4), 2, or 3 acridines (Figure 1-5), only to produce biological data that contradicted each other's reports (*10, 11*). Recently, the group led by Vinogradov has demonstrated promising in vitro results with a tri-acridine-PEG-NLS construct (Figure 1-6) when used in combination with a variety of cationic condensing reagents (*7-9*). Upon observing the complexity of the compounds used in the previous studies, it is understandable why many investigators were not eager to develop their acridine conjugates further, considering the meager increases in biological results. Additionally, it is clear that other than Szoka, the potential utility of acridine to bind reversibly and deliver nucleic acids was not fully realized in the context that intercalation was the primary mode of interaction between the carrier and nucleic acid.

The first goal of this thesis project was to demonstrate the basic proof of principle evidence regarding the appropriateness of developing polyacridine as a gene delivery vehicle. This was accomplished through the reducible or non-reducible attachment of melittin to a polyacridine peptide. The biophysical data demonstrates polyacridine-melittin is capable of binding to DNA through a thiazole orange assay (Figure 2-4). Furthermore, a reducible polyacridine-melittin produced gene transfer activity comparable to PEI-DNA polyplexes. Additionally, a 1000-fold difference in gene transfer efficiency between a non-reducibly and a reducibly linked melittin demonstrates the importance of linkage between polyacridine and melittin (Figure 2-6). Due to the

chemical complexity regarding the synthesis of polyacridine peptides and limited potential for SAR studies, an alternative approach to incorporate acridine was investigated.

A new generation of polyacridine peptides were synthesized by SPPS by adapting and modifying the methods to produce the Fmoc-Lys(Acr)-OH (Scheme 2-4) amino acid as reported by Chiu, Tung, and Ueyama, respectively (*120-122, 137, 138*). The SPPS approach to produce polyacridine peptides allowed us conduct SAR in regard to polyacridine peptide length, spacer identity, and nature of melittin linkage using an in vitro gene transfer assay as a positive readout. The in vitro gene transfer results found in Chapter 3 identified the ideal polyacridine chain length of 4 acridine moieties separated by arginine as the spacing amino acid, resulting in $(Acr\text{-}Arg)_4$-Cys. Optimal in vitro gene transfer was observed with $(Acr\text{-}Arg)_4$-SS-melittin which was nearly equivalent to PEI control and 100-1000 fold more potent than its' non-reducible counterpart $(Acr\text{-}Arg)_4$-Mal-melittin in three different cell lines (Figure 3-9). Interestingly, the importance of reducibility was observed for both $(Acr\text{-}Lys)_4$-SS-melittin and $(Acr\text{-}Leu)_4$-SS-melittin analogues in the three cell lines tested as well (Figure 3-9). The importance of polyacridine to gene transfer was confirmed by the synthesis of a control peptide in which acridine was substituted with an acetyl group on lysine's ε-amine, resulting in $(Lys(Ac)\text{-}Arg)_4$-SS-melittin peptide. This substitution of acetyl for acridine resulted in a 100-1000 fold decrease in gene transfer activity as compared to $(Acr\text{-}Arg)_4$-SS-melittin. Gene transfer with reducible polyacridine-melittin peptides containing Lys and Leu as spacing amino acids produced gene transfer levels 10-1000 fold lower than those containing Arg as the spacing amino acid (Figure 3-9).

The identification of $(Acr\text{-}Arg)_4$-Cys as the lead polyacridine peptide allowed for further study in vivo through functionalization with PEG and triantennary N-glycan to produce a multi-component complex with DNA (Figure 1-7). At a 5 μg dose of DNA polyplex, expression levels were not detectible by BLI after standard tail vein dose.

Following a 5 min delay after initial dose, a stimulatory HD dose was given. This resulted in similar expression levels that were observed by Chen and colleagues with the melittin formulation. However a 5 μg stimulated dose consisting of 90% $(Acr\text{-}Arg)_4$-Cys-Mal-PEG and 10% $(Acr\text{-}Arg)_4$-Cys-TRI produced a BLI response of $10^9$ photons/sec/ $cm^2$/sr (Figure 3-10), comparable to a direct 5 μg HD dose of pGL3 (*26, 142*).

This discovery permitted further synthesis and optimization of the polyacridine anchor peptide as PEGylated analogues using hydrodynamic stimulation as a tool to study this unique gene transfer system in vivo. Initial studies with $(Acr\text{-}Arg)_4$-PEG sought to investigate the importance of reducible or non-reducible linkage between PEG and polyacridine peptide. Unlike the polyacridine-melittin study, there was no dependence on level of stimulated expression versus a disulfide or maleimide linked PEG peptides (Figure 4-9A).

These initial studies also allowed us to investigate the maximum dwell time between initial dosing and hydrodynamic stimulation with $(Acr\text{-}Arg)_4$-Cys-Mal-PEG polyplexes. Figure 4-9B demonstrates that the ability to HD stimulate is lost after 30 minutes, which is later confirmed to be due to polyplex degradation (Figure 4-12, Panels A, B, and D). Studies relating to identity of the spacing amino acid revealed cationic residues are capable of producing stimulated expression, while PEGylated polyacridine peptide polyplexes containing the neutrally charged Leu and negatively charged Glu spacing amino acid produced background levels of expression (Figure 4-10A). Further optimization of the peptide to DNA ratio for $(Acr\text{-}Arg)_4$-Cys-Mal-PEG and $(Acr\text{-}Lys)_4$-Cys-Mal-PEG revealed slightly higher stimulated transfections efficiencies over a broader range of stoichiometries tested (Figure 4-10B), warranting an investigation of polyacridine chain length with Lys as the spacing amino acid. Figure 4-10C demonstrates nearly equivalent stimulated gene expression between polyplexes formulated with 0.8 nmol of $(Acr\text{-}Lys)_4$-Cys-Mal-PEG per μg DNA and 0.2 nmol of $(Acr\text{-}Lys)_6$-Cys-Mal-PEG per μg, while polyplexes formulated with 0.2 nmol of $(Acr\text{-}Lys)_8$-Cys-Mal-PEG per

μg demonstrate a subtle decrease in gene expression and $(Acr\text{-}Lys)_2$-Cys-Mal-PEG produced negligible expression.

$(Acr\text{-}Lys)_6$-Cys-Mal-PEG was then selected for further investigation regarding optimal peptide to DNA stoichiometry, where it demonstrated stable expression over a broad range of stoichiometries from 0.2 to 0.8 nmol peptide per μg DNA (Figure 4-11A). It was stimulatable with up to a 60 min dwell time and demonstrated a 100-fold decrease in gene expression after a delay of 120 min between formulation dose and HD stimulation (Figure 4-11B). Plasmid dose response also revealed a 1 μg dose of pGL3 polyplexed with $(Acr\text{-}Lys)_6$-Cys-Mal-PEG with 5 min delayed stimulation generates 5-fold higher gene expression versus HD pGL3 (Figure 4-11C).

In addition to $(Acr\text{-}Lys)_6$-Cys-Mal-PEG stimulatory transfection capabilities, this peptide demonstrated similar pharmacokinetic and biodistribution profiles upon comparison of $(Acr\text{-}Lys)_4$-Cys-Mal-PEG and superior properties as compared to naked DNA and $(Acr\text{-}Lys)_2$-Cys-Mal-PEG (Figure 4-12 A and B). $(Acr\text{-}Lys)_6$-Cys-Mal-PEG also demonstrated the ability to protect DNA in the blood for up two hours (Figure 4-12F) where naked DNA is almost immediately degraded (Figure 4-12A) and $(Acr\text{-}Lys)_2$-Cys-Mal-PEG offers minimal protection in the blood (Figure 4-12C). The results taken as a whole demonstrates the unique properties of $(Acr\text{-}Lys)_6$-Cys as a non-viral gene delivery vehicle and identified the peptide for further development for use in a targeted multi-component plasmid DNA delivery vectors.

The biological success of $(Acr\text{-}Lys)_6$-Cys necessitated a substantial synthetic improvement to isolate the peptide in high yield and purity when initial synthesis revealed a highly heterogeneous product when judged by RP-HPLC (Figure 4-2A). Upon optimization of the SPPS parameters, the crude $(Acr\text{-}Lys)_6$-Cys quality was much improved by incorporating triple coupling cycles for the spacing amino acid, substitution of the standard coupling agent HBTU with HATU, and preactivation of Fmoc-Lys(Acr)-

OH with HATU (Figure 4-2C). These optimization steps increased the final purified yield to 40% from an initial yield of 1.6% (Table 4-1 and 5-2).

The final chapter of my thesis project entails the synthesis of various polyacridine peptides based upon the $(Acr\text{-}Lys)_6$-Cys and related $(Acr\text{-}His)_6$-Cys scaffolds to address the barriers to efficient non-viral gene delivery in vivo (Table 5-1 and 5-3). These polyacridine peptides possessed endosomal escape agents (melittin, PC-4, or JTS-1), chimeric NLS-fusogen analogues, PEG peptides, and hepatocyte targeting ligands. The in vitro gene transfer potential of $(Acr\text{-}Lys)_6$-fusogen constructs were investigated in CHO cells to confirm activity. $(Acr\text{-}Lys)_6$-SS-K-melittin and $(Acr\text{-}Lys)_6$-SS-NLS-K-melittin mediated expression similar to PEI-DNA while PC-4 and NLS-PC-4 chimeras mediated expression levels similar to polyplexes formed with the control condensing peptide $WK_{18}$ (Figure 5-3). The apparent lack of fusogenic activity of PC-4 is surprising considering Peterson's report confirming early endosomal escape mediated by the peptide in CHO cells (*93*).

Multi-component polyplexes were formed with discrete amounts of PEG peptide, targeting ligand, and fusogenic peptide or NLS-fusogen chimera and the mol percent incorporated within a polyplex was quantified by spin assay after analysis by analytical RP-HPLC (Figure 5-5) to ensure incorporation of all components. The results reveal a considerable loss of targeting ligand and PEG peptide once fusogen input ratio is increased above 20% (Table 5-4 and 5-5).

Standard i.v. tail vein dosing of multi-component complexes with 1 μg of pGL3 with polyacridine-melittin or PC-4 resulted in undetectable luciferase expression as measured by BLI (Figure 5-7). Upon increasing the pGL3 dose to 25 μg, formulations including polyacridine PC-4 or NLS-PC-4 chimeras mediated a detectable BLI response as did formulations composed of 90% $(Acr\text{-}Lys)_6$-SS-PEG and 10% $(Acr\text{-}Lys)_6$-Cys-TRI, or 100% $(Acr\text{-}Lys)_6$-SS-PEG (Figure 5-7). The results demonstrate a non-specific gene expression phenomenon independent of polyacridine-PC-4 linkage (reducible versus non

reducible), inclusion and placement of NLS within the PC-4 sequence (N versus C-terminus), nuclear localization (NLS versus control NLS) and hepatocyte targeting ligand (TRI versus Agal-TRI). While the luciferase expression is not as efficient as a direct 1 μg HD dose of pGL3, it does represent a step forward in the development of a first generation polyacridine gene delivery system capable of producing detectable gene transfer by BLI.

In a recent report by Harris and co-workers, the BLI response mediated by a cationic polymer polyplexes ion paired with an anionic peptide maximally mediated $10^7$ photons/sec/cm$^2$/sr with a 50 μg dose of pCMV-LUC polyplexes and uncoated cationic polyplexes produced approximately $10^6$ photons/sec/cm$^2$/sr (*171*). Comparison of our in vivo gene transfer result with 25 μg of pGL3 polyplexed with 90% PEG and 10% TRI to the uncoated polymer result at a 50 μg pCMV-LUC dose. This result reveals almost a 2-fold increase in delivery efficiency based on plasmid dose for the polyacridine multi-component system. Furthermore, the result of the anionic peptide coated formulation suggests the importance of producing anionically charged polyplexes (*171*). This observation is exemplified with the in vivo gene transfer results of multi-component complexes formulated with the cationic fusogen melittin, which all formations failed to produce a detectable BLI response (Figure 5-9). Interestingly enough, polyplexes formed with an NLS-PC-4 analogue in combination with melittin resulted in the loss of detectible expression, negating the expression levels observed with many of the PC-4 formulations (Figure 5-8). This result suggests a negative correlation between polyplex cationic charge in regards to promoting gene transfer, perhaps due to undesirable aggregation within the blood, leading premature plasmid degradation (*44, 124, 171*). The active shielding of polyacridine polyplexes with an anionic peptide represents a unique opportunity to further mask any residual cationic charge and perhaps increase gene transfer efficiency.

The negative results observed with multi-component complexes formed with melittin prompted the investigation of polyplexes incorporating the anionic fusogen JTS-

1. Surprisingly, 25 μg pGL3 formulations dosed with 20% $(Acr\text{-}Lys)_6$-SS-JTS-1 or $(Acr\text{-}Lys)_8$-SS-JTS-1 could not mediate detectable luciferase expression (Figure 5-10) even though polyacridine-JTS-1 peptides were capable of binding DNA with nearly equivalent affinity as compared to PEG and TRI components (Figure 5-3). JTS-1's inability to promote non-stimulated expression may be rationalized by an undesirable ionic interaction created between glutamic acid residues with the polyacridine anchor of PEG and TRI during formulation. This phenomenon weakens the binding affinity of polyacridine PEG and TRI for DNA, which subsequently leads to premature polyplex disruption and DNA degradation. Due to JTS-1's high propensity to be non-specifically bound to plastics and filter membranes, the spin assay cannot be utilized to diagnose or test this hypothesis.

Non-stimulated dosing of polyplexes formed with the endosomal buffering peptide $(Acr\text{-}His)_6$-SS-PEG with or without $(Acr\text{-}His)_6$-Cys-TRI also failed to promote detectible luciferase expression at 1, 5, and 25 μg of pGL3 (Figure 5-11). However, a formulation consisting of 100% $(Acr\text{-}His)_6$-SS-PEG produced similar stimulated expression as compared to the expression produced by $(Acr\text{-}Lys)_6$-Mal-PEG, demonstrating potential utility of $(Acr\text{-}His)_6$-Cys in a stimulatable gene transfer system (Figure 5-10).

In summary, this thesis project involved the development and synthesis of novel polyacridine gene delivery peptides in an effort to strengthen the DNA-vector interaction and improve upon the deficiencies offered by purely cationic gene delivery systems. Furthermore, the hypothesis focuses on the targeted delivery of polyplexes containing multiple components in efforts to circumvent the various barriers to efficient non-stimulated in vivo gene delivery to the liver. Through these efforts, we have indentified the polyacridine peptide $(Acr\text{-}Lys)_6$-Cys as the ideal candidate on which to base future gene delivery systems upon. Furthermore, $(Acr\text{-}Lys)_6$-PEG and $(Acr\text{-}Lys)_6$-Cys-TRI are demonstrating potential utility as hepatocyte targeted siRNA delivery agents in vivo.

Additionally, other polyacridine analogues such as $(Acr\text{-}His)_6$-Cys may have potential use in gene transfer systems stimulated by physical methods as well (hydrodynamic dosing and electroporation).

To overcome the barriers that limit robust and target specific gene expression in vivo will require novel approaches and development of synthetically challenging and intricate bioconjugates. One approach could be the integration of phospholipase enzymes capable of degrading cellular membranes as an alternative endosomal escape mechanism to using fusogenic peptides or endosomal buffering agents (*172, 174, 175*). Furthermore, transgenic modification of a phospholipase enzyme to include an NLS moiety could result in the permeablization of the nuclear envelope to allow free passage of plasmid DNA through a reported pore of 10 μm (*176*). However, one must be cautious when integrating enzymes or viral proteins into a non-viral system as there is potential to illicit an immune response and limit the therapeutic potential due to the same issues that plague viral gene therapy.

Another possible strategy to increase gene transfer in vivo regards the incorporation of anionic moieties within the polyplex in an effort to actively shield or neutralize the overall positive charge and increase blood compatibility (*171*). Possible strategies to incorporate polyanions within the nanoparticle includes synthesis of poly-glutamic or aspartic acid containing peptides ligated to polyacridine or as separate entities used to coat the nanoparticle and impart an overall negative charge. Furthermore, to increase the polyplex binding strength of the polyanionic peptide, analogues could be synthesized with terminal cysteine residues to generate template driven polymers. An added benefit of incorporating polyanions within the polyplex involves the possibility of producing an endosomal buffering effect due to the pKa properties of the glutamic and aspartic acid side chains. Furthermore, successful incorporation of anionic endosomal buffering entities will not increase the nanoparticles overall positive charge, which is a common concern for polymers such as PEI or polyhistidine peptide systems.

To increase a non-viral vector's probability of producing potent gene expression in vivo without physical stimulation necessitates the development of systems incorporating components attempting to circumvent the multitude of delivery barriers preventing efficient gene transfer. Furthermore, production of successful gene delivery vectors must incorporate novel and perhaps unconventional methods of enhancing nanoparticle endosomal escape and nuclear localization, perhaps the more elusive barriers to overcome. Regardless of strategy, polyacridine peptides hold great therapeutic potential due to their modular design and unique nucleic acid binding properties to produce DNA delivery vehicles capable of mediating efficient gene transfer in vivo.

# REFERENCES


(1) Glover, D. J., Lipps, H. J., and Jans, D. A. (2005) Towards safe, non-viral therapeutic gene expression in humans. *Nat Rev Genet 6*, 299-310.

(2) Jackson, D. A., Juranek, S., and Lipps, H. J. (2006) Designing Nonviral Vectors for Efficient Gene Transfer and Long-Term Gene Expression. *Mol Ther 14*, 613-26.

(3) Wolff, J. A., and Rozema, D. B. (2008) Breaking the bonds: non-viral vectors become chemically dynamic. *Mol Ther 16*, 8-15.

(4) Grigsby, C. L., and Leong, K. W. Balancing protection and release of DNA: tools to address a bottleneck of non-viral gene delivery. *J R Soc Interface 7 Suppl 1*, S67-82.

(5) Bostanci, A. (2002) Gene therapy. Blood test flags agent in death of Penn subject. *Science 295*, 604-5.

(6) Kaiser, J. (2007) Clinical research. Death prompts a review of gene therapy vector. *Science 317*, 580.

(7) Zhang, H., Mitin, A., and Vinogradov, S. V. (2009) Efficient transfection of blood-brain barrier endothelial cells by lipoplexes and polyplexes in the presence of nuclear targeting NLS-PEG-acridine conjugates. *Bioconjug Chem 20*, 120-8.

(8) Vinogradov, S. V., Zhang, H., Mitin, A., and Warren, G. (2008) Intercalating Conjugates of Peg with Nuclear Localization Signal (Nls) Peptide. *Polymer Prepr 49*, 434-435.

(9) Zhang, H., and Vinogradov, S. V. (2010) Short biodegradable polyamines for gene delivery and transfection of brain capillary endothelial cells. *J Control Release 143*, 359-66.

(10) Shiraishi, T., Hamzavi, R., and Nielsen, P. E. (2005) Targeted Delivery of Plasmid DNA into the Nucleus of Cells via Nuclear Localization Signal Peptide Conjugated to DNA Intercalating Bis- and Trisacridines *Bioconjugate Chemistry 16*, 1112-1116.

(11) Boulanger, C., Di Giorgio, C., and Vierling, P. (2005) Synthesis of acridine-nuclear localization signal (NLS) conjugates and evaluation of their impact on lipoplex and polyplex-based transfection. *Eur J Med Chem 40*, 1295-306.

(12) Mahato, R. I. (1999) Non-viral peptide-based approaches to gene delivery. *Journal of Drug Targeting 7*, 249-268.

(13) Zanta, M. A., Belguise-Valladier, P., and Behr, J. P. (1999) Gene delivery: A single nuclear localization signal peptide is sufficient to carry DNA to the cell nucleus. *Proc. Natl. Acad. Sci. 96*, 91-96.

(14) Miller, A. M., and Dean, D. A. (2009) Tissue-specific and transcription factor-mediated nuclear entry of DNA. *Adv Drug Deliv Rev 61*, 603-13.

(15) Grigsby, C. L., and Leong, K. W. (2010) Balancing protection and release of DNA: tools to address a bottleneck of non-viral gene delivery. *J R Soc Interface 7 Suppl 1*, S67-82.

(16) Martin, M. E., and Rice, K. G. (2008) A Novel Class of Intrinsic Proteasome Inhibitory Gene Transfer Peptides. *Bioconjugate Chemistry 19*, 370-376.

(17) Martin, M. E., and Rice, K. G. (2007) Peptide-Guided Gene Delivery. *The AAPS Journal 9*, E18-E29.

(18) Kim, J., Chen, C.-P., and Rice, K. G. (2005) The proteasome metabolizes peptide-mediated nonviral gene delivery systems. *Gene Therapy 12*, 1581-1590.

(19) Wu, G. Y., and Wu, C. H. (1987) Receptor-mediated in vitro gene transformation by a soluble DNA carrier system [published erratum appears in J Biol Chem 1988 Jan 5;263(1):588]. *Journal of Biological Chemistry 262*, 4429-32.

(20) Wu, G. Y., and Wu, C. H. (1988) Evidence for Targeted Gene Delivery to Hep G2 Hepatoma Cells in Vitro. *Biochemistry 27*, 887-892.

(21) Wu, G. Y., and Wu, C. H. (1988) Receptor-mediated Gene Delivery and Expression In Vivo. *J. Biol. Chem. 263*, 14621-14624.

(22) Wadhwa, M. S., Collard, W. T., Adami, R. C., McKenzie, D. L., and Rice, K. G. (1997) Peptide-mediated gene delivery: influence of peptide structure on gene expression. *Bioconjugate Chemistry 8*, 81-8.

(23) Tang, M. X., and Szoka, F. C. (1997) The influence of polymer structure on the interactions of cationic polymers with DNA and morphology of the resulting complexes. *Gene Therapy 4*, 823-832.

(24) Tiera, M. J., Winnik, F. O., and Fernandes, J. C. (2006) Synthetic and natural polycations for gene therapy: state of the art and new perspectives. *Currernt Gene Therapy 6*, 59-71.

(25) El-Aneed, A. (2004) An overview of current delivery systems in cancer gene therapy. *Journal of Controlled Release 94*, 1-14.

(26) Chen, C. p., Kim, J. s., Liu, D., Rettig, G. R., McAnuff, M. A., Martin, M. E., and Rice, K. G. (2007) Synthetic PEGylated Glycoproteins and Their Utility in Gene Delivery. *Bioconjugate Chemistry 18*, 371-378.

(27) Haines, A. M., Irvine, A. S., Mountain, A., Charlesworth, J., Farrow, N. A., Husain, R. D., Hyde, H., Ketteringham, H., McDermott, R. H., Mulcahy, A. F., Mustoe, T. L., Reid, S. C., Rouquette, M., Shaw, J. C., Thatcher, D. R., Welsh, J. H., Williams, D. E., Zauner, W., and Phillips, R. O. (2001) CL22 - a novel cationic peptide for efficient transfection of mammalian cells. *Gene Therapy 8*, 99-110.

(28) Chan, W. C., and White, P. D. (2000) *Fmoc solid phase peptide synthesis : a practical approach*, Oxford University Press, Oxford ; New York.

(29) McKenzie, D. L., Collard, W. T., and Rice, K. G. (1999) Comparative gene transfer efficiency of low molecular weight polylysine DNA-condensing peptides. *Journal of Peptide Research 54*, 311-8.

(30) Adami, R. C., Collard, W. T., Gupta, S. A., Kwok, K. Y., Bonadio, J., and Rice, K. G. (1998) Stability of Peptide-Condensed Plasmid DNA Formulations. *Journal of Pharmaceutical Sciences 87*, 678-683.

(31) Gottschalk, S., Sparrow, J. T., Hauer, J., Mims, M. P., Leland, F. E., Woo, S. L. C., and Smith, L. C. (1996) A novel DNA-peptide complex for efficient gene transfer and expression in mammalian cells. *Gene Therapy 3*, 448-457.

(32) Adami, R. C., and Rice, K. G. (1999) Metabolic stability of glutaraldehyde cross-linked peptide DNA condensates. *Journal of Pharmaceutical Sciences 88*, 739-746.

(33) McKenzie, D. L., Kwok, K. Y., and Rice, K. G. (2000) A potent new class of reductively activated peptide gene delivery agents. *Journal of Biological Chemistry 275*, 9970-9977.

(34) McKenzie, D., Smiley, B., Kwok, K. Y., and Rice, K. G. (2000) Low molecular weight disulfide cross-linking peptides as nonviral gene delivery carriers. *Bioconjugate Chemistry 11*, 901-909.

(35) Kwok, K. Y., McKenzie, D. L., Evers, D. L., and Rice, K. G. (1999) Formulation of highly soluble poly(ethylene glycol)-peptide DNA condensates. *Journal of Pharmaceutical Sciences 88*, 996-1003.

(36) Collard, W. T., Yang, Y., Kwok, K. Y., Park, Y., and Rice, K. G. (2000) Biodistribution, metabolism, and *in vivo* gene expression of low molecular weight glycopeptide polyethylene glycol peptide DNA co-condensates. *Journal of Pharmaceutical Sciences 89*, 499-512.

(37) Yang, Y., Man, S., Park, Y., and Rice, K. G. (2001) Biodistribution, cellular localization and in vivo gene expression of mannose glycopeptide polyethylene glycol peptide DNA co-condensates. *J. Biol. Chem.*, in preparation.

(38) Chiu, M. H., Tamura, T., Wadhwa, M. S., and Rice, K. G. (1994) In vivo targeting function of N-linked oligosaccharides with terminating galactose and N-acetylgalactosamine residues. *J. Biol. Chem. 269*, 16195-16202.

(39) Yang, Y., Park, Y., Man, S., Liu, Y., and Rice, K. G. (2001) Cross-linked low molecular weight glycopeptide-mediated gene delivery: relationship between DNA metabolic stability and the level of transient gene expression in vivo. *J Pharm Sci 90*, 2010-22.

(40) Park, Y., Kwok, K. Y., Boukarim, C., and Rice, K. G. (2002) Synthesis of Sulfhydryl Crosslinking Poly (ethylene glycol) Peptides and Glycopeptides as Carriers for Gene Delivery. *Bioconjugate Chemistry 13*, 232-239.

(41) Kwok, K. Y., Park, Y., Yongsheng, Y., McKenzie, D.L., Rice, K.G. (2003) In Vivo Gene Transfer using Sulfhydryl Crosslinked PEG-peptide/Glycopeptide DNA Co-Condensates. *J Pharm Sci 92*, 1174-1185.

(42) Chen, C.-P., Kim, J.-s., Steenblock, E., Liu, D., and Rice, K. G. (2006) Gene transfer with poly-melittin peptides. *Bioconjugate Chemistry 17*, 1057-62.

(43) Burke, R. S., and Pun, S. H. (2008) Extracellular barriers to in Vivo PEI and PEGylated PEI polyplex-mediated gene delivery to the liver. *Bioconjug Chem 19*, 693-704.

(44) Dash, P. R., Read, M. L., Barrett, L. B., Wolfert, M. A., and Seymour, L. W. (1999) Factors affecting blood clearance and in vivo distribution of polyelectrolyte complexes for gene delivery. *Gene Therapy 6*, 643-650.

(45) Gupta, B., Levchenko, T. S., and Torchilin, V. P. (2005) Intracellular delivery of large molecules and small particles by cell-penetrating proteins and peptides. *Adv Drug Deliv Rev 57*, 637-51.

(46) Ogris, M., Carlisle, R. C., Bettinger, T., and Seymour, L. W. (2001) Melittin Enables Efficient Vesicular Escape and Enhanced Nuclear Access of Nonviral Gene Delivery Vectors. *Journal of Biological Chemistry 276*, 47550-47555.

(47) Boeckle, S., Wagner, E., and Ogris, M. (2005) C-Versus N-terminally Linked Melittin-Polyethylenimine Conjugates: The Site of Linkage Strongly Influences Activity of DNA Polyplexes. *J. Gene Medicine 7*, 1335-1347.

(48) Boeckle, S., Fahrmeir, J., Roedl, W., Ogris, M., and Wagner, E. (2006) Melittin analogs with high lytic activity at endosomal pH enhance transfection with purified targeted PEI polyplexes. *J Control Release 112*, 240-8.

(49) Walker, G. F., Fella, C., Pelisek, J., Fahrmeir, J., Boeckle, S., Ogris, M., and Wagner, E. (2005) Toward synthetic viruses: endosomal pH-triggered deshielding of targeted polyplexes greatly enhances gene transfer in vitro and in vivo. *Mol Ther 11*, 418-25.

(50) Parente, R. A., Nadasdi, L., Subbarao, N. K., and Szoka, F. C., Jr. (1990) Association of a pH-sensitive peptide with membrane vesicles: role of amino acid sequence. *Biochemistry 29*, 8713-9.

(51) Parente, R. A., Nir, S., and Szoka, F. C., Jr. (1990) Mechanism of leakage of phospholipid vesicle contents induced by the peptide GALA. *Biochemistry 29*, 8720-8.

(52) Wyman, T. B., Nicol, F., Zelphati, O., Scaria, P. V., Plank, C., and Szoka, F. C. (1997) Design, synthesis and characterization of a cationic peptide that binds to nucleic acids and permeabilizes bilayers. *Biochemistry 36*, 3008-3017.

(53) Lochmann, D., Jauk, E., and Zimmer, A. (2004) Drug delivery of oligonucleotides by peptides. *European Journal of Pharmaceutics & Biopharmaceutics 58*, 237-51.

(54) Boussif, O., Lezoualc'h, F., Zanta, M. A., Mergny, M. D., Scherman, D., Demeneix, B., and Behr, J. P. (1995) A versatile vector for gene and oligonucleotide transfer into cells in culture and in vivo: polyethylenimine. *Proceedings of the National Academy of Sciences of the United States of America 92*, 7297-301.

(55) Thomas, M., and Klibanov, A. M. (2002) Enhancing polyethylenimine's delivery of plasmid DNA into mammalian cells. *Proc Natl Acad Sci U S A 99*, 14640-5.

(56) Douglas, K. L. (2008) Toward development of artificial viruses for gene therapy: a comparative evaluation of viral and non-viral transfection. *Biotechnol Prog 24*, 871-83.

(57) Pichon, C., Goncalves, C., and Midoux, P. (2001) Histidine-rich peptides and polymers for nucleic acids delivery. *Adv Drug Deliv Rev 53*, 75-94.

(58) Pichon, C., Roufai, M. B., Monsigny, M., and Midoux, P. (2000) Histidylated oligolysines increase the transmembrane passage and the biological activity of antisense oligonucleotides. *Nucleic Acids Res 28*, 504-12.

(59) Midoux, P., Kichler, A., Boutin, V., Maurizot, J. C., and Monsigny, M. (1998) Membrane permeabilization and efficient gene transfer by a peptide containing several histidines. *Bioconjugate Chem. 9*, 260-267.

(60) Midoux, P., and Monsigny, M. (1999) Efficient gene transfer by histidylated polylysine/pDNA complexes. *Bioconjugate Chemistry 10*, 406-11.

(61) Midoux, P., LeCam, E., Coulaud, D., Delain, E., and Pichon, C. (2002) Histidine containing peptides and polypeptides as nucleic acid vectors. *Somat Cell Mol Genet 27*, 27-47.

(62) Kichler, A., Leborgne, C., Marz, J., Danos, O., and Bechinger, B. (2003) Histidine-rich amphipathic peptide antibiotics promote efficient delivery of DNA into mammalian cells. *Proceedings of the National Academy of Sciences of the United States of America 100*, 1564-8.

(63) Midoux, P., Pichon, C., Yaouanc, J. J., and Jaffres, P. A. (2009) Chemical vectors for gene delivery: a current review on polymers, peptides and lipids containing histidine or imidazole as nucleic acids carriers. *Br J Pharmacol 157*, 166-78.

(64) Leng, Q., Goldgeier, L., Zhu, J., Cambell, P., Ambulos, N., and Mixson, A. J. (2007) Histidine-lysine peptides as carriers of nucleic acids. *Drug News Perspect 20*, 77-86.

(65) Zhu, J., Luther, P. W., Leng, Q., and Mixson, A. J. (2006) Synthetic histidine-rich peptides inhibit Candida species and other fungi in vitro: role of endocytosis and treatment implications. *Antimicrob Agents Chemother 50*, 2797-805.

(66) Leng, Q., Scaria, P., Ioffe, O. B., Woodle, M., and Mixson, A. J. (2006) A branched histidine/lysine peptide, H2K4b, in complex with plasmids encoding antitumor proteins inhibits tumor xenografts. *J Gene Med 8*, 1407-15.

(67) Leng, Q., Scaria, P., Zhu, J., Ambulos, N., Campbell, P., and Mixson, A. J. (2005) Highly branched HK peptides are effective carriers of siRNA. *J Gene Med 7*, 977-86.

(68) Deshayes, S., Morris, M. C., Divita, G., and Heitz, F. (2005) Cell-penetrating peptides: tools for intracellular delivery of therapeutics. *Cell Mol Life Sci 62*, 1839-49.

(69) Cho, Y. W., Kim, J. D., and Park, K. (2003) Polycation gene delivery systems: escape from endosomes to cytosol. *J Pharm Pharmacol 55*, 721-34.

(70) Blondelle, S. E., and Houghten, R. A. (1991) Hemolytic and Antimicrobial Activities of the Twenty-Four Individual Omission Analogues of Melittin. *Biochemistry 30*, 4671-4678.

(71) Mahato, R. I., Monera, O. D., Smith, L. C., and Rolland, A. (1999) Peptide-based gene delivery. *Curr Opin Mol Ther 1*, 226-43.

(72) Wagner, E., Plank, C., Zatloukal, K., Cotten, M., and Birnstiel, M. L. (1992) Influenza virus hemagglutinin HA-2 N-terminal fusogenic peptides augment gene transfer by transferrin-polylysine-DNA complexes: Toward a synthetic virus-like gene-transfer vehicle. *Proc. Natl. Acad. Sci. USA 89*, 7934-7938.

(73) Plank, C., Oberhauser, B., Mechtler, K., Koch, C., and Wagner, E. (1994) The Influence of Endosome-disruptive Peptides on Gene Transfer Using Synthetic. *J. Biol. Chem. 269*, 12918-12924.

(74) Plank, C., Zauner, W., and Wagner, E. (1998) Application of membrane-active peptides for drug and gene delivery across cellular membranes. *Advanced Drug Delivery Reviews 34*, 21-35.

(75) Subbarao, N. K., Parente, R. A., Szoka, F. C., Jr., Nadasdi, L., and Pongracz, K. (1987) pH-dependent bilayer destabilization by an amphipathic peptide. *Biochemistry 26*, 2964-72.

(76) Vlasov, G. P., Lesina, E. A., Korol'kov, V. I., Gur'ianov, I. A., Baianova, N. V., Baranov, A. N., Kisilev, A. V., and Baranov, V. S. (2005) [Optimization of transfection properties of DNA-lysine dendrimer complexes]. *Bioorg Khim 31*, 167-74.

(77) Vlasov, G. P., Korol'kov, V. I., Pankova, G. A., Tarasenko, II, Baranov, A. N., Glazkov, P. B., Kiselev, A. V., Ostapenko, O. V., Lesina, E. A., and Baranov, V. S. (2004) [Dendrimers based lysine and their "starburst" polymeric derivatives: prospects of use in compacting DNA and in vitro delivery of genetic constructs]. *Bioorg Khim 30*, 15-24.

(78) Rittner, K., Benavente, A., Bompard-Sorlet, A., Heitz, F., Divita, G., Brasseur, R., and Jacobs, E. (2002) New basic membrane-destabilizing peptides for plasmid-based gene delivery in vitro and in vivo. *Molecular Therapy: the Journal of the American Society of Gene Therapy. 5*, 104-14.

(79) Rozema, D. B., Ekena, K., Lewis, D. L., Loomis, A. G., and Wolff, J. A. (2003) Endosomolysis by masking of a membrane-active agent (EMMA) for cytoplasmic release of macromolecules. *Bioconjugate Chemistry 14*, 51-7.

(80) Legendre, J. Y., Bohrmann, T. B., Deuschle, U., Kitas, E., and Supersaxo, A. (1997) Dioleoymelittin as a Novel Serum-Insensitive Reagent for Efficient Transfections of Mammalian Cells. *Bioconjug. Chem. 8*, 57-63.

(81) Goto, Y., and Hagihara, Y. (1992) Mechanism of the conformational transition of melittin. *Biochemistry 31*, 732-8.

(82) Terwilliger, T. C., and Eisenberg, D. (1982) The structure of melittin. II. Interpretation of the structure. *Journal of Biological Chemistry 257*, 6016-22.

(83) Subbalakshmi, C., Nagaraj, R., and Sitaram, N. (1999) Biological activities of C-terminal 15-residue synthetic fragment of melittin: design of an analog with improved antibacterial activity. *FEBS Letters 448*, 62-6.

(84) Dempsey, C. E. (1990) The actions of melittin on membranes. *Biochim. Biophys. Acta 1031*, 143-161.

(85) Dempsey, C. E., Bazzo, R., Harvey, T. S., Syperek, I., Boheim, G., and Campbell, I. D. (1991) Contribution of proline-14 to the structure and actions of melittin. *FEBS Lett 281*, 240-4.

(86) Park, S. C., Kim, M. H., Hossain, M. A., Shin, S. Y., Kim, Y., Stella, L., Wade, J. D., Park, Y., and Hahm, K. S. (2008) Amphipathic alpha-helical peptide, HP (2-20), and its analogues derived from Helicobacter pylori: pore formation mechanism in various lipid compositions. *Biochim Biophys Acta 1778*, 229-41.

(87) Yang, L., Harroun, T. A., Weiss, T. M., Ding, L., and Huang, H. W. (2001) Barrel-stave model or toroidal model? A case study on melittin pores. *Biophys J 81*, 1475-85.

(88) Ladokhin, A. S., Selsted, M. E., and White, S. H. (1997) Sizing membrane pores in lipid vesicles by leakage of co-encapsulated markers: pore formation by melittin. *Biophys J 72*, 1762-6.

(89) Rozema, D. B., Lewis, D. L., Wakefield, D. H., Wong, S. C., Klein, J. J., Roesch, P. L., Bertin, S. L., Reppen, T. W., Chu, Q., Blokhin, A. V., Hagstrom, J. E., and Wolff, J. A. (2007) Dynamic PolyConjugates for targeted in vivo delivery of siRNA to hepatocytes. *Proc Natl Acad Sci U S A 104*, 12982-7.

(90) Meyer, M., Dohmen, C., Philipp, A., Kiener, D., Maiwald, G., Scheu, C., Ogris, M., and Wagner, E. (2009) Synthesis and Biological Evaluation of a Bioresponsive and Endosomolytic siRNA-Polymer Conjugate. *Molecular Pharmaceutics 6*, 752-762.

(91) Meyer, M., Philipp, A., Oskuee, R., Schmidt, C., and Wagner, E. (2008) Breathing life into polycations: functionalization with pH-responsive endosomolytic peptides and polyethylene glycol enables siRNA delivery. *Journal of the American Chemical Society 130*, 3272-3.

(92) Hirosue, S., and Weber, T. (2006) pH-Dependent lytic peptides discovered by phage display. *Biochemistry 45*, 6476-87.

(93) Sun, Q., Cai, S., and Peterson, B. R. (2008) Selective disruption of early/recycling endosomes: release of disulfide-linked cargo mediated by a N-alkyl-3beta-cholesterylamine-capped peptide. *J Am Chem Soc 130*, 10064-5.

(94) Stoffler, D., Feja, B., Fahrenkrog, B., Walz, J., Typke, D., and Aebi, U. (2003) Cryo-electron tomography provides novel insights into nuclear pore architecture: implications for nucleocytoplasmic transport. *J Mol Biol 328*, 119-30.

(95) Bremner, K. H., Seymour, L. W., and Pouton, C. W. (2001) Harnessing nuclear localization pathways for transgene delivery. *Current Opinion in Molecular Therapeutics 3*, 170-177.

(96) Bremner, K. H., Seymour, L. W., Logan, A., and Read, M. L. (2004) Factors influencing the ability of nuclear localization sequence peptides to enhance nonviral gene delivery. *Bioconjugate Chemistry 15*, 152-61.

(97) Nigg, E. A. (1997) Nucleocytoplasmic transport: signals, mechanisms and regulation. *Nature 386*, 779-87.

(98) Goldfarb, D. S., Gariepy, J., Schoolnik, G., and Kornberg, R. D. (1986) Synthetic peptides as nuclear localization signals. *Nature 322*, 641-644.

(99) Gorlich, D., and Mattaj, I. W. (1996) Nucleocytoplasmic transport. *Science 271*, 1513-8.

(100) Gorlich, D., and Kutay, U. (1999) Transport between the cell nucleus and the cytoplasm. *Annu Rev Cell Dev Biol 15*, 607 - 660.

(101) Lanford, R. E., Kanda, P., and Kennedy, R. C. (1986) Induction of nuclear transport with a synthetic peptide homologous to the SV40 T antigen transport signal. *Cell 46*, 575-82.

(102) Collas, P., and Alestrom, P. (1997) Nuclear localization signals: a driving force for nuclear transport of plasmid DNA in zebrafish. *Biochemistry & Cell Biology 75*, 633-40.

(103) Collas, P., and Alestrom, P. (1996) Nuclear localization signal of SV40 T antigen directs import of plasmid DNA into sea urchin male pronuclei in vitro. *Mol Reprod Dev 45*, 431-8.

(104) Collas, P., Husebye, H., and Alestrom, P. (1996) The nuclear localization sequence of the SV40 T antigen promotes transgene uptake and expression in zebrafish embryo nuclei. *Transgenic Res 5*, 451-8.

(105) Collas, P., and Alestrom, P. (1997) Rapid targeting of plasmid DNA to zebrafish embryo nuclei by the nuclear localization signal of SV40 T antigen. *Mol Mar Biol Biotechnol 6*, 48-58.

(106) Lanford, R. E., and Butel, J. S. (1984) Construction and characterization of an SV40 mutant defective in nuclear transport of T antigen. *Cell 37*, 801-13.

(107) Kalderon, D., Richardson, W. D., Markham, A. F., and Smith, A. E. (1984) Sequence requirements for nuclear location of simian virus 40 large-T antigen. *Nature 311*, 33-8.

(108) Kalderon, D., Roberts, B. L., Richardson, W. D., and Smith, A. E. (1984) A short amino acid sequence able to specify nuclear location. *Cell 39*, 499-509.

(109) Graebe, C., and Lagodzinski, K. (1893) Ueber Oxyderivate des Anthracholinchinons *Justus Liebigs Annalen der Chemie 276*.

(110) Rettig, G. R., and Rice, K. G. (2007) Non-viral gene delivery: from the needle to the nucleus. *Expert Opin Biol Ther 7*, 799-808.

(111) Rebuffat, A., Bernasconi, A., Ceppi, M., Wehrli, H., Verca, S. B., Ibrahim, M., Frey, B. M., Frey, F. J., and Rusconi, S. (2001) Selective enhancement of gene transfer by steroid-mediated gene delivery. *Nat Biotechnol 19*, 1155-61.

(112) Sebestik, J., Hlavacek, J., and Stibor, I. (2007) A role of the 9-aminoacridines and their conjugates in a life science. *Curr Protein Pept Sci 8*, 471-83.

(113) Sebestik, J., Safarik, M., Stibor, I., and Hlavacek, J. (2006) Acridin-9-yl exchange: a proposal for the action of some 9-aminoacridine drugs. *Biopolymers 84*, 605-14.

(114) Sebestik, J., Stibor, I., and Hlavacek, J. (2006) New peptide conjugates with 9-aminoacridine: synthesis and binding to DNA. *J Pept Sci 12*, 472-80.

(115) Kukowska-Kaszuba, M., and Dzierzbicka, K. (2007) Synthesis and Structure-Activity Studies of Peptide-Acridine/Acridone Conjugates. *Current Medicinal Chemistry 14*, 3079-3104.

(116) Graebe, C., and Caro, H. (1870) Ueber Acridin. *Chemische Berichte 3*, 746.

(117) Albert, A., and Ritchie, B. (1955) 9-Aminoacridine. *Organic Syntheses 3*, 53.

(118) Karup, G., Meldal, M., Nielsen, P. E., and Buchardt, O. (1988) 9-Acridinylpeptides and 9-acridinyl-4-nitrophenylsulfonylpeptides. Synthesis, binding to DNA, and photoinduced DNA cleavage. *Int J Pept Protein Res. 32*, 331-343.

(119) Dupre, D. J., and Robinson, F. A. (1945) N-Substituted 5-Aminoacridines. *Journal of the Chemical Society none*, 549-551.

(120) Ueyama, H., Takagi, M., Waki, M., and Takenaka, S. (2001) DNA binding behavior of peptides carrying acridinyl units: First example of effective poly-intercalation. *NUCLEIC ACIDS SYMP SER (OXF) 1*, 163-164.

(121) Tung, C., Zhu, T., Lackland, H., and Stein, S. (1992) An acridine amino acid derivative for use in Fmoc peptide synthesis. *Peptide Research 5*, 115-8.

(122) Chiu, F. C. K., Brownlee, R. T. C., and Phillips, D. R. (1993) Cupric Ion Chelation Assisted Synthesis of Nα-protected Nω-Acridin-9-yl αω-Diamino carboxylic Acids. *Australian Journal of Chemistry 46*, 1207-1212.

(123) Haensler, J., and Szoka, J. F. C. (1993) Synthesis and characterization of a trigalactosylated bisacridine compound to target DNA to hepatocytes. *Bioconjug. Chem. 4*, 85-93.

(124) Read, M. L., Logan, A., and Seymour, L. W. (2005) Barriers to Gene Delivery Using Synthetic Vectors, in *Advances in Genetics* (Hall, J. C., Dunlap, J. C., Friedmann, T., and van Heyningen, V., Eds.) pp 19-46, Academic Press.

(125) Van Dyke, R. W. (1996) Acidification of lysosomes and endosomes. *Sub-Cellular Biochemistry 27*, 331-60.

(126) Rich, D. H., Gesellchen, P. D., Tong, A., Cheung, A., and Buckner, C. K. (1975) Alkylating derivatives of amino acids and peptides. Synthesis of N-maleoylamino acids, [1-(N-maleoylglycyl)cysteinyl]oxytocin, and [1-(N-maleoyl-11-aminoundecanoyl)cysteinyl]oxytocin. Effects on vasopressin-stimulated water loss from isolated toad bladder. *Journal of Medicinal Chemistry 18*, 1004-1010.

(127) Ruiz-Gayo, M., Royo, M., Fernandez, I., Albericio, F., Giralt, E., and Pons, M. (1993) Unequivocal synthesis and characterization of a parallel and an antiparallel bis-cystine peptide. *The Journal of Organic Chemistry 58*, 6319-6328.

(128) Smith, P. K., Krohn, R. I., Hermanson, G. T., Mallia, A. K., Gartner, F. H., Provenzano, M. D., Fujumoto, E. K., Goeke, N. M., Olson, B. J. and Klenk, D. C. (1985) Measurement of protein using bicinchoninic acid. *Analytical Biochemistry 150*, 76-85.

(129) Combet, C., Blanchet, C., Geourjon, C., and Deleage, G. (2000) Network Protein Sequence Alingment. *TIBS 25*, 147-150.

(130) Legendre, J. Y., and Szoka, F. C., Jr. (1993) Cyclic amphipathic peptide-DNA complexes mediate high-efficiency transfection of adherent mammalian cells. *Proceedings of the National Academy of Sciences of the United States of America 90*, 893-7.

(131) Schuster, M. J., Wu, G. Y., Walton, C. M., and Wu, C. H. (1999) Multicomponent DNA carrier with a vesicular stomatitis virus G-peptide greatly enhances liver-targeted gene expression in mice. *Bioconjugate Chemistry 10*, 1075-1083.

(132) Nishikawa, M., Yamauchi, M., Morimoto, K., Ishida, E., Takakura, Y., and Hashida, M. (2000) Heptocyte-targeted *in vivo* gene expression by intraveneous injection of plasmid DNA complexed with synthetic multi-functional gene delivery system. *Gene Therapy 7*, 548-555.

(133) Li, W., Nicol, F., and Szoka Jr, F. C. (2004) GALA: a designed synthetic pH-responsive amphipathic peptide with applications in drug and gene delivery. *Adv Drug Deliv Rev 56*, 967-985.

(134) Read, M. L., Bremner, K. H., Oupicky, D., Green, N. K., Searle, P. F., and Seymour, L. W. (2003) Vectors based on reducible polycations facilitate intracellular release of nucleic acids. *J Gene Med 5*, 232-45.

(135) Zhou, Q.-H., Wu, C., Manickam, D., and Oupický, D. (2009) Evaluation of Pharmacokinetics of Bioreducible Gene Delivery Vectors by Real-time PCR. *Pharmaceutical Research 26*, 1581-1589.

(136) Nielsen, P. E. (2005) Systemic delivery: the last hurdle? *Gene Ther 12*, 956-7.

(137) Ueyama, H., Waki, M., Takagi, M., and Takenaka, S. (2000) Novel synthesis of a tetra-acridinyl peptide as a new DNA polyintercalator. *Nucleic Acids Symp Ser*, 133-4.

(138) Ueyama, H., Takagi, M., and Takenaka, S. (2002) Tetrakis-acridinyl peptide: a novel fluorometric reagent for nucleic acid analysis based on the fluorescence dequenching upon DNA binding. *Analyst 127*, 886-8.

(139) Mosmann, T. (1983) Rapid colorimetric assay for cellular growth and survival: application to proliferation and cytotoxicity assays. *J. Immunol. Methods 65*, 55-63.

(140) Liu, F., Song, Y., and Liu, D. (1999) Hydrodynamics-based transfection in animals by systemic administration of plasmid DNA. *Gene Ther 6*, 1258-66.

(141) Zhang, G., Budker, V., and Wolff, J. A. (1999) High levels of foreign gene expression in hepatocytes after tail vein injections of naked plasmid DNA. *Human Gene Therapy 10*, 1735-1737.

(142) Rettig, G., McAnuff, M., Kim, J., Liu, D., and Rice, K. G. (2006) Quantitative Bioluminscence Imaging of Transgene Expression In Vivo. *Analytical Biochemistry 335*, 90-94.

(143) Terebesi, J., Kwok, K. Y., and Rice, K. G. (1998) Iodinated plasmid DNA as a tool for studying gene delivery. *Analytical Biochemistry 263*, 120-123.

(144) Boeckle, S., von Gersdorff, K., van der Piepen, S., Culmsee, C., Wagner, E., and Ogris, M. (2004) Purification of polyethylenimine polyplexes highlights the role of free polycations in gene transfer. *Journal of Gene Medicine 6*, 1102-11.

(145) Rudolph, C., Schillinger, U., Plank, C., Gessner, A., Nicklaus, P., Muller, R., and Rosenecker, J. (2002) Nonviral gene delivery to the lung with copolymer-protected and transferrin-modified polyethylenimine. *Biochimica et Biophysica Acta. 1573*, 75-83.

(146) Guillaume, C., Delepine, P., Droal, C., Montier, T., Tymen, G., and Claude, F. (2001) Aerosolization of cationic lipid-DNA complexes: lipoplex characterization and optimization of aerosol delivery conditions. *Biochemical & Biophysical Research Communications. 286*, 464-71.

(147) Mahato, R. I., Anwer, K., Tagliaferri, F., Meaney, C., Leonard, P., Wadhwa, M. S., Logan, M., French, M., and Rolland, A. (1998) Biodistribution and gene expression of lipid/plasmid complexes after systemic administration. *Hum Gene Ther 9*, 2083-99.

(148) Li, S., Rizzo, M. A., Bhattacharya, S., and Huang, L. (1998) Characterization of cationic lipid-protamine-DNA (LPD) complexes for intravenous gene delivery. *Gene Therapy 5*, 930-7.

(149) Liu, F., Qi, H., Huang, L., and Liu, D. (1997) Factors controlling the efficiency of cationic lipid-mediated transfection in vivo via intravenous administration. *Gene Therapy 4*, 517-23.

(150) Felgner, P. L., Tsai, Y. J., Sukhu, L., Wheeler, C. J., Manthorpe, M., Marshall, J., and Cheng, S. H. (1995) Improved cationic lipid formulations for in vivo gene therapy. *Annals of the New York Academy of Sciences 772*, 126-39.

(151) Al-Dosari, M. S., Knapp, J. E., and Liu, D. (2005) Hydrodynamic Delivery, in *Advances in Genetics* pp 65-82, Academic Press.

(152) Molnar, M. J., Gilbert, R., Lu, Y., Liu, A. B., Guo, A., Larochelle, N., Orlopp, K., Lochmuller, H., Petrof, B. J., Nalbantoglu, J., and Karpati, G. (2004) Factors influencing the efficacy, longevity, and safety of electroporation-assisted plasmid-based gene transfer into mouse muscles. *Mol Ther 10*, 447-55.

(153) Dean, D. A., Machado-Aranda, D., Blair-Parks, K., Yeldandi, A. V., and Young, J. L. (2003) Electroporation as a method for high-level nonviral gene transfer to the lung. *Gene Ther 10*, 1608-15.

(154) Fattori, E., La Monica, N., Ciliberto, G., and Toniatti, C. (2002) Electro-gene-transfer: a new approach for muscle gene delivery. *Somat Cell Mol Genet. 27*, 75-83.

(155) Li, S., MacLaughlin, F. C., Fewell, J. G., Gondo, M., Wang, J., Nicol, F., Dean, D. A., and Smith, L. C. (2001) Muscle-specific enhancement of gene expression by incorporation of SV40 enhancer in the expression plasmid. *Gene Ther 8*, 494-7.

(156) Liu, F., and L, H. (2002) A Syringe Electrode Device for Simultaneous Injection of DNA and Electrotransfer. *Molecular Therapy 5*, 323-328.

(157) Heyes, J., Palmer, L., Chan, K., Giesbrecht, C., Jeffs, L., and MacLachlan, I. (2007) Lipid encapsulation enables the effective systemic delivery of polyplex plasmid DNA. *Mol Ther 15*, 713-20.

(158) Ogris, M., Brunner, S., Schuller, S., Kircheis, R., and Wagner, E. (1999) PEGylated DNA/transferrin-PEI complexes: reduced interaction with blood components, extended circulation in blood and potential for systemic gene delivery. *Gene Ther 6*, 595-605.

(159) Blessing, T., Kursa, M., Holzhauser, R., Kircheis, R., and Wagner, E. (2001) Different Strategies for Formation of PEGylated EGF-Conjugated PEI/DNA Complexes for Targeted Gene Delivery. *Bioconj. Chem 12*, 529-537.

(160) Mannisto, M., Vanderkerken, S., Toncheva, V., Elomaa, M., Ruponen, M., Schacht, E., and Urtti, A. (2002) Structure-activity relationships of poly(L-lysines): effects of pegylation and molecular shape on physicochemical and biological properties in gene delivery. *Journal of Controlled Release. 83*, 169-82.

(161) Baumhover, N. J., Anderson, K., Fernandez, C. A., and Rice, K. G. (2010) Synthesis and In Vitro Testing of New Potent Polyacridine-Melittin Gene Delivery Peptides. *Bioconjugate Chemistry 21*, 74-86.

(162) Anderson, K., Fernandez, C. A., and Rice, K. G. (2010) N-Glycan Targeted Gene Delivery to the Dendritic Cell SIGN Receptor. *Bioconjugate Chemistry*, submitted.

(163) Fernandez, C., A., Baumhover, N., J., Anderson, K., and Rice, K., G. (2010) Discovery of Metabolically Stablized Electronegative Polyacridine-PEG Peptide DNA Open Polyplexes. *Bioconjugate Chemistry*, in press.

(164) Kaiser, E., Colescott, R. L., Bossinger, C. D., and Cook, P. I. (1979) Color test for detection of free terminal amino groups in the solid-phase synthesis of peptides. *Analytical Biochemistry 34*, 595-598.

(165) Kaiser, E., Colescott, R. L., Bossinger, C. D., and Cook, P. I. (1970) Color test for detection of free terminal amino groups in the solid-phase synthesis of peptides. *Anal Biochem 34*, 595-8.

(166) Abdallah, B., Hassan, A., Benoist, C., Goula, D., Behr, J. P., and Demeneix, B. A. (1996) A powerful nonviral vector for in vivo gene transfer into the adult mammalian brain: polyethylenimine. *Human Gene Therapy 7*, 1947-54.

(167) Blessing, T., Remy, J. S., and Behr, J. P. (1998) Monomolecular collapse of plasmid DNA into stable virus-like particles. *Proceedings of the National Academy of Sciences of the United States of America 95*, 1427-31.

(168) Bello Roufai, M., and Midoux, P. (2001) Histidylated polylysine as DNA vector: elevation of the imidazole protonation and reduced cellular uptake without change in the polyfection efficiency of serum stabilized negative polyplexes. *Bioconjug Chem 12*, 92-9.

(169) Fajac, I., Allo, J. C., Souil, E., Merten, M., Pichon, C., Figarella, C., Monsigny, M., Briand, P., and Midoux, P. (2000) Histidylated polylysine as a synthetic vector for gene transfer into immortalized cystic fibrosis airway surface and airway gland serous cells. *J Gene Med 2*, 368-78.

(170) Boeckle, S., and Wagner, E. (2006) Optimizing targeted gene delivery: chemical modification of viral vectors and synthesis of artificial virus vector systems. *Aaps J 8*, E731-42.

(171) Harris, T. J., Green, J. J., Fung, P. W., Langer, R., Anderson, D. G., and Bhatia, S. N. (2010) Tissue-specific gene delivery via nanoparticle coating. *Biomaterials 31*, 998-1006.

(172) Le, H. T., Rao, G. A., Hirko, A. C., and Hughes, J. A. (2010) Polymeric Nanoparticles Containing Conjugated Phospholipase A2 for Nonviral Gene Delivery. *Mol Pharm*.

(173) Girod, A., Wobus, C. E., Zadori, Z., Ried, M., Leike, K., Tijssen, P., Kleinschmidt, J. A., and Hallek, M. (2002) The VP1 capsid protein of adeno-associated virus type 2 is carrying a phospholipase A2 domain required for virus infectivity. *Journal of General Virology 83*, 973-8.

(174) Grieger, J. C., Johnson, J. S., Gurda-Whitaker, B., Agbandje-McKenna, M., and Samulski, R. J. (2007) Surface-exposed adeno-associated virus Vp1-NLS capsid fusion protein rescues infectivity of noninfectious wild-type Vp2/Vp3 and Vp3-only capsids but not that of fivefold pore mutant virions. *J Virol 81*, 7833-43.

(175) Girod, A., Wobus, C. E., Zadori, Z., Ried, M., Leike, K., Tijssen, P., Kleinschmidt, J. A., and Hallek, M. (2002) The VP1 capsid protein of adeno-associated virus type 2 is carrying a phospholipase A2 domain required for virus infectivity. *J Gen Virol 83*, 973-8.

(176) Afrin, R., Zohora, U. S., Uehara, H., Watanabe-Nakayama, T., and Ikai, A. (2009) Atomic force microscopy for cellular level manipulation: imaging intracellular structures and DNA delivery through a membrane hole. *J Mol Recognit 22*, 363-72.